CATALYTIC ASYMMETRIC DESYMMETRISATION AND KINETIC RESOLUTION OF UNSATURATED AMIDES VIA HALOFUNCTIONALIZATION

Ву

Yi Yi

A DISSERTATION

Submitted to
Michigan State University
in partial fulfillment of the requirements
for the degree of

Chemistry – Doctor of Philosophy

2018

ABSTRACT

CATALYTIC ASYMMETRIC DESYMMETRISATION AND KINETIC RESOLUTION OF UNSATURATED AMINDES VIA HALOFUNCTIONALIZATION

By

Yi Yi

My doctorate research work with professor Borhan is mainly focused on developing new asymmetric halofunctionalization reactions. Chapter 1 describes the catalytic asymmetric desymmetrisation of dienes via chlorocyclization. Chapter 2 describes the kinetic resolution of propargyl amides via chlorocyclization. Both desymmetrisation and kinetic resolution using cinchona alkaloid (DHQD)₂PHAL as catalyst afford good diastereoselectivity and enantioselectivity. Chapter 3 discloses efforts to develop asymmetric *ipso*-halocyclization via dearomatization of phenol derivatives. Chapter 4 describes a novel and practical method to access *N,O*-acetals using commercially available XtalFluor-E® as catalyst.



ACKNOWLEDGMENTS

Firstly I would like to express my sincere gratitude to my advisor Prof. Borhan for the continuous support of my Ph.D study and research, for his patience, motivation, and immense knowledge in these years. He has always been my role model in science who inspire me to be dedicated to chemistry, and to stay curious.

Secondly I would like to thank all my committee members: Prof. William Wulff, Prof. Ned Jackson and Prof. Mitch Smith. They provided me a lot of guidance about scientific research. I would also like to give regards to other faculty and staff, specifically Dr Daniel Holmes for his help for NMR analysis and Dr Richard Staples for his help for X-ray crystallography. Besides, for those who helped me during my research, specifically Dr Arvind Jaganathan, Dr Kumar Ashtekar, Hadi Gholami, Xiaopeng Yin and my undergraduate Mengke Fan I would like to offer my sincere thanks.

Last but not the least, I would like to thank my parents and family who always support me with extensive love and understanding.

TABLE OF CONTENTS

LIST OF TABLES	viii
LIST OF FIGURES	x
LIST OF SCHEMES	xi
KEY TO ABBREVIATIONS	xv
CHAPTER ONE Catalytic Enantioselective Desymmetrisation of Dienes via	
Chlorocyclization	
1.1 Introduction	
1.2 Results and discussion	
1.2.1 Preliminary results	
1.2.2 Solvents study	
1.2.3 Chlorine source study	
1.2.4 Additive study	
1.2.5 Screen of other conditions	
1.2.6 Summary of optimal condition	
1.3 Substrate scope	
1.3.1 Initial application of optimal condition	
1.3.2 Substrate scope	
1.4 Derivatization of oxazine products	
1.5 Substrate synthesis	
1.6 Summary	
1.7 Experimental section	
1.7.2 General procedure for synthesis of substrates	
1.7.3 Analytical data for dienones	
1.7.4 Analytical data for substrates	
1.7.5 General procedure for desymmetrisation	
1.7.6 Analytical data for desymmetrisation products	
1.7.7 Derivatization of oxazine product	
1.8 X-ray crystal structure data	
1.8.1 X-ray crystal structure for I-77	
1.8.2 X-ray crystal structure for I-118	
1.8.3 X-ray crystal structure for I-119	
REFERENCES	
CHAPTER TWO Kinetic Resolution of Propargyl Amides in a Chlorocyclization	
Reaction	100
2.1 Introduction	100

2.2 Results and discussion	.112
2.2.1 Evaluate the efficiency of kinetic resolution	.112
2.2.2 Screening of halogen sources	.113
2.2.3 Screening of solvents	.114
2.2.4 Catalyst study	.116
2.2.5 Temperature study	.117
2.2.6 Variations from standard conditions	.119
2.2.7 Substrates scope with TFE as solvent	
2.2.8 Substrate scope with HFIP as solvent	
2.2.9 Substrate scope with TFE-DCM as solvent at low temperature	
2.2.10 Large scale reaction	
2.3 Kinetic resolution of racemic amides by dehalogenation	
2.4 Summary	
2.5 Acknowledgement	
2.6 Experimental section	
2.6.1 General information	. 130
2.6.2 General procedure for screening and optimization of kinetic resolution	. 131
2.6.3 Analytical data for cyclized products	
2.6.4 General procedure for synthesis of substrates	. 145
2.6.5 Analytical data for kinetic resolution substrates and intermediates	. 147
2.7 ¹ H NMR study	
2.8 X-ray crystallography structure data	. 165
2.8.1 X-ray crystal structure data of II-55	
2.8.2 X-ray crystal structure data of II-79	. 170
REFERENCES	. 175
CHAPTER THREE Intramolecular <i>ipso</i> -Halocyclization to Construct a Chiral	470
Spiro-Center	
3.1 Introduction	
3.2 Results and discussion	. 190
3.2.1 Screen the halogen source with <i>N</i> -(4-methoxyphenyl)-4-methyl- <i>N</i> -(3-	400
	. 190
3.2.2 Asymmetric <i>ipso</i> -halocyclization of N-(4-methoxy-2-methylphenyl)-4-	404
methyl-N-(3-phenylprop-2-yn-1-yl)benzenesulfonamide	. 191
3.2.3 Asymmetric <i>ipso</i> -halocyclization with 2-bromo- 4-methoxy- 1-((3-	400
phenylprop-2-yn-1-yl) oxy) benzene	
3.2.4 Use of Brønsted acid (R)-VANOL dihydrogenphosphate as catalyst	. 195
3.2.5 Asymmetric <i>ipso</i> -halocyclization with <i>N</i> -(4-methoxy-2-methylphenyl)-3-	107
phenyl- <i>N</i> -tosylpropiolamide	. 197
3.2.6 Asymmetric <i>ipso</i> -halocyclization with <i>N</i> -(2-hydroxyphenyl)- <i>N</i> -methyl-3-	201
phenylpropiolamide	
3.3 Summary and future work	
3.4.1 General information	
3.4.2 Synthesis of substrate III-48, III-52	
บ. - ८ บูที่เมื่องเง บา จนมจน สเซ เม-ฯบ , เม-มะ	. ८००

3.4.3 General procedure of screening and optimization of <i>ipso</i> -halocyclization	ı of
substrate III-48 and III-52	. 209
3.4.4 Procedure of synthesis and ipso-halocyclization of substrate III-54	.214
3.4.5 Synthesis and <i>ipso</i> -cyclization of substrate III-61	
3.4.6 Synthesis and <i>ipso</i> -cyclization of substrate III-72	.219
3.5 X-ray crystallography data	
3.5.1 X-ray crystallography data of III-53	. 224
3.5.2 X-ray crystal structure data of III-55	. 228
3.5.3 X-ray crystallography data of III-82	. 231
3.5.4 X-ray crystallography data of III-57	. 236
3.5.5 X-ray crystallography data of III-72	. 240
3.5.6 X-ray crystallography data of III-81	. 244
REFERENCES	. 248
CHAPTER FOUR XtalFluor- E^{\otimes} Mediated Proto-functionalization of <i>N</i> -vinyl Amides:	
Access to N-acetyl N,O-acetals	
4.1 Introduction	
4.2 Results and discussion	
4.2.1 Optimization for intermolecular hydroalkoxylation of enamide	
4.2.2 The scope for intermolecular hydroalkoxylation of enamides	
4.2.3 Mechanistic studies	
4.2.4 HBF ₄ catalyzed hydroalkoxylation	
4.2.5 Study of intramolecular hydroalkoxylation	
4.2.6 Attempts of constructing C-N/C-C bond mediated by XtalFluor-E®	
4.2.7 Summary	
4.3 Experimental section	
4.3.1 General information	
4.3.2 General procedure A for screening and optimization	
4.3.3 Analytical data for products	. 276
4.3.4 General procedure for synthesis of unsaturated amides and analytical	
data	_
4.4 Acknowledgement	. 297
REFERENCES	298

LIST OF TABLES

Table 1.1 The study of TFE-HFIP cosolvent system	19
Table 1.2 The study of other solvents	20
Table 1.3 Electrophilic chlorine source study	21
Table 1.4 The study of additives	22
Table 1.5 The study of catalyst	23
Table 2.1 Screening of electrophilic halogen source	114
Table 2.2 Screening of solvent	116
Table 2.3 Catalyst loading study	117
Table 2.4 Temperature study for different substrates	118
Table 2.5 Variations from standard condition	120
Table 2.6 Substrate scope using TFE as solvent	122
Table 2.7 Substrate scope using HFIP as solvent	123
Table 2.8 Substrate scope using TFE-DCM as solvent at -30 °C	124
Table 2.9 Kinetic resolution of racemic allyl amides via dichlorination	127
Table 2.10 Screen variations from standard condition to improve dr	129
Table 3.1 Halogen screening for substrate III-48	191
Table 3.2 Optimization of reaction conditions for substrate III-52	192
Table 3.3 Catalyst screen for substrate III-54	194
Table 3.4 Evaluation of (R)-VANOL-hydrogen phosphate	196
Table 3.5 Halogen screening for substrate III-61	198
Table 3.6 Optimization of reaction conditions for substrate III-61	200

Table 3.7 Screen of different electrophilic halogen reagent for III-72	203
Table 3.8 Catalyst screening for III-72	204
Table 3.9 Evaluation of chiral ligand with different Lewis acid	205
Table 4.1 Reaction condition optimization	263
Table 4.2 Substrates scope	265
Table 4.3 Control experiments with increasing loadings of XtalFluor-E [®]	266
Table 4.4 Control experiments of nucleophiles with different nucelophilicity and acidity	267
Table 4.5 Comparison of yields between XtalFluor-E [®] and HBF₄•OEt₂ as catalyst	271
Table 4.6 Intramolecular cyclization mediated by XtalFluor-E®	272

LIST OF FIGURES

Figure 1.1	The ¹ H NMR of substrate I-76 before and after recrystalization	17
Figure 2.1	a) plot of <i>ee</i> of recovered starting material vs conversion as a function b) plot of <i>ee</i> of product vs conversion as a function of <i>S</i>	•
•	2 Stoichiometric NMR studies of substrate-catalyst mixtures in CF ₃ CH ₂ O emperature and 0.02 M concentration of substrate and catalyst	
Figure 4.1	¹⁹ F NMR spectrum of a) XtalFluor-E [®] ; b) XtalFluor-E [®] + 1 equiv MeOH XtalFluor-E [®] + 2 equiv MeOH; d) XtalFluor-E [®] + 4 equiv MeOH; e) XtalFluor-E [®] + 5 equiv MeOH; f) XtalFluor-E [®] + 10 equiv MeOH (δ 63. was from standard compound benzotrifluoride 1 equiv.)	21

LIST OF SCHEMES

Scheme 1.1 Desymmetrization of dienes	2
Scheme 1.2 Desymmetrization of diynes	3
Scheme 1.3 Desymmetrization of anhydrides	4
Scheme 1.4 Desymmetrization of <i>meso</i> -diol	4
Scheme 1.5 Desymmetrization via alkylation and Michael addition	5
Scheme 1.6 Desymmetrization via alkylation	6
Scheme 1.7 Two types of desymmetrization via halofunctionalization	7
Scheme 1.8 The first enantioselective halocyclization with practical ee and Titanium complex catalyzed iodocylization	8
Scheme 1.9 Desymmetrization of cyclohexadiene via bromo-lactonization	9
Scheme 1.10 Henneck's work of organocatalyzed enantioselective desymmetrization	10
Scheme 1.11 Yeung's work of organocatalyzed enantioselective desymmetrization	11
Scheme 1.12 Desymmetrization of cyclopropyl carboaldehyde by 1,3-dichlorination through umploung aldehyde iminium activation	12
Scheme 1.13 Our group's previous work	14
Scheme 1.14 First snapshot of desymmetrization of diene amide	15
Scheme 1.15 Optimal conditions for substrate I-76	.24
Scheme 1.16 Initial test of three different optimal conditions	. 25
Scheme 1.17 Substrate scope using TFE-HFIP (v/v 7:3) as solvent	.27
Scheme 1.18 Substrate scope using TFE-DCM (v/v 7:3) as solvent	29

Scheme 1.19 The substrate scope	31
Scheme 1.20 Derivatization of products	33
Scheme 1.21 Other failed derivatizations	35
Scheme 1.22 Synthesis of aryl substituted diene	36
Scheme 1.23 Mitsunobu strategy to access aryl substituted dienes	37
Scheme 1.24 Reductive amination strategy to access aryl substituted dienes	37
Scheme 1.25 S _N 2 strategy to access to aryl substituted diene	38
Scheme 1.26 Reduction of oxime to access aryl substituted dienes	39
Scheme 1.27 Synthesis of aliphatic substituted diene	40
Scheme 1.28 Synthesis of bis(aryl)-amides	41
Scheme 1.29 Synthesis of bis(alkyl)-amides	43
Scheme 2.1 Catalytic kinetic resolution	101
Scheme 2.2 Early landmark studies in kinetic resolution of alkene	105
Scheme 2.3 a) Cobalt-salen catalyzed HKR; b) Mechanism of HKR	106
Scheme 2.4 (DHQD) ₂ AQN catalyzed alcoholysis of meso UNCA	107
Scheme 2.5 DKR of lactone II-15 catalyzed by a thiourea-based bifunctional catalyst	108
Scheme 2.6 Kinetic resolution of 2-oxindole catalyzed by cinchona-alkaloid squaramide	108
Scheme 2.7 Kinetic resolution of unsaturated amine and alcohols	110
Scheme 2.8 Access to propargylic amines by coupling of alkyne and aldimine	111
Scheme 2.9 Our group's previous work and proposed work	112
Scheme 2.10 Two distinct stereoselective steps leading to diastereomers	126
Scheme 2 11 Kinetic resolution of II-82	120

Scheme 3.1 C-O bond forming <i>ipso</i> -cyclization	178
Scheme 3.2 ipso-cyclization catalyzed by Iridium catalyst	179
Scheme 3.3 ipso-cyclization catalyzed by a Palladium catalyst	180
Scheme 3.4 ipso-cyclization of an activated alkyne by single electron oxidation path	181
Scheme 3.5 Silver catalyzed dearomatization of indole	182
Scheme 3.6 C-N bond forming <i>ipso</i> -cyclization	183
Scheme 3.7 Types of dearomatization via halofunctionalization	184
Scheme 3.8 Fluorocyclization of tryptamine and tryptophol	185
Scheme 3.9 Enantioselective <i>ipso</i> -chlorocyclization of indoles	186
Scheme 3.10 Larock's ipso-iodocyclization	187
Scheme 3.11 Electrophilic <i>ipso</i> -iodocyclization with <i>para</i> -activiting group	188
Scheme 3.12 Electrophilic <i>ipso</i> -iodocyclization without <i>para</i> -activiting group	188
Scheme 3.13 ipso-iodocyclization to access spiro-pyrimidine/coumarin	189
Scheme 3.14 Ipso-chlorocylization of O-linker Substrate	193
Scheme 3.15 ipso-bromocyclization of benzoyl protected N-tethered substrate	196
Scheme 3.16 ortho-directing group assisted nucleophilic substitution of propargylic alcohols	
Scheme 3.17 Evaluation of NBS with chiral dihydrogen phosphate	205
Scheme 3.18 Reactions of other derivatives	206
Scheme 3.19 Gold catalyzed <i>ipso</i> -cylclization	207
Scheme 3.20 Other substrates for <i>ipso</i> -halocyclization	207
Scheme 4.1 Catalytic intramolecular hydroalkoxylation	253
Scheme 4.2 TfOH catalyzed intermolecular hydroalkoxylation	253

Scheme 4.3 Intramolecular alkoxylation catalyzed by I ₂ and PhSiH ₃	254
Scheme 4.4 Access to <i>N</i> -acetyl- <i>N</i> , <i>O</i> -acetals via condensation of amide with aldehyde	255
Scheme 4.5 Access to <i>N</i> -acetyl- <i>N</i> , <i>O</i> -acetals via activation of nitrile	256
Scheme 4.6 Chiral phosphoric acid catalyzed addition of alcohol to imine	256
Scheme 4.7 Chiral phosphoric acid catalyzed oxyfluorination	257
Scheme 4.8 Sulfur-based fluorinating reagent	258
Scheme 4.9 XtalFluor-E® as deoxofluorinating reagent	259
Scheme 4.10 XtalFluor-E® mediated benzylation	260
Scheme 4.11 XtalFluor-E® mediated aziridine opening	261
Scheme 4.12 Reaction scheme	262
Scheme 4.13 Proposed mechanism	270
Scheme 4.14 Other attempts of intramolecular cyclization	273
Scheme 4.15 Constructing C-N bond	273
Scheme 4.16 Attempts of constructing C-C bond	275

KEY TO ABBREVIATIONS

[a] specific rotation

 δ chemical shift

Å angstrom

ACN acetonitrile

AcOH acetic acid

Ar aromatic

BF₃•OEt₂ boron trifluoride diethyl ether

BINOL 1,1'-Bi-2-naphthol

Bz benzoyl

cm centimeter

CHCl₃ chloroform

d doublet

DABCO 1,4-diazabicyclo[2,2,2]octane

DBDMH 1,3-dibromo-5,5-dimethylhydantoin

DCDMH 1,3-dichloro-5,5-dimethylhydantoin

DCM dichloromethane

DMAP 4-diaminopyridine

DMF N,N-dimethylformamide

(DHQ)₂AQN dihydroquinine(anthraquinone-1,4-diyl)-diether

(DHQ)₂PHAL dihydroquinine 1,4-phthalazinediyl diether

(DHQD)₂PHAL dihydroquinidine 1,4-phthalazinediyl diether

(DHQD)₂Pyr dihydroquinidine-2,5-diphenyl-4,6-pyrimidinediyl diether

ee enantiomeric excess

Et₃N triethylamine

Et₂O diethyl ether

EtOAc ethyl acetate

equiv equivalents

g gram(s)

h hour(s)

HPLC high pressure liquid chromatography

HRMS high resolution mass spectrometry

Hz hertz

*i*Pr *iso*propyl

J coupling constant

m multiplet

m-CPBA 3-chloroperoxybenzoic acid

MeOH methanol

min minutes

mg milligram

MHz megahertz

mmol millimole

m. p. melting point

M molar

NBS N-bromosuccinimide

NCP N-chlorophthalamide

NCS N-chlorosuccinimide

NaHCO₃ sodium bicarbonate

NaOH sodium hydroxide

Na₂SO₄ sodium sulfate

Na₂S₂O₃ sodium thiosulfate

NMR nuclear magnetic resonance

Ph phenyl

q quartet

s singlet

R_f retention factor

rt room temperature

TBAF tetrabutylammonium fluoride

TBS *t*-butyldimethylsilyl

TCCA trichloroisocyanuric acid

TFA trifluoroacetic acid

THF tetrahydrofuran

TLC thin layer chromatography

Ts tosyl

UV ultraviolet-visible spectrosco

CHAPTER ONE

Catalytic Enantioselective Desymmetrisation of Dienes via Chlorocyclization

1.1 Introduction

Desymmetrization of achiral or meso molecules is an important strategy to yield enantioenriched products. Normally people define desymmetrization as a transformation which converts an achiral or meso compound to an enantiomerically enriched chiral product by the destruction of a symmetry element. The substrates for desymmetrization are wide, including but not limited to C₂-symmetric dienes, diynes, anhydrides, epoxides, aziridines, diols and dicarbonyl compounds. Among various desymmetrization strategies, the desymmetrization of *meso*-dienes, not surprisingly, is one of the most widely investigated category considering the importance of olefin functionalization in organic synthesis. To name a few (Scheme 1.1), the Schreiber group reported desymmetrization of meso-dienes I-1 using Sharpless asymmetric epoxidation. 2-3 Landais used (DHQ)₂PYR as catalyst to desymmetrise silyl-substituted cyclohexadiene I-3 via dihydroxylation.4 Belley used Sharpless asymmetric dihydroxylation on substituted dienes I-5 to access enantio- enriched pentols I-6.5 Martin desymmetrized diene I-7 to get cyclo-propanedelta-lactone I-8 and I-9 via rhodium carboximide I-10 catalyzed enantioselective intramolecular cyclopropanation.6

Desymmetrization of *meso*-dienes by epoxidation:

Desymmetrization of cyclohexadiene by AD reaction:

Desymmetrization of *meso*-dienes by dihydroxylation:

Desymmetrization of *meso*-dienes by cyclopropanation:

Scheme 1.1 Desymmetrization of dienes

Similarly, desymmetrization of dignes has also been studied. For example, Helquist's group desymmetrized dignes **I-11** via silver catalyzed intramolecular hydroamination

(Scheme 1.2). This strategy can be applied to the synthesis of monomorine I.⁷ Yamada incorporated CO₂ into bispropargylic alcohol **I-13** to form chiral cyclic carbonates using catalytic silver acetate and chiral Schiff base ligand **I-15**.⁸ Fu used Rh(ToI-BINAP) to catalyze the cyclization of meso-diynes **I-16** to generate cyclopentanones **I-17** in excellent yield and *ee*.⁹

Scheme 1.2 Desymmetrization of diynes

More recently, impressive advances have been seen in organocatalyzed enantioselective desymmetrization. Among these, cinchona-alkaloid derived catalysts play an important role, especially in desymmetrization of *meso*-anhydrides. A large body of work for desymmetrization via nucleophilic ring-opening of anhydrides by alcohols have been reported. List *et al.* reported a novel textile supported cinchona alkaloid derived

sulfonamide catalyst **I-19** to desymmetrise anhydrides **I-18** by metholysis (Scheme 1.3).¹⁰ Hamersak et al used quinine or quinidine to catalyze the desymmetrization of anhydride **I-21** to afford half ester **I-22** by using benzyl alcohol (Scheme 1.3).¹¹ The products can be further derivatized into Rolipram.

Scheme 1.3 Desymmetrization of anhydrides

Besides anhydrides, *meso*-1,2-diols **I-23** have been desymmetrized by NBS induced mono-oxidation using quinine-derived urea catalyst **I-24** (Scheme 1.4).¹² This method furnish α -hydroxy ketones **I-25** in good yield and enantioselectivity.

Scheme 1.4 Desymmetrization of *meso*-diol

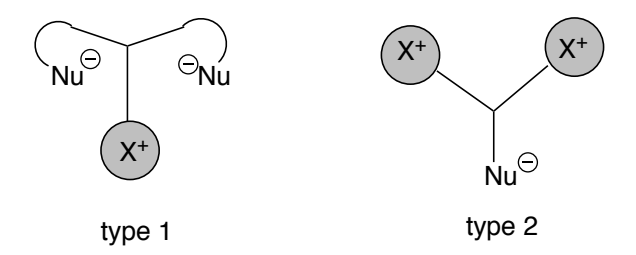
Melchiorre used cinchona alkaloid based primary amine **I-28** as catalyst in a highly selective α -alkylation of 4-substituted cyclohexanones reaction (Scheme 1.5).¹³ You and co-workers employed cinchonine derived urea catalyst **I-31** for an intramolecular Michael addition between cyclohexadienone and a pendant biphenylsulfonyl methylene (Scheme 1.5).¹⁴

Scheme 1.5 Desymmetrization via alkylation and Michael addition

Mukherjee developed an allylic alkylation reaction of prochiral 1,3-dinitropropane **I-33** using quinidine derived thiourea catalyst **I-35** (Scheme 1.6).¹⁵ The catalyst is a bifunctional catalyst which contains a Lewis basic tertiary amine and a Brønsted acidic thiourea moiety. Similarly, he also developed an alkylative desymmetrization of prochiral cyclopentene-1,3-diones **I-37** by a quinine-based urea catalyst **I-38** (Scheme 1.6).¹⁶

Scheme 1.6 Desymmetrization via alkylation

Cinchona-alkaloid catalysts have been widely used in halofunctionalization recently as well. However, the use of halofunctionalization as a strategy to achieve desymmetrization is relatively underdeveloped. Based on literature reports, desymmetrization involved halofunctionalization can be roughly divided into two types in terms of substrates (Scheme 1.7): 1) substrates that contain only one site for formation of halonium and two symmetrical nucleophilic sites that can be trapped by halonium ion;¹⁷⁻²¹ 2) substrates that contain two symmetrical sites that can form halonium and only one site to be trapped by halonium.^{17, 22-24}



Scheme 1.7 Two types of desymmetrization via halofunctionalization

Enantioselective desymmetrization via halofunctionalization was first reported in 1992 by Taguchi's group (Scheme 1.8). 19 They desymmerized prochiral diallyl(hydroxyl)acetic acids and C₂-symmetric diols through an iodolactonization process by using stoichiometric chiral Titanium(IV) complex based on a TADDOL derivative. Treatment of I-40 with Ti(iOPr)₄, pyridine, I₂ and TADDOL derived I-41 leads to cyclized *trans*-tetrahydrofuran derivative I-42 with 36% ee. The iodolactonization of symmetric diene I-44 with the same condition gave lactone I-45 with higher *ee* (67%). This was also the first example of an enantioselective halocyclization with practical *ee*. Later they reported Titanium TADDOL complex I-47 can induce highly enantioselective carbocyclization of 4-pentenylmalonate I-46 (Scheme 1.8). 17 The high enantioselectivity was due to the strong coordination between the malonate substrate and the Titanium complex.

Scheme 1.8 The first enantioselective halocyclization with practical *ee* and Titanium complex catalyzed iodocylization

More recently several groups reported organocatalyzed desymmetrization using a halofunctionalization strategy (Scheme 1.9). Kan reported a catalytic desymmetrization of cyclohexadiene derivatives **I-49** via asymmetric bromolactonization.²² NBS was used as a brominating reagent and (DHQD)₂PHAL as catalyst. For most cyclohexadiene substrates, the *ee*s were low to moderate (40% - 80% *ee*). Similarly, Marin's group reported a single example of desymmetrization of prochiral cyclodienoic acid **I-51** by bromolactonization, although only 46% *ee* was achieved.²³ They applied a BINOL derived bifunctional catalyst **I-52** which contains both acidic phenol and basic amidine.

Scheme 1.9 Desymmetrization of cyclohexadiene via bromo-lactonization

Henneck *et al.* reported another desymmetrization approach of bromolactonization of dialkynoic acids **I-54** catalyzed by (DHQD)₂PHAL (Scheme 1.10).²⁴ They proposed that the pyridazine unit of the catalyst can activate the carboxylic acid by hydrogen bonding. Besides, they reported a haloetherification reaction of a symmetric diol **I-56**. The success of this reaction depends on the selective opening of the *in situ*-generated *meso*-halonium ions. The chiral counteranion of BINOL-phosphoric acid circumvents the erosion of enantioselectivity caused by halonium olefin-to-olefin transfer.²⁵

$$\begin{array}{c} O \\ HO \\ \hline \\ R^{1} \\ \hline \\ R^{2} \\ \hline \\ I-54 \\ \hline \\ I-56 \\ \hline \\ I-56 \\ \hline \\ \\ I-56 \\ \hline \\ \\ I-57 \\ \hline \\ \\ I-20 \\ \hline \\ I-20$$

Scheme 1.10 Henneck's work of organocatalyzed enantioselective desymmetrization

Yeung's group reported bromocyclization of symmetric olefinic 1,3-dicarbonyl compounds **I-59** giving rise to functionalized dihydrofurans (Scheme 1.11).²¹ They used quinidine-derived-amino-thiocarbamate **I-60** as the catalyst and NBS as the bromination source. Even though moderate to high *ees* were reported for most substrates, reactions were sluggish and took 4 days to complete. They believe that the amino-thiocarbamate is a bifunctional catalyst: the Lewis basic sulfur can activate Br in NBS and the quinuclidine moiety in the catalyst can deprotonate the α-H of the carbonyl. Similar work from Yeung's group is the desymmetrization of trisubstituted alkenoic 1,3-diols **I-62** via bromoetherification using Lewis basic C₂-symmetric cyclic sulfide **I-63** as catalyst (Scheme 1.11).¹⁸ They believe that chiral cyclic sulfide can activate the NBS to give a chiral bromine species and the chiral bromine is then delivered to the olefin. MsOH can facilitate the formation of sulfide-Br species by protonation of the succinimide. Likewise, Yeung developed a desymmetrization of diolefinic diols **I-65** by enantioselective bromoetherification using quinidine-derived thiocarbamate catalyst **I-66**.²⁶ They proposed

that the acidic proton of the 1,3-diol may interact with the quinuclidine nitrogen atom of the catalyst and an intramolecular hydrogen bond can help lock the substrate in a pseudo six-membered ring chair conformation.

Scheme 1.11 Yeung's work of organocatalyzed enantioselective desymmetrization

Most of the reported enantioselective desymmetrizations which use halofunctionalization strategy involve the formation of a C-Br bond. The exception is that

by Gilmour and coworkers who developed an iminium catalyzed 1,3-dichlorination of cyclopropane carboxaldehyde **I-68** (Scheme 1.12).²⁷ He used Macmillan's first-generation chiral imidazolidinone catalyst to activate cyclopropane carboxaldehydes. Collidine hydrochloride and perchlorinated quinone were used as nucleophilic and electrophilic chlorinating reagents, respectively. However, this method does not belong to olefin halofunctionalization. Up to this time, catalytic enantioselective desymmetrization which involves olefin chloro-functionalization is absent.

Scheme 1.12 Desymmetrization of cyclopropyl carboaldehyde by 1,3-dichlorination through umploung aldehyde iminium activation

In 2010 our group developed the chlorolactonization of 4-substituted 4-pentenoic acid I-70 (Scheme 1.13). This method was the first catalytic enantioselective chlorolactonization with synthetically useful *ees*. Since then we realized that (DHQD)₂PHAL can be a promising candidate for catalyzing other chlorofunctionalization reactions. In 2011, our group reported a highly stereoselective chlorocyclization of unsaturated amides I-72 giving rise to the highly functionalized oxazine motif using (DHQD)₂PHAL as catalyst.²⁸ In that study dichlorodiphenylhydantoin (DCDPH) was found superior to other electrophilic chlorine sources. More interestingly, we found

trifluoroethanol (TFE) as an optimal solvent after exhaustive solvent screening. TFE revealed its uniqueness, which has also been demonstrated in a later study, as a highly polar, protic, weak nucleophilic and noncoordinating counteranion solvent. TFE greatly promoted the enantioselectivity of the reaction. The reaction scope is general in terms of the olefin substitution pattern. Both aliphatic and aromatic substituents are well tolerated. Based on this methodology our group developed a highly diastereoselective kinetic resolution of racemic olefinic amides **I-74** via chlorocyclization.²⁹ We proposed that (DHQD)₂PHAL concomitantly differentiates the chirality of racemates as well as induces high face selectivity of the olefin. The K_{rel} value for some substrates are up to 50 which is sufficient to get both substrate and product in pure enantioform. In the terms of mechanism, we proposed that the stereoinduction results from the protonated (DHQD)₂PHAL, which could be Brønsted acid catalysis or Lewis base assisted Brønsted acid catalysis (LBBA).³⁰

The first example of catalytic enantioselective halolactonization:

Chlorocyclization of unsaturated amides:

Kinetic resolution of unsaturated amides:

Ph 0.55 equiv NCP 0.5 mol% (DHQD)₂PHAL
$$R^2$$
 CF_3CH_2OH (0.1M), R^2 $R^$

Scheme 1.13 Our group's previous work

Inspired by the work mentioned above, a symmetric diene skeleton with amide was designed as nucleophile. The strategy of chlorocyclization has been applied to bisallylamide to afford highly functionalized oxazines with three contiguous stereo-centers and a remaining double bond which can be further derivatized. The chirality of oxazine can be used to induce stereoinduction to the double bond without external chiral catalysts.

1.2 Results and discussion

1.2.1 Preliminary results

Dr. Jaganathan first started this project. After the success with kinetic resolution of alkenoic amides with (DHQD)₂PHAL, desymmetrization of *meso*-alkenoic amides seemed like a reasonable possibility. Initially he employed the same conditions for the chlorocyclization of amides to the kinetic resolution of the *meso* compound **I-76**. In the presence of 10 mol% of (DHQD)₂PHAL and 1.1 equiv NCP, the reaction afforded the cyclized product in good diastereoselectivity (>9:1 *dr*) and enantioselectivity (89% *ee*) but with incomplete conversion (70%) and low isolated yield (30%) at room temperature after 30 min (Scheme 1.14). The absolute stereochemistry of the product was confirmed by X-ray crystallography. Encouraged by this result, we began optimization studies of reaction conditions.

Scheme 1.14 First snapshot of desymmetrization of diene amide

The reaction was first repeated with the same substrate and used the same condition of the first snapshot by Arvind (Scheme 1.14). Instead of 30 min the reaction time was increased to 17 h. However, the reaction was still not complete after 17 h and only reached 66% conversion (34% isolated yield) with 93% ee. The major side-product is the TFE incorporated product I-78, which has also been observed in the kinetic resolution of alkenoic amides. The TFE incorporated product is due to the excess electrophilic chlorine source in the reaction reacting with the cyclized product. Trifluoroethanol (TFE) is a nucleophilic solvent and excess amount of TFE in the reaction is prone to be trapped by chlorinium ion. Besides the TFE incorporated product, it was also found that the purity of substrate is an important factor and can erode the yield. Even though the substrate looks pure by NMR, some polymers or inorganic salts generated in the synthesis of the substrate can be separated by column chromatography only with difficulty (I will discuss the substrate synthesis in a later part). As can be seen in Figure 1.1, spectrum a is the substrate I-76 after recrystalization, spectrum **b** is the substrate I-76 after purification through column chromatography, spectrum **c** is the impurity trace in **b**. Although spectrum **b** has almost all the correct peaks of the substrate (except for the NH hydrogen shifts), there is a broad peak in the aromatic region (6.75 ppm-7.75 ppm) which was initially neglected. Spectrum c shows the isolated material buried under the aromatic region (6.75 ppm-7.75 ppm). The ¹H NMR absorption of this fraction are too messy to characterize, they may be due to some polymer or inorganic salts. The very pure form of the substrate **I-76** should be white flakes which can be obtained from recrystallization.

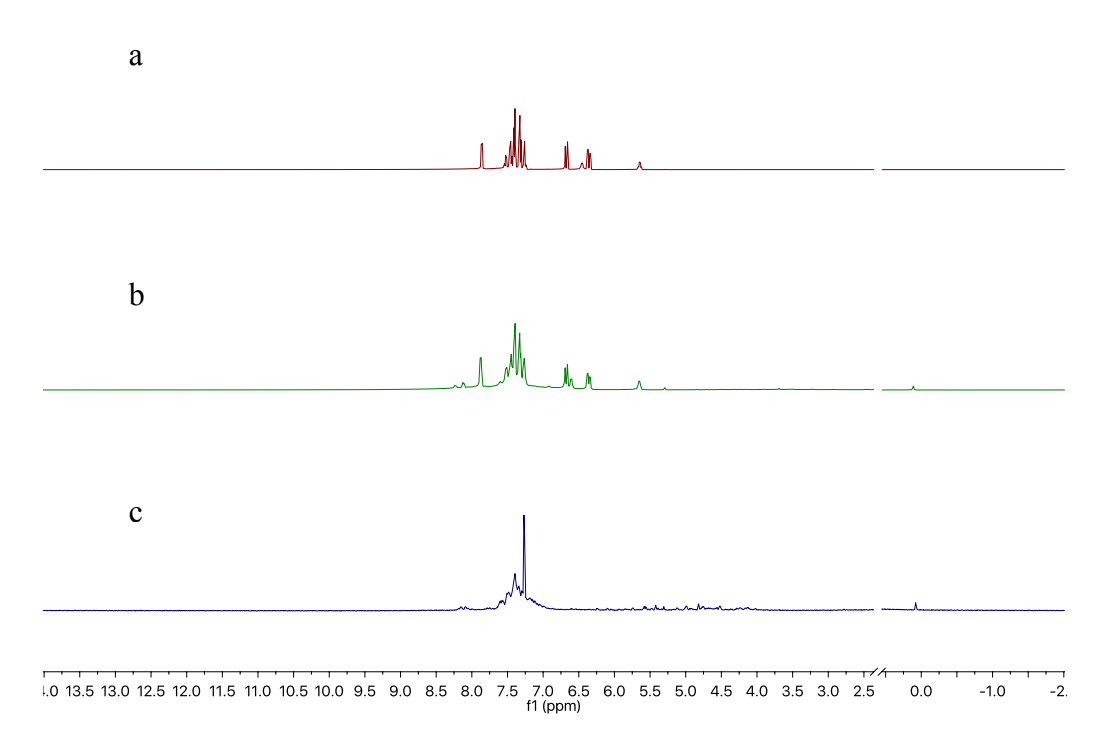


Figure 1.1 The ¹H NMR of substrate I-76 before and after recrystalization 1.2.2 Solvents study

From the initial study, it was realized that the incomplete conversion was one of the biggest issues. The reaction is not complete

in TFE after an extended time. TFE proved to be superior to any other solvents in our previous study of chlorocyclizations as well as for the dichlorination of unsaturated amides in terms of enantioselectivity. However, the *meso*-diene substrate and the desymmetrized product have poor solubility in TFE, which presumably leads to the incompletion of the reaction. An attempt was made to find an ideal solvent which can provide better soluability than TFE and meanwhile not deteriorate the enantioselectivity. We proposed that TFE can facilitate hydrogen bonding between catalyst and substrate or that its acidity can protonate the quinuclidine nitrogen of (DHQD)₂PHAL.²⁹ Based on this principle, an

attempt was made to find an alternative solvent which was also protic, acidic and highly polar. Another commonly used fluorinated solvent is HFIP (hexafluoroisopropanol). The reaction was investigated with HFIP instead of TFE while keeping the other conditions the same. Gratifyingly the reaction was much faster and was complete within 2 h at room temperature. However, the increased the reaction rate resulted in sacrificed diastereoselectivity (dr = 4.5:1) while the enantioselctivity was reduced somewhat (Table 1.1, entry 2). Aside from giving better solubility, HFIP also inhibits the generation of a major sideproduct arising from TFE incorporation, therefore the yield is much higher (95%). Then the TFE-HFIP cosolvent system was explored trying to find a ratio that can give high yield as well as good selectivity (Table 1.1). By varying the TFE-HFIP ratio from 3:7 to 7:3, a clear trend was observed: the more HFIP that was used the reaction is faster but gives a lower dr, the more TFE the higher enantioselectivity but the lower yield (Table 1.1, entry 4, 6, 7). Another trend, as can be seen from Table 1.1 is that lowering the temperature from room temperature to -10 °C greatly increases the ee (entry 3 and entry 8). But further cooling to -30 °C did not make too much difference to the ee, although reaction was slower (entry 5 and entry 6).

Table 1.1 The study of TFE-HFIP cosolvent system

entry	CI+ (equiv)	temp (°C)	solvent (ratio)	time (h)	%yield (I-77) ^a	%yield (I-78) ^a	<i>dr</i> (I-77) ^b	% <i>ee</i> (I-77) ^c
1	NCS (1.0)	rt	TFE	18	61 (76)	10	> 20:1	93
2	NCS (1.1)	rt	HFIP	2	95	=	4.5 : 1	91
3	NCP (1.0)	rt	TFE-HFIP (3:7)	12	91 (100)	=	4.5 : 1	91
4	NCP (1.1)	-30	TFE-HFIP (7:3)	17	58 (71)	10	> 20:1	98
5	NCP (1.1)	-10	TFE-HFIP (1:1)	3	99 (100)	-	6:1	96
6	NCP (1.1)	-30	TFE-HFIP (1:1)	12	96 (100)	-	6:1	97
7	NCP (1.1)	-30	TFE-HFIP (6:4)	17	91 (100)	=	6.8 : 1	95
8	NCP (1.0)	-10	TFE-HFIP (3:7)	19	69 (70)	-	21 : 1	97

^a yield of isolated product is reported and conversion is in the parentheses; ^b dr was determined form ¹H NMR;

Since TFE /HFIP co-solvent did not solve the problem, the investigation was extended to other solvents (see Table 1.2). Other non-protic and less polar solvents like dichloromethane and acetonitrile, not surprisingly lead to poor results. There was no reaction at all using DCM as solvent at –30 °C. The reaction in MeCN at room temperature was very sluggish and the enantioselectivity dropped significantly (Table 1.2, entry 2). It turned out that TFE is essential and plays an important role. Then mixtures of TFE with other non-fluorinated solvents were examined. TFE-MeCN did not lead to a complete reaction after 22 h (Table1.2, entry 3), even though the *ee* and *dr* were good. The reaction was even slower in the more polar solvent combination of TFE-DMF, and the *ee* was just moderate. Finally, it was found that the TFE-DCM solvent system greatly increases the reaction rate, giving 91% yield, predominantely as a single diastereomer in 98% *ee* (Table1.2, entry 5). The substrate is more soluble in DCM than in TFE alone. However, TFE is very crucial as well and did make a big difference (Table 1.2, entry 1 and entry 5).

^c ee was determined by chiral HPLC column.

Table 1.2 The study of other solvents

entry	CI+ (equiv)	temp (°C)	solvent (ratio)	time (h)	%yield (I-77) ^a	<i>dr</i> (I-77) ^b	% <i>ee</i> (I-77) ^c
1	NCP (1.1)	-30	DCM	24	0	-	-
2	NCS (1.1)	rt	MeCN	28	32 (41)	3.8 : 1	47
3	NCP (1.1)	-30	TFE-MeCN (1:1)	22	68 (85)	> 20:1	84
4	NCP (1.1)	-30	TFE-DMF (1:1)	48	59 (76)	10 : 1	51
5	NCP (1.1)	-30	TFE-DCM (7:3)	3	91 (100)	> 20 : 1	98

^a yield of isolated product is reported and conversion is in the parentheses; ^b *dr* was determined form ¹H NMR;

1.2.3 Chlorine source study

The TFE-incorporation product **I-78** (the major side product) was formed due to the excess of electrophilic chlorine source in the presence of TFE solvent. To get rid of this side product, the effect of adding different amounts of electrophilic chlorine reagent were studied. When 2 equiv of a CI+ source (NCS or NCP) was used the reaction became messy and the expected product was not obtained (Table 1.3, entry 1 and 2). The major product was only the TFE incorporated product **I-78**. When only 1 equiv of NCP was used at –10 °C, the reaction proceeds to 70% completion (Table 1.3, entry 3). If just a little bit excess (1.3 equiv) of NCP was added in TFE-HFIP (3:7) solvent, the reaction was complete in 3 h and no TFE incorporated product was observed (Table 1.3, entry 4, although the *dr* was only 4:1. It is noteworthy that *N*-chlorophthalimide (NCP) was more reactive than *N*-chlorosuccinimide (NCS) and meanwhile gave higher yield, NCS lead to more TFE incorporated side product (Table 1.3, entries 6 and 7). Another electrophilic

^c ee was determined by chiral HPLC column.

chlorine reagent DCDMH was more reactive and gave a complex mixture of products and only 15% of the desired product was isolated (Table 1.3, entry 5).

Table 1.3 Electrophilic chlorine source study

entry	CI+ (equiv)	temp (°C)	solvent (ratio)	time (h)	%yield (I-77) ^a	%yield (I-78) ^a	dr (I-77) ^b	% <i>ee</i> (I-77) ^c
1	NCS (2.0)	-10	TFE-HFIP (7:3)	4	0	44	6.7 : 1 ^d	-
2	NCP (2.0)	-10	TFE-HFIP (3:7)	17	0	17	-	-
3	NCP (1.0)	-10	TFE-HFIP (3:7)	19	69 (70)	-	21:1	97
4	NCP (1.3)	-10	TFE-HFIP (3:7)	3	94 (100)	=	4.4 :1	94
5	DCDMH (1.0)	-30	TFE-HFIP (1:1)	12	15 (100)	-	-	-
6	NCP (1.1)	-30	TFE-HFIP (7:3)	17	58 (71)	10	-	98
7	NCS (1.1)	-30	TFE-HFIP (7:3)	24	29 (67)	31	-	98

^a yield of isolated product is reported and conversion is in the parentheses; ^b dr was determined form ¹H NMR;

1.2.4 Additive study

To understand other factors that affect the reaction outcome the effect of addition of some additives was studied (Table 1.4). These additives include bases, Lewis acids, Brønsted acids and Lewis bases. When 1 equiv NaHCO₃ was added to the reaction at -30 °C, the product was obtained in lower yield and with reduced *ee* and *dr* (Table 1.1, entry 6 and Table 1.4, entry 1). Stoichiometric amounts of a Lewis base (PPh₃) and a Brønsted acid (benzoic acid) both decreased the reaction rate significantly while not affecting the *dr* and *ee* that much (Table 1.4, entries 2 and 3). Interestingly a catalytic amount of the Lewis acid Yt(OTf)₃ speeds up the reaction and improved the conversion within the same time frame from 71% to 95% (Table 1.1, entry 4 and Table 1.4, entry 4). The combination of 0.1 equiv Yt(OTf)₃ with 1.1 equiv NCS can push the reaction to

^c ee was determined by chiral HPLC column; ^d dr was for product **1-78**.

completetion within 17 h and afford the product in 90% yield, 19:1 dr and 98% ee (Table 1.4, entry 5). Under the latter reaction conditions, 7% of the TFE incorporated product was observed. However, other triflate salts such as AgOTf and $Zn(OTf)_2$ did not affect the reaction rate. It is still not clear how $Yt(OTf)_3$ speeds up the reaction. Adding molecular sieves in the reaction did not accelerate the reaction and some starting material was left after 24 h, albeit the yield and dr were high.

Table 1.4 The study of additives

entry	CI+ (equiv)	Additives (equiv)	solvent (ratio)	time (h)	%yield (I-77) ^a	<i>dr</i> (I-77) ^b	%ee (I-77) ^c
1	NCP (1.1)	NaHCO ₃ (1.0)	TFE-HFIP (1 : 1)	12	91 (100)	5.5 : 1	93
2	NCP (1.1)	PPh ₃ (1.0)	TFE-HFIP (1:1)	12	26 (38)	5.2 : 1	95
3	NCP (1.1)	BzOH (1.0)	TFE-HFIP (1:1)	17	48 (53)	7.9 : 1	94
4	NCP (1.1)	Yt(OTf) ₃ (0.1)	TFE-HFIP (7:3)	17	90 (95)	> 20 : 1	99
5 ^d	NCS (1.1)	Yt(OTf) ₃ (0.1)	TFE-HFIP (7:3)	17	90 (100)	19:1	98
6	NCS (1.1)	AgOTf (0.1)	TFE-HFIP (7:3)	24	73 (88)	16 : 1	-
7	NCS (1.1)	Zn(OTf) ₂ (0.1)	TFE-HFIP (7:3)	24	59 (70)	> 20 : 1	-
8	NCS (1.1)	4A MS	TFE-HFIP (7:3)	24	80 (82)	> 20 : 1	-

^a yield of isolated product is reported and conversion is in the parentheses; ^b dr was determined form ¹H NMR;

1.2.5 Screen of other conditions

Last but not the least, we screened other organocatalysts. The reaction with the qunidine derived thiourea catalyst **A** was slower than using (DHQD)₂PHAL and gave racemic products (Table 1.5, entry 1). The reaction did not proceed at all with the chiral Brønsted acid catalyst (*R*)-TRIP (Table 1.5, entry 2). Running the reaction at lower concentration (0.025 M) of the substrate gave 80% yield of **I-77** in 94% *ee* while moderate *dr* (Table 1.5, entry 3).

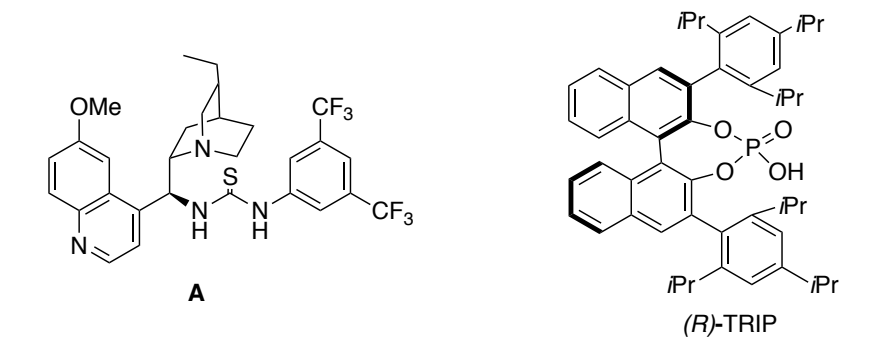
^c ee was determined by chiral HPLC column; ^d 7% of **I-78** was observed.

Table 1.5 The study of catalyst

entry	catalyst	temp (°C)	solvent (ratio)	time (h)	%yield (I-77) ^a	<i>dr</i> (I-77) ^b	% <i>ee</i> (I-77) ^c
1	A	-30	TFE-HFIP (1:1)	17	59 (60)	1:4	2
2	(<i>R</i>)-TRIP	-30	toluene	48	0 (0)	-	-
3 ^d	(DHQD) ₂ PHAL	-30	TFE-HFIP (1:1)	12	80 (100)	7 : 1	94

^a yield of isolated product is reported and conversion is in the parentheses; ^b dr was determined form ¹H NMR;

^c ee was determined by chiral HPLC column; ^d reaction concentration is 0.025 M.



1.2.6 Summary of optimal condition

After screening the solvent, temperature, catalyst and chlorine reagent, two comparable optimal conditions were identified (Scheme 1.15). When the *meso*-Diene substrate **I-76** is exposed to 1.1 equiv NCP, 10 mol% (DHQD)₂PHAL with TFE-DCM (v/v 7:3) as solvent at -30 °C the cyclized product **I-77** was obtained in 91% yield as single diastereomer in 98% *ee* (condition A). Similar results can be achieved by using TFE-HFIP (v/v 7:3) and 10 mol% Yt(OTf)₃ as additive (condition B). However later studies of the substrate scope suggested that the effect of Yt(OTf)₃ is substrate dependent. For example, *o*-Me substituted phenyl diene gave lower *dr* with Yt(OTf)₃ than without the

additive in TFE-HFIP (v/v 7:3). Interestingly for some substrates, the TFE-HFIP solvent system without any other additives gave better selectivities than TFE-DCM system. For most of the substrates both conditions were applied leading to the comparable results. This will be discussed in the substrate scope in later sections of this chapter.

condition A:

condition B:

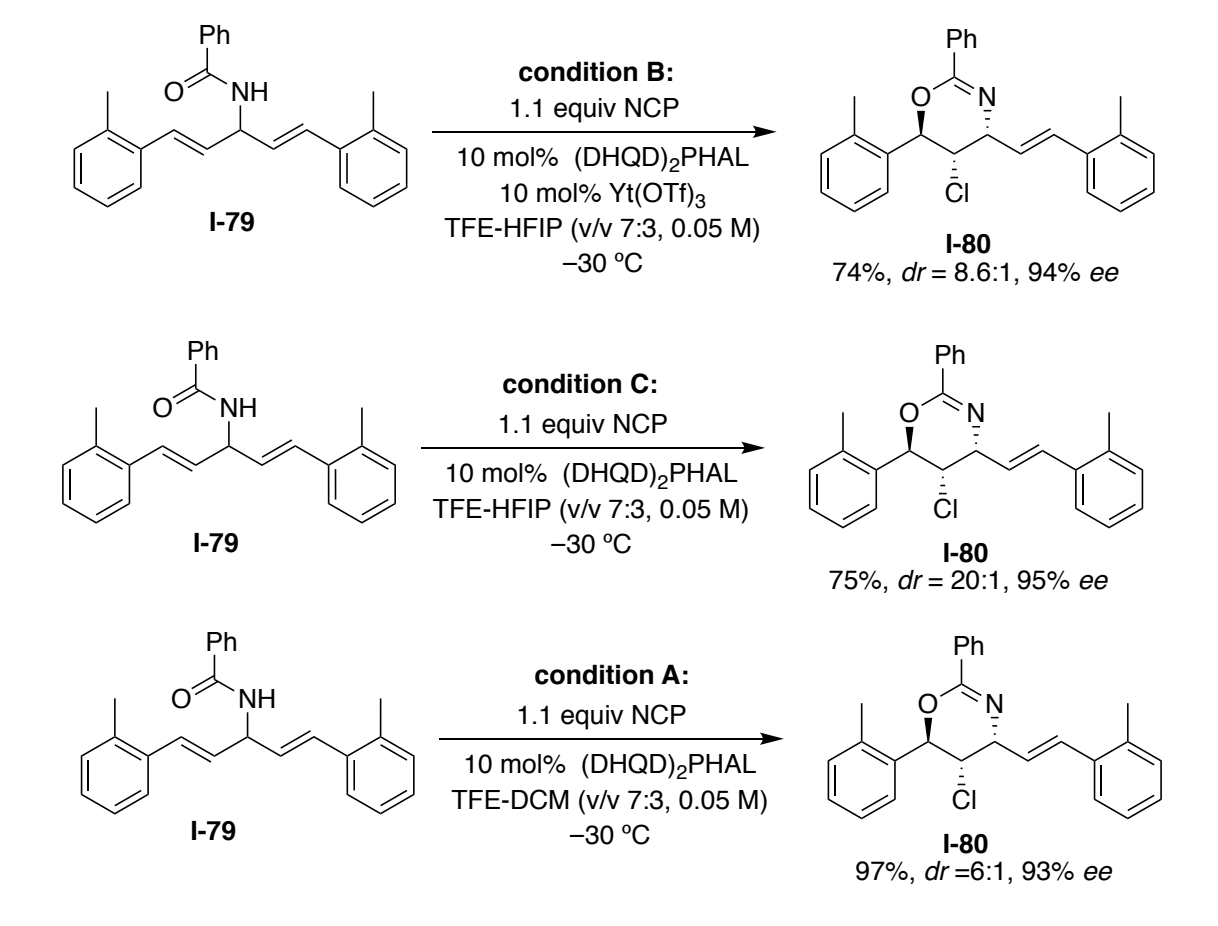
Scheme 1.15 Optimal conditions for substrate I-76

1.3 Substrate scope

1.3.1 Initial application of optimal condition

With optimal conditions in hand, other substrates bearing varied substituents on the phenyl ring were exposed to the reaction conditions. First the *o*-Me phenyl diene substrate **I-79** (Scheme 1.16) was tried. The combination of 10 mol% Yt(OTf)₃ as additive and TFE-HFIP (v/v 7:3) as solvent gave moderate yield and 94% *ee* but low *dr* (condition B) of the product **I-80**. Another optimal condition with TFE-DCM (v/v 7:3) as solvent gave higher yield but still low *dr* (condition A). Surprisingly the reaction was complete within 12 h

without $Yt(OTf)_3$ as additive and gave much better dr with comparable yield and ee in TFE-HFIP (condition C).



Scheme 1.16 Initial test of three different optimal conditions

1.3.2 Substrate scope

To obtain the best result for each substrate, both solvent systems were tested. First the TFE-HFIP (v/v 7:3) solvent system was used. A number of aryl substituted diene amides were evaluated by exposing to 1.1 equiv NCP and 10 mol% (DHQD)₂PHAL at -30 °C in TFE-HFIP (Scheme 1.17). *O*-methyl substituted phenyl substrate **I-79** reacted to give moderate yield with decent *dr* and *ee*. Electron-withdrawing substituents on phenyl ring like *p*-F **I-82** and *p*-CF₃ **I-85** lead to a single diastereomeric product in high yield and excellent *ee*. Electron-rich phenyl substituents like *p*-OMe **I-87** and *p*-Me **I-81** substituents

furnished poor stereoselectivity, giving both poor *dr* and *ee*. For the less electron-rich *m*-MeO substituted phenyl substrate **I-86**, *dr* increased a little bit to 4:1 while the *ee* was high (97%). These data suggest that the intermediate in the reaction is likely a carbocation, which can be highly stabilized by an electron-donating group and therefore the face selectivity of nucleophilic capture by the amide is scrambled and hence the selectivity is eroded. Both *m*-Br and *p*-Br substituted phenyl substrates **I-83** and **I-84** provide good *ee* and *dr*, however the reactions are not complete in an extended time range probably due to the poor solubility of substrates in TFE-HFIP. For the alkyl substituted substrate *tert*-butyl substituted diene **I-88**, the diastereoselectivity is good but *ee* is poor.

^a yield of isolated product is reported and conversion is in the parentheses; ^b *dr* was determined form ¹H NMR;

Scheme 1.17 Substrate scope using TFE-HFIP (v/v 7:3) as solvent

To further improve the outcome of the reaction, the TFE-DCM (v/v 7:3) solvent system was evaluated by applying to the same substrates in addition to others (Scheme 1.18). An obvious drop in diastereoselectivity was observed for o-Me substituted phenyl substrate **I-79** compared with the results in TFE-HFIP. A similar trend was also seen for the p-CF $_3$ substituted phenyl substrate **I-85** whose dr decreased from 20:1 to 8:1. The switch of solvent had minor effect on yield and dr of the p-Me substituted substrate **I-81**.

^c ee was determined by chiral HPLC column

The p-F substituted phenyl substrate I-82 gave quantitative yield and comparable selectivity except for a minor drop in ee. The brominated phenyl substrates **I-83** and **I-84**, in contrast to what was observed in TFE-HFIP, all afforded products in very good yields, drs and ees. The TFE-DCM solvent system did not lead to the full consumption of the p-MeO phenyl substrate **I-87** after 24 h. The diastereoselectivity of m-MeO phenyl substrate I-86 could not be improved by using TFE-DCM as solvent but the yield increased significantly (71% to 92%). In general, reactions are faster and cleaner in TFE-DCM solvent system presumably because solubility is better, so the reaction is faster and side products are suppressed. Disubstituted phenyl substrate, like 2,6-dichlorinated phenyl substituted diene I-92 was tested but gave no discernable reaction. Naphthyl and heteroaromatic substituents are not compatible with this system. The furan substituted substrate I-94 gave only 36% conversion after 2 days. Thiophene substituted substrate I-100 was more reactive as compared to furan substituted I-94, leading to 82% conversion, but producing a complex mixture of products. Only a 26% yield of six-member ring products were obtained in poor *dr* and *ee*.

Scheme 1.18 Substrate scope using TFE-DCM (v/v 7:3) as solvent

The tolerance of different substitution patterns and electronic properties were tested, as feasible, since the synthesis of the *meso*-diene amides is not routine. Alkyl substituted dienes were examined. *t*-Butyl substituted **I-88** failed to give high selectivity, its steric hindrance might be a reason. More general alkyl substituents such as *n*-butyl **I-95** and cyclohexyl **I-96** substituents have been evaluated. It turned out that they both gave excellent *dr* and *ee* in good yield. This result was within our expectation based on Arvind's

^a yield of isolated product is reported and conversion is in the parentheses; ^b *dr* was determined form 1H NMR; ^c *ee* was determined by chiral HPLC column. ND = none determined

work on the chlorocyclization of alkenoic amides where he reported aliphatic substituted substrates gave excellent enantioselectivity.²⁸

Another variable that can be tuned is the nature of the aryl amide (Scheme 1.19). p-MeO benzoyl and p-Br benzoyl protected amides **I-97** and **I-98** both gave excellent diastereoselectivity and enantioselectivity but not the acetyl protection group **I-99** which led to complete loss of stereoinduction and poor yield. The complete loss of stereoinduction with the acetyl group might be due to the absence of π interaction between catalyst and substrate. Our previous reports of successful (DHQD)₂PHAL catalyzed chlorofunctionalization of unsaturated amides, include chlorocyclization, kinetic resolution and dichlorination, all used benzoyl type protection group. The specific preference of the amide might suggest that there is a π interaction existing between catalyst and substrate which can direct the nucleophilic trap of a chlorenium from a specific face. However, at this stage we don't have any evidence to support this assumption. Scheme 1.19 shows the complete substrate scope.

1.1 equiv NCP

I-81 70%^a, *dr* = 1.6 : 1, 47% *ee*

87%^a, dr > 20 : 1, 96% ee

I-97

77%, dr > 20 : 1, 95% ee

I-85

86%^a, dr > 20 : 1, 90% ee

41%, *dr* = 2.8 : 1, 56% *ee*

I-88

66%^a, dr > 20 : 1, 41% ee

67%, dr > 20:1, 98% ee

I-99

53%, *dr* = 2 : 1, 3% *ee*

 $^{\rm a}$ TFE : HFIP (v/v, 7 : 3, 0.05 M) as solvent; $^{\rm b}$ (DHQ)2PHAL was used as catalyst.

Scheme 1.19 The substrate scope

I-98

66%, dr > 20:1, > 99.9 % ee

1.4 Derivatization of oxazine products

To demonstrate the application of this methodology, further functionalization of the oxazine products were performed (Scheme 1.20). One of the merits of this desymmetrization method is that we can access oxazine bearing a double bond. Functionalization of olefins is one of the most well studied and important transformations. Since this methodology provides a highly stereoselective access to oxazine rings, new chiral centers can be introduced onto the neighboring double bond in the absence of an external chiral catalyst. After an exhaustive screen, it was found that subjecting the oxazine product (98% ee, dr > 20:1) to Upjohn dihydroxylation conditions affording the diol product I-118 in 86% yield with more than 20:1 dr. More importantly, the dr of diol I-118 was not eroded. The double bond could be epoxidized by using m-CPBA and expoxide product I-119 was obtained with a slight decrease in dr in 67% yield. The absolute stereochemistry of diol and expoxide was determined by X-ray crystallography. The oxazine product can be hydrolyzed in HCI to afford the corresponding amino alcohol I-120 in quantitative yield but with diminished dr.

Dihydroxylation

Epoxidation:

Scheme 1.20 Derivatization of products

Other transformations have been attempted including dihalogenation, chloroetherification, cyclopropanation, aziridination and hydroxyamination (Scheme 1.21). However, most of those transformations failed. The double bond next to the oxazine ring is unreactive for these reactions. Starting material was recovered for most of the transformations. Notably dichlorination developed by our group using DCDMH and LiCl in the absence of (DHQD)₂PHAL failed to give the desired product.³¹ Likewise chloroetherification in the presence of (DHQD)₂PHAL did not induce any reaction as well. Dichlorination using PCl₅ gave the dichloride product I-134 in 1:1 *dr*.

aziridination:

dihalogenation:

chloro-etherification:

hydroxyamination:

cyclopropanation:

$$\begin{array}{c|c} Ph & 2 \text{ equiv } \text{Et}_2\text{Zn} \\ 2 \text{ equiv } \text{CH}_2\text{I}_2 \\ \hline \hline \text{DCM, 24 h} \\ \hline \text{I-77} \\ \end{array} \qquad \text{N.R}$$

Scheme 1.21 Other failed derivatizations

1.5 Substrate synthesis

The biggest challenge encountered in this project was the synthesis of bis-allylamide substrates. The symmetrical *meso* alkenyl amides have not been reported before, nor have the *meso* alkenyl amines been previously synthesized. It was desired to find a short and high yielding route to access these substrates. After exhaustive attempts, a four-step sequence was found to access the aryl substituted substrates, although with low yield overall (Scheme 1.22). First, the dienones **I-121-I-133** were synthesized by adol reaction of acetone and the corresponding benzaldehyde in more than 90% yield for most substrates. The dienone was subjected to excess LiHMDS followed by excess benzoyl chloride to give an imine. No purification was needed for the imine intermediate which tend to decompose on a column of silica gel. The imine was reduced with NaBH4 to deliver the final product. The yield for the last three steps is between 10 - 30%.

Scheme 1.22 Synthesis of aryl substituted dienes

It is worth to summarize some of the failed routes. One path utilized the Mitsunobu reaction. We reduced the dieone **I-125** to the secondary alcohol **I-135**, but several conditions for the Mitsunobu reaction did not work. The combination of PPh₃, DIAD and phthalimide failed to give any conversion. While DPPA with DBU can transform the secondary alcohol to azide **I-136**, *n*Bu₃P could not reduce the azide. Also it was hard to

selectively reduce the azide in the presense of double bonds using other reduction methods, for example hydrogenation.

Scheme 1.23 Mitsunobu strategy to access aryl substituted dienes

Reductive amination is another commonly used strategy to transform ketones to amines. We attempted to use Ti(OiPr)4 to induce amination. Ammonia/EtOH solution could not yield the imine product I-137; after adding NaBH4 in one pot alcohol was obtained. Consisitent bubbling of ammonia gas followed by refluxing for 24 h only give partial conversion and most of the ketone was recovered.

Route 3:

Scheme 1.24 Reductive amination strategy to access anyl substituted dienes

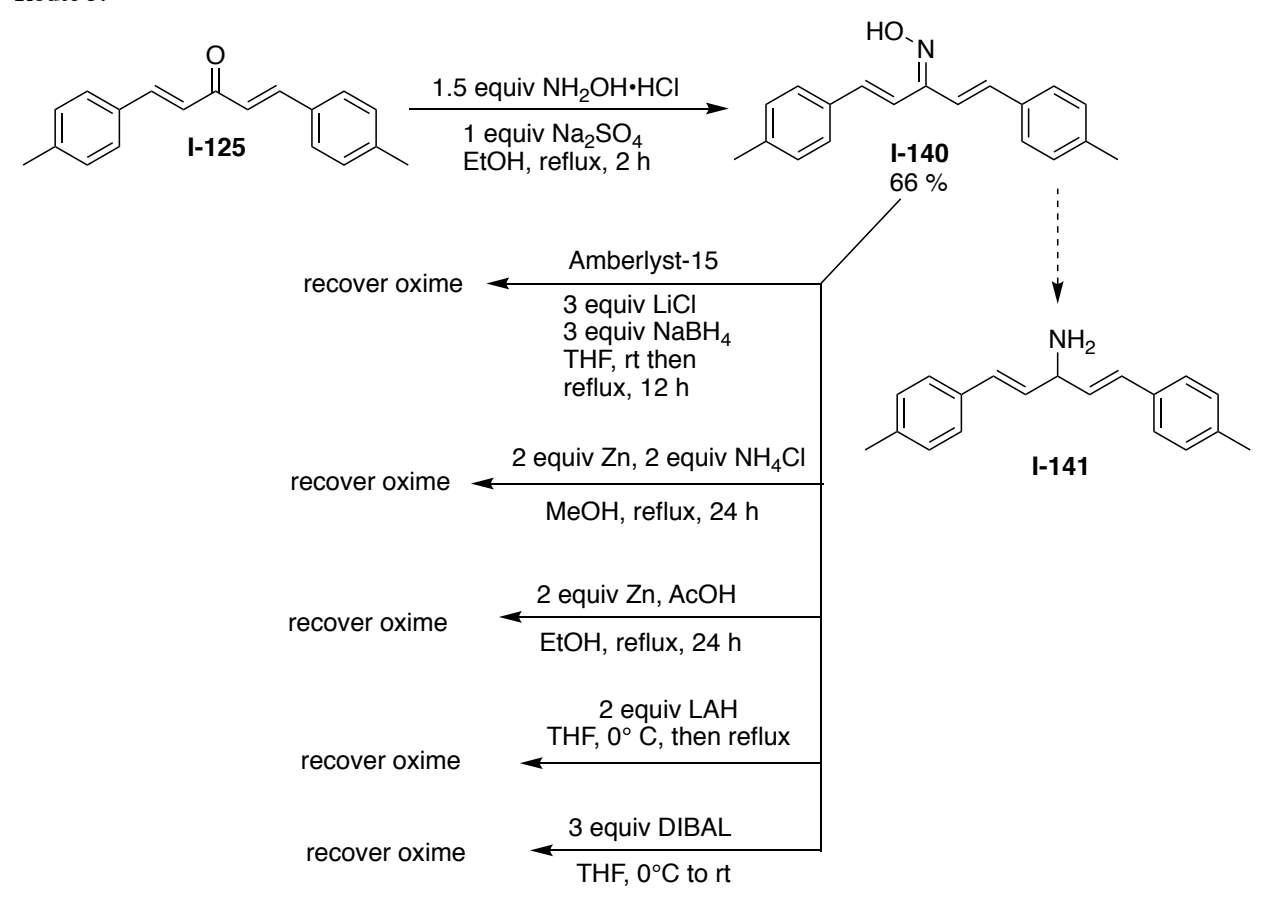
We also used the strategy that converts the secondary alcohol to a good leaving group and then reacting with a nitrogen nucleophile via an S_N2 pathway (Scheme 1.25). The secondary alcohol could be easily protected to give the methyl sulfonyl chloride **I-138**. However, when sodium azide was used as nucleophile, the sequence of S_N2 followed by [3,3] sigmatropic rearrangement of azide occurred to yield **I-139**.

Route 4:

Scheme 1.25 S_N2 strategy to access to aryl substituted dienes

There are reports of oxime synthesis from ketone and subsequent reduction of the oxime to amine.³²⁻³³ The preparation of oxime **I-140** from dienone **I-125** was achieved in moderate yields. However varied methods for the reduction of the oxime failed, leading to the recovery of the oxime in most cases (Scheme 1.26).

Route 5:



Scheme 1.26 Reduction of oxime to access aryl substituted dienes

For the aliphatic substituted diene substrates, the four steps sequence using LiHMDS did not work. The Mitsunobu reaction was used to install the nitrogen group (Scheme 1.27). Starting from the corresponding alkyne I-142, an aldol reaction afforded the *meso*-propargyl alcohol (I-101, I-102). Reduction of the triple bond with Red-Al® gave exclusively the *E* bis-allyl alcohol I-143 which was ready for Mitsunobu reaction. The resulting phthalimide I-145 was removed by hydrazine hydrate and the resulted amine was protected with benzoyl chloride. However, the reduction step with Red-Al always gave the over-reduced product which could not be separated from the diene product.

(R = cyclohexyl, n-butyl)

Scheme 1.27 Synthesis of aliphatic substituted dienes

1.6 Summary

A useful and efficient desymmetrization of *meso*-diene amides via catalytic enantioselective chlorocyclization has been successfully developed. Many aryl and alkyl substituted dienes substrates are well tolerated. The reaction can furnish a highly functionalized oxazine with good yield and excellent enantioselectivity and diastereoselectivity.

1.7 Experimental section

1.7.1 General information

All reagents were purchased from commercial sources and were used without purification. (DHQD)₂PHAL and *N*-chlorophthalimide were purchased from Aldrich.

Trifluoroethanol and hexafluoro-*iso*propanol were purchased from Combi-Blocks. TLC analyses were performed on silica gel plates (pre-coated on glass; 0.20 mm thickness with fluorescent indicator UV254) and were visualized by UV or charred in KMnO₄ stains.

¹H and ¹³C NMR spectra were collected on 500 MHz NMR spectrometers (Agilent) using CDCl₃. Chemical shifts are reported in parts per million (ppm) and are referenced to residual solvent peaks. For HRMS (ESI) analysis, a Water 2795 (Alliance HT) instrument was used and referenced against Polyethylene Glycol (PEG-400-600). Flash silica gel (32-63 μm, Silicycle 60 Å) was used for column chromatography. All known compounds were characterized by ¹H and ¹³C NMR and are in complete agreement with samples reported elsewhere. All new compounds were characterized by ¹H and ¹³CNMR, HRMS, and melting point (where appropriate). Enantiomeric excesses were determined using chiral HPLC (instrument: HP series 1100, Agilent 1260 infinity).

1.7.2 General procedure for synthesis of substrates

Scheme 1.28 Synthesis of bis(aryl)-amides

General procedure A: Dienone was synthesized according to reported literature.³⁴ To a solution of the corresponding benzaldehyde (2 equiv) and acetone (1 equiv) in the solvent of Ethanol (1M), 6M NaOH (2 M) was added dropwise (approximately 2 drops/sec to avoid formation of side products). The reaction mixture warmed up rapidly forming a cloudy suspension. The mixture was allowed to stir at room temperature for another hour. The reaction was neutralized with the addition of HCI (concentrated), followed by extraction with dichlormethane. The combined organic extracts were washed with brine, dried over sodium sulfate, and finally subjected to purification by silica gel flash column chromatography or by recrystallization.

The corresponding dienone was dissolved in freshly distilled THF (0.5 M) and stirred at -78 °C for 10 min. LiHMDS (1 M in THF) was added dropwise to the solution under Ar balloon. The reaction mixture was gradually warmed to room temperature and stirred for further 4 hr. The reaction was cooled down to -78 °C and benzoyl chloride was added in one portion. After strirring at room temperature for 2 hr, the reaction was quenched by addition of saturated ammonium chloride solution. The reaction was extracted with EtOAc and the combined organic layers were dried with Na₂SO₄ and the solvent was removed under reduced pressure. The residue was dissolved in MeOH and NaBH₄ was added at 0 °C. The reaction was gradually warmed to room temperature and stirred for 8 hr. Once the reaction was complete, H₂O was added to quench the reaction. The reaction was extracted with EtOAc and the combined organics were dried with Na₂SO₄ and filtered. The solvent was removed under reduced pressure to afford the crude product. The product was purified with silica column chromatography using EtOAc/Hex as eluent.

Scheme 1.29 Synthesis of bis(alkyl)-amides

General procedure B: To a round bottom flask under Ar atmosphere add cyclohexylacetylene (13.9 mmol, 1,5 g) and freshly distilled THF (20 mL) was added, then *n*-BuLi solution in hexane (2.5 M, 15.2 mmol, 6.1 mL) was added dropwise to the alkyne solution at –78 °C. After stirring for 5 min, ethyl formate (6.95 mmol, 515 mg) was added in one portion at –78 °C. The reaction was then gradually warmed up to room temperature. After reaction was complete, saturated NH₄Cl solution (20 mL) was added to work up the reaction. The organics were separated and washed with DCM for three times. The combined organics were dried with Na₂SO₄ and the solvent were removed under reduced pressure. The propargyl alcohol product was purified in a flash column to afford 98% yield.

The propargylic alcohol was then reduced by Red-Al[®]. To a solution of propargylic alcohol (6.9 mmol) in freshly distilled THF (50 mL) was added Red-Al® (42 mmol, 70% in toluene) and then the solution was stirred at room temperature for 12 hr. To guench the reaction, saturated Rochelle salt solution was added carefully and then the resulting mixture was stirred for 1h until two clear layers were seen. The mixture was extracted with EtOAc three times, and the combined extracts were dried over Na₂SO₄. The combined organic layers were concentrated under reduced pressure to afford crude residue, which was purified by chromatography on silica gel with EtOAc/Hexane as eluent (75% yield). The allyl alcohol (4.67 mmol, 1 equiv) was dissolved in distilled THF (25 mL). Triphenylphosphine (5.14 mmol, 1.1 equiv), phthalimide (5.14 mmol, 1.1 equiv) and DIAD (5.14 mmol, 1.1 equiv) were added subsequently to the reaction mixture at 0 °C. After the reaction was complete, water was added to quench the reaction. The organic layers were separates and dried over the Na₂SO₄. The solvent was removed under reduced pressure to afford the crude product. The product was purified by column chromatography on silica gel with 3% EtOAc/Hexane as eluent.

1.7.3 Analytical data for dienones:

General procedure **A** with benzaldehyde (5.4 mmol) gave 90% yield of the pure product as yellow needle shaped crystals, mp. 111 °C.

¹H NMR (500 MHz, CDCl₃) δ 7.73 (2H, d, J = 15.6 Hz), 7.61-7.60 (4H, m), 7.41-7.60 (6H, m), 7.07 (2H, d, J = 16.2 Hz).

¹³C NMR (125 MHz, CDCl₃) δ 188.9, 143.3, 134.8, 130.5, 129.0, 128.4, 125.4 ppm.

General procedure **A** with *m*-anisaldehyde (5.4 mmol) gave 55% yield of the pure product as yellow oil.

¹H NMR (500 MHz, CDCl₃) δ 7.71 (2H, d, J = 16.0 Hz), 7.34 (2H, t, J = 8.0 Hz), 7.20-7.24 (2H, m), 7.12-7.16 (2H, m), 7.07 (2H, d, J = 15.5 Hz), 6.97 (2H, dd, J = 8.0 Hz, 2.5 Hz), 3.86 (6H, s).

¹³C NMR (125 MHz, CDCl₃) δ 188.9, 159.9, 143.3, 136.2, 130.0, 125.7, 121.1, 116.4, 113.2, 55.4.

General procedure **A** with p-anisaldehyde (5.4 mmol) gave 62% yield of the pure product as yellow solid, mp. 120 °C.

¹H NMR (500 MHz, CDCl₃) δ 7.70 (2H, d, J = 15.5 Hz), 7.54-7.60 (4H, m), 6.91-6.98 (6H, m), 3.85 (6H, s).

 ^{13}C NMR (125 MHz, CDCl₃) δ 188.8, 161.5, 142.6, 130.1, 127.6, 123.5, 114.4, 55.4.

General procedure **A** with *o*-tolualdehyde (5.4 mmol) gave 83% yield of the pure product as yellow solid, mp.70 °C.

¹H NMR (500 MHz, CDCl₃) δ 8.05 (2H, d, J = 16.0 Hz), 7.64-7.68 (2H, m), 7.29-7.34 (2H, m), 7.22-7.27 (2H, m), 7.00 (2H, d, J = 15.5 Hz), 2.49 (6H, s).

¹³C NMR (125 MHz, CDCl₃) δ 188.9, 140.9, 138.2, 133.8, 130.9, 130.2, 126.7, 126.4, 126.4, 19.9.

General procedure **A** with *p*-tolualdehyde (5.4 mmol) gave 73% yield of the pure product as yellow solid, mp. 166 °C.

¹H NMR (500 MHz, CDCl₃) δ 7.72 (2H, d, J = 16.0 Hz), 7.52 (4H, d, J = 8.5 Hz), 7.22 (4H, d, J = 8.5 Hz), 7.05 (2H, d, J = 15.5 Hz) 2.39 (6H, s).

¹³C NMR (125 MHz, CDCl₃) δ 189.1, 143.2, 141.0, 132.1, 129.7, 128.4, 124.6, 21.5 ppm.

General procedure **A** with *o*-fluorobenzaldehyde (5.4 mmol) gave 49% yield of the pure product as yellow solid, mp. 68 °C.

¹H NMR (500 MHz, CDCl₃) δ 7.87 (2H, d, J = 16.0 Hz), 7.61-7.67 (2H, m), 7.35-7.42 (2H, m), 7.10-7.23 (6H, m).

¹³C NMR (125 MHz, CDCl₃) 189.0, 162.6 (d, ${}^{1}J_{C,F} = 252.4$ Hz.), 136.1 (d, ${}^{4}J_{C,F} = 2.9$ Hz.), 131.9 (d, ${}^{3}J_{C,F} = 8.5$ Hz.), 129.3 (d, ${}^{4}J_{C,F} = 2.8$ Hz.), 127.6 (d, ${}^{3}J_{C,F} = 6.6$ Hz.), 124.5 (d, ${}^{3}J_{C,F} = 3.9$ Hz.), 122.8 (d, ${}^{2}J_{C,F} = 11.4$ Hz.), 116.3 (d, ${}^{2}J_{C,F} = 21.9$ Hz.).

General procedure **A** with *p*-bromobenzaldehyde (5.4 mmol) gave 97% yield of the pure product as yellow solid, mp. 205 °C.

¹H NMR (500 MHz, CDCl₃) δ 7.67 (2H, d, J = 15.5 Hz), 7.55 (4H, d, J = 8.0 Hz), 7.47 (4H, d, J = 8.0 Hz), 7.05 (2H, d, J = 16.0 Hz).

¹³C NMR (125 MHz, CDCl₃) δ 188.3, 142.2, 133.6, 132.2, 129.7, 125.7, 124.9.

General procedure **A** with *m*-bromobenzaldehyde (5.4 mmol) gave 85% yield of the pure product as yellow solid, mp. 93-97 °C.

¹H NMR (500 MHz, CDCl₃) δ 7.78 (t, J = 1.9 Hz, 2H), 7.66 (dd, J = 15.9, 2.0 Hz, 2H), 7.54 (t, J = 7.6 Hz, 3H), 7.35 – 7.24 (m, 3H), 7.06 (dd, J = 15.9, 2.0 Hz, 2H).

¹³C NMR (125 MHz, CDCl₃) δ 188.13, 141.89, 136.75, 133.34, 130.88, 130.49, 127.16, 126.34, 123.11.

General procedure **A** with *p*-chlorpbenzaldehyde (5.4 mmol) gave 98% yield of the pure product as yellow solid, mp. 170 °C.

¹H NMR (500 MHz, CDCl₃) δ 7.73 (2H, d, J = 16.0 Hz), 7.61 (4H, d, J = 8.5 Hz), 7.45 (4H, d, J = 9.0 Hz), 7.09 (2H, d, J = 15.5 Hz).

¹³C NMR (125 MHz, CDCl₃) δ 188.3, 142.1, 136.5, 133.2, 129.5, 129.3, 129.2, 125.7.

General procedure **A** with 3-furaldehdye (5.4 mmol) gave 95% yield of the pure product as yellow crystal, mp. 89-94°C.

¹H NMR (500 MHz, CDCl₃) δ 7.73 (dd, J = 1.5, 0.8 Hz, 2H), 7.63 (d, J = 15.7 Hz, 2H), 7.51 – 7.39 (m, 2H), 6.77 (d, J = 15.8 Hz, 2H), 6.67 (dd, J = 1.9, 0.8 Hz, 2H).

¹³C NMR (126 MHz, CDCl₃) δ 188.55, 145.27, 144.49, 133.09, 125.30, 123.10, 107.40.

General procedure **A** with 2-naphthaldehyde (5.4 mmol) gave 27% yield of the pure product as yellow solid, 113 °C.

¹H NMR (500 MHz, CDCl₃) δ 8.66 (2H, d, J = 16.0 Hz), 8.29 (2H, d, J = 9.0 Hz), 7.87-7.98 (6H, m), 7.51-7.65 (6H, m), 7.25 (2H, d, J = 14.5 Hz).

¹³C NMR (125 MHz, CDCl₃) δ 188.6, 140.4, 133.7, 132.2, 131.7, 130.8, 128.8, 128.1, 127.0, 126.3, 125.5, 125.2, 123.4.

General procedure **A** with 4-*tert*-butylbenzaldehyde (5.4 mmol) gave 50% yield of the pure product as yellow solid

¹H NMR (500 MHz, CDCl₃) δ 7.71 (d, J = 15.9 Hz, 2H), 7.55 (d, J = 8.4 Hz, 4H), 7.42 (d, J = 8.4 Hz, 4H), 7.04 (d, J = 15.9 Hz, 2H), 1.32 (s, 18H).

¹³C NMR (126 MHz, CDCl₃) δ 189.12, 154.08, 143.07, 132.08, 128.25, 125.94, 124.77, 34.95, 31.17.

General procedure **A** with 4-(trifluoromethyl)benzaldehyde gave 34% yield of the pure product as yellow solid, mp.135-140 °C.

¹H NMR (500 MHz, CDCl₃) δ 7.75 (d, J = 15.9 Hz, 2H), 7.75 – 7.66 (m, 8H), 7.15 (d, J = 15.9 Hz, 2H).

¹³C NMR (126 MHz, CDCl₃) δ 188.08, 141.92, 137.94, 132.06 (d, J_{C-F} = 32.6 Hz), 128.52, 127.17, 125.96 (q, J_{C-F} =3.8 Hz), 124.86.

General procedure **A** with 4-fluorobenzaldehyde gave 95% yield of the pure product as yellow solid, mp.124-128 °C.

¹H NMR (500 MHz, CDCl₃) δ 7.72 (d, J = 15.9 Hz, 2H), 7.67 – 7.56 (m, 4H), 7.17 – 7.07 (m, 4H), 7.00 (d, J = 15.9 Hz, 2H).

¹³C NMR (126 MHz, CDCl₃) δ 188.45, 164.05 (d, $J_{\text{C-F}}$ = 252.0 Hz), 142.10, 130.97 (d, $J_{\text{C-F}}$ = 3.3 Hz), 130.28 (d, $J_{\text{C-F}}$ = 8.5 Hz), 125.06 (d, $J_{\text{C-F}}$ = 2.4 Hz), 116.17 (d, $J_{\text{C-F}}$ = 21.9 Hz).

1.7.4 Analytical data for substrates

General procedure **A** with dienone **I-121**(2.00 g, 8.54 mmol) gave **I-76** in 30% yield.

white snowflake solids; M.P.: 203-205 °C

Rf: 0.54 (30% EtOAc in Hexane, UV)

¹H NMR (500 MHz, CDCl₃) δ 7.86 (d, J = 7.8 Hz, 2H), 7.57 – 7.49 (m, 1H), 7.46 (d, J = 7.5 Hz, 2H), 7.40 (d, J = 7.0 Hz, 4H), 7.33 (t, J = 7.5 Hz, 4H), 7.26 (td, J = 7.3, 1.3 Hz, 2H), 6.67 (d, J = 16.0 Hz, 2H), 6.45 (d, J = 8.4 Hz, 1H), 6.36 (dd, J = 16.0, 6.1 Hz, 2H), 5.70 – 5.56 (m, 1H).

¹³C NMR (125 MHz, CDCl₃) δ 166.5, 136.4, 134.4, 131.8, 131.7, 128.7, 128.6, 128.0, 127.9, 127.0, 126.5, 52.8

HRMS analysis (ESI): calculated for (M+H): C₂₄H₂₁CINO 374.1312; found: 374.1346.

General procedure **A** with dienone **I-124** (1.30 g, 5 mmol) gave **I-79** in 19% yield white solids; M.P.: 145-150 °C

R_f: 0.22 (15% EtOAc in Hexane, UV)

¹H NMR (500 MHz, CDCl₃) δ 7.82 (d, J = 6.9 Hz, 2H), 7.52 – 7.49 (m, 1H), 7.46 – 7.43 (m, 4H), 7.15 (ddd, J = 8.6, 5.2, 3.7 Hz, 6H), 6.89 (d, J = 1.5 Hz, 2H), 6.31 (d, J = 8.3 Hz, 1H), 6.21 (dd, J = 15.8, 6.1 Hz, 2H), 5.67 – 5.62 (m, 1H), 2.33 (s, 1H).

¹³C NMR (125 MHz, CDCl₃) δ 166.54, 135.62, 134.54, 131.63, 130.33, 129.87, 129.49, 128.67, 127.78, 126.95, 126.12, 125.73, 53.42, 19.85.

HRMS analysis (ESI): calculated for (M+H): C₂₆H₂₅NO 368.2014; found: 368.2014.

General procedure **A** with dienone **I-125** (1.50 g, 5.7 mmol) gave **I-81** in 16% yield white solids; M.P. :165-175 °C

Rf: 0.14 (15% EtOAc in Hexane, UV)

¹H NMR (500 MHz, CDCl₃) δ 7.83 (dt, J = 7.2, 1.4 Hz, 2H), 7.54 – 7.40 (m, 3H), 7.28 (d, J = 7.8 Hz, 4H), 7.11 (d, J = 7.8 Hz, 4H), 6.61 (d, J = 15.8 Hz, 2H), 6.36 – 6.24 (m, 3H), 5.59 (q, J = 7.5, 6.8 Hz, 1H), 2.32 (s, 6H).

¹³C NMR (125 MHz, CDCl₃) δ 166.44, 137.71, 134.45, 133.66, 131.57, 129.30, 128.62, 127.13, 127.03, 126.48, 126.44, 52.81, 21.23.

HRMS analysis (ESI): calculated for (M-H): C₂₆H₂₄NO 366.1858; found: 366.1853.

General procedure A with dienone I-133 (1.00 g, 2.7 mmol) gave I-85 in 9% yield

white solids; M.P.: 156-162 °C

R_f: 0.14 (15% EtOAc in Hexane, UV)

¹H NMR (500 MHz, CDCl₃) δ 7.84 (d, J = 7.0 Hz, 2H), 7.57 – 7.50 (m, 5H), 7.49 – 7.42 (m, 6H), 6.71 – 6.67 (m, 2H), 6.43 (dd, J = 16.0, 6.1 Hz, 2H), 6.38 (d, J = 8.3 Hz, 1H), 5.68 – 5.63 (m, 1H).

¹³C NMR (125 MHz, CDCl₃) δ 166.55, 139.65, 133.97, 131.94, 130.86, 130.23, 129.95, 129.70, 128.75, 127.01, 126.73, 125.66, 125.63, 125.60, 125.57, 52.73.

HRMS analysis (ESI): calculated for (M+H): C₂₆H₂₀NOF₆ 476.1449; found: 476.1451

General procedure A with dienone I-145 (2.00g, 7.40 mmol) gave I-82 in 10% yield.

white solids; M.P.: 148-152 °C

R_f: 0.12 (15% EtOAc in Hexane, UV)

¹H NMR (500 MHz, CDCl₃) δ 7.83 – 7.81 (m, 2H), 7.56 – 7.41 (m, 3H), 7.36 (ddd, J = 8.5, 5.1, 2.2 Hz, 4H), 7.00 (td, J = 8.7, 2.2 Hz, 4H), 6.62 (d, J = 15.9 Hz, 2H), 6.28 (s, 1H), 6.24 (ddd, J = 15.9, 6.2, 2.2 Hz, 2H), 5.58 (d, J = 7.4 Hz, 1H).

¹³C NMR (125 MHz, CDCl₃) δ 166.44, 162.47 (d, J = 247.4 Hz), 134.22, 132.48 (d, J = 3.4 Hz), 131.75, 130.75, 128.67, 128.08 (d, J = 8.1 Hz), 127.66 (d, J = 2.2 Hz), 126.98, 115.55 (d, J = 21.6 Hz), 52.80.

HRMS analysis (ESI): calculated for (M+H): C₂₄H₂₀NOF₂ 376.1513; found: 376.1507

General procedure **A** with dienone **I-128** (1.10 g, 2.8 mmol) gave **I-83** in 8% yield white solids; M.P.: 120-125 °C

R_f: 0.20 (15% EtOAc in Hexane, UV)

¹H NMR (500 MHz, CDCl₃) δ 7.83 (d, J = 7.5 Hz, 2H), 7.57 – 7.48 (m, 3H), 7.44 (t, J = 7.6 Hz, 2H), 7.36 (dd, J = 7.8, 1.9 Hz, 2H), 7.28 (d, J = 7.8 Hz, 2H), 7.17 (t, J = 7.8 Hz, 2H), 6.57 (d, J = 15.9 Hz, 2H), 6.37 (d, J = 8.3 Hz, 1H), 6.31 (dd, J = 15.9, 6.1 Hz, 2H), 5.60 (q, J = 6.8 Hz, 1H).

¹³C NMR (125 MHz, CDCl₃) δ 166.51, 138.39, 134.06, 131.84, 130.82, 130.64, 130.14, 129.33, 129.25, 128.70, 127.01, 125.30, 122.80, 52.66.

HRMS analysis (ESI): calculated for (M-H): C₂₄H₁₈NOBr₂ 493.9755; found: 493.9740

General procedure **A** with dienone **I-127** (1.44 g, 2.55 mmol) gave **I-84** in 9.5% yield.

white solids; M.P.: 180-186 °C

R_f: 0.13 (15% EtOAc in Hexane, UV)

¹H NMR (500 MHz, CDCl₃) δ 7.85 – 7.77 (m, 2H), 7.56 – 7.47 (m, 1H), 7.47 – 7.36 (m, 6H), 7.27 – 7.18 (m, 4H), 6.58 (d, *J* = 16.0 Hz, 2H), 6.30 (dd, *J* = 15.8, 6.3 Hz, 3H), 5.57 (q, *J* = 6.8 Hz, 1H).

¹³C NMR (125 MHz, CDCl₃) δ 166.47, 135.20, 134.11, 131.81, 131.74, 130.86, 128.69, 128.53, 128.05, 126.99, 121.79, 52.77.

HRMS analysis (ESI): calculated for (M-H): C₂₄H₁₈NOBr₂ 493.9755; found: 493.9752

General procedure **B** with (3E,6E)-2,2,8,8-tetramethylnona-3,6-dien-5-ol (630 mg, 3.2 mmol) gave 31% yield of **I-88** in 3 steps.

Rf: 0.70 (20% EtOAc in Hexane, UV)

¹H NMR (500 MHz, CDCl₃) δ 7.83 – 7.75 (m, 2H), 7.54 – 7.40 (m, 3H), 6.17 – 6.10 (m, 1H), 5.66 (dd, J = 15.7, 2H), 5.39 (dd, J = 15.7, 5.8 Hz, 2H), 5.19 (ddt, J = 10.0, 5.8, 1.4 Hz, 1H), 1.01 (s, 18H).

¹³C NMR (125 MHz, CDCl₃) δ 166.50, 143.02, 131.35, 128.52, 126.94, 126.88, 124.13, 51.81, 32.94, 29.57.

HRMS analysis (ESI): calculated for (M+H): C₂₀H₃₀NO 300.2327; found: 300.2342

General procedure **A** with dienone **I-122** (1.89 g, 6.42 mmol) gave **I-86** in 23% yield white solids; M.P.: 110-115 °C

R_f: 0.17 (15% EtOAc in Hexane, UV)

¹H NMR (500 MHz, CDCl₃) δ 7.85 – 7.79 (m, 2H), 7.53 – 7.48 (m, 1H), 7.47 – 7.41 (m, 2H), 7.24 – 7.18 (m, 2H), 6.98 (dt, J = 7.8, 1.2 Hz, 2H), 6.92 (dd, J = 2.6, 1.6 Hz, 2H),

6.80 (ddd, J = 8.2, 2.6, 0.9 Hz, 2H), 6.63 (dd, J = 15.9, 1.4 Hz, 2H), 6.33 (dd, J = 16.0, 6.1 Hz, 3H), 5.65 – 5.56 (m, 1H), 3.79 (s, 6H).

¹³C NMR (125 MHz, CDCl₃) δ 166.44, 159.81, 137.82, 134.32, 131.79, 131.70, 129.61, 128.67, 128.30, 127.00, 119.17, 113.71, 111.73, 109.98, 55.26, 52.68.

HRMS analysis (ESI): calculated for (M+Na): C₂₆H₂₅NO₃Na 422.1732; found: 422.1734

General procedure **A** with bis(4-methoxybenzylidene)acetone (6.0 mmol) gave **I-87** in 10% yield.

white solids; M.P.: 157-161 °C

Rf: 0.25 (30% EtOAc in Hexane, UV)

¹H NMR (500 MHz, CDCl₃) ¹H NMR (500 MHz, Chloroform-*d*) δ 7.85 – 7.78 (m, 2H), 7.54 – 7.39 (m, 3H), 7.35 – 7.25 (m, 4H), 6.91 – 6.77 (m, 4H), 6.59 (dd, *J* = 15.9, 1.4 Hz, 2H), 6.29 (d, *J* = 8.3 Hz, 1H), 6.19 (dd, *J* = 15.9, 6.1 Hz, 2H), 5.61 – 5.49 (m, 1H), 3.79 (s, 6H). ¹³C NMR (125 MHz, CDCl₃) δ 166.37, 159.36, 134.46, 131.59, 131.14, 129.20, 128.62, 127.72, 126.98, 125.99, 113.98, 55.29, 52.89.

HRMS analysis (ESI): calculated for (M+H): C₂₆H₂₆NO₃ 400.1913; found: 400.1908.

General procedure **A** with dienone **I-129** (1.08 g, 3.56 mmol) gave **I-90** in 7% yield white solids; M.P.: 152-162 °C

R_f: 0.33 (15% EtOAc in Hexane, UV)

¹H NMR (500 MHz, CDCl₃) δ 7.83 (d, J = 7.0 Hz, 1H), 7.54 – 7.49 (m, 1H), 7.47 – 7.40 (m, 2H), 7.32 – 7.24 (m, 9H), 6.59 (dd, J = 15.9, 1.5 Hz, 2H), 6.38 (d, J = 8.3 Hz, 1H), 6.28 (dd, J = 15.9, 6.1 Hz, 2H), 5.58 (dddd, J = 8.0, 6.2, 4.6, 1.5 Hz, 1H).

¹³C NMR (125 MHz, CDCl₃) δ 166.48, 134.77, 134.13, 133.61, 131.80, 130.76, 128.79, 128.68, 128.44, 127.74, 127.01, 52.78.

HRMS analysis (ESI): calculated for (M+H): C₂₂H₂₀Cl₂NO 408.0922; found: 408.0918

General procedure **A** with dienone **I-126** (0.83 g, 3.07 mmol) gave **I-89** in 15% yield. white solids; M.P. 155-158 °C

Rf: 0.59 (30% EtOAc in Hexane, UV)

¹H NMR (500 MHz, CDCl₃) δ 7.87 – 7.78 (m, 2H), 7.54 – 7.48 (m, 1H), 7.45 (ddd, J = 8.9, 7.1, 1.6 Hz, 4H), 7.24 – 7.16 (m, 2H), 7.14 – 7.04 (m, 3H), 6.80 (dd, J = 16.1, 1.4 Hz, 2H), 6.45 (dd, J = 16.1, 6.0 Hz, 2H), 6.33 (d, J = 8.3 Hz, 1H), 5.68 – 5.59 (m, 1H).

¹³C NMR (125 MHz, CDCl₃) δ 166.63, δ 160.31 (d, J = 249.8 Hz), 134.30, 131.70, 130.61 (d, J = 5.3 Hz), 129.18 (d, J = 8.3 Hz), 128.65, 127.80 (d, J = 3.6 Hz), 127.08, 124.52 (d, J = 3.2 Hz), 124.25, 124.15 (d, J = 3.4 Hz), 115.80 (d, J = 22.1 Hz), 53.41.

HRMS analysis (ESI): calculated for (M+Na): C₂₄H₁₉F₂NONa 398.1332; found: 398.1336

General procedure **A** with dienone **I-132** (800 mg, 2.3 mmol) gave **I-91** in 14.4% yield.

Rf: 0.28 (15% EtOAc in Hexane, UV)

¹H NMR (500 MHz, CDCl₃) δ 7.84 – 7.78 (m, 2H), 7.54 – 7.37 (m, 3H), 7.33 (s, 8H), 6.63 (dd, J = 15.9, 1.5 Hz, 2H), 6.34 – 6.24 (m, 3H), 5.63 – 5.57 (m, 1H), 1.29 (s, 18H).

¹³C NMR (125 MHz, CDCl₃) δ 166.39, 151.01, 134.48, 133.64, 131.60, 131.51, 128.63, 127.34, 126.96, 126.23, 125.53, 52.72, 34.59, 31.26.

HRMS analysis (ESI): calculated for (M+Na): C₃₂H₃₇NONa 474.2773; found: 474.2778

General procedure **A** with **I-130** (1.59 g, 7.4 mmol) gave **I-94** in 10.3% yield yellow solid; Melting point: 135-142 °C

Rf: 0.45 (30% EtOAc in Hexane, UV)

¹H NMR (500 MHz, CDCl₃) δ 7.81 (dd, J = 7.7, 1.6 Hz, 2H), 7.55 – 7.45 (m, 1H), 7.47 – 7.27 (m, 5H), 6.55 – 6.43 (m, 4H), 6.36 (d, J = 8.3 Hz, 1H), 6.02 (dd, J = 15.8, 6.0 Hz, 2H), 5.49 (dt, J = 7.8, 5.9 Hz, 1H).

¹³C NMR (126 MHz, CDCl₃) δ 166.42, 143.65, 140.87, 134.30, 131.67, 128.62, 127.61, 127.03, 123.43, 121.61, 107.44, 107.44, 52.66.

HRMS analysis (ESI): calculated for (M-H): C₂₀H₁₆NO₃ 318.1130; found: 318.1118

General procedure **A** of 1,5-bis(2,6-dichlorophenyl)penta-1,4-dien-3-one (2.20 g, 5.9 mmol) gave **I-89** in 30% yield.

white solid; Melting point: 145-150 °C

¹H NMR (500 MHz, CDCl₃) δ 7.83 (dd, J = 7.5, 1.6 Hz, 2H), 7.56 – 7.39 (m, 3H), 7.30 (d, J = 8.1 Hz, 4H), 7.09 (t, J = 8.1 Hz, 2H), 6.76 (dd, J = 16.4, 1.5 Hz, 2H), 6.43 (dd, J = 16.3, 5.6 Hz, 2H), 6.32 (d, J = 8.5 Hz, 1H), 5.82 – 5.71 (m, 1H).

¹³C NMR (126 MHz, CDCl₃) δ 166.70, 136.02, 134.44, 133.98, 131.69, 128.70, 128.43, 128.41, 127.01, 126.00, 125.29, 52.87.

HRMS analysis (ESI): calculated for (M-H): C₂₄H₁₆NOCl₄ 473.9986; found: 473.9980

General procedure **A** with 1,5-bis(thiophene-2-yl)1,4-pentadien-3-one (2.2 g, 8.9 mmol) gave **I-100** in 10% yield.

yellow solid; Melting point: 160-163 °C

¹H NMR (500 MHz, CDCl₃) δ 7.89 – 7.73 (m, 2H), 7.58 – 7.33 (m, 3H), 7.16 (dt, J = 4.8, 0.9 Hz, 2H), 7.02 – 6.85 (m, 4H), 6.86 – 6.67 (m, 2H), 6.27 (d, J = 8.3 Hz, 1H), 6.13 (dd, J = 15.8, 6.1 Hz, 2H), 5.67 – 5.44 (m, 1H).

¹³C NMR (126 MHz, CDCl₃) δ 166.39, 141.35, 134.19, 131.74, 128.66, 127.46, 127.20, 127.01, 126.40, 125.32, 124.66, 52.47.

HRMS analysis (ESI): calculated for (M-H): C₂₀H₁₆NOS₂ 350.0673; found: 350.0670.

General procedure **B**: Cyclohexyl acetylene (1.5 g, 13.9 mmol) was used to yield the propargyl alcohol (1.7g, 99% yield).

R_f: 0.67 (15% EtOAc in Hexane, UV)

¹H NMR (500 MHz, CDCl₃) δ 5.13 (dt, *J* = 7.2, 1.9 Hz, 1H), 2.46 – 2.37 (m, 2H), 2.09 – 1.98 (m, 1H), 1.85 – 1.75 (m, 4H), 1.73 – 1.65 (m, 4H), 1.55 – 1.39 (m, 4H), 1.38 – 1.19 (m, 8H).

¹³C NMR (125 MHz, CDCl₃) δ 88.9, 78.2, 52.6, 32.3, 28.9, 25.8, 24.8

General procedure **B**: Cycloacetylene (1.5 g, 13.9 mmol) was used to yield allyl alcohol 1.16g (75% yield for two steps). Allyl alcohol (1.16 g 4.67 mmol) was subjected to Mitsunobu reaction to obtain phthalimide (950 mg, 54% yield). Phthalimide (950 mg, 2.52 mmol) was hydrolyzed and protected to furnish final product (400 mg, 45% yield).

This compound could not be purified from a side product.

R_f: 0.58 (15% EtOAc in Hexane, UV)

¹H NMR (500 MHz, CDCl₃) δ 7.76 (dd, J = 9.7, 7.8 Hz, 2H), 7.52 – 7.38 (m, 4H), 6.03 (d, J = 8.5 Hz, 1H), 5.94 (d, J = 8.6 Hz, 0.27H), 5.58 (dd, J = 15.5, 6.5 Hz, 2.27H), 5.42 (dd, J = 15.6, 5.7 Hz, 2H), 5.35 (dd, J = 15.6, 6.2 Hz, 0.27H), 5.15 (q, J = 6.5 Hz, 1H), 4.61 –

4.50 (m, 0.27H), 1.94 (dddd, *J* = 14.5, 11.0, 6.5, 3.1 Hz, 2H), 1.75 – 1.50 (m, 15H), 1.35 – 0.93 (m, 13H).

¹³C NMR (125 MHz, CDCl₃) δ 166.19, 138.03, 137.68, 134.87, 131.35, 131.27, 128.53, 127.47, 126.92, 126.85, 126.61, 52.29, 51.55, 40.40, 37.58, 33.39, 33.33, 32.91, 32.89, 32.84, 26.65, 26.36, 26.15, 26.04.

HRMS analysis (ESI): calculated for (M+H): C₂₄H₃₄NO 352.2640; found: 352.2661

General procedure **B**: 1-Hexyne (1.5 g, 18.26 mmol) was used to yield propargyl alcohol (1.6g, 91% yield).

Rf: 0.67 (20% EtOAc in Hexane, UV)

¹H NMR (500 MHz, CDCl₃) δ 5.10 (dq, J = 7.1, 2.1 Hz, 1H), 2.24 (td, J = 7.1, 2.0 Hz, 4H), 2.12 – 2.05 (m, 1H), 1.55 – 1.46 (m, 4H), 1.46 – 1.34 (m, 4H), 0.92 (t, J = 7.2 Hz, 6H).

 ^{13}C NMR (125 MHz, CDCl₃) δ 85.12, 78.01, 52.57, 30.41, 21.93, 18.41, 13.59.

General procedure **B**: 1-Hexyne (1.5 g, 18.26mmol) was used to yield allyl alcohol (1.0 g, 61% yield for two steps). Allyl alcohol (940 mg, 4.79 mmol) was subjected to Mitsunobu reaction to obtain phthalimide (620 mg, 40% yield). Phthalimide (310 mg, 0.953 mmol) was hydrolyzed and protected to furnish final product (180 mg, 63% yield).

This compound could not be purified from a side product.

Rf: 0.58 (15% EtOAc in Hexane, UV)

¹H NMR (500 MHz, CDCl₃) δ 7.83 – 7.74 (m, 5H), 7.53 – 7.41 (m, 7H), 6.08 (d, J = 8.2 Hz, 1H), 5.98 (d, J = 8.5 Hz, 0.87H), 5.68 (ddtd, J = 15.4, 8.5, 6.7, 1.3 Hz, 3.87H), 5.51 (ddt, J = 15.4, 5.8, 1.4 Hz, 2H), 5.43 (ddt, J = 15.4, 6.4, 1.5 Hz, 0.87H), 5.22 – 5.13 (m, 1H), 4.65 – 4.56 (m, 0.87H), 2.06 (qd, J = 6.9, 4.7 Hz, 7H), 1.66 – 1.53 (m, 3H), 1.44 – 1.20 (m, 21H), 0.90 (td, J = 6.7, 6.1, 2.1 Hz, 14H).

¹³C NMR (125 MHz, CDCl₃) δ 166.54, 166.23, 134.98, 134.78, 132.46, 131.99, 131.34, 131.25, 129.97, 128.93, 128.50, 128.49, 126.91, 126.85, 52.45, 51.40, 35.50, 32.00, 31.99, 31.76, 31.34, 31.28, 29.13, 25.85, 22.59, 22.23, 22.20, 14.07, 13.93.

HRMS analysis (ESI): calculated for (M+H): C₂₀H₃₀NO 300.2327; found: 300.2346

General procedure **A** with dienone **I-121** (1.00 g, 4.3 mmol) gave **I-97** in 10% yield. white solids; M.P.: 188-193 °C

Rf: 0.39 (30% EtOAc in Hexane, UV)

¹H NMR (500 MHz, CDCl₃) δ 7.80 (d, J = 8.8 Hz, 2H), 7.41 – 7.35 (m, 5H), 7.34 – 7.26 (m, 5H), 7.27 – 7.21 (m, 2H), 6.92 (d, J = 8.8 Hz, 2H), 6.64 (dd, J = 16.0, 1.4 Hz, 2H), 6.38 – 6.26 (m, 3H), 5.65 – 5.56 (m, 1H), 3.83 (s, 3H).

¹³C NMR (125 MHz, CDCl₃) δ 165.96, 162.29, 136.44, 131.67, 128.84, 128.59, 128.24, 127.84, 126.58, 126.53, 113.80, 55.43, 52.68.

HRMS analysis (ESI): calculated for (M+H): C₂₅H₂₄NO₂ 370.1807; found: 370.1812

General procedure A with dienone I-121 (1.40 g, 6 mmol) gave I-98 in 15% yield.

white solids; M.P.: 215-220 °C

Rf: 0.65 (30% EtOAc in Hexane, UV)

¹H NMR (500 MHz, CDCl₃) δ 7.69 (d, J = 8.6 Hz, 2H), 7.58 (d, J = 8.6 Hz, 2H), 7.42 – 7.35 (m, 4H), 7.35 – 7.27 (m, 4H), 7.25 (d, J = 7.6 Hz, 2H), 6.65 (dd, J = 16.0, 1.4 Hz, 2H), 6.32 (dd, J = 15.9, 6.1 Hz, 2H), 6.27 (d, J = 8.2 Hz, 1H), 5.63 – 5.54 (m, 1H). ¹³C NMR (125 MHz, CDCl₃) δ 165.47, 136.27, 133.15, 132.08, 131.88, 128.64, 128.63, 127.99, 127.72, 126.54, 126.38, 52.98.

HRMS analysis (ESI): calculated for (M+H): C₂₄H₂₁BrNO 418.0807; found: 418.0791

General procedure A with dienone I-121 (1.93 g, 8 mmol) gave I-99 in 5% yield.

white solids; M.P.: 172-176 °C

R_f: 0.43 (30% EtOAc in Hexane, UV)

¹H NMR (500 MHz, CDCl₃) δ 7.40 – 7.35 (m, 4H), 7.31 (dd, J = 8.5, 6.8 Hz, 4H), 7.27 – 7.21 (m, 2H), 6.57 (dd, J = 16.0, 1.4 Hz, 2H), 6.25 (dd, J = 16.0, 6.0 Hz, 2H), 5.69 (d, J = 8.5 Hz, 1H), 5.51 – 5.35 (m, 1H), 2.43 (hept, J = 6.9 Hz, 1H), 1.21 (d, J = 6.9 Hz, 6H) ¹³C NMR (125 MHz, CDCl₃) δ 175.92, 136.48, 131.43, 131.43, 128.60, 128.30, 127.83, 126.50, 77.29, 77.04, 76.78, 51.95, 35.85, 19.71

HRMS analysis (ESI): calculated for (M-H): C₂₁H₂₂NO 304.1701; found: 304.1695

1.7.5 General procedure for desymmetrisation

General procedure C: Diene substrate (I-76, I-79, I-81-I-99) (0.1 mmol, 1 equiv) was dissolved in TFE/DCM (1 mL, 7:3, v/v), followed by adding (DHQD)₂PHAL (0.01 mmol, 0.1 equiv) as catalyst. After the reaction mixture was stirred at -30 °C for 5 min, NCP (0.11 mmol, 1.1 equiv) was added. Reaction was stirred at -30 °C until completion, evident by TLC. Most of the solvent was removed under reduced pressure, and 10% aq. Na₂SO₃ (1 mL) and DCM were added to dissolve the residue. Aqueous layers were extracted with DCM (3X). The combined organics were dried over Na₂SO₄. After filtration, the solvent was removed under reduced pressure to deliver the crude product. The crude product was purified via the column chromatography with silica gel using EtOAc in hexane as eluent.

General procedure D: Diene substrate (I-76, I-79, I-81-I-99) (0.1 mmol, 1 equiv) was dissolved in TFE/HFIP (1 mL, 7:3, v/v), followed by adding (DHQD)₂PHAL (0.01 mmol, 0.1 equiv) as catalyst. After the reaction mixture was stirred at -30 °C for 5 min, NCP (0.11 mmol, 1.1 equiv) was added in one portion. The reaction was stirred at -30 °C until completion as evident from TLC. Most of the solvent was removed under reduced

pressure, and 10% aq. Na₂SO₃ (1 mL) and DCM were added to dissolve the residue. Aqueous layers were extracted with DCM (3X). The combined organics were dried over Na₂SO₄. After filtration, the solvent was removed under reduced pressure to deliver the crude product. The crude product was purified via column chromatography with silica gel using EtOAc in hexane as eluent.

1.7.6 Analytical data for desymmetrisation products

Procedure **C** with **I-76** (136 mg, 0.4 mmol) gave **I-77** (121.00 mg, 81%).

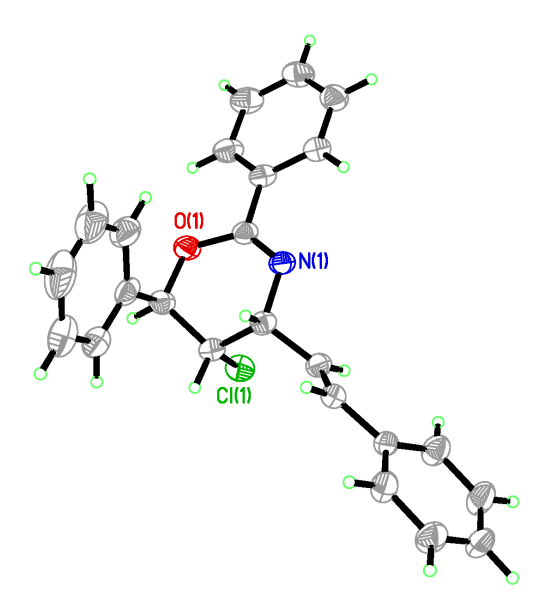
Rf: 0.54 (15% EtOAc in Hexane, UV)

¹H NMR (500 MHz, CDCl₃) δ 8.14 – 8.07 (m, 2H), 7.51 – 7.19 (m, 13H), 6.69 (d, J = 15.7 Hz, 1H), 6.43 (dd, J = 15.8, 5.6 Hz, 1H), 5.47 (d, J = 6.1 Hz, 1H), 4.51 (t, J = 4.9 Hz, 1H), 4.43 – 4.36 (m, 1H).

¹³C NMR (125 MHz, CDCl₃) δ 154.42, 137.74, 136.75, 133.38, 132.58, 131.12, 128.95, 128.88, 128.53, 128.24, 127.69, 127.60, 127.11, 126.67, 126.23, 79.16, 58.29, 54.84. HRMS analysis (ESI): calculated for (M+H): C₂₄H₂₁CINO 374.1312; found: 374.1346. Resolution of enantiomers: Daicel Chiralpak IA, 5% IPA-Hex, 1 mL/min; 254 nm, RT1 = 8.76 min, RT2 = 9.84 min.

$$[\alpha]_{D^{20}} = +29.5^{\circ} \text{ (C 1.0, CH}_{2}\text{Cl}_{2}, \textit{ee} = 98\%)$$

X-ray crystallography:



Procedure **D** with **I-79** (18.4 mg, 0.05 mmol) gave **I-80** (15.10 mg, 75%).

R_f: 0.53 (15% EtOAc in Hexane, UV)

¹H NMR (500 MHz, CDCl₃) δ 8.13 – 8.03 (m, 2H), 7.52 – 7.37 (m, 4H), 7.34 – 7.20 (m, 4H), 7.19 – 7.10 (m, 3H), 6.95 (dd, J = 15.5, 1.5 Hz, 1H), 6.26 (dd, J = 15.6, 5.6 Hz, 1H), 5.75 (d, J = 5.4 Hz, 1H), 4.56 (s, 1H), 4.39 (dd, J = 5.4, 3.9 Hz, 1H), 2.42 (s, 3H), 2.34 (s, 3H).

¹³C NMR (125 MHz, CDCl₃) δ 154.70, 136.20, 135.98, 135.63, 135.19, 132.67, 131.50, 131.07, 130.94, 130.18, 128.81, 128.77, 128.23, 127.56, 127.55, 126.70, 126.09, 126.05, 125.78, 76.86, 57.23, 54.65, 19.92, 19.22.

HRMS analysis (ESI): calculated for (M+H): C₂₆H₂₅CINO 402.1625; found: 402.1648.

Resolution of enantiomers: Daicel Chiralpak IA, 5% IPA-Hex, 1 mL/min; 254 nm, RT1 = 5.4 min, RT2 = 7.9 min.

 $[\alpha]_D^{20} = +33.9^{\circ} (C 1.0, CH_2Cl_2, ee = 95\%)$

Procedure **D** with **I-81** (0.05 mmol, 18.4 mg) gave **I-103** (14.07 mg, 70%).

Rf: 0.79 (30% EtOAc in Hexane, UV)

For major diastereomer: ¹H NMR (500 MHz, CDCl₃) δ 8.14 – 8.02 (m, 2H), 7.53 – 7.37 (m, 2H), 7.31 (d, J = 8.1 Hz, 2H), 7.28 – 7.17 (m, 6H), 7.11 (d, J = 7.8 Hz, 2H), 6.63 (dd, J = 15.8, 1.4 Hz, 1H), 6.38 (dd, J = 15.8, 5.6 Hz, 1H), 5.40 (d, J = 6.3 Hz, 1H), 4.50 (ddd, J = 5.7, 4.1, 1.5 Hz, 1H), 4.37 (dd, J = 6.3, 4.1 Hz, 1H), 2.36 (s, 3H), 2.32 (s, 3H). ¹³C NMR (125 MHz, CDCl₃) δ 154.52, 138.85, 137.50, 134.76, 133.97, 133.23, 132.63, 131.05, 129.51, 129.20, 128.19, 127.59, 126.56, 126.23, 126.04, 78.99, 58.43, 55.06, 21.23, 21.21.

HRMS analysis (ESI): calculated for (M+H): C₂₆H₂₅CINO 402.1625; found: 402.1648.

Resolution of enantiomers: Daicel Chiralpak OD-H, 5% IPA-Hex, 0.5 mL/min; 280 nm, RT1 = 10.0 min, RT2 = 11.4 min.

 $[\alpha]_D^{20} = +8.6^{\circ} (C \ 0.4, \ CH_2Cl_2, \ ee = 47\%)$

Procedure **D** with **I-85** (19.02 mg, 0.04 mmol) gave **I-104** (17.54 mg, 86%).

Rf: 0.43 (15% EtOAc in Hexane, UV)

¹H NMR (500 MHz, CDCl₃) δ 8.09 (dd, J = 8.2, 3.5 Hz, 2H), 7.69 (dd, J = 8.4, 3.4 Hz, 2H), 7.50 (dddd, J = 29.0, 24.7, 8.4, 4.5 Hz, 9H), 6.73 (dd, J = 15.9, 3.5 Hz, 1H), 6.54 (dt, J = 15.9, 4.6 Hz, 1H), 5.47 (dd, J = 6.7, 3.6 Hz, 1H), 4.54 (t, J = 4.6 Hz, 1H), 4.39 (dt, J = 7.8, 3.8 Hz, 1H).

¹³C NMR (125 MHz, CDCl₃) δ 154.38, 141.24, 139.99, 132.55, 132.06, 131.45, 131.17, 129.73, 129.47, 129.26, 128.36, 127.57, 126.87, 126.83, 125.92(q), 125.52(q), 125.21, 78.30, 57.52, 54.99.

HRMS analysis (ESI): calculated for (M+H): C₂₆H₁₉ClF₆NO 510.1059; found: 510.1074

Resolution of enantiomers: Daicel Chiralpak IA, 5% IPA- Hex, 1 mL/min; 254 nm, RT1 = 6.5 min, RT2 = 9.4 min.

 $[\alpha]_{D^{20}} = +13.8^{\circ} \; (C \; 1.0, \; CH_{2}CI_{2}, \; ee = 90\%)$

Procedure **D** with **I-82** (19 mg, 0.0506 mmol) gave **I-105** (18.04 mg, 87%).

Rf: 0.48 (15% EtOAc in Hexane, UV)

¹H NMR (500 MHz, CDCl₃) δ 8.09 – 8.04 (m, 2H), 7.52 – 7.46 (m, 1H), 7.46 – 7.28 (m, 6H), 7.10 (t, J = 8.4 Hz, 2H), 7.00 (t, J = 8.5 Hz, 2H), 6.63 (d, J = 15.7 Hz, 1H), 6.37 (dd, J = 15.8, 5.5 Hz, 1H), 5.38 (d, J = 6.8 Hz, 1H), 4.55 – 4.49 (m, 1H), 4.34 (dd, J = 6.8, 4.4 Hz, 1H).

¹³C NMR (125 MHz, CDCl₃) δ 163.94, 163.40, 161.97, 161.44, 154.49, 133.36, 133.33, 132.83, 132.80, 132.57, 132.34, 131.26, 128.33, 128.29, 128.26, 128.25, 128.18, 127.57, 126.46, 126.44, 115.97, 115.80, 115.56, 115.38, 78.23, 58.16, 55.28.

HRMS analysis (ESI): calculated for (M+H): C₂₄H₁₉CINOF₂ 410.1123; found: 410.1129
Resolution of enantiomers: Daicel Chiralpak IA, 5% IPA- Hex, 1 mL/min; 254 nm, RT1 = 9.2 min, RT2 = 13.4 min.

 $[\alpha]_D^{20} = +25.5^{\circ} (C \ 1.0, CDCl_3, ee = 95\%)$

Procedure C with I-83 (12 mg, 0.024 mmol) gave I-106 (12.25 mg, 96%).

Rf: 0.53 (15% EtOAc in Hexane, UV)

¹H NMR (500 MHz, CDCl₃) δ 8.10 – 8.04 (m, 2H), 7.57 (d, J = 1.8 Hz, 1H), 7.55 – 7.47 (m, 3H), 7.43 (dd, J = 8.2, 6.9 Hz, 2H), 7.37 – 7.26 (m, 4H), 7.17 (t, J = 7.8 Hz, 1H), 6.62 (dd, J = 15.8, 1.5 Hz, 1H), 6.46 – 6.40 (m, 1H), 5.39 – 5.24 (m, 1H), 4.55 – 4.51 (m, 1H), 4.35 (dd, J = 6.6, 4.3 Hz, 1H).

¹³C NMR (125 MHz, CDCl₃) δ 154.36, 139.67, 138.75, 132.37, 132.20, 132.16, 131.33, 130.62, 130.43, 130.07, 129.47, 128.32, 128.25, 127.59, 125.38, 125.11, 122.97, 122.75, 78.19, 57.67, 54.94.

HRMS analysis (ESI): calculated for (M+H): C₂₄H₁₉CINOBr₂ 529.9522; found: 529.9539 Resolution of enantiomers: Daicel Chiralpak AD-H, 5% IPA- Hex, 1 mL/min; 254 nm, RT1 = 9.3 min, RT2 = 10.6 min.

 $[\alpha]_D^{20} = +8.1^{\circ} (C 1.0, CH_2CI_2, ee = 97\%)$

Procedure **C** with **I-84** (12 mg, 0.024 mmol) gave **I-107** (11.87 mg, 93%).

Rf: 0.49 (15% EtOAc in Hexane, UV)

¹H NMR (500 MHz, CDCl₃) δ 8.06 (dt, J = 8.5, 1.3 Hz, 2H), 7.56 – 7.51 (m, 2H), 7.52 – 7.46 (m, 1H), 7.46 – 7.37 (m, 4H), 7.25 (ddd, J = 21.2, 8.3, 1.1 Hz, 4H), 6.61 (d, J = 15.8 Hz, 1H), 6.45 – 6.31 (m, 1H), 5.36 (d, J = 6.6 Hz, 1H), 4.50 (dt, J = 5.5, 2.8 Hz, 1H), 4.33 (ddd, J = 6.6, 4.3, 1.1 Hz, 1H).

¹³C NMR (125 MHz, CDCl₃) δ 154.41, 136.50, 135.55, 132.60, 132.22, 132.05, 131.66, 131.32, 128.31, 128.21, 128.10, 127.56, 127.49, 123.14, 121.60, 78.32, 57.78, 55.12. HRMS analysis (ESI): calculated for (M+H): C₂₄H₁₉CINOBr₂ 529.9522; found: 529.9521 Resolution of enantiomers: Daicel Chiralpak IA, 5% IPA- Hex, 1 mL/min; 254 nm, RT1 = 10.4 min, RT2 = 13.8 min

 $[\alpha]_D^{20} = +20.0^{\circ} (C \ 1.0, CH_2Cl_2, ee = 90\%)$

Procedure C with I-86 (19 mg, 0.048 mmol) gave I-108 (19.16 mg, 92%).

Rf: 0.46 (20% EtOAc in Hexane, UV)

¹H NMR (500 MHz, CDCl₃) δ 8.10 (dt, J = 7.1, 1.4 Hz, 2H), 7.51 – 7.45 (m, 1H), 7.42 (dd, J = 8.3, 6.8 Hz, 2H), 7.32 (t, J = 7.9 Hz, 1H), 7.27 – 7.18 (m, 1H), 7.02 (dt, J = 7.7, 1.2 Hz, 1H), 6.99 – 6.85 (m, 4H), 6.79 (ddd, J = 8.3, 2.6, 0.9 Hz, 1H), 6.66 (dd, J = 15.8, 1.5 Hz, 1H), 6.42 (dd, J = 15.8, 5.5 Hz, 1H), 5.44 (d, J = 5.8 Hz, 1H), 4.50 (ddd, J = 5.6, 4.0, 1.5 Hz, 1H), 4.40 (dd, J = 5.8, 4.1 Hz, 1H), 3.79 (d, J = 5.6 Hz, 6H).

¹³C NMR (125 MHz, CDCl₃) δ 159.92, 159.75, 154.36, 139.31, 138.21, 133.23, 132.55, 131.12, 130.01, 129.50, 128.24, 127.59, 127.51, 119.31, 118.34, 114.12, 113.45, 112.02, 111.86, 79.12, 58.17, 55.32, 55.25, 54.72.

HRMS analysis (ESI): calculated for (M+H): $C_{26}H_{25}CINO_3$ 434.1523; found: 434.1518 Resolution of enantiomers: Daicel Chiralpak AD-H, 3% IPA- Hex, 1 mL/min; 250 nm, major diastereomer: RT1 = 24.8 min, RT2 = 27.3 min

 $[\alpha]_D^{20} = -18.1^{\circ} (C 1.0, CH_2Cl_2, ee = 97\%)$

Procedure **C** with **I-90** (20 mg, 0.05 mmol) gave **I-109** (21.92 mg, 99%).

R_f: 0.67 (15% EtOAc in Hexane, UV)

¹H NMR (500 MHz, CDCl₃) δ 8.09 – 8.03 (m, 2H), 7.53 – 7.45 (m, 1H), 7.45 – 7.25 (m, 10H), 6.62 (dd, J = 15.8, 1.5 Hz, 1H), 6.42 (dd, J = 15.8, 5.5 Hz, 1H), 5.38 (d, J = 6.7 Hz, 1H), 4.51 (td, J = 4.3, 2.2 Hz, 1H), 4.33 (dd, J = 6.7, 4.3 Hz, 1H).

¹³C NMR (125 MHz, CDCl₃) δ 154.43, 135.97, 135.10, 134.97, 133.42, 132.53, 132.24, 131.31, 129.10, 128.71, 128.30, 127.88, 127.81, 127.56, 127.36, 78.26, 57.89, 55.13.

HRMS analysis (ESI): calculated for (M+H): C₂₄H₁₉Cl₃NO 442.0532; found: 442.0552

Resolution of enantiomers: Daicel Chiralpak IA, 5% IPA-Hex, 1 mL/min; 254 nm, RT1 = 9.5 min, RT2 = 12.4 min

 $[\alpha]_D^{20} = +23.2^{\circ} (C 1.0, CH_2Cl_2, ee = 94.7\%)$

Procedure C with I-89 (36 mg, 0.1 mmol) gave I-110 (40.57 mg, 99%).

R_f: 0.57 (15% EtOAc in Hexane, UV)

¹H NMR (500 MHz, CDCl₃) δ 8.14 – 8.08 (m, 2H), 7.50 (tq, J = 6.6, 1.7 Hz, 2H), 7.47 – 7.35 (m, 3H), 7.31 (td, J = 7.6, 1.7 Hz, 1H), 7.23 – 7.05 (m, 4H), 7.02 (ddd, J = 10.7, 8.2, 1.2 Hz, 1H), 6.89 (d, J = 15.9 Hz, 1H), 6.48 (dd, J = 15.9, 5.4 Hz, 1H), 5.80 (d, J = 5.0 Hz, 1H), 4.55 (t, J = 4.4 Hz, 1H), 4.50 – 4.43 (m, 1H).

¹³C NMR (125 MHz, CDCl₃) δ 161.29, 160.58, 159.30, 158.61, 154.17, 132.42, 131.21, 130.80, 130.73, 129.82, 129.77, 129.00, 128.93, 128.27, 127.86, 127.83, 127.62, 127.58,

125.89, 125.87, 125.11, 125.01, 124.78, 124.75, 124.60, 124.50, 124.09, 124.06, 116.07, 115.91, 115.82, 115.64, 74.84, 74.82, 56.39, 56.37, 54.67.

HRMS analysis (ESI): calculated for (M+H): C₂₄H₁₉CINOF₂ 410.1123; found: 410.1150

Resolution of enantiomers: Daicel Chiralpak IA, 5% IPA-Hex, 1mL/min; 254 nm, RT1 = 6.4 min, RT2 = 8.9 min

 $[\alpha]_D^{20} = +39.7^{\circ} (C 1.0, CH_2Cl_2, ee = 96\%)$

Procedure C with I-91 (22.6 mg, 0.05 mmol) gave I-111 (9.96 mg, 41%).

R_f: 0.89 (30% EtOAc in Hexane, UV)

Major diasteromer: ¹H NMR (500 MHz, CDCl₃) δ 8.13 – 8.04 (m, 2H), 7.51 – 7.30 (m, 9H), 7.26 (d, J = 8.3 Hz, 2H), 6.66 (d, J = 15.9 Hz, 1H), 6.39 (dd, J = 15.8, 5.5 Hz, 1H), 5.43 (d, J = 6.0 Hz, 1H), 4.53 – 4.49 (m, 1H), 4.38 (dd, J = 6.0, 4.1 Hz, 1H), 1.30 (d, J = 8.2 Hz, 18H).

¹³C NMR (125 MHz, CDCl₃) δ 166.63, 161.31, 159.32, 134.30, 131.70, 130.63, 130.58, 129.21, 129.14, 128.65, 127.81, 127.78, 127.08, 124.53, 124.51, 124.25, 124.16, 124.13, 115.89, 115.71, 53.41.

HRMS analysis (ESI): calculated for (M+H): C₃₂H₃₇CINO 486.2564; found: 486.2571

Resolution of enantiomers: Daicel Chiralpak IA, 1% IPA-Hex, 1 mL/min; 254 nm, RT1 = 8.2 min, RT2 = 9.1 min

Procedure **C** with **I-96** (28 mg, 0.08 mmol) gave **I-112** (27.17 mg, 88%).

Rf: 0.89 (30% EtOAc in Hexane, UV)

¹H NMR (500 MHz, CDCl₃) δ 8.03 – 7.85 (m, 2H), 7.51 – 7.30 (m, 3H), 5.61 (qd, J = 15.5, 5.7 Hz, 2H), 4.35 (t, J = 5.0 Hz, 1H), 4.22 (dd, J = 7.9, 4.6 Hz, 1H), 4.08 (dd, J = 7.9, 4.4 Hz, 1H), 2.02 (dq, J = 5.0, 2.7, 2.0 Hz, 1H), 1.89 – 1.49 (m, 11H), 1.44 (qd, J = 12.5, 3.5 Hz, 1H), 1.36 – 1.04 (m, 9H).

¹³C NMR (125 MHz, CDCl₃) δ 154.41, 141.03, 133.07, 130.74, 128.09, 127.39, 124.52, 79.69, 77.22, 56.53, 54.90, 40.63, 38.95, 32.87, 32.80, 29.35, 26.29, 26.25, 26.22, 26.18, 26.04, 25.78.

HRMS analysis (ESI): calculated for (M+H): C₂₄H₃₃CINO 386.2251; found: 386.2263

Resolution of enantiomers: Daicel Chiralpak IA, 1% IPA-Hex, 1 mL/min; 254 nm, RT1 = 5.6 min, RT2 = 11.7 min

 $[\alpha]_{D^{20}} = +91^{\circ} (C 1.0, CH_{2}CI_{2}, ee = 100\%)$

Procedure C with I-95 (30 mg, 0.1 mmol) gave I-113 (22.37 mg, 67%).

R_f: 0.64 (15% EtOAc in Hexane, UV)

¹H NMR (500 MHz, CDCl₃) δ 7.99 – 7.90 (m, 2H), 7.51 – 7.30 (m, 3H), 5.80 – 5.55 (m, 2H), 4.38 – 4.35 (m, 1H), 4.28 (td, J = 8.3, 3.2 Hz, 1H), 4.04 (dd, J = 7.9, 4.6 Hz, 1H), 2.13 – 2.05 (m, 2H), 1.96 – 1.86 (m, 1H), 1.76 – 1.56 (m, 2H), 1.51 – 1.22 (m, 7H), 0.94 (t, J = 7.2 Hz, 3H), 0.87 (t, J = 7.2 Hz, 3H).

¹³C NMR (125 MHz, CDCl₃) δ 154.29, 135.40, 133.02, 130.74, 128.06, 127.38, 126.75, 76.06, 57.29, 56.54, 32.61, 32.17, 31.24, 26.85, 22.49, 22.24, 13.99, 13.93.

HRMS analysis (ESI): calculated for (M+H): $C_{20}H_{29}CINO$ 334.1938; found: 334.1942

Resolution of enantiomers: Daicel Chiralpak IA, 1% IPA-Hex, 1 mL/min; 254 nm, RT1 = 4.6 min, RT2 = 5.8 min

 $[\alpha]_D^{20} = +83.1^{\circ} (C 1.0, CH_2Cl_2, ee = 98\%)$

Procedure **C** with **I-97** (37 mg, 0.1 mmol) gave **I-114** (31.10 mg, 77%).

Rf: 0.77 (30% EtOAc in Hexane, UV)

White solids, M.P.=148-152 °C

¹H NMR (500 MHz, CDCl₃) δ 8.08 – 8.02 (m, 2H), 7.45 – 7.28 (m, 10H), 7.26 – 7.20 (m, 1H), 6.95 – 6.89 (m, 2H), 6.68 (dd, J = 15.8, 1.5 Hz, 1H), 6.43 (dd, J = 15.8, 5.6 Hz, 1H),

5.44 (d, J = 6.1 Hz, 1H), 4.48 (ddd, J = 5.6, 4.1, 1.6 Hz, 1H), 4.39 (dd, J = 6.2, 4.1 Hz, 1H), 3.85 (s, 3H).

¹³C NMR (125 MHz, CDCl₃) δ 162.01, 154.23, 137.84, 136.80, 133.31, 129.28, 128.90, 128.84, 128.52, 127.64, 127.29, 126.67, 126.28, 125.04, 113.51, 79.02, 58.41, 55.41, 54.86.

HRMS analysis (ESI): calculated for (M+H): C₂₅H₂₃CINO₂ 404.1417; found: 404.1457 Resolution of enantiomers: Daicel Chiralpak IA, 15% IPA-Hex, 1 mL/min; 250 nm, RT1 = 16.3 min, RT2 = 19.7 min

 $[\alpha]_D^{20} = +2.8^{\circ} (C \ 1.0, CH_2Cl_2, ee = 95\%)$

Procedure **C** with **I-98** (21 mg, 0.05 mmol) gave **I-115** (14.94 mg, 66%).

R_f: 0.74 (30% EtOAc in Hexane, UV)

White solids, M.P.= 128 -134 °C

¹H NMR (500 MHz, CDCl₃) δ 7.96 (d, J = 8.6 Hz, 2H), 7.55 (d, J = 8.6 Hz, 2H), 7.45 – 7.37 (m, 5H), 7.34 – 7.26 (m, 4H), 7.27 – 7.19 (m, 1H), 6.66 (dd, J = 15.8, 1.4 Hz, 1H), 6.40 (dd, J = 15.8, 5.6 Hz, 1H), 5.46 (d, J = 5.8 Hz, 1H), 4.47 (ddd, J = 5.6, 4.0, 1.5 Hz, 1H), 4.39 (dd, J = 5.9, 4.0 Hz, 1H).

¹³C NMR (125 MHz, CDCl₃) δ 153.64, 137.56, 136.64, 133.43, 131.48, 131.45, 129.21, 129.04, 128.94, 128.55, 127.76, 126.91, 126.66, 126.12, 125.86, 79.35, 58.10, 54.75. HRMS analysis (ESI): calculated for (M+H): C₂₄H₂₀ClBrNO 452.0417; found: 452.0415 Resolution of enantiomers: Daicel Chiralpak IA, 5% IPA-Hex, 1 mL/min; 250 nm, RT1 = 12.7 min, RT2 = 17.1 min

 $[\alpha]_D^{20} = +4.8^{\circ} (C \ 1.0, CH_2Cl_2, ee = 100\%)$

Procedure **C** with **I-99** (30.5 mg, 0.1 mmol) gave **I-116** (18.01 mg, 53%).

colorless oil

R_f: major diastereomer: 0.74; minor diastereomer: 0.82 (30% EtOAc in Hexane, UV) For the major diastereomer: 1 H NMR (500 MHz, CDCl₃) δ 7.39 (dtd, J = 8.6, 6.5, 4.9 Hz, 5H), 7.33 – 7.26 (m, 4H), 7.23 – 7.20 (m, 1H), 6.60 – 6.53 (m, 1H), 6.39 – 6.30 (m, 1H), 5.23 (d, J = 5.8 Hz, 1H), 4.26 (dq, J = 5.9, 4.0 Hz, 2H), 2.67 (p, J = 6.9 Hz, 1H), 1.29 (dd, J = 6.9, 2.9 Hz, 6H).

¹³C NMR (126 MHz, CDCl₃) δ 163.57, 138.00, 136.77, 133.14, 128.85, 128.78, 128.51, 127.64, 127.30, 126.63, 126.17, 78.68, 58.48, 53.99, 34.48, 20.11, 20.01.

HRMS analysis (ESI): calculated for (M-H): C₂₁H₂₁CINO 338.1312; found: 338.129

Resolution of enantiomers: Daicel Chiralpak IA, 15% IPA-Hex, 1 mL/min; 250 nm, RT1 = 5.27 min, RT2 = 7.50 min

Procedure **C** with **I-100** (0.06 mmol, 21 mg) gave **I-117** as diastereomers mixture (6.02 mg, 26%).

pale yellow oil

Rf: 0.77 (30% EtOAc in Hexane, UV)

For the major diastereomer: ¹H NMR (500 MHz, CDCl₃) δ 8.08 – 8.02 (m, 2H), 7.51 – 7.38 (m, 3H), 7.36 (dd, J = 5.0, 1.2 Hz, 1H), 7.16 (dt, J = 5.2, 0.9 Hz, 1H), 7.12 (dt, J = 3.6, 1.1 Hz, 1H), 7.03 (dd, J = 5.0, 3.6 Hz, 1H), 7.00 – 6.92 (m, 2H), 6.86 – 6.78 (m, 1H), 6.29 (dd, J = 15.6, 5.3 Hz, 1H), 5.65 (dd, J = 6.6, 0.9 Hz, 1H), 4.61 (ddd, J = 5.6, 4.3, 1.7 Hz, 1H), 4.40 (dd, J = 6.6, 4.3 Hz, 1H).

¹³C NMR (126 MHz, CDCl₃) δ 154.09, 141.80, 140.47, 132.39, 131.18, 128.23, 127.60, 127.39, 127.14, 126.76, 126.24, 126.21, 126.14, 126.13, 124.47, 75.36, 58.11, 55.18. HRMS analysis (ESI): calculated for (M+H): C₂₀H₁₇NOS₂Cl 386.0440; found: 386.0435. Resolution of enantiomers: Daicel Chiralpak AD-H, 5% IPA-Hex, 1 mL/min; 254 nm, RT1 = 12.6 min, RT2 = 14.2 min

Procedure **C** with **I-87** (17 mg, 0.042 mmol) gave **I-146** (9.66 mg, 53%).

colorless oil, R_f: 0.67 (30% EtOAc in Hexane, UV)

¹H NMR (500 MHz, CDCl₃) δ 8.12 – 8.04 (m, 2H), 7.55 – 7.39 (m, 3H), 7.39 – 7.33 (m, 2H), 7.32 – 7.27 (m, 2H), 6.96 – 6.90 (m, 2H), 6.89 – 6.82 (m, 2H), 6.66 – 6.57 (m, 1H), 6.33 (dd, J = 15.8, 5.7 Hz, 1H), 5.39 (d, J = 6.7 Hz, 1H), 4.54 (ddd, J = 5.7, 4.2, 1.5 Hz, 1H), 4.37 (dd, J = 6.7, 4.2 Hz, 1H), 3.83 (s, 3H), 3.81 (s, 3H).

¹³C NMR (126 MHz, CDCl₃) δ 159.97, 159.26, 154.57, 132.88, 132.64, 131.03, 129.72, 129.55, 128.19, 127.85, 127.71, 127.58, 124.76, 114.16, 113.91, 78.60, 58.59, 55.39, 55.33, 55.30.

HRMS analysis (ESI): calculated for (M+H): C₂₆H₂₅NO₃Cl 434.1523; found: 434.1509.

Resolution of enantiomers: Daicel Chiralpak IA, 5% IPA-Hex, 1 mL/min; 254 nm, RT1 = 16.2 min, RT2 = 22.2 min

1.7.7 Derivatization of oxazine product

The oxazine substrate I-77 (0.048 mmol, 16 mg) was dissolved in a mixture of acetone (1.8 mL), *t*-BuOH (0.1 mL) and H₂O (0.1 mL). To the colorless solution was added OsO₄ (0.0165 mmol, 4.2 mg), followed by NMO (0.053 mmol, 6.2 mg) at room temperature. The reaction turned to brown. After the completion, solvent was removed and passed the residue thru a flash column to afford 16.8 mg white solid as product.

Rf: 0.51 (30% EtOAc in Hexane, UV)

Brown solids, M.P.=142-150 °C

¹H NMR (500 MHz, CDCl3) δ 8.16 – 8.11 (m, 2H), 7.58 – 7.51 (m, 1H), 7.48 (dd, J = 8.3, 6.8 Hz, 2H), 7.43 (d, J = 7.6 Hz, 2H), 7.39 – 7.31 (m, 5H), 7.30 – 7.25 (m, 1H), 7.24 – 7.20 (m, 2H), 5.78 (s, 1H), 5.44 (s, 1H), 4.74 – 4.66 (m, 1H), 4.03 (ddd, J = 9.0, 6.7, 2.0 Hz, 1H), 3.73 (s, 1H), 3.64 (dd, J = 9.2, 3.0 Hz, 1H), 2.03 – 1.92 (br, 1H).

¹³C NMR (125 MHz, CDCl₃) δ 154.08, 141.57, 138.27, 132.31, 131.32, 129.12, 128.71, 128.37, 128.32, 127.50, 126.27, 124.77, 81.39, 74.60, 72.72, 56.18, 51.81.

HRMS analysis (ESI): calculated for (M+H): C₂₄H₂₃CINO₃ 408.1366; found: 408.1391 The absolute stereochemistry was determined by X-ray crystallography:

Ph Ph Ph DCM (0.5 M) Ph
$$\tilde{C}l$$
 Ph $\tilde{C}l$ Ph $\tilde{C}l$

The oxazine substrate **I-77** (0.1 mmol, 38 mg) was dissolve in DCM (2 mL), followed by adding *m*-CPBA (77% wt, 0.2 mmol, 44 mg). The reaction was stirred at room temperature for 4 h. Then add water to the reaction and separate the organic portion. The

organic portion was dried over Na₂SO₄ and remove the solvent under reduced pressure. The crude residue was purified through a silica gel column (10% EtOAc in hexane as eluent) and afforded 26 mg product as colorless wax. The absolute stereochemistry was determined by X-ray crystallography.

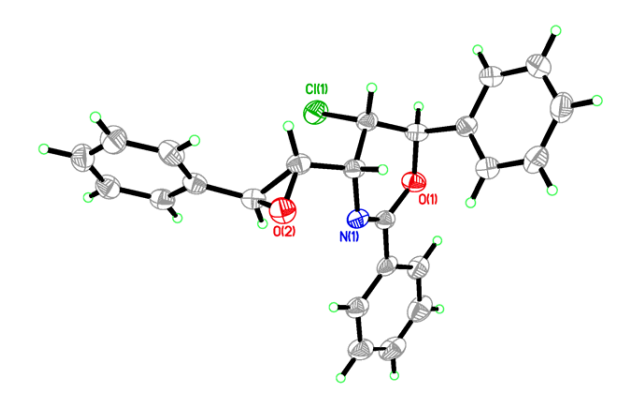
Rf: 0.78 (30% EtOAc in Hexane, UV)

¹H NMR (500 MHz, CDCl3) δ 8.17 – 8.07 (m, 2H), 7.55 – 7.31 (m, 11H), 7.30 – 7.25 (m, 2H), 5.75 (d, J = 2.1 Hz, 1H), 4.61 (dd, J = 3.2, 2.2 Hz, 1H), 3.99 (d, J = 1.9 Hz, 1H), 3.58 (dd, J = 5.5, 3.1 Hz, 1H), 3.29 (dd, J = 5.5, 2.0 Hz, 1H).

¹³C NMR (125 MHz, CDCl₃) δ 154.31, 138.06, 136.96, 132.40, 131.25, 129.18, 128.87, 128.41, 128.23, 128.20, 127.59, 125.84, 124.88, 80.52, 62.74, 57.87, 55.69, 51.87.

HRMS analysis (ESI): calculated for (M+H): C₂₄H₂₁CINO₂ 390.1261; found: 390.1273

The absolute stereochemistry was determined by X-ray crystallography:



Hydrolysisi of oxazine was done following reported literature with **I-77** (34 mg, 0.091 mmol).²⁸

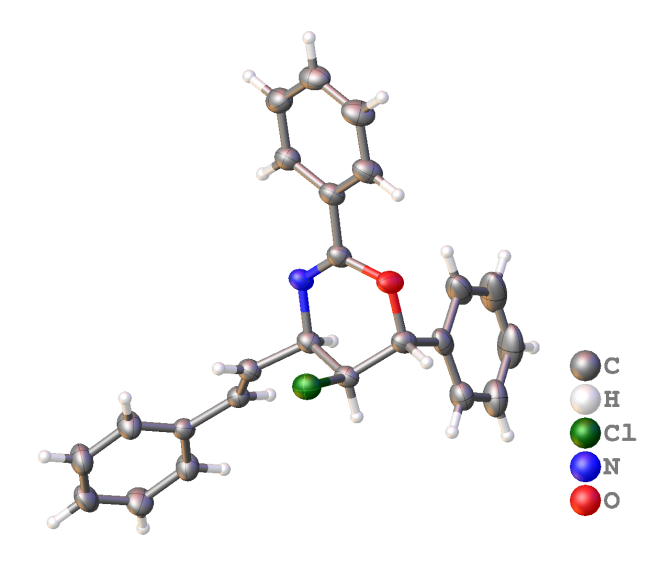
Rf: 0.65 (30% EtOAc in Hexane, UV)

¹H NMR (500 MHz, CDCl₃) δ 8.03 – 7.97 (m, 2H), 7.56 – 7.49 (m, 5H), 7.40 – 7.24 (m, 7H), 6.65 (dd, J = 15.8, 1.3 Hz, 1H), 6.48 (d, J = 9.2 Hz, 1H), 6.28 (dd, J = 15.8, 6.2 Hz, 1H), 6.18 (d, J = 7.8 Hz, 1H), 5.62 (ddt, J = 9.5, 6.2, 1.8 Hz, 1H), 4.66 (dd, J = 7.8, 2.0 Hz, 1H).

¹³C NMR (125 MHz, CDCl₃) δ 165.48, 164.90, 136.61, 133.32, 132.97, 131.83, 129.73, 129.03, 128.68, 128.65, 128.63, 128.45, 128.15, 127.69, 126.64, 75.98, 66.63, 51.24. HRMS analysis (ESI): calculated for (M-H): C₂₄H₂₀NO₂ClBr 468.0366; found: 468.0366.

1.8 X-ray crystal structure data

1.8.1 X-ray crystal structure for I-77



Experimental

Single colourless chunk-shaped crystals of (**BB817B**) were used as received. A suitable crystal ($0.30\times0.22\times0.12$) mm³ was selected and mounted on a nylon loop with paratone oil on a Bruker APEX-II CCD diffractometer. The crystal was kept at T=173(2) K during data collection. Using **Olex2** (Dolomanov et al., 2009), the structure was solved with the XT (Sheldrick, 2015) structure solution program, using the Intrinsic Phasing solution method. The model was refined with version of **XL** (Sheldrick, 2008) using Least Squares minimisation.

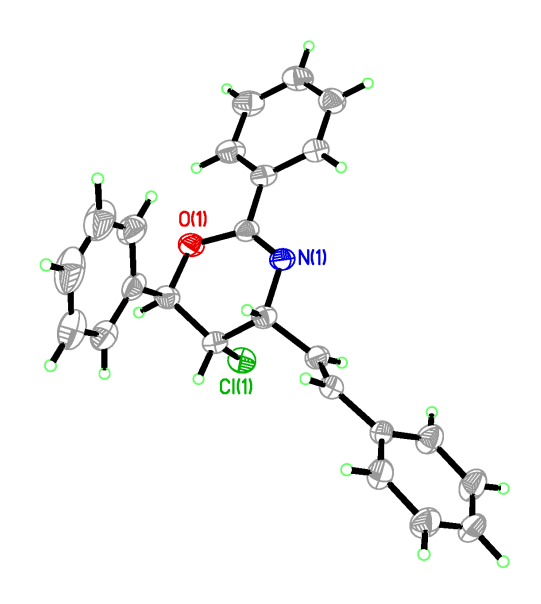
Crystal Data

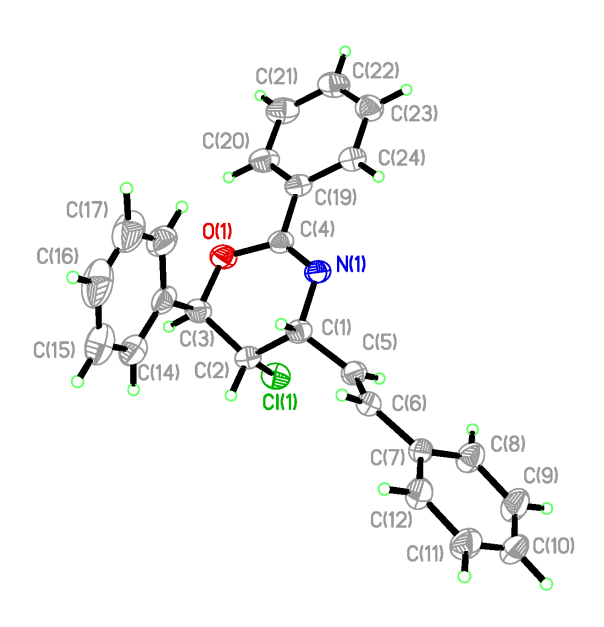
C₂₄H₂₀CINO, M_r = 373.86, orthorhombic, P2₁2₁2₁ (No. 19), a = 9.3060(8) Å, b = 9.6574(9) Å, c = 21.8911(19) Å, $\alpha = \beta = \gamma = 90^{\circ}$, V = 1967.4(3) Å³, T = 173(2) K, Z = 4, Z' = 1, μ (MoK $_{\alpha}$) = 0.207, 14580 reflections measured, 3615 unique ($R_{int} = 0.0335$) which were used in all calculations. The final wR_2 was 0.0784 (all data) and R_1 was 0.0332 (I > 2(I)).

Crystal data and structure refinement

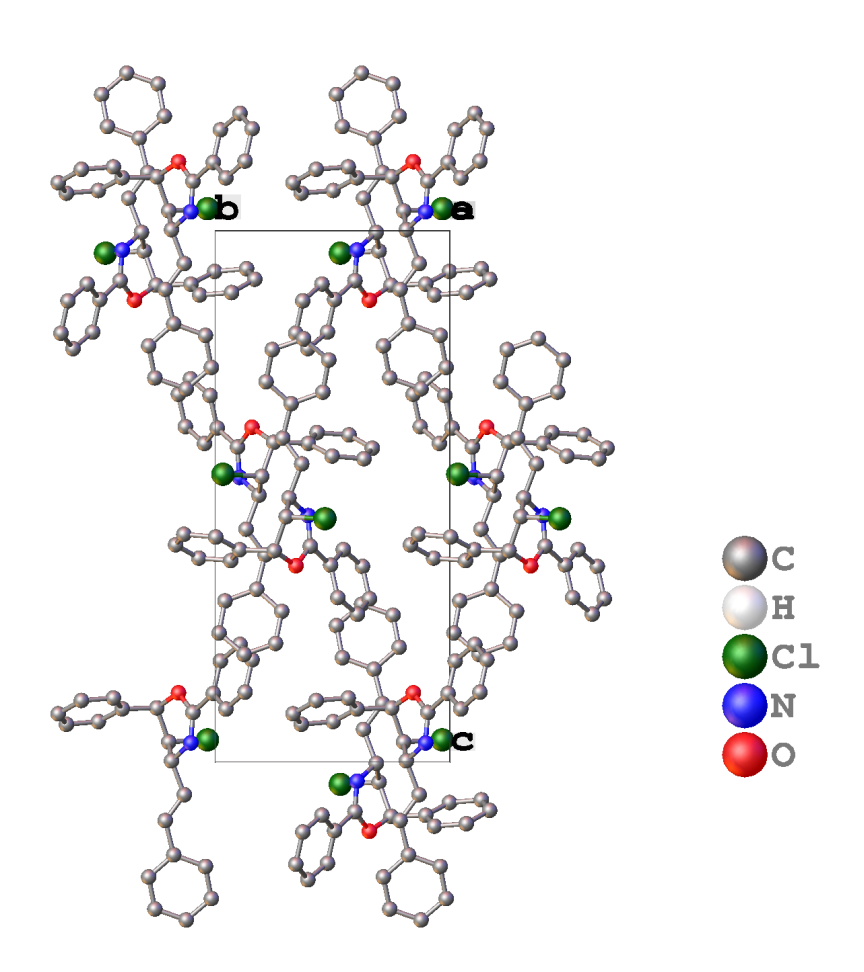
Compound	BB817B
Formula	C ₂₄ H ₂₀ CINO
Dcalc./ g cm ⁻³	1.262
μ/mm ⁻¹	0.207
Formula Weight	373.86
Colour	colourless
Shape	chunk
Size/mm ³	0.30×0.22×0.12
T/K	173(2)
Crystal System	orthorhombic
Flack Parameter	0.02(3)
Hooft Parameter	0.04(3)
Space Group	P2 ₁ 2 ₁ 2 ₁
a/Å	9.3060(8)
b/Å	9.6574(9)
c/Å	21.8911(19)
$lpha f^{\circ}$	90
$eta f^{\circ}$	90
γl°	90
V/Å ³	1967.4(3)
Z	4
<i>Z'</i>	1
Wavelength/Å	0.710730
Radiation type	MoK_{lpha}
Θ_{min} / $^{\circ}$	1.861
$\Theta_{max}/\!\!\!/^{\circ}$	25.393
Measured Refl.	14580
Independent Refl.	3615
Reflections Used	3255
Rint	0.0335
Parameters	244
Restraints	0
Largest Peak	0.161
Deepest Hole	-0.165
GooF	1.059
wR_2 (all data)	0.0784
wR ₂	0.0749
R_1 (all data)	0.0384

The Model has Chirality at C1 (Chiral SPGR) R Verify; The Model has Chirality at C2 (Chiral SPGR) S Verify; The Model has Chirality at C3 (Chiral SPGR) R Verify:





Packing diagram of BB817B:

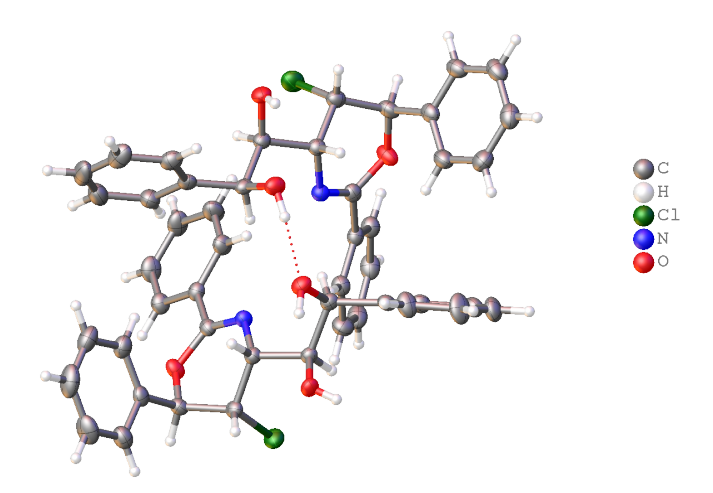


Citations

- 1.COSMO-V1.61 Software for the CCD Detector Systems for Determining Data Collection Parameters, Bruker axs, Madison, WI (2000).
- 2. O.V. Dolomanov and L.J. Bourhis and R.J. Gildea and J.A.K. Howard and H. Puschmann, Olex2: A complete structure solution, refinement and analysis program, *J. Appl. Cryst.*, (2009), **42**, 339-341.
- 3. Sheldrick, G.M., A short history of ShelX, Acta Cryst., (2008), A64, 339-341.

Software for the Integration of CCD Detector System Bruker Analytical X-ray Systems, 4. Bruker axs, Madison, WI (after 2013)

1.8.2 X-ray crystal structure for I-118



Experimental. Single colourless needle-shaped crystals of (**BB717D**) were used as received. A suitable crystal (0.34×0.08×0.06) mm³ was selected and mounted on a nylon loop with paratone oil on a Bruker APEX-II CCD diffractometer. The crystal was kept at *T* = 173(2) K during data collection. Using **Olex2** (Dolomanov et al., 2009), the structure was solved with the **SheIXT** (Sheldrick, 2015) structure solution program, using the Intrinsic Phasing solution method. The model was refined with version of **XL** (Sheldrick, 2008) using Least Squares minimisation.

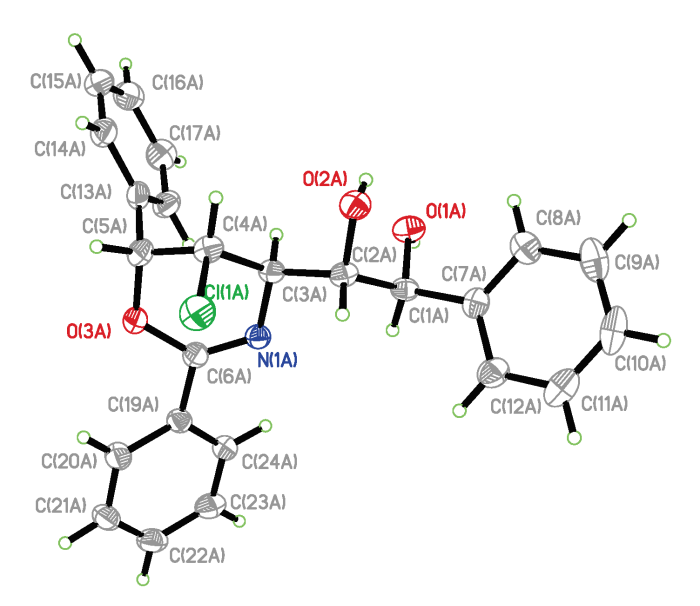
Crystal Data. C₂₄H₂₂CINO₃, M_r = 407.87, monoclinic, P2₁ (No. 4), a = 10.39310(10) Å, b = 9.62820(10) Å, c = 20.5187(2) Å, β = 98.2450(10)°, α = γ = 90°, V = 2032.02(4) Å³, T = 173(2) K, Z = 4, Z' = 2, μ (CuK $_{\alpha}$) = 1.869, 27382 reflections measured, 7691 unique (R_{int} = 0.0470) which were used in all calculations. The final wR_2 was 0.0732 (all data) and R_1 was 0.0306 (I > 2(I)).

Crystal data and structure refinement

Compound	BB717D
Formula	C ₂₄ H ₂₂ CINO ₃
D_{calc} / g cm ⁻³	1.333
μ/mm ⁻¹	1.869
Formula Weight	407.87
Colour	colourless
Shape	needle
Size/mm ³	0.34×0.08×0.06
7/K	173(2)
Crystal System	monoclinic
Flack Parameter	0.018(6)
Hooft Parameter	0.010(7)
Space Group	P2 ₁
a/Å	10.39310(10)
b/Å	9.62820(10)
c/Å	20.5187(2)
$\alpha / $	90
βf°	98.2450(10)
y °	90
// V/Å ³	2032.02(4)
Z	4
	2
Wavelength/Å	1.541838
Radiation type	CuK_lpha
$arTheta_{min}$ / $^{\circ}$	4.298
$\Theta_{ extit{max}}/\!\!\!/^{\circ}$	72.150
Measured Refl.	27382
Independent Refl.	7691
Reflections Used	7125
Rint	0.0470
Parameters	539
Restraints	1
Largest Peak	0.159
Deepest Hole	-0.186
GooF	1.027
wR₂ (all data)	0.0732
wR ₂	0.0710
R_1 (all data)	0.0346
R_1	0.0306

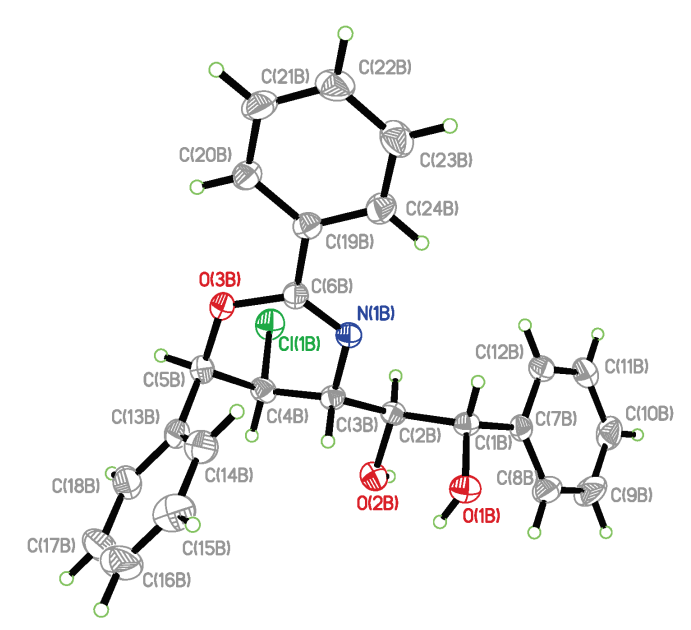
The following are 50% thermal ellipsoidal drawings of the molecule in the asymmetric cell with various amount of labeling:

The Model has Chirality at C1A (Chiral SPGR) S Verify; The Model has Chirality at C2A (Chiral SPGR) S Verify; The Model has Chirality at C3A (Chiral SPGR) R Verify; The Model has Chirality at C4A (Chiral SPGR) S Verify; The Model has Chirality at C5A (Chiral SPGR) R Verify:

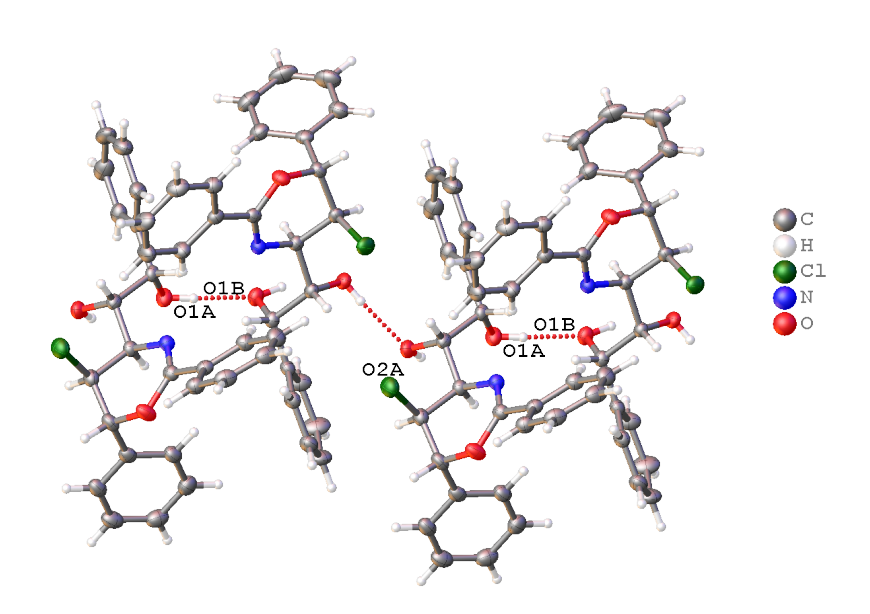


The Model has Chirality at C1B (Chiral SPGR) S Verify; The Model has Chirality at C2B (Chiral SPGR) S Verify; The Model has Chirality at C3B (Chiral SPGR) R Verify; The Model has Chirality at C4B (Chiral SPGR) S Verify; The Model has Chirality at C5B (Chiral

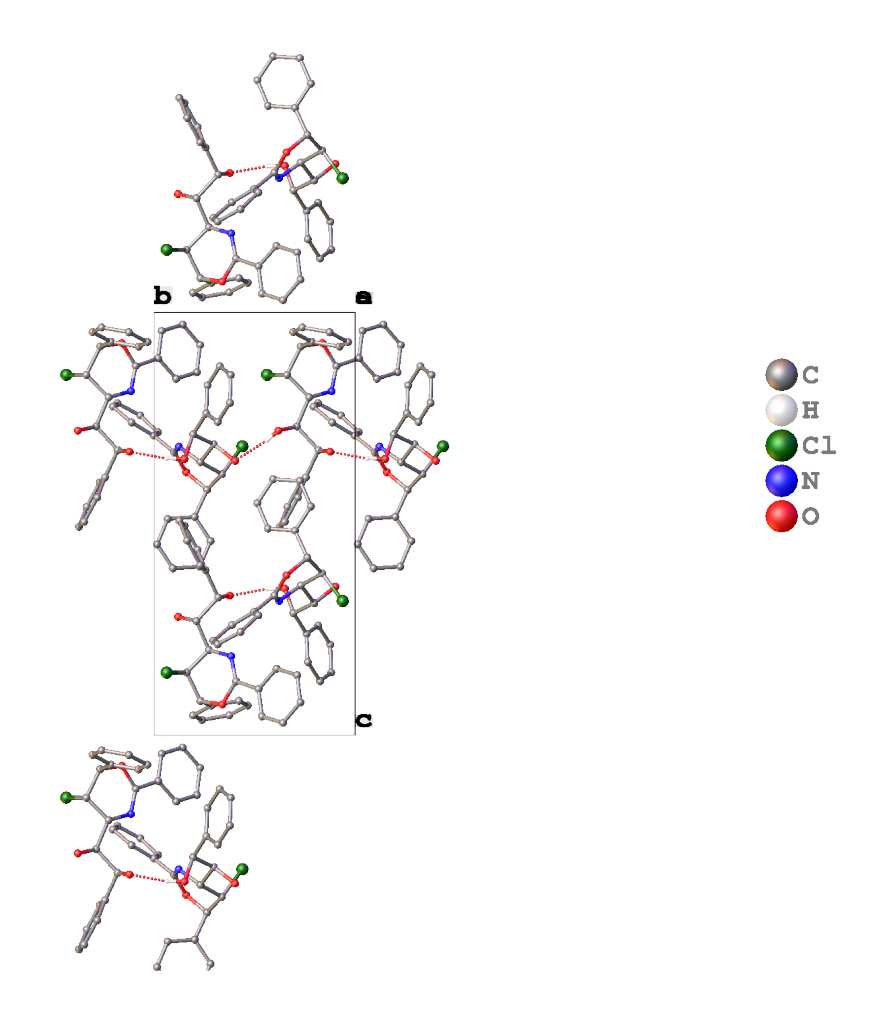
SPGR) R Verify:



The following hydrogen bonding interactions with a maximum D-D distance of 3.1 Å and a minimum angle of 110 ° are present in **BB717D**: O1A-O1B: 2.668 Å, O2A-O1A: 2.673 Å, O1B-O2B: 2.685 Å, O2B-O2A_1: 2.718 Å:



Packing diagram of BB717D:



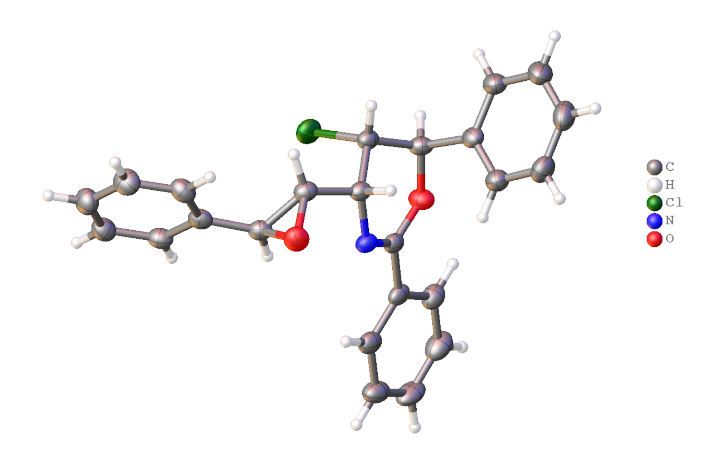
Citations

- 1.COSMO-V1.61 Software for the CCD Detector Systems for Determining Data Collection Parameters, Bruker axs, Madison, WI (2000).
- 2.O.V. Dolomanov and L.J. Bourhis and R.J. Gildea and J.A.K. Howard and H. Puschmann, Olex2: A complete structure solution, refinement and analysis program, *J. Appl. Cryst.*, (2009), **42**, 339-341.
- 3. Sheldrick, G.M., A short history of ShelX, Acta Cryst., (2008), A64, 339-341.
- 4. Sheldrick, G.M., ShelXT-Integrated space-group and crystal-structure determination,

Acta Cryst., (2015), A71, 3-8.

5. Software for the Integration of CCD Detector System Bruker Analytical X-ray Systems, Bruker axs, Madison, WI (after 2013).

1.8.3 X-ray crystal structure for I-119



Experimental. Single colourless needle-shaped crystals of (**BB717A**) were used as received. A suitable crystal $(0.22\times0.10\times0.08)$ mm³ was selected and mounted on a nylon loop with paratone oil on a Bruker APEX-II CCD diffractometer. The crystal was kept at T = 173(2) K during data collection. Using **Olex2** (Dolomanov et al., 2009), the structure was solved with the XT (Sheldrick, 2015) structure solution program, using the Intrinsic Phasing solution method. The model was refined with version of **XL** (Sheldrick, 2008) using Least Squares minimisation.

Crystal Data. C₂₄H₂₀CINO₂, M_r = 389.86, orthorhombic, P2₁2₁2₁ (No. 19), a = 10.0607(3) Å, b = 10.4054(3) Å, c = 19.2999(5) Å, $\alpha = \beta = \gamma = 90^{\circ}$, V = 2020.42(10) Å³, T = 173(2) K, Z = 4, Z' = 1, μ (CuK $_{\alpha}$) = 1.820, 12613 reflections measured, 3804 unique (R_{int} = 0.0423) which were used in all calculations. The final wR_2 was 0.0793 (all data) and R_1 was 0.0323 (I > 2(I)).

Crystal data and structure refinement

Compound **BB717A** Formula C₂₄H₂₀CINO₂ D_{calc.}/ g cm⁻³ 1.282 μ /mm⁻¹ 1.820 Formula Weight 389.86 Colour colourless Shape needle Size/mm³ 0.22×0.10×0.08 T/K 173(2) Crystal System orthorhombic Flack Parameter 0.041(10) **Hooft Parameter** 0.031(10) Space Group P212121 a/Å 10.0607(3) b/Å 10.4054(3) c/Å 19.2999(5) $\alpha/^{\circ}$ 90 $\beta / \hat{}$ 90 ηſ° 90 V/Å³ 2020.42(10) Ζ 4 Z'1 Wavelength/Å 1.541838 Radiation type CuK_{α} 4.582 $\Theta_{min}I^{\circ}$ 69.898 $\Theta_{max}I^{\circ}$ Measured Refl. 12613 Independent Refl. 3804 Reflections Used 3403 Rint 0.0423 **Parameters** 253 Restraints 0 Largest Peak 0.154 Deepest Hole -0.193GooF 1.029 wR_2 (all data) 0.0793 wR_2 0.0761 R_1 (all data) 0.0385

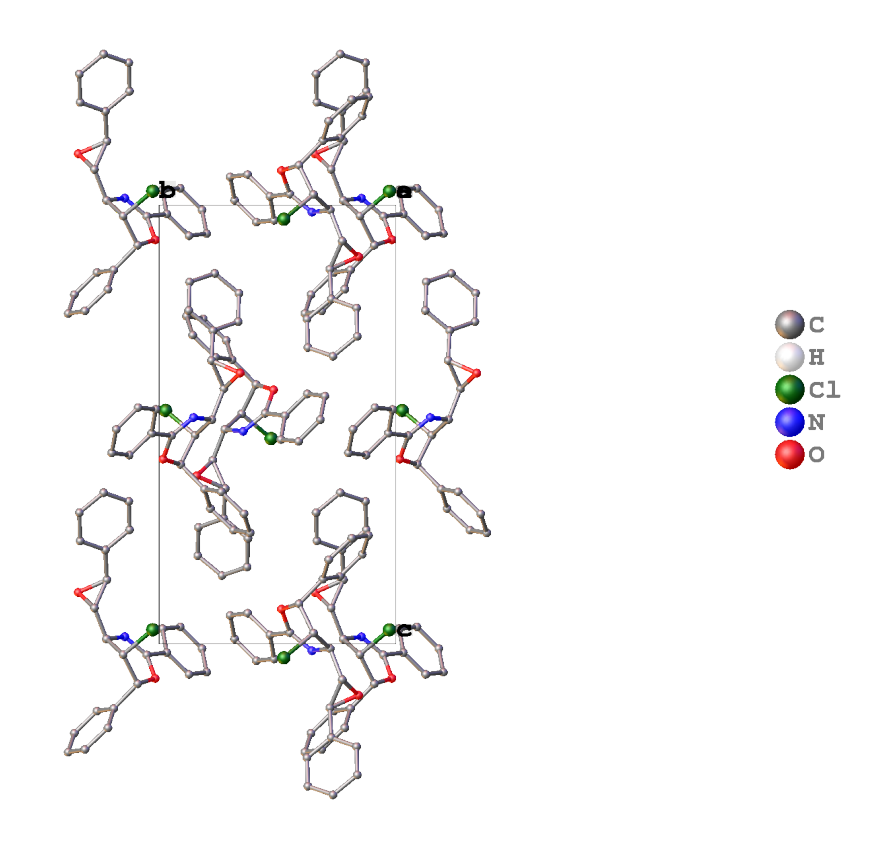
0.0323

 R_1

The following are 50% thermal ellipsoidal drawings of the molecule in the asymmetric cell with various amount of labeling:

The Model has Chirality at C2 (Chiral SPGR) R Verify; The Model has Chirality at C3 (Chiral SPGR) S Verify; The Model has Chirality at C4 (Chiral SPGR) R Verify; The Model has Chirality at C5 (Chiral SPGR) S Verify; The Model has Chirality at C6 (Chiral SPGR) S Verify:

Packing diagram of BB717A:



Citations

- 1.COSMO-V1.61 Software for the CCD Detector Systems for Determining Data Collection Parameters, Bruker axs, Madison, WI (2000).
- 2. O.V. Dolomanov and L.J. Bourhis and R.J. Gildea and J.A.K. Howard and H. Puschmann, Olex2: A complete structure solution, refinement and analysis program, *J. Appl. Cryst.*, (2009), **42**, 339-341.
- 3. Sheldrick, G.M., A short history of ShelX, Acta Cryst., (2008), A64, 339-341.
- 4. Software for the Integration of CCD Detector System Bruker Analytical X-ray Systems, Bruker axs, Madison, WI (after 2013).

REFERENCES

REFERENCES

- 1. Borissov, A.; Davies, T. Q.; Ellis, S. R.; Fleming, T. A.; Richardson, M. S. W.; Dixon, D. J., Organocatalytic enantioselective desymmetrisation. *Chemical Society Reviews* **2016**, *45* (20), 5474-5540.
- 2. Schreiber, S. L.; Schreiber, T. S.; Smith, D. B., Reactions that proceed with a combination of enantiotopic group and diastereotopic face selectivity can deliver products with very high enantiomeric excess: experimental support of a mathematical model. *Journal of the American Chemical Society* **1987**, *109* (5), 1525-1529.
- 3. Smith, D. B.; Zhaoyin, W.; Schreiber, S. L., The asymmetric epoxidation of divinyl carbinols: theory and applications. *Tetrahedron* **1990**, *46* (13), 4793-4808.
- 4. Angelaud, R.; Landais, Y., Desymmetrization of a Silyl-2,5-cyclohexadiene. Synthesis of (+)-Conduritol E and (–)-2-Deoxy-allo-inositol. *The Journal of Organic Chemistry* **1996**, *61* (16), 5202-5203.
- 5. Belley, M. L.; Hill, B.; Mitenko, H.; Scheigetz, J.; Zamboni, R., Asymmetric Dihydroxylation of Dienes: Synthesis of Tetrols. *Synlett* **1996**, *1996* (01), 92-94.
- 6. Martin, S. F.; Spaller, M. R.; Liras, S.; Hartmann, B., Enantio- and Diastereoselectivity in the Intramolecular Cyclopropanation of Secondary Allylic Diazoacetates. *Journal of the American Chemical Society* **1994**, *116* (10), 4493-4494.
- 7. Reddy Iska, V. B.; Verdolino, V.; Wiest, O.; Helquist, P., Mild and Efficient Desymmetrization of Diynes via Hydroamination: Application to the Synthesis of (±)-Monomorine I. *The Journal of Organic Chemistry* **2010**, *75* (4), 1325-1328.
- 8. Yoshida, S.; Fukui, K.; Kikuchi, S.; Yamada, T., Silver-Catalyzed Enantioselective Carbon Dioxide Incorporation into Bispropargylic Alcohols. *Journal of the American Chemical Society* **2010**, *132* (12), 4072-4073.
- 9. Tanaka, K.; Fu, G. C., Enantioselective Synthesis of Cyclopentenones via Rhodium-Catalyzed Kinetic Resolution and Desymmetrization of 4-Alkynals. *Journal of the American Chemical Society* **2002**, *124* (35), 10296-10297.
- 10. Lee, J.-W.; Mayer-Gall, T.; Opwis, K.; Song, C. E.; Gutmann, J. S.; List, B., Organotextile Catalysis. *Science* **2013**, *341* (6151), 1225-1229.
- 11. Ivšić, T.; Hameršak, Z., A simple enantioselective route toward (*R*)- and (*S*)-Rolipram via anhydride desymmetrization. *Tetrahedron: Asymmetry* **2013**, *24* (4), 217-222.

- 12. Rong, Z.-Q.; Pan, H.-J.; Yan, H.-L.; Zhao, Y., Enantioselective Oxidation of 1,2-Diols with Quinine-Derived Urea Organocatalyst. *Organic Letters* **2014**, *16* (1), 208-211.
- 13. Arceo, E.; Bahamonde, A.; Bergonzini, G.; Melchiorre, P., Enantioselective direct α -alkylation of cyclic ketones by means of photo-organocatalysis. *Chemical Science* **2014**, *5* (6), 2438-2442.
- 14. Gu, Q.; You, S.-L., Desymmetrization of Cyclohexadienones via Asymmetric Michael Reaction Catalyzed by Cinchonine-Derived Urea. *Organic Letters* **2011**, *13* (19), 5192-5195.
- 15. Singha Roy, S. J.; Mukherjee, S., Enantioselective desymmetrization of prochiral 1,3-dinitropropanes via organocatalytic allylic alkylation. *Chemical Communications* **2014**, *50* (1), 121-123.
- 16. Manna, M. S.; Mukherjee, S., Organocatalytic Enantioselective Formal C(sp2)–H Alkylation. *Journal of the American Chemical Society* **2015**, *137* (1), 130-133.
- 17. Inoue, T.; Kitagawa, O.; Kurumizawa, S.; Ochiai, O.; Taguchi, T., Enantioselective iodocarbocyclization of 4-alkenylmalonate derivatives using a chiral titanium complex. *Tetrahedron Letters* **1995**, *36* (9), 1479-1482.
- 18. Ke, Z.; Tan, C. K.; Chen, F.; Yeung, Y.-Y., Catalytic Asymmetric Bromoetherification and Desymmetrization of Olefinic 1,3-Diols with C2-Symmetric Sulfides. *Journal of the American Chemical Society* **2014**, *136* (15), 5627-5630.
- 19. Kitagawa, O.; Hanano, T.; Tanabe, K.; Shiro, M.; Taguchi, T., Enantioselective halocyclization reaction using a chiral titanium complex. *Journal of the Chemical Society, Chemical Communications* **1992,** (14), 1005-1007.
- 20. Müller, C. H.; Rösner, C.; Hennecke, U., Enantioselective Haloetherifications Catalyzed by 1,1'-Bi-2-naphthol (BINOL) Phosphates: From Symmetrical Alkenediols to Simple Alkenols. *Chemistry An Asian Journal* **2014**, *9* (8), 2162-2169.
- 21. Zhao, Y.; Jiang, X.; Yeung, Y.-Y., Catalytic, Enantioselective, and Highly Chemoselective Bromocyclization of Olefinic Dicarbonyl Compounds. *Angewandte Chemie International Edition* **2013**, *52* (33), 8597-8601.
- 22. Ikeuchi, K.; Ido, S.; Yoshimura, S.; Asakawa, T.; Inai, M.; Hamashima, Y.; Kan, T., Catalytic Desymmetrization of Cyclohexadienes by Asymmetric Bromolactonization. *Organic Letters* **2012**, *14* (23), 6016-6019.
- 23. Paull, D. H.; Fang, C.; Donald, J. R.; Pansick, A. D.; Martin, S. F., Bifunctional Catalyst Promotes Highly Enantioselective Bromolactonizations To Generate

- Stereogenic C-Br Bonds. *Journal of the American Chemical Society* **2012**, *134* (27), 11128-11131.
- 24. Wilking, M.; Mück-Lichtenfeld, C.; Daniliuc, C. G.; Hennecke, U., Enantioselective, Desymmetrizing Bromolactonization of Alkynes. *Journal of the American Chemical Society* **2013**, *135* (22), 8133-8136.
- 25. Hennecke, U.; Müller, C. H.; Fröhlich, R., Enantioselective Haloetherification by Asymmetric Opening of meso-Halonium Ions. *Organic Letters* **2011**, *13* (5), 860-863.
- 26. Tay, D. W.; Leung, G. Y. C.; Yeung, Y.-Y., Desymmetrization of Diolefinic Diols by Enantioselective Amino-thiocarbamate-Catalyzed Bromoetherification: Synthesis of Chiral Spirocycles. *Angewandte Chemie International Edition* **2014**, *53* (20), 5161-5164.
- 27. Sparr, C.; Gilmour, R., Cyclopropyl Iminium Activation: Reactivity Umpolung in Enantioselective Organocatalytic Reaction Design. *Angewandte Chemie International Edition* **2011**, *50* (36), 8391-8395.
- 28. Jaganathan, A.; Garzan, A.; Whitehead, D. C.; Staples, R. J.; Borhan, B., A Catalytic Asymmetric Chlorocyclization of Unsaturated Amides. *Angewandte Chemie International Edition* **2011**, *50* (11), 2593-2596.
- 29. Jaganathan, A.; Staples, R. J.; Borhan, B., Kinetic Resolution of Unsaturated Amides in a Chlorocyclization Reaction: Concomitant Enantiomer Differentiation and Face Selective Alkene Chlorination by a Single Catalyst. *Journal of the American Chemical Society* **2013**, *135* (39), 14806-14813.
- 30. Sakakura, A.; Sakuma, M.; Ishihara, K., Chiral Lewis Base-Assisted Brønsted Acid (LBBA)-Catalyzed Enantioselective Cyclization of 2-Geranylphenols. *Organic Letters* **2011**, *13* (12), 3130-3133.
- 31. Soltanzadeh, B.; Jaganathan, A.; Yi, Y.; Yi, H.; Staples, R. J.; Borhan, B., Highly Regio- and Enantioselective Vicinal Dihalogenation of Allyl Amides. *Journal of the American Chemical Society* **2017**, *139* (6), 2132-2135.
- 32. Bruenker, H.-G.; Adam, W., Diastereoselective and Regioselective Singlet Oxygen Ene Oxyfunctionalization (Schenck Reaction): Photooxygenation of Allylic Amines and Their Acyl Derivatives. *Journal of the American Chemical Society* **1995**, *117* (14), 3976-3982.
- 33. Hyster, T. K.; Rovis, T., Pyridine synthesis from oximes and alkynesviarhodium(iii) catalysis: Cp* and Cpt provide complementary selectivity. *Chemical Communications* **2011**, *47* (43), 11846-11848.

34. Ashtekar, K. D.; Ding, X.; Toma, E.; Sheng, W.; Gholami, H.; Rahn, C.; Reed, P.; Borhan, B., Mechanistically Inspired Route toward Hexahydro-2H-chromenes via Consecutive [4 + 2] Cycloadditions. *Organic Letters* **2016**, *18* (16), 3976-3979.

CHAPTER TWO

Kinetic Resolution of Propargyl Amides in a Chlorocyclization Reaction

2.1 Introduction

Kinetic resolution is the process of using a chiral reagent or chiral catalyst to promote the reaction of one enantiomer over the other, resulting in a mixture of resolved starting material and converted product (Scheme 2.1). It is an important strategy for accessing enantioenriched molecules, as an alternative to using the chiral pool or enantioselective synthesis. The chiral pool is using enantio-pure starting materis provided by nature, however this method is always limited to the range and the stereochemistry of available natural products. Therefore, kinetic resolution and enantioselective synthesis using chiral reagents or chiral catalysts play a critical role in organic synthesis. Kinetic resolution can be criticized for its inherent inelegance and poor atom economy because the maximum theoretical yield is 50%. On the other hand, if one can transform racemic starting materials to some other useful enantio-enriched products in the process of resolution, it would counterbalance this disadvantage to some degree. Many factors determine the efficiency and practicality of kinetic resolution. Jacobsen has highlighted several features of a practical and efficient kinetic resolution:

- 1 The starting material is readily accessible.
- 2 Products are obtained in quantitative yield or with minimal byproducts.
- 3 The chiral catalyst is inexpensive.
- 4 The resolved starting material and product are easily isolated.
- 5 The reaction can be processed in large scale.

6 Reaction time must be short.

$$S_S$$
 + S_R + reagent $\xrightarrow{\text{chiral catalyst}}$ S_S + P_R racemic substrate

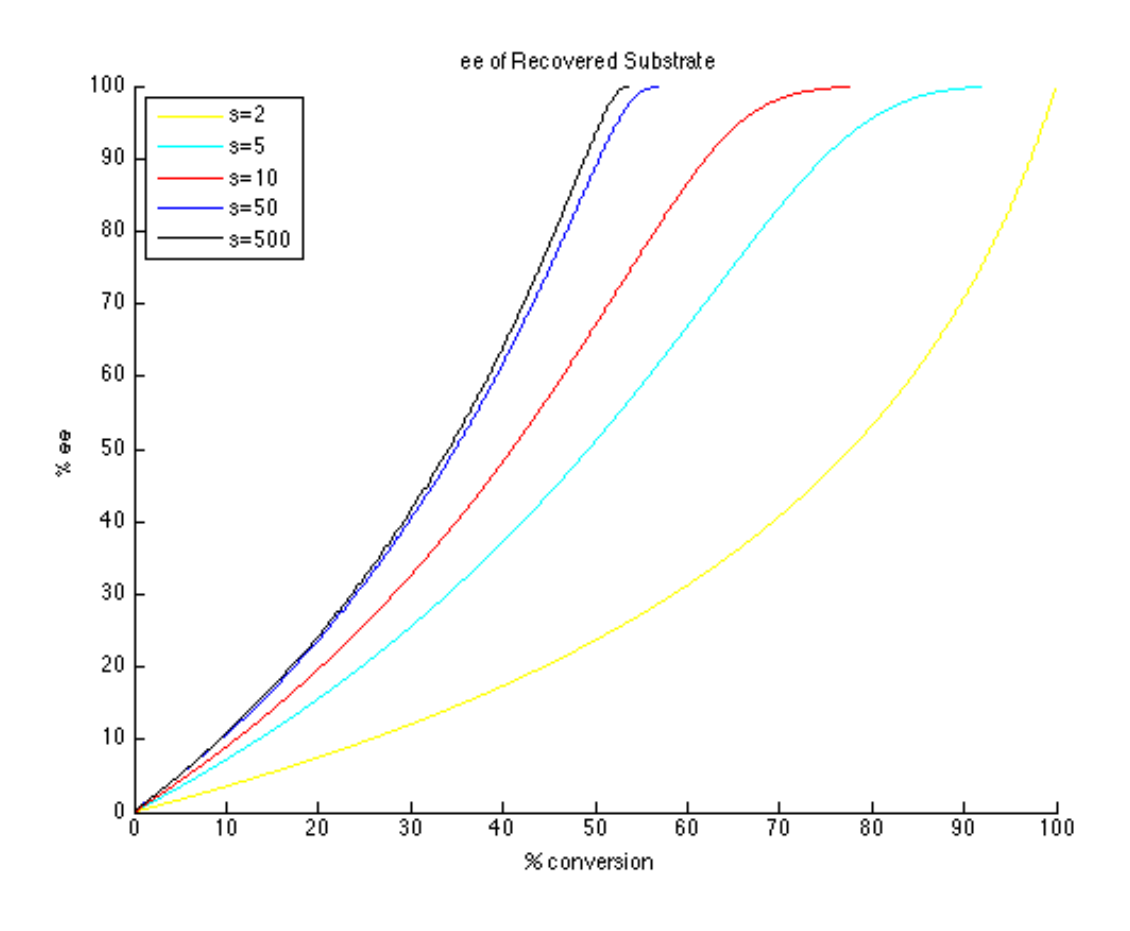
$$S = K_{rel} = K_{fast}/K_{slow} = e^{\Delta \Delta G_{\pm}/RT}$$

Scheme 2.1 Catalytic kinetic resolution

People usually use the *selectivity factor* (S or K_{rel}) to evaluate the efficiency of a kinetic resolution. In general, systems with $K_{rel} > 10$ are useful. K_{rel} is defined as the relative reaction rate of two enantiomers, so it is correlated with the energy difference of diastereomeric transition states (Scheme 2.1). S can also be defined using the formula of ee and conversion. The ee of the recovered substrate and converted product varies as a function of conversion (Figure 2.1). As you can see from plot **a** below, even though the S is only 5, recovered starting material can also be obtained in more than 90% ee by controlling the conversion at 70%. In contrast, high selectivity factor is required if you want to get the converted product in high ee (see Figure 2.1, plot b). S is an important factor to evaluate the efficacy of kinetic resolution in many of the reported kinetic resolution studies, however, it is to some degree oversimplifying the process of kinetic resolution for three reasons. First, the correlation between ee and conversion plotted in Figure 2.1 is based on the assumption that the reaction is first order with respect to the substrate. Second, the selectivity factor only accounts for the conversion of substrate and assumes that the reaction only leads to one converted product, but some reported kinetic resolutions have side products and the isolated yield of the converted product is less than the conversion. Finally, a minor change in conversion will significantly affect the selectivity

factor. Jacobsen also mentioned that most S values reported in the literature are inaccurate. Therefore simply using S is not an accurate, or at least not a comprehensive way to describe the efficacy of a kinetic resolution. The yield and ee of the converted product and resolved starting material are required.

a)

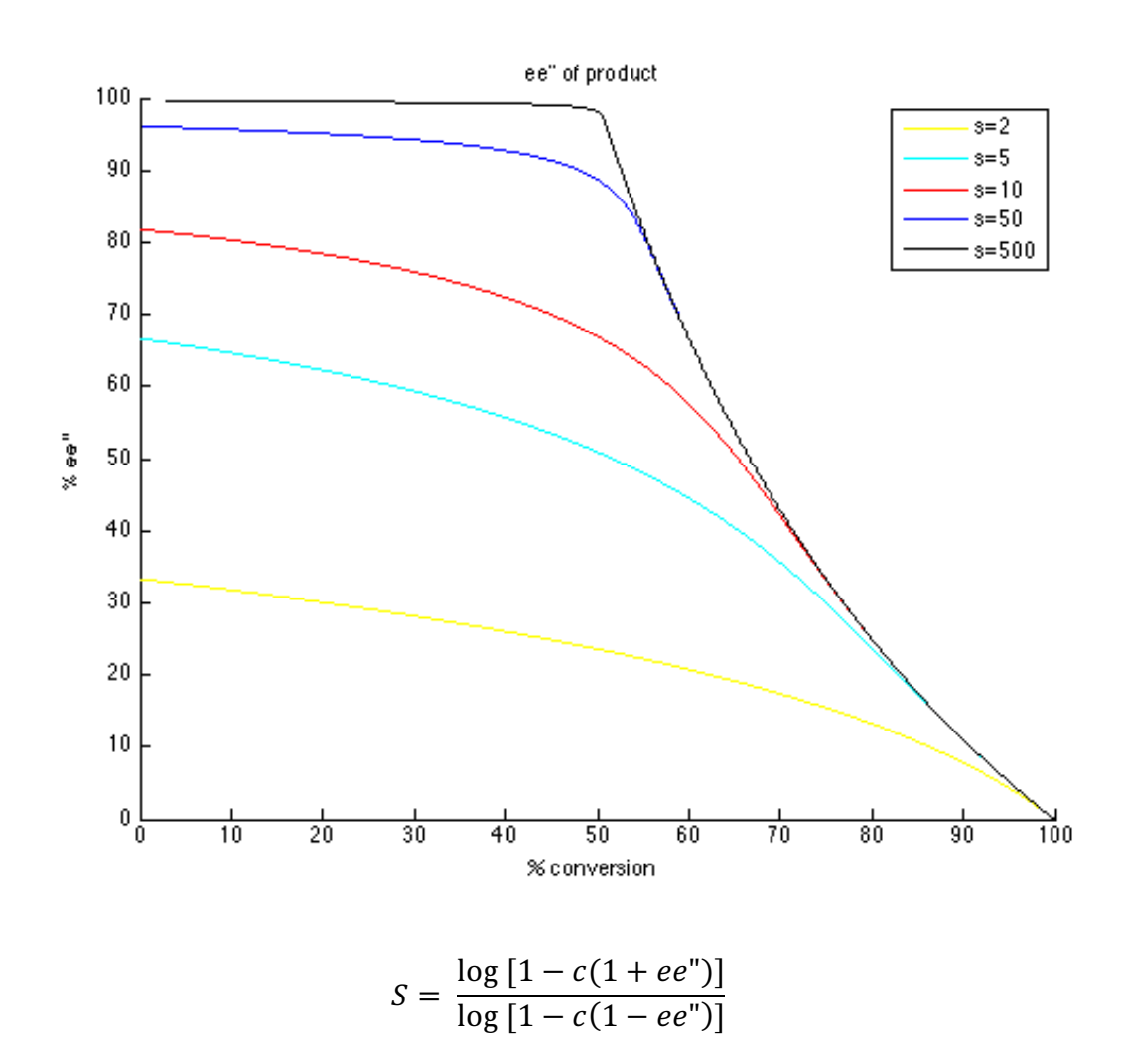


 $S = \frac{Ln[(1-c)(1-ee)]}{Ln[(1-c)(1+ee)]}$

Figure 2.1 a) plot of *ee* of recovered starting material vs conversion as a function of S; b) plot of *ee* of product vs conversion as a function of S^1 .

Figure 2.1(cont'd)

b)



Although it is hard to meet all the aforementioned criteria for a perfect kinetic resolution, many great examples have been reported that demonstrate the practical utility of this important synthetic strategy. One of the earliest examples is the landmark work of Sharpless for the kinetic resolution of allylic alcohol (Scheme 2.2, a).² He used titanium alkoxide tartrate complex to epoxidize prochiral allylic alcohols. It was observed that the *S* enantiomer reacts 104 times faster than the *R* enantiomer to give a 98:2 *erythro to threo*

product ratio when L-(+)-DIPT was used. If Ti(O-*i*-Pr)₄ is used alone, the *threo* product is predominant. He also showed that the resolution process can proceed under catalytic conditions by using 25 mol% titanium alkoxide tartrate complex but with an extended time range. This work represents the earliest non-enzymatic resolution using a synthetic catalyst. Since then alkenes have become the most studied category in kinetic resolution. Corey reported the kinetic resolution of allylic 4-methoxybenzoate by asymmetric dihydroxylation using cinchona alkaloid catalyst **II-5** (Scheme 2.2, b).³ Noyori reported the Ru-catalyzed oxidative kinetic resolution of benzylic alcohols. This method merits the high selectivity and quantitative yield for a variety of benzylic and allylic alcohols (Scheme 2.2, c).⁴

Transition-metal-salen complexes are another class of privileged catalysts for hydrolytic kinetic resolution (HKR) of epoxides. HKR provides a good way to access chiral epoxides other than direct enantioselective epoxidation of olefins since racemic epoxides are readily synthesized from alkenes. Chiral salen complexes of Cr and Co can catalyze the opening of epoxides with a variety of nucleophiles, such as carboxylic acids, phenols, azides, and water. Jacobsen's (salen)-Co catalyzed kinetic resolution of terminal epoxides results in high selectivity and generate the corresponding diols in excellent *ee* (Scheme 2.3, a).⁵ The HKR is second-order for the catalyst, proceeding via simultaneous activation of epoxide and nucleophile. Surprisingly the high selectivity is not caused by different binding constants between the two epoxide enantiomers with the catalyst, since they are comparable. The high selectivity arises from the preferential ring-opening process of one of the diastereomeric catalyst-epoxide adducts (Scheme 2.3, b). The

active form of catalyst is (salen)Co(OH), which is generated after (salen)Co(OAc) or (salen)Co(CI) is added to the epoxide.

a. OH TBHP
$$\frac{OH}{II-1}$$
 $\frac{OH}{II-2}$ $\frac{OH}{II-3}$ $\frac{OH}{II-2}$ $\frac{OH}{II-3}$ $\frac{OH}{II-3}$ $\frac{(O-PP)_4}{II-2}$ $\frac{OH}{II-3}$ $\frac{(CO_3)_6}{II-4}$ $\frac{(K_2CO_3)_6}{II-4}$ $\frac{(K_2CO_3)_6}{II-5}$ $\frac{(K_2CO_3)_6}{II-6}$ $\frac{(K_2CO_3)_6}{II-6}$ $\frac{(K_2CO_3)_6}{II-6}$ $\frac{(CO_3)_6}{II-6}$ $\frac{(CO_3)_6}{II-6}$

Scheme 2.2 Early landmark studies for thr kinetic resolution of alkenes.

b.
$$X = CI$$
, OAC $X = CI$, OAC OAC

Scheme 2.3 a) Cobalt-salen catalyzed HKR; b) Mechanism of HKR.

Since the time that Sharpless used cinchona alkaloid derivatives as catalysts in kinetic resolution during the 1980s, a number of other groups studying kinetic resolutions started using this type of catalyst. Deng reported cinchona alkaloid catalyzed kinetic resolution of urethane protected α -amino acid N-carboxyanhydride (UNCA) II-12 that leads to α -amino acid derivatives II-13 and II-14 (Scheme 2.4).6 (DHQD)₂AQN catalyzed the alcoholysis of meso UNCA to generate the amino ester II-13 with S up to 170. This work

indicates that small-molecule catalyzed kinetic resolution of carbonyl derivatives can be as efficient as the enzyme catalyzed processes.

Scheme 2.4 (DHQD)₂AQN catalyzed alcoholysis of *meso* UNCA.

More recently Wang's group reported that the cinchona-alkaloid derived amine thiourea bifunctional catalyst **II-17** can catalyze a highly enantioselective transesterification process to generate chiral biaryl products (Scheme 2.5). Biaryl lactone **II-15** can undergo dynamic kinetic resolution (DKR) by reacting with alcohol **II-16**. The synergistic activation of lactones and alcohols by the thiourea and amine, respectively, is crucial for achieving high yield and enantioselectivity.

Scheme 2.5 DKR of lactone **II-15** catalyzed by a thiourea-based bifunctional catalyst.

Scheme 2.6 Kinetic resolution of 2-oxindole catalyzed by cinchona-alkaloid squaramide.

Kinetic resolution of 2-oxindole **II-19** through an enolate alkylation process catalyzed by cinchona-alkaloid derived squaramide catalyst **II-20** has been reported by Connon's group (Scheme 2.6). The S_N2 reaction is taking place in a biphasic solvent system using a phase transfer catalyst, leading to a single diastereomer with S up to 261.

This chapter describes kinetic resolution of propargyl amides via chlorocyclization catalyzed by a cinchona-alkaloid catalyst. Kinetic resolution of propargyl or allyl amines and propargyl alcohols have been reported. Most of the kinetic resolutions of propargyl amines are through N-acetylation processes. For example, Cossy's group used N-acetyl-1,2-bis-trifluoromethanesulfon-amidocyclo-hexane II-23 as a chiral acetylating reagent to react with primary propargyl amine II-22, affording acetamide II-24 with high selectivity (Scheme 2.7, a).9 Siedel also reported the first small-molecule catalyzed kinetic resolution of racemic allylic amines by an acylation reaction (Scheme 2.7, b). He utilized a dual catalyst system which contains a nucleophile catalyst PPY and a chiral hydrogen bonding catalyst II-27. The nucleophilic catalyst and the acylating reagent generate an ion pair which can form hydrogen bond with the chiral catalyst, leading to a chiral ion pair. Fu reported a Rh-catalyzed kinetic resolution of 4-alkynals II-29 (Scheme 2.7, c). 10 Rh-(Tol-BINAP) complex catalyze the cyclization of 4-alkynals leading to cyclopentenone product II-31. Similarly a Rh(I)-BINAP complex can catalyze the kinetic resolution of secondary propargylic alcohol **II-32** by isomerization into α,β -enones (Scheme 2.7, d).¹¹ The isomerization proceeds through 1,2 or 1,3-hydrogen migration.

Scheme 2.7 Kinetic resolution of unsaturated amines and alcohols.

Propargyl amines in pure enantiomeric form are important and versatile building blocks in organic synthesis. Conventional routes for the preparation of chiral propargylic amines include:1) nucleophilic 1,2-addition to activated aldimines; 2) kinetic resolution of racemic propargyl amines. For route (1) a three-component coupling of an aldehyde, an alkyne and an amine catalyzed by a chiral catalyst is used to access to enantiopure propargylic amines (Scheme 2.8).¹²⁻¹⁴ This method usually requires the activation of the C-H bond of terminal alkyne by a transition metal catalyst. As mentioned above, there are also reported kinetic resolutions of propargylic amines employing chiral acylating reagents.⁹ However, kinetic resolution of propargylic amines by halofunctionalization has not been reported yet.

$$R = [M] \xrightarrow{R^2 N} R^2 N + R^2 N + R^2 N + R^1$$

Scheme 2.8 Access to propargylic amines by coupling of alkyne and aldimine.

In 2013, our group reported the first example of kinetic resolution via chlorofunctionalization of olefins (Scheme 2.9). 15 This was a captivating piece of work for several reasons. First, the C-Cl bond generated can be a functional handle for further functionalization. Second, the kinetic resolution leads to a product with three contiguous chiral centers. Thirdly, (DHQD)₂PHAL as a catalyst can not only show high olefin face selectivity with a chlorenium donor, but also effectively discriminate the chirality of propargylic amides. This proposed method for the kinetic resolution of propargylic amides was inspired by our previous work on organocatalytic enantioselective chlorocyclization

of olefinic amides. Based on previous work it was proposed that propargylic amides should be able to undergo similar kinetic resolution via chlorocyclization.

previous work:

Ph NH
$$\frac{0.55 \text{ equiv NCP}}{0.5 \text{ mol}\% \text{ (DHQD)}_2\text{PHAL}}$$
 $\frac{R^2}{CF_3\text{CH}_2\text{OH} \text{ (0.1 M)}}$ $\frac{R^2}{CI}$ $\frac{R^2}{R^2}$ $\frac{R^2}{R^2}$

Scheme 2.9 Our group's previous work and proposed work

2.2 Results and Disscussion

2.2.1 Evaluate the efficiency of kinetic resolution

Generally, people use K_{rel} or S to evaluate the efficiency of a kinetic resolution. However, as mentioned above, S usually is not an accurate and reliable value since minor variation on conversion can change the S by several folds. Therefore, it really depends on how accurately we measure the conversion of a reaction. During the development of this project, different ways to measure the conversion were attempted. Each of those methods has *pros and cons*. Crude ¹HNMR was used to evaluate conversion by adding methyl *tert*-butyl ether as internal standard, which is an easy and fast way to get the conversion. However, the error can be notable sometimes since MTBE is volatile. Besides, using methyl and t-butyl as standard, respectively, gave different integration of products. Alternatively, GC was used to determine conversion. This method

requires plotting a standard curve using a stock solution of different percentage products or substrates along with a high boiling point internal standard such as undecane. For the method to be accurate, each time you need to make a stock solution of crude and subject it to GC analysis, which is not an efficient way for high throughput screening. Another way is using the isolated yield of the recovered substrate to decide the conversion. This method is more straightforward, however, is not accurate when running small scale reactions. During the project, for those conversions decided by isolated yield, reactions were carried out on 0.2 mmol–0.5 mmol scale. Recently, many that study kinetic resolution, use the following equation to calculate conversion:

$$conversion (HPLC) = \frac{ee(sm)}{ee(sm) + ee(p)}$$

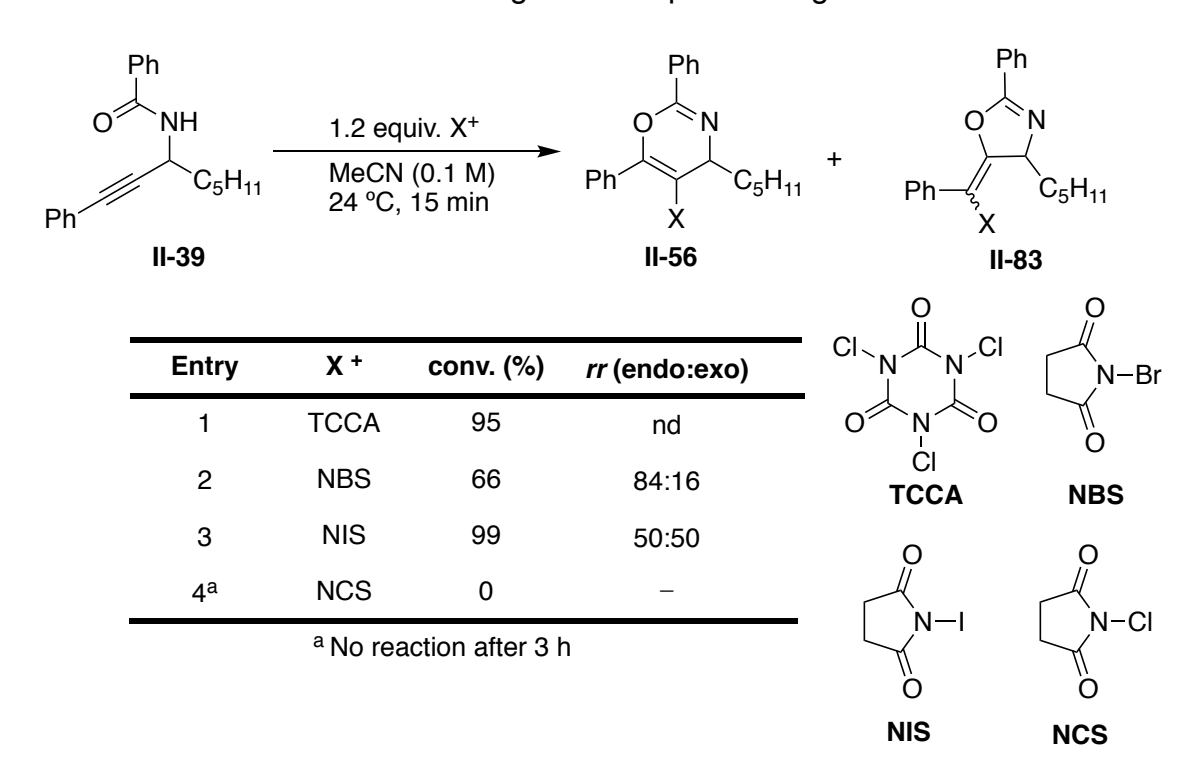
where ee_{sm} is enantiomeric excess of the recovered substrate and ee_p is the enantiomeric excess of product. In this case, conversion is only determined by ee which is measured by HPLC. To some degree, this helps to avoid the errors caused by direct measuring conversion. From now on, this conversion will be designated as C_{HPLC} wherever it appears.

2.2.2 Screening of the halogen sources

I started screening the reaction by choosing a halogen source that results in less background reaction. Substrate **II-39** was exposed to different types of electrophilic halogen sources in acetonitrile without adding catalyst. Reactions were quenched after 15 min to evaluate the background reaction rate. The more reactive electrophilic chlorine reagent trichloro*iso*cyanuric acid (TCCA) resulted in complicated products and the reaction was done after 15 min. *N*-bromosuccinimide leads to 66% conversion with both six-membered ring and five-membered ring regioisomer formation (84:16 ratio). Not

surprisingly the more electrophilic *N*-iodosuccinimide gave 99% conversion and endo/exo isomers in 1:1 ratio. Finally it was found that NCS (*N*-chlorosuccinimide) gave no reaction even after 3 hours at room temperature. Therefore, NCS was chosen as the optimal halogen source for catalytic reactions.

Table 2.1 Screening of electrophilic halogen source



2.2.3 Screening of solvents

With NCS as an optimal electrophilic chlorine reagent in hand, substrate **II-38** was used for screening solvent (Table 2.2). Chlorinated solvents including dichloromethane, dichloroethane and chloroform gave low conversion and ee for the recovered substrate. The selectivity factor for all reactions was around 2. Acetonitrile and CHCl₃/hexane led to incomplete reactions, even after extended time. More polar protic solvent *iso*-propanol still did not give full conversion, however they did increase the *ee* of the recovered substrate, the selectivity factor in *iso*-propanol went up to 9. This suggested that polar

protic solvents might be important for good enantioselectivity. The more polar trifluoroethanol (TFE) increased the reaction rate and ee greatly, but led to a 6% yield of the TFE incorporated side product **II-72**. Another fluorinated solvent hexafluoro-isopropanol (HFIP) avoided this side product and gave higher yield, however the enantioselectivity was lower, with S=29, while S=40 for TFE. Based on this, it was assumed that both good yield and enantioselectivity might be achieved through using different ratios of TFE/HFIP co-solvent system. However, it turned out that ee was generally worse than TFE alone when HFIP was used as a cosolvent and the TFE incorporated product **II-72** was always observed. Using other co-solvent combination, i.e. TFE and other non-fluorinated solvents like CHCl₃ and DCM led to decreased enantioselectivity, with S around 20 (Scheme 2.10, entry 12 and 13). Finally, TFE, HFIP and TFE-DCM (7:3) were used respectively for substrate scope analysis.

Table 2.2 Screening of solvent

entry	solvent	%conv ^a (%yield) ^b	%ee (II-55) ^c	% <i>ee</i> (<i>(S)</i> -II-38
1	DCM	14	75	9
2	DCE	20	72	10
3	CHCl ₃	20	68	13
4	MeCN	11	77	8
5	<i>i</i> -propanol	30	72	32
6	CHCl ₃ : hexane (1:1) 14	20	4
7	TFE	52 (44)	80	92
8	TFE: HFIP (1:1)	51(44)	80	84
9	TFE: HFIP (3:7)	51(44)	80	84
10	TFE: HFIP (1:9)	52 (43)	72	72
11	HFIP	51 (48)	78	86
12	CHCl ₃ : TFE (5:1)	37 (33)	89	51
13	DCM: TFE (5:1)	44 (40)	90	52
14	CH ₃ CN: TFE (5:1)	24	80	21

^a conversion is based on GC yields of unreacted substrate using undecane as internal standard; ^b yield of isolated product is reported;

2.2.4 Catalyst Study

Different loadings of catalyst were tried (Table 2.3). Typically, 10 mol% (DHQD)₂PHAL was used as catalyst. When the catalyst loading was 2 mol% and 5 mol%, *S* was 25 and 27 respectively, which are lower than that of 10 mol% catalyst. Therefore, 10 mol% (DHQD)₂PHAL was used as the optimal loading. For large scale reactions, the catalyst can be recycled by column chromatography using MeOH/EtOAc as eluent.

^c ee was determined by chiral HPLC.

Table 2.3 Catalyst loading study

catalyst loading	conversion% ^a	ratio (II-55:II-72) ^b	<i>ee</i> (II-55) ^c	<i>ee</i> (II-72) ^c	<i>ee</i> ((<i>S</i>)-II-38) ^c
2 mol%	50	7:1	81	88	82
5 mol%	50	6:1	82	86	83
10 mol%	52	6:1	80	88	92

^a conversion is based on GC yields of unreacted substrate using undecane as internal standard;

2.2.5 Temperature Study

Another important variable for screening is temperature. Low temperatures were tried for those substrates which gave low *ee* at room temperature, such as *p*-MeO phenyl and *p*-Me phenyl substrates **II-41** and **II-40** (Table 2.4). When the temperature was decreased to –10 °C, the reaction rate for both substrates reduced greatly. *p*-MeO phenyl substrate **II-41** only gave 42% conversion after 12 h in contrast of 50% conversion at room temperature after 1.5 h. Besides, the enantioselectivity was almost the same as that at room temperature in terms of *S*. For **II-40**, S was even worse at –10 °C than that at room temperature. For substrates that gave good enantioselectivity at room temperature, lowering the temperature had a drastic improvement in *S*. For example, S of phenyl substrate **II-39** increased from 18 to 27 when temperature was decreased from room temperature to –10 °C. Further decreasing the temperature from –10 °C to –30 °C increased the *S* further, albeit using a different solvent.

^b ratio is based on ¹H NMR; ^c ee is determined by chiral HPLC

Table 2.4 Temperature study for different substrates

temp (°C)	conv (%)	ee % ((<i>S</i>)-II-41)	ee % (II-59)	s ♭
23	50	20	4	1.8
-10	42	21	10	2.2
-30 ^a	57	32	22	2

t	emp (°C)	conv (%)	ee % ((<i>S</i>)-II-40)	ee % (II-58)	S ⁵
	23	55	63	86	11.5
	-10	30	25	29	4.8
	-30 ^a	52	82	76	18

temp (°C)	conv (%)	ee % ((<i>S</i>)-II-39)	ee % (II-56)	S ^b
23	56	91	91	18.5
-10	59	99	70	27
-30 ^a	51	99	91	210

 $^{^{\}rm a}$ TFE-DCM(V/V, 7:3) was used as solvent; $^{\rm b}$ conversion was determined by recovered substrate.

To get better solubility, TFE-DCM (v/v, 7:3) was used as solvent at -30 °C. Although reactions take longer time to complete, the enantioselectivity increased quite a bit. S for phenyl substrate **II-39** can be up to 210, which is almost as efficient as an enzyme

catalyzed kinetic resolution. But for *p*-MeO phenyl substrate **II-41**, *S* remains the same even at low temperature (–30 °C). *p*-Me phenyl substrate **II-40** had a slightly higher *S* at –30 °C as compared to room temperature. In summary, low temperature could help further increase the *S* of substrates that work well at room temperature, however, for those that gave poor enantioselectivity at room temperature, low temperature does not make a large difference.

2.2.6 Variations from standard condition

Other variables including catalyst and halogen sources were also investigated (Table 2.5). It is noteworthy that other C₂-symmetric cinchona alkaloid catalysts like (DHQD)₂Pyr and (DHQD)₂AQN did not induce any enantioselectivity and gave almost racemic products. Other halogenated succinimide, including NBS and NIS, gave no enantioselectivity as well.

Table 2.5 Variations from standard condition

entry	variaton from "standard" conditons	%ee (II-57) ^a	% <i>ee</i> ((<i>S</i>)-II-38) ^a
1	none	78	86
2	(DHQD) ₂ Pyr instead of (DHQD) ₂ PHAL	2	2
3	(DHQD)2AQN instead of (DHQD)2PHAL	7	6
4	NBS instead of NCS	2	0
5	NIS instead of NCS	0	0

a ee was determined by chiral HPLC

2.2.7 Substrates scope with TFE as solvent

After screening different conditions, TFE turned out to be the best solvent in terms of enantioselectivity. Substrates bearing a range of sterically and electronically diverse functionalities were tried using TFE as solvent, NCS as chlorinating reagent and (DHQD)₂PHAL as catalyst at room temperature. The TFE incorporated product was observed for most substrates (between 5% to 10%). The ratio of cyclized product to TFE incorporated product was indicated for some substrates. As shown in Scheme 2.6, the ees of some TFE incorporated products were as good as those of the cyclized products. The absolute stereochemistry of TFE incorporated product was not determined. However, based on indirect evidence based on the simple math of ee and conversion, it was

hypothesized that the TFE incorporated product has the same stereochemistry as the cyclized product. Phenyl substituted alkynes with less bulky R₂ (R₂ = pentyl, methyl) gave good enantioselectivity (Table 2.6, entries 1 and 2). Substrates with bulky R₂ groups, like t-butyl had slower reactions and poor enantioselectivity (Table 2.6, entry 11), leading to almost racemic cyclized product when conversion was 25% after 24 h. Besides alkyl substituents, aryl groups were also substituted for R₂, **II-47** was produced with moderate enantioselectivity (Table 2.6, entry 10). The electronic effect on R₁ was obvious and substituents on phenyl have a drastic effect on enantioselectivity. In general, electron rich phenyl and very electron poor aryls lead to lower ee, examples are p-MeO phenyl II-41 and p-NO₂ phenyl **II-45** (Table 2.6, entries 3 and 8). Reaction of **II-45** is sluggish with NCS as the chlorinating reagent and only 20% conversion was obtained when the more reactive DCDMH was used. If there is a strong electron donating group at the meta position of phenyl, the ee was still good (Table 2.6, entry 4). Moderately electron rich substituents such as p-Me and o-Me phenyl gave moderate ee (Table 2.6, entries 5 and 6). However, alkyl substituted alkynes were not compatible with this system (Table 2.6, entry 9). No enantioselectivity was observed for the alkyl substituted alkyne II-46. In terms of selectivity factor K_{rel} , as shown in Table 2.6, those for phenyl substituted alkynes K_{rel} were around 50, and for methyl substituted phenyls were slightly lower K_{rel} (36 and 48). Surprisingly, the electron-withdrawing F goup leads to a K_{rel} of up to 65, while the p-NO₂ substituted phenyl substrate was not resolved at all. Although K_{rel} is not an accurate parameter because of the reasons previously discussed, especially considering that side

products are formed, it still can be a straightforward reference to roughly compare the efficiency of a kinetic resolution.

Table 2.6 Substrate scope using TFE as solvent

$$\begin{array}{c} \text{NHBz} \\ \text{R}_{2} \\ \text{II-38-II-48} \end{array} \begin{array}{c} 0.55 \text{ equiv. NCS} \\ \hline 10 \text{ mol } \% \text{ (DHQD)}_{2}\text{PHAL,} \\ \text{TFE } (0.1 \text{ M}), \text{ rt} \\ \hline \end{array} \begin{array}{c} \text{Ph} \\ \text{O} \\ \text{N} \\ \text{R}_{1} \\ \end{array} \begin{array}{c} \text{NHBz} \\ \text{R}_{2} \\ \text{R}_{1} \\ \end{array} \begin{array}{c} \text{NHBz} \\ \text{R}_{2} \\ \end{array} \begin{array}{c} \text{BzHN} \\ \text{R}_{2} \\ \end{array} \begin{array}{c} \text{R}_{2} \\ \text{R}_{1} \\ \end{array} \begin{array}{c} \text{F}_{3}\text{CH}_{2}\text{CO} \\ \text{R}_{1} \\ \end{array} \begin{array}{c} \text{CI} \\ \text{R}_{1} \\ \end{array}$$

entry	substrate	R ₁	R ₂	%conv. ^a (%yield ^b)	<i>ee</i> % (II-55-II-63) ^c	<i>ee</i> % (II-38-II-48) ^c	ee % (II-72-II-76) ^f	\textit{K}_{rel}^{d}
1	II-38	Ph	methyl	50 (42)	80	89	90 (5%)	51
2	II-39	Ph	pentyl	54 (45)	84	98	83 (4%)	50
3	II-41	4-OMe-Ph	pentyl	50	21	20	-	2
4	II-42	3-OMe-Ph	pentyl	53 (41)	84	96	82 (9%)	48
5	II-40	4-Me-Ph	pentyl	56 (48)	86	63	-	5
6	II-43	2-Me-Ph	pentyl	55 (48)	74	97	77 (5%)	36
7	II-44	4-F-Ph	pentyl	53 (43)	85	98	78 (3%)	65
8 g	II-45	4-NO ₂ -Ph	pentyl	37 (15)	75	11	-	2
9 ^e	II-46	pentyl	pentyl	20	2	2	-	1
10	II-47	Ph	Ph	49 (35)	40	52	-	5
11	II-48	Ph	<i>t</i> -butyl	25	7	?	-	-

^a conversion was determined by recovered substrate yield;

2.2.8 Substrate scope with HFIP as solvent

Since the TFE incorporated product was always been observed when TFE was used as solvent, a polar, more acidic and non-nucleophilic alternative HFIP was tried (Table 2.7). The yield generally improved for most substrates, but the ee eroded slightly. Notably, p-CF $_3$ phenyl substrate II-49 gave much higher enantioselectivity as compared to the similarly electron-deficient p-NO $_2$ phenyl substrate II-45. Other aryl substituted substrates, such as 1-naphthalenyl, gave moderate enantioselectivity. Besides benzoyl, other amine protecting groups, including p-F benzoyl and p-Me benzoyl also performed well. The 4-F

^b yield of isolated cyclized product is reported;

^c ee was determined by chiral HPLC.

^d K_{rel} was calculated using equation $K_{rel} = \ln[(1-c)(1-ee)]/\ln[(1-c)(1+ee)]$, c is the conversion that determined by recoverd substrate

^e DCDMH was used instead of NCS, MeCN was used as solvent instead of TFE

f yield in parenthesis was for TFE incorporated product

⁹ DCDMH was used instead of NCS

benzoyl protecting group **II-51** gave lower *ee*, while the 4-Me benzoyl protecting group **II-52** gave better *ee* than benzoyl (Table 2.7, entries 2 and 12, entries 1 and 13).

Table 2.7 Substrate scope using HFIP as solvent

entry	substrate	e R ₁	R_2	R_3	%conv.a (%yieldb)	<i>ee</i> % (II-55-II-70) ^c	<i>ee</i> % (II-38-II-53) ^c	K_{rel}^{d}
1	II-38	Ph	methyl	Bz	51 (48)	77	80	18
2	II-39	Ph	pentyl	Bz	53 (51)	80	94	39
3	II-41	4-OMe-Ph	pentyl	Bz	42 (40)	22	19	2
4	II-42	3-OMe-Ph	pentyl	Bz	51 (51)	86	84	25
5	II-40	4-Me-Ph	pentyl	Bz	55 (52)	38	56	4
6	II-43	2-Me-Ph	pentyl	Bz	55 (51)	64	82	12
7	11-44	4-F-Ph	pentyl	Bz	55 (50)	80	92	23
8	II-45	4-NO2-Ph	pentyl	Bz	14	2	6	2
9	II-49	4-CF ₃ -Ph	methyl	Bz	37 (28)	64	42	9
10	II-50 1	-Naphthalenyl	methyl	Bz	55 (53)	48	66	6
11	II-46	pentyl	pentyl	Bz	20	2	0	1
12	II-51	Ph	pentyl	4-F-Bz	55 (53)	78	80	11
13	II-52	Ph	methyl	4-Me-Bz	54 (40)	73	97	43
14	II-47	Ph	Ph	Bz	50 (40)	44	52	5
15	II-53	Ph	Су	Bz	48 (43)	67	49	5

^a conversion was determined by recovered substrate yield;

2.2.9 Substrate scope with TFE-DCM as solvent at low temperature

From temperature studies, it was realized that low temperature can increase the enantioselectivity for most substrates. As a result, the scope of the transformation at –30 °C using TFE-DCM (v/v, 7/3) as co-solvent was evaluated. DCM can facilitate the solubility of substrates. The general trend is consistent with the results at room temperature. Phenyl rings bearing electron-donating substituents (4-OMe, 4-Me, 2-Me) led to a lower selectivity factor (Table 2.8, entries 3, 5 and 6). When R₂ is some sterically

^b yield of isolated cyclized product is reported;

c ee was determined by chiral HPLC;

 $^{^{\}rm d}$ K_{rel} was calculated using equation K_{rel} =ln[(1-c)(1-ee)]/ln[(1-c)(1+ee)], c is the conversion that is determined from recovered substrate.

demanding group, such as cyclohexyl and TBS protected silyl ether, K_{rel} dropped. Besides, aryl substituent R₂ (R₂ = phenyl) was not well tolerated in this system (Table 2.8, entry 10). Both electron-deficient and electron-rich protecting groups of amine gave good enantioselectivity (Table 2.8, entries 8 and 13). The efficiency of the kinetic resolution greatly improved under low temperature for most substrates. K_{rel} were generally above 100 for substrates that only gave K_{rel} up to 50 at room temperature in TFE. Substrate II-39 even gave K_{rel} up to 210, which is comparable with enzyme catalyzed kinetic resolution.

Table 2.8 Substrate scope using TFE-DCM as solvent at -30 °C

entry	substrate	e R ₁	R ₂	R ₃	%conv. ^a (%yield ^b)	<i>ee</i> % (II-55-II-71) ^c	ee % ((S)-II-38-II-54) ^c	<i>k</i> _{rel} ^d
1	II-38	Ph	methyl	Bz	50 (42)	88.7	94.6	132
2	II-39	Ph	pentyl	Bz	51 (46)	91	99	210
3	II-41	4-OMe-Ph	pentyl	Bz	57 (49)	22	32	2
4	II-42	3-OMe-Ph	pentyl	Bz	52 (40)	84	99.9	116
5	II-40	4-Me-Ph	pentyl	Bz	52 (45)	76	82	18
6	II-43	2-Me-Ph	pentyl	Bz	50 (38)	90	83	28
7	II-44	4-F-Ph	pentyl	Bz	51 (47)	94	97	119
8	II-51	Ph	pentyl	p-F-Bz	50 (44)	90	92	79
9	II-50	naphthalenyl	methyl	Bz	56 (49)	72	95	25
10	II-47	Ph	Ph	Bz	40 (33)	60	37	5
11	II-53	Ph	cyclohexyl	Bz	46 (42)	77	67	17
12	II-54	Ph p	ropyl-OTBS	Bz	48 (36)	92	77	21
13	II-52	Ph	methyl	p-Me-Bz	z 52 (40)	87	99	116

^a conversion was determined from recovered substrate yield;

2.2.10 Large scale reaction

Large scale kinetic resolutions were performed to evaluate its practicality. Substrate II-38 (0.84 g) was subjected to reaction conditions with TFE as solvent at ambient

^b yield of isolated cyclized product is reported;

^c ee was determined by chiral HPLC;

 $^{^{\}rm d}$ $K_{\rm rel}$ was calculated using equation $K_{\rm rel}$ =ln[(1-c)(1-ee)]/ln[(1-c)(1+ee)], c is the conversion that is determined from recovered substrate.

temperature. Considering the high cost of catalyst on large scale, catalyst loading was decreased to 2 mol%. The chlorocyclized product **II-55** was obtained in 68% *ee* and 45% of the substrate was recovered in 87% *ee*. Compared with the small-scale reaction, K_{rel} dropped greatly (K_{rel} is from 51 to 14).

Scheme 2.9 Large scale reaction

2.3 Kinetic resolution of racemic amides by dihalogenation

After developing the kinetic resolution of unsaturated amides via intramolecular cyclization, it was of interest to assess whether kinetic resolution of unsaturated amides can be achieved by intermolecular halofunctionalization. The Borhan group recently developed a highly regio-, diastereo-, and enantioselective vicinal dichlorination of allyl amides using (DHQD)₂PHAL as catalyst.¹⁷ This method represents an excellent catalyst-controlled stereo-discrimination process. Similarly, a successful kinetic resolution of racemic allyl amides requires a series of highly catalyst-controlled processes (Scheme 2.10). First, the catalyst should be able to discriminate between two enantiomers of allyl amides. Second, high face selectivity is required for olefin capture of electrophilic chlorine source, while potential olefin-to-olefin transfer can erode the stereochemical fidelity of the chlorenium intermediate. Third, the regioselectivity of chloride opening of chiral chlorenium ion will determine the *dr* and *ee* of the dichlorinated products.

Scheme 2.10 Two distinct stereoselective steps leading to diastereomers.

It has already been demonstrated that excellent catalyst control is possible in dichlorination of allyl amides,¹⁷ and thus the next step is to examine whether (DHQD)₂PHAL can efficiently resolve the two enantiomers of racemic allyl amides via dichlorination. The alkyl substituted (*Z*)-olefin **II-77** was subjected to the dichlorination condition, in which DCDMH and a large excess of LiCl was used as the electrophilic and nucleophilic chlorine source, respectively. However, the dichlorinated products were obtained in almost 1:1 *dr*. One of the diastereomers **II-78** had much higher *ee* than **II-79**. The absolute stereochemistry of the diastereomer **II-78** that had higher *ee* was confirmed by X-ray crystallography. This stereochemical outcome was consistent with the dichlorination of allyl amides which also lead to *anti*-dichlorination. The less reactive chlorine reagent NCS also gave 1:1 *dr* but good *ee* for the dichlorination product. To determine if both enantiomers can be pushed to dichlorination or undergo dynamic kinetic

resolution by adding 1.1 equiv NCS, however 33% of the starting material in almost pure enantiomeric form remained unreacted, suggesting a big difference for the reaction rate between the two enantiomers.

Table 2.9 Kinetic resolution of racemic allyl amides via dichlorination

CI+	Yield(II-78 and II-79) % ^a	Yield(II-77 recover) % ^a	dr (II-78:II-79) ^b	<i>ee</i> (II-78) % ^c	<i>ee</i> (II-79)% ^c	<i>ee</i> (II-77 recover) % ^c
DCDMH	53	36	1.1:1	88	47	100
NCS	44	40	1.2:1	100	60	65
NCSd	67	24	1.1:1	86	42	97

^a yield of isolated product is reported; ^b dr is determined from crude ¹H NMR;

Next the focus shifted to improving the diastereoselectivity of the reaction. Various conditions including changes in concentration, chloride source and catalyst were screened. The concentration of the reaction did not have an influence on *dr*. Other electrophilic chlorine sources like NCP gave 1:1 *dr* as well. The basic additive Na₂CO₃ did not improve *dr*. Other cinchona alkaloid dimer catalysts including (DHQD)₂Pyr and (DHQD)₂AQN gave 1:1 *dr* as well and proved sluggish in promoting the reaction. Quinidine derived thiocarbamate catalyst **II-80** gave chloro-cyclization product **II-81** instead of dichlorination product. When 100 equiv KCI was used as the nucleophilic chloride source, no dichlorination product was observed and instead the 5-member ring

^c ee was determined by chiral HPLC; ^d 1.1 equiv NCS was used.

product **II-81** was obtained. Since (DHQD)₂PHAL can effectively resolve aryl substituted allyl amides via chlorocyclization,¹⁵ the phenyl substituted substrate **II-82** was subjected to dichlorination condition, however complicated products were obtained. So far the catalytic system that has been developed is not capable of kinetic resolution of racemic amides through dichlorination.

Table 2.10 Screen variations from standard condition to improve dr

variations from standard condition	Yield(II-78 and II-79) %a	dr (II-78:II-79) ^b	
none	44	1.2:1	Ph. S =
0.1 M TFE instead of 0.2 M	46	1.2:1	N U
0.4 M TFE instead of 0.2 M	48	1.3:1	N.
NCP instead of NCS	42	1.2:1	
10 equiv LiCl instead of 100 equiv	50	1.2:1	OMe
add 1 equiv Na ₂ CO ₃	48	1.2:1	NO ₂
100 equiv KCl instead of LiCl	37 ^c	_	
10 mol% (DHQD) ₂ PHAL instead of 5 mol%,	rt 46	1.1:1	0
10 mol% (DHQD) ₂ Pyr instead of (DHQD) ₂ PHA	AL, rt 11	1.3:1	CI
10 mol% (DHQD) ₂ AQN instead of (DHQD) ₂ PH	AL, rt 21	1.2:1	II-81
10 mol II-80 instead of (DHQD) ₂ PHAL	23 ^c	_	01

^a yield of isolated products is reported; ^b *dr* is determined from crude ¹H NMR;

Scheme 2.11 Kinetic resolution of II-82

2.4 Summary

We have developed an efficient and practical kinetic resolution of propargyl amides via chlorocyclization using (DHQD)₂PHAL as the catalyst. *Kreis* were generally >20 and reached up to 210. This catalytic system is tolerated with various aryl substituted

^c yield was for cyclized product **II-81**.

propargyl amides. Electronic and steric modification of the aryl substituents have drastic impact on the K_{rel} . However, this kinetic resolution is not compatible with alkyl substituted propargyl amides. Kinetic resolution of allyl amides via intermolecular dichlorination was also evaluated. After exhaustive screening, the downside of poor dr of dichlorination products could not be circumvented.

2.5 Acknowledgement

Thanks are due to Mr. Mengke Fan who worked as an undergraduate research assistant in the lab during the duration of this project. He helped with the synthesis of substrates and executed many experiments.

2.6 Experimental Section

2.6.1 General Information

All reagents were purchased from commercial sources and were used without purification. (DHQD)₂PHAL and *N*-chlorosuccinimide were purchased from Aldrich. Trifluoroethanol and hexafluoro-*iso*propanol were purchased from Combi-Blocks. TLC analyses were performed on silica gel plates (pre-coated on glass; 0.20 mm thickness with fluorescent indicator UV254) and were visualized by UV or charred in KMnO₄ stains. ¹H and ¹³C NMR spectra were collected on 500 MHz NMR spectrometers (Agilent) using CDCl₃. Chemical shifts are reported in parts per million (ppm) and are referenced to residual solvent peaks. For HRMS (ESI) analysis, a Water 2795 (Alliance HT) instrument was used and referenced against Polyethylene Glycol (PEG-400-600). Flash silica gel (32-63 μm, Silicycle 60 Å) was used for column chromatography. All known compounds were characterized by ¹H and ¹³C

NMR and are in complete agreement with samples reported elsewhere. All new compounds were characterized by ¹H and ¹³C NMR, HRMS, and melting point (where appropriate). Enantiomeric excesses were determined using chiral HPLC (instrument: HP series 1100, Agilent 1260 infinity).

2.6.2 General Procedure for Screening and Optimization of Kinetic Resolution

A 5 mL vial equipped with a magnetic stir bar was charged with the substrate (0.2 mmol, 1 equiv) and catalyst (0.1 equiv). The mixture was dissolved in the appropriate solvent (0.1M) and was stirred at designated temperature for 5 min. *N*-chlorosuccinimide was then added to the reaction mixture and the reaction was stirred at the designated temperature until completion. The reaction was then quenched with saturated Na₂SO₃ and extracted with dichloromethane. The combined organics were dried over anhydrous Na₂SO₄ and filtered. Conversions were decided by GC analysis or ¹H NMR. Pure products and unreacted substrate were isolated by column chromatography on silica gel as stationary phase (EtOAc/Hexanes gradient).

2.6.3 Analytical data for cyclized products:

colorless gum, Rf: 0.85 (30% EtOAc in Hexane, UV)

¹H NMR (500 MHz, CDCl₃) δ 7.99 (d, *J* = 7 Hz, 2H), 7.78 (d, *J* = 7 Hz, 2H), 7.49 - 7.39 (m, 6H), 4.40 (q, *J* = 7 Hz, 1H), 1.57 (d, *J* = 6.5 Hz, 3H).

¹³C NMR (125 MHz, CDCl₃) δ 151.3, 143.3, 131.6, 131.4, 131.2, 129.3, 128.3, 128.2, 128.1, 127.4, 113.2, 54.5, 22.4

HRMS analysis (ESI): calculated for (M+H): $C_{17}H_{14}CINO$ 284.0842; found: 284.0857 Resolution of enantiomers: Daicel Chiralpak AD-H, 1% IPA- Hex, 0.5 mL/min; 254 nm, RT1 = 8.6 min, RT2 = 10.7 min.

$$[\alpha]_D^{20} = -27.8 \text{ (C 1.0, CH}_2\text{Cl}_2, ee = 89\%)$$

The structure and absolute stereochemistry was confirmed by X-ray crystallography:

colorless oil, R_f: 0.81 (30% EtOAc in Hexane, UV)

¹H NMR (500 MHz, CDCl₃) δ 7.99 (d, J = 7.5 Hz, 2H), 7.78 (d, J = 7.5 Hz, 2H), 7.49 - 7.39 (m, 6H), 4.39 (dd, J = 4 Hz, 2.5 Hz, 1H), 1.95 - 1.85 (m, 2H), 1.58 - 1.32 (m, 6H), 0.93 (t, J = 7 Hz, 3H).

¹³C NMR (125 MHz, CDCl₃) δ 163.9, 161.9, 151.3, 143.2, 131.4, 131.2, 130.4, 130.3, 128.3, 127.4, 115.3, 58.5, 34.9, 31.7, 23.9, 22.6, 14.1

HRMS analysis (ESI): calculated for (M+H): $C_{21}H_{22}CINO$ 340.1468; found: 340.1484 Resolution of enantiomers: Daicel Chiralpak AD-H, 1% IPA- Hex, 0.5 mL/min; 254 nm, RT1 = 8.07 min, RT2 = 8.75 min.

 $[\alpha]_D^{20} = -31.5$ (C 1.0, CH₂Cl₂, *ee* = 91%)

colorless oil, R_f: 0.77 (30% EtOAc in Hexane, UV)

¹H NMR (500 MHz, CDCl₃) δ 7.95 (d, J = 7 Hz, 2H), 7.48 - 7.25 (m, 7H), 4.47 (dd, J = 4 Hz, 2 Hz, 1H), 2.41 (s, 3H), 1.98 - 1.89 (m, 2H), 1.64 – 1.45 (m, 2H), 1.42 - 1.36 (m, 4H), 0.93 (t, J = 7 Hz, 3H).

¹³C NMR (125 MHz, CDCl₃) δ 171.2, 151.3, 145.3, 137.4, 131.4, 131.0, 130.4, 130.1, 129.7, 128.2, 127.5, 125.7, 113.0, 57.8, 34.8, 31.8, 23.9, 22.7, 19.5, 14.1

HRMS analysis (ESI): calculated for (M+H): C₂₂H₂₄CINO 354.1625; found: 354.1638

Resolution of enantiomers: Daicel Chiralpak IA, 1% IPA- Hex, 0.5 mL/min; 254 nm, RT1 = 7.57 min, RT2 = 9.6 min.

$$[\alpha]_D^{20} = -12.0 \text{ (C } 1.0, \text{ CH}_2\text{Cl}_2, ee = 90\%)$$

colorless oil, Rf: 0.88 (30% EtOAc in Hexane, UV)

¹H NMR (500 MHz, CDCl₃) δ 7.98 (d, J = 7.5 Hz, 2H), 7.65 (d, J = 7.5 Hz, 2H), 7.48 - 7.38 (m, 3H), 7.25 (d, J = 7.5 Hz, 2H), 4.36 (dd, J = 4 Hz, 2 Hz, 1H), 2.39 (s, 3H), 1.92 - 1.82 (m, 2H), 1.57 - 1.42 (m, 2H), 1.37 - 1.29 (m, 4H), 0.88 (t, J = 7 Hz, 3H).

¹³C NMR (125 MHz, CDCl₃) δ 151.5, 144.1, 139.4, 131.5, 131.1, 128.8, 128.3, 128.2, 127.5, 111.4, 58.6, 35.0, 31.8, 23.9, 22.6, 21.5, 14.1

HRMS analysis (ESI): calculated for (M+H): C₂₂H₂₅CINO 354.1625; found: 354.1640

Resolution of enantiomers: Daicel Chiralpak AD-H, 1% IPA- Hex, 0.5 mL/min; 254 nm, RT1 = 8.4 min, RT2 = 10.0 min.

 $[\alpha]D^{20} = -17.0 \text{ (C } 1.0, \text{ CH}_2\text{Cl}_2, ee = 76\%)$

colorless oil, R_f: 0.80 (30% EtOAc in Hexane, UV)

¹H NMR (500 MHz, CDCl₃) δ 7.97 (d, J = 7.5 Hz, 2H), 7.71 (d, J = 8.5 Hz, 2H), 7.48 - 7.38 (m, 3H), 6.96 (d, J = 8.5 Hz, 2H), 4.35 (dd, J = 4 Hz, 2 Hz, 1H), 3.84 (s, 3H), 1.95 - 1.79 (m, 2H), 1.57 – 1.40 (m, 2H), 1.35 - 1.30 (m, 4H), 0.88 (t, J = 7 Hz, 3H).

¹³C NMR (125 MHz, CDCl₃) δ 160.1, 151.5, 143.8, 131.6, 131.1, 129.7, 128.3, 127.4, 124.1, 113.5, 110.8, 58.6, 55.3, 35.0, 31.8, 23.9, 22.6, 14.1

HRMS analysis (ESI): calculated for (M+H): C₂₂H₂₅CINO₂ 370.1574; found: 370.1590 Resolution of enantiomers: Daicel Chiralpak AD-H, 1% IPA- Hex, 0.5 mL/min; 254 nm, RT1 = 10.3 min, RT2 = 11.4 min.

 $[\alpha]_D^{20} = +0.6 \text{ (C 1.0, CH}_2\text{Cl}_2, ee = 7\%)$

colorless oil, R_f: 0.76 (30% EtOAc in Hexane, UV)

¹H NMR (500 MHz, CDCl₃) δ 7.97 (d, J = 7.5 Hz, 2H), 7.47 - 7.29 (m, 6H), 6.95 (m, 1H), 4.36 (dd, J = 4 Hz, 2 Hz, 1H), 3.84 (s, 3H), 1.94 - 1.81 (m, 2H), 1.57 – 1.40 (m, 2H), 1.35 - 1.30 (m, 4H), 0.88 (t, J = 7 Hz, 3H).

¹³C NMR (125 MHz, CDCl₃) δ 159.2, 151.4, 143.9, 132.9, 131.4, 131.2, 129.2, 128.3,
127.5, 120.7, 114.9, 114.0, 112.2, 58.7, 55.4, 35.0, 31.8, 23.9, 22.6, 14.2

HRMS analysis (ESI): calculated for (M+H): C₂₂H₂₅CINO₂ 370.1574; found: 370.1604

Resolution of enantiomers: Daicel Chiralpak IA, 100% Hex, 0.2 mL/min; 254 nm, RT1 = 23.77 min, RT2 = 25.94 min.

 $[\alpha]_D^{20} = -10.5$ (C 1.0, CH₂Cl₂, ee = 84%)

colorless oil, Rf: 0.77 (30% EtOAc in Hexane, UV)

¹H NMR (500 MHz, CDCl₃) δ 8.03 (d, J= 10 Hz, 2H), 7.81 (dd, J= 1.5 Hz, 8 Hz, 2H), 7.49 – 7.32 (m, 11H), 5.36 (s, 1H)

¹³C NMR (125 MHz, CDCl₃) δ 151.7, 143.6, 141.2, 131.5, 131.4, 131.2, 129.6, 128.8, 128.4, 128.3, 128.2, 127.9, 127.7, 111.6, 58.7, 63.1

HRMS analysis (ESI): calculated for (M+H): C₂₂H₁₆CINO 346.0999; found: 346.1011

Resolution of enantiomers: Daicel Chiralpak AD-H, 2% IPA-Hex, 0.5 mL/min; 254 nm, RT1 = 11.38 min, RT2 = 15.9 min.

 $[\alpha]_D^{20} = -28.5$ (C 1.0, CH₂Cl₂, *ee* = 60%)

colorless oil, R_f: 0.77 (30% EtOAc in Hexane, UV)

¹H NMR (500 MHz, CDCl₃) δ 7.96 (d, *J* = 7 Hz, 2H), 7.75 (dd, *J* = 4 Hz, 5.5 Hz, 2H), 7.48 – 7.38 (m, 3H), 7.12 (t, *J* = 10 Hz, 2H), 4.36 (dd, J = 4.5 Hz, 2 Hz, 1H), 1.96 - 1.81 (m, 2H), 1.57 – 1.40 (m, 2H), 1.35 - 1.30 (m, 4H), 0.88 (t, *J* = 7 Hz, 3H).

¹³C NMR (125 MHz, CDCl₃) δ 163.9, 161.9, 151.3, 143.2, 131.2, 130.3, 129.7, 128.3, 127.8, 115.3, 111.9, 58.6, 34.9, 31.7, 23.9, 22.6, 14.1

HRMS analysis (ESI): calculated for (M+H): C₂₁H₂₁CIFNO 358.1374; found: 358.1390

Resolution of enantiomers: Daicel Chiralpak AD-H, 1% IPA-Hex, 0.5 mL/min; 254 nm, RT1 = 8.37 min, RT2 = 9.72 min.

 $[\alpha]_D^{20} = -6.3$ (C 1.0, CH₂Cl₂, ee = 94%)

colorless oil, Rf: 0.81 (30% EtOAc in Hexane, UV)

¹H NMR (500 MHz, CDCl₃) δ 8.28 (d, J = 8.5 Hz, 2H), 7.96 (d, J = 8.5 Hz, 3H), 7.50 – 7.40 (m, 4H), 4.38 (dd, J = 4.5 Hz, 2 Hz, 1H), 1.98 - 1.80 (m, 2H), 1.57 – 1.40 (m, 2H), 1.35 - 1.30 (m, 4H), 0.88 (t, J = 7 Hz, 3H)

¹³C NMR (125 MHz, CDCl₃) δ 150.9, 147.8, 142.2, 137.7, 131.4, 129.1, 128.8, 128.4, 127.4, 123.5, 115.2, 58.6, 34.9, 31.7, 23.9, 22.6, 14.1

HRMS analysis (ESI): calculated for (M+H): $C_{21}H_{21}CIN_2O_3$ 385.1319; found: 385.1337 Resolution of enantiomers: Daicel Chiralpak AD-H, 1% IPA-Hex, 1 mL/min; 254 nm, RT1 = 6.35 min, RT2 = 8.07 min.

 $[\alpha]_D^{20} = 6.2 \text{ (C 1.0, CH}_2\text{Cl}_2, ee = 75\%)$

$$O_2N$$
 O_2N
 O_1
 O_2N
 O_3
 O_4
 O_5
 O_7
 O_7
 O_7
 O_8
 O

colorless oil, Rf: 0.86 (30% EtOAc in Hexane, UV)

¹H NMR (500 MHz, CDCl₃) δ 8.40 – 8.25 (m, 2H), 8.09 – 7.95 (m, 4H), 7.68 – 7.40 (m, 3H), 5.25 (dd, J = 7.5, 3.3 Hz, 1H), 2.31 – 2.11 (m, 1H), 1.99 (dddd, J = 13.8, 10.4, 7.5, 5.1 Hz, 1H), 1.52 – 1.20 (m, 6H), 1.00 – 0.78 (m, 3H).

¹³C NMR (126 MHz, CDCl₃) δ 160.87, 156.44, 146.44, 141.13, 132.39, 128.79, 128.17, 127.92, 125.72, 123.50, 107.61, 72.21, 31.78, 31.55, 24.51, 22.51, 14.04.

HRMS analysis (ESI): calculated for (M+H): C₂₁H₂₁CIN₂O₃ 385.1319; found: 385.1329

colorless oil, Rf: 0.85 (30% EtOAc in Hexane, UV)

¹H NMR (500 MHz, CDCl₃) δ 7.86 (d, J = 8.5 Hz, 2H), 7.76 (d, J = 9 Hz, 2H), 7.45 - 7.40 (m, 3H), 7.20 (d, J = 8.5 Hz, 2H), 4.37 (q, J = 7 Hz, 1H), 2.39 (s, 3H), 1.55 (d, J = 7 Hz, 3H).

¹³C NMR (125 MHz, CDCl₃) δ 151.4, 143.3, 141.5, 131.7, 129.3, 129.0, 128.7, 128.3, 128.1, 127.4, 113.3, 54.5, 22.4, 21.5

HRMS analysis (ESI): calculated for (M+H): C₁₈H₁₇CINO 298.0999; found: 298.1006

Resolution of enantiomers: Daicel Chiralpak IA, 3% IPA- Hex, 0.5 mL/min; 254 nm, RT1

= 8.6 min, RT2 = 11.0 min.

 $[\alpha]_D^{20} = -23.7$ (C 1.0, CH₂Cl₂, *ee* = 87%)

colorless oil, Rf: 0.85 (30% EtOAc in Hexane, UV)

¹H NMR (500 MHz, CDCl₃) δ 7.98 (dd, J = 5 Hz, 3.5 Hz, 2H), 7.74 (dd, J = 8 Hz, 4 Hz, 2H), 7.46 - 7.39 (m, 3H), 7.07 (t, J = 8.5 Hz, 2H), 4.35 (q, J = 4 Hz, 2 Hz, 1H), 1.92 - 1.82 (m, 2H), 1.58 - 1.30 (m, 6H), 0.88 (t, J = 7 Hz, 3H)

¹³C NMR (125 MHz, CDCl₃) δ 165.7, 150.6, 144.0 137.7, 131.6, 129.7, 129.6, 129.4, 128.2, 128.1, 115.4, 58.5, 34.9, 31.7, 23.9, 22.6, 14.1

HRMS analysis (ESI): calculated for (M+H): $C_{21}H_{21}CIFNO$ 358.1374; found: 358.1389 Resolution of enantiomers: Daicel Chiralpak IA, 0.1% IPA-Hex, 0.3 mL/min; 254 nm, RT1 = 20.0 min, RT2 = 23.5 min.

 $[\alpha]_D^{20} = -29.6$ (C 1.0, CH₂Cl₂, *ee* = 88%)

colorless oil, Rf: 0.89 (30% EtOAc in Hexane, UV)

¹H NMR (500 MHz, CDCl₃) δ 8.02 – 7.79 (m, 4H), 7.70 (d, J = 8.2 Hz, 2H), 7.60 – 7.33 (m, 3H), 4.40 (q, J = 6.7 Hz, 1H), 1.57 (d, J = 6.8 Hz, 3H).

¹³C NMR (125 MHz, CDCl₃) δ 150.91, 142.13, 135.03, 135.02, 131.33, 131.12, 128.60, 128.36, 127.37, 125.14 (q, $J_{\text{C-F}}$ = 3.7 Hz), 125.11, 114.90, 54.47, 22.31.

HRMS analysis (ESI): calculated for (M+H): $C_{18}H_{13}CIF_3NO$ 352.0740; found: 352.0728 Resolution of enantiomers: Daicel Chiralpak AD-H, 1% IPA- Hex, 0.5 mL/min; 254 nm, RT1 = 8.2 min, RT2 = 9.0 min.

 $[\alpha]D^{20} = -26.0 \text{ (C 1.0, CH}_2\text{Cl}_2, ee = 64\%)$

R_f: 0.77 (30% EtOAc in Hexane, UV)

¹H NMR (500 MHz, CDCl₃) δ 7.97 - 7.88 (m, 5H), 7.65 (d, J = 7 Hz, 1H), 7.55 - 7.50 (m, 3H), 7.43 - 7.31 (m, 3H), 4.51 (q, J = 7 Hz, 1H), 1.66 (d, J = 7 Hz, 3H).

¹³C NMR (125 MHz, CDCl₃) δ 151.2, 143.6, 133.7, 131.4, 131.2, 130.9, 130.2, 129.1, 128.7, 128.6, 128.3, 127.6, 126.9, 126.2, 125.2, 125.1, 115.8, 54.0, 22.8

HRMS analysis (ESI): calculated for (M+H): $C_{21}H_{16}CINO$ 334.0999; found: 334.1016 Resolution of enantiomers: Daicel Chiralpak AD-H, 1% IPA- Hex, 1 mL/min; 254 nm, RT1 = 4.6 min, RT2 = 5.6 min.

 $[\alpha]_D^{20} = -37.9$ (C 1.0, CH₂Cl₂, ee = 72%)

colorless oil, R_f: 0.78 (30% EtOAc in Hexane, UV)

¹H NMR (500 MHz, CDCl₃) δ 8.0 (d, J = 7 Hz, 2H), 7.77 (d, J = 7 Hz, 2H), 7.49 - 7.38 (m, 6H), 4.24 (d, J = 3.5 Hz, 1H), 1.98 -1.59 (m, 7H), 1.35 -1.10 (m, 4 H)

¹³C NMR (125 MHz, CDCl₃) δ 151.5, 144.6, 131.8, 131.4, 129.3, 128.3, 128.1, 127.5, 111.1, 63.6, 42.2, 29.3, 26.9, 26.6, 26.4, 26.2

HRMS analysis (ESI): calculated for (M+H): C₂₂H₂₂CINO 352.1468; found: 352.1486

Resolution of enantiomers: Daicel Chiralpak AD-H, 1% IPA- Hex, 0.5 mL/min; 254 nm, RT1 = 8.5 min, RT2 = 9.7 min.

 $[\alpha]_D^{20} = -24.0 \text{ (C 1.0, CH}_2\text{Cl}_2, ee = 77\%)$

colorless oil, R_f: 0.87 (30% EtOAc in Hexane, UV)

¹H NMR (500 MHz, CDCl₃) δ 7.98 (dt, J = 7.3, 1.4 Hz, 2H), 7.84 – 7.68 (m, 2H), 7.57 – 7.32 (m, 6H), 4.41 (dd, J = 6.4, 3.9 Hz, 1H), 3.68 (t, J = 6.5 Hz, 2H), 2.08 – 1.59 (m, 4H), 0.87 (s, 9H), 0.03 (s, 6H).

¹³C NMR (125 MHz, CDCl₃) δ 151.50, 144.15, 131.63, 131.36, 131.15, 129.34, 128.26, 128.13, 127.45, 111.75, 63.04, 58.31, 31.35, 27.65, 25.98, 18.36, -5.24, -5.25.

HRMS analysis (ESI): calculated for (M+H): C₂₅H₃₃CINO₂Si 442.1969; found: 442.1974

Resolution of enantiomers: Daicel Chiralpak IA, 0.1% IPA- Hex, 1 mL/min; 254 nm, RT1

= 5.1 min, RT2 = 6.0 min.

 $[\alpha]_D^{20} = -33.2$ (C 1.0, CH₂Cl₂, ee = 92%)

colorless oil, Rr: 0.82 (30% EtOAc in Hexane, UV)

¹H NMR (500 MHz, CDCl₃) δ 8.10 – 7.91 (m, 2H), 7.84 – 7.66 (m, 2H), 7.55 – 7.32 (m, 6H), 4.07 (s, 1H), 1.11 (s, 9H).

¹³C NMR (126 MHz, CDCl₃) δ 152.16, 145.92, 132.01, 131.27, 131.09, 129.40, 128.60, 128.41, 128.20, 127.68, 110.15, 68.79, 39.49, 26.54.

HRMS analysis (ESI): calculated for (M+H): C₂₀H₂₁CINO 326.1312; found: 326.1316

colorless oil, Rf: 0.85 (30% EtOAc in Hexane, UV)

¹H NMR (500 MHz, CDCl₃) δ 7.96 (d, J = 7.5 Hz, 2H), 7.72 (d, J = 7.5 Hz, 2H), 7.50 - 7.38 (m, 6H), 4.45 (q, J = 7 Hz, 1H), 1.57 (d, J = 7 Hz, 3H)

¹³C NMR (125 MHz, CDCl₃) δ 151.5, 144.8, 132.7, 131.4, 131.2, 129.5, 128.7, 128.3, 128.1, 127.4, 104.0, 56.0, 23.0

HRMS analysis (ESI): calculated for (M+H): C₁₇H₁₅NOBr 328.0337; found: 328.0346

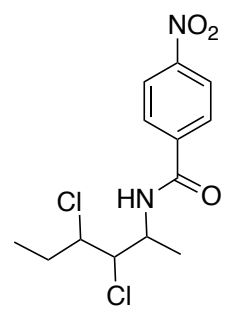
Resolution of enantiomers: Daicel Chiralpak AD-H, 1% IPA- Hex, 1 mL/min; 254 nm, RT1 = 4.3 min, RT2 = 5.1 min.

 $[\alpha]_D^{20} = +3.3 \text{ (C 1.0, CH}_2\text{Cl}_2, ee = 3\%)$

¹H NMR (500 MHz, CDCl₃) δ 7.80 – 7.74 (m, 2H), 7.53 – 7.46 (m, 3H), 7.47 – 7.34 (m, 5H), 6.32 (d, J = 8.1 Hz, 1H), 5.79 (dq, J = 8.1, 6.8 Hz, 1H), δ 4.27 (dq, J = 11.9, 8.6 Hz, 1H), 3.84 (dq, J = 11.8, 8.4 Hz, 1H), 1.46 (d, J = 6.8 Hz, 3H).

¹³C NMR (126 MHz, CDCl₃) δ 166.53, 148.81, 134.44, 131.61, 130.98, 130.75, 129.70, 129.66, 128.63, 128.44, 126.95, 124.31, 66.5 (q, J_{C-F} =34.78) 44.59, 18.86.

HRMS analysis (ESI): calculated for (M-H): C₁₉H₁₆NO₂CIF₃ 382.0822; found: 382.0820



II-78, II-79

major diastereomer ((*R*,*R*,*R*)-**II-78**):

¹H NMR (500 MHz, CDCl₃) δ 8.29 (d, J = 8.7 Hz, 2H), 7.97 – 7.82 (m, 2H), 6.59 (d, J = 8.4 Hz, 1H), 4.58 (ddd, J = 8.4, 6.7, 4.6 Hz, 1H), 4.39 (t, J = 4.8 Hz, 1H), 4.11 (dt, J = 8.2, 4.9 Hz, 1H), 2.00 – 1.84 (m, 2H), 1.42 (d, J = 6.7 Hz, 3H), 1.10 (t, J = 7.3 Hz, 3H). ¹³C NMR (126 MHz, CDCl₃) δ 164.74, 149.75, 139.54, 128.18, 123.93, 68.09, 64.99, 48.97, 29.01, 16.06, 10.68.

HRMS analysis (ESI): calculated for (M+H): C₁₃H₁₇N₂O₃Cl₂ 319.0616; found: 319.0623

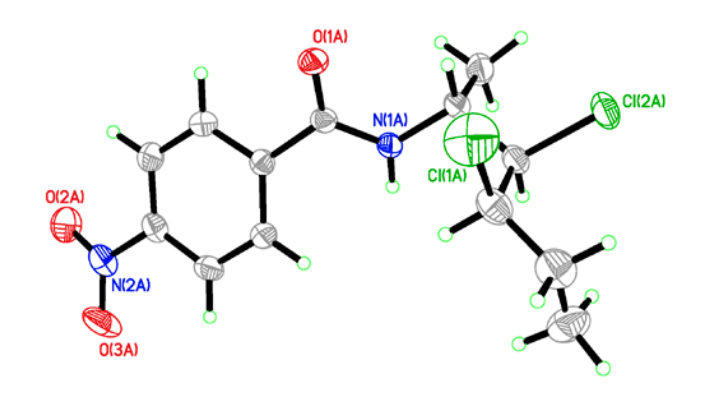
Resolution of enantiomers: Daicel Chiralpak OJ-H, 10% IPA- Hex, 1 mL/min; 254 nm, RT1 = 27.8 min, RT2 = 34.8 min.

minor diastereomer (II-79):

¹H NMR (500 MHz, Chloroform-*d*) δ 8.29 (d, J = 8.7 Hz, 2H), 7.97 – 7.82 (m, 2H), 6.59 (d, J = 8.4 Hz, 1H), 4.58 (ddd, J = 8.4, 6.7, 4.6 Hz, 1H), 4.39 (t, J = 4.8 Hz, 1H), 4.11 (dt, J = 8.2, 4.9 Hz, 1H), 2.00 – 1.84 (m, 2H), 1.42 (d, J = 6.7 Hz, 3H), 1.10 (t, J = 7.3 Hz, 3H). ¹³C NMR (126 MHz, cdcl₃) δ 164.74, 149.72, 139.76, 128.17, 123.95, 69.23, 65.87, 48.00, 28.73, 20.12, 11.04.

HRMS analysis (ESI): calculated for (M+H): $C_{13}H_{17}N_2O_3Cl_2$ 319.0616; found: 319.0625 Resolution of enantiomers: Daicel Chiralpak OJ-H, 15% IPA- Hex, 1 mL/min; 254 nm, RT1 = 18.1 min, RT2 = 27.9 min.

X-ray crystallography structure of the major diastereomer ((R,R,R)-II-78):



2.6.4 General procedure for synthesis of substrates:

General pathway A:

General pathway B:

General procedure for Mitsunobu reaction: To a solution of 3-butyn-2-ol (2.0 g, 28.5 mmol), pthalimide (8.2 g, 31.4 mmol) and triphenylphosphine (4.6 g, 31.4 mmol) in freshly distilled tetrahydrofuran was added dropwise di-*iso*propyl azodicarboxylate (6.3 g, 31.4 mmol) at 0 °C. Then the reaction mixture was stirred at room temperature for 3 h. Solvent was removed and the residue was triturated with ether to precipitate out

triphenylphosphine oxide. The white solid was filtered off and the filtrate was concentrated and purified on silica gel (15% EtOAc in hexane) to give 4.8 g of **II-84** as white solid (85% yield).

General procedure for Sonogashira coupling: CuI (2 mol%) and Pd(PPh₃)₂Cl₂ (1 mol%) were added to an oven-dried round bottom flask equipped with a stir bar. Anhydrous Et₃N (0.4 M) was added and flush with Argon. Propargyl phthalimide (1equiv) and corresponding aryl iodide (1 equiv) were then added into the reaction mixture. The reaction was stirred at room temperature for 8 h. After the reaction was complete, Et₃N was removed under reduced pressure. The crude residue was purified by silica column chromatography.

General procedure for cleavage of phthalimide: To a solution of phthalimide (3 mmol, 1 equiv) in EtOH (15 mL) was added hydrazine hydrate (18 mmol, 6 equiv) dropwise. The resulting mixture was stirred at 60 °C for 3 h. The formed white precipitate was then filtered through a thin layer of celite, washed with Et₂O and the solvent was removed under reduced pressure. The crude residue was purified by flash column chromatography over silica gel to afford the propargyl amine.

General procedure for protection of amine: Propargyl amine (1 equiv) was dissolved in freshly distilled dichloromethane at 0 °C. Et₃N (1.1 equiv) was added to the solution dropwise, followed by addition of benzoyl chloride (1 equiv) in one portion. After the reaction was complete, water was added to the reaction mixture. The organic layer was separated and dried over Na₂SO₄. The crude residue, obtained after removal of solvent was purified by column chromatography with silica gel.

General pathway C:

$$Ph = + R O = \frac{1.1 \text{ equiv } n\text{-BuLi}}{\text{THF, } -78 \text{ °C to rt}} = \frac{OH}{R} = \frac{1.1 \text{ equiv } PPh_3}{1.1 \text{ equiv } DIAD} = \frac{1.1 \text{ equiv } DIAD} = \frac{1.1 \text{ eq$$

Procedure for the synthesis of propargyl alcohol: To a solution of phenyl acetylene (6 mmol, 1 equiv) in anhydrous THF (24 mL) at –78 °C was added a solution of *n*-BuLi (2.5 M in THF, 6 mmol, 2.4 mL) dropwise. After stirring at the same temperature for 15 min, the corresponding aldehyde (6 mmol, 1 equiv) was added and was stirred for 1 h before saturated NH₄Cl (30 mL) was added. The organic layer was separated and the aqueous phase was extracted twice with EtOAc (2X20 mL). The combined organic layers were dried over anhydrous Na₂SO₄, filtered and concentrated. The crude was purified by column chromatography over silica gel to afford propargyl alcohol.

From propargyl alcohol to amide, the procedure is same as the **path A** and **path B** sequence: Mitsunobu reaction, cleavage of phthalimide and protection of amine.

2.6.5. Analytical data for kinetic resolution substrates and intermediates:

II-84 was synthesized through general procedure for Mitsunobu reaction with 3-butyn-2-ol (2.00 g, 28.50 mmol) in 85% yield.

Rf: 0.57 (30% EtOAc in Hexane, UV)

white solids; M.P.: 80 °C -85 °C

¹H NMR (500 MHz, CDCl₃) δ 7.84 (dd, J = 5.4, 3.1 Hz, 2H), 7.71 (dd, J = 5.5, 3.0 Hz, 2H), 5.20 (qd, J = 7.2, 2.5 Hz, 1H), 2.33 (d, J = 2.5 Hz, 1H), 1.70 (d, J = 7.2 Hz, 3H).

¹³C NMR (126 MHz, CDCl₃) δ 166.88, 134.13, 131.83, 123.44, 81.08, 71.19, 36.85, 20.06.

HRMS analysis (ESI): calculated for (M+H): C₁₂H₁₀NO₂ 200.0712; found: 200.0712

II-85 was synthesized through general procedure for Mitsunobu reaction with 1-octyn-2-ol(1.00g, 7.92 mmol) in 85% yield.

yellow oil, Rf: 0.69 (30% EtOAc in Hexane, UV)

¹H NMR (500 MHz, CDCl₃) δ 7.87 (dd, J = 5.4, 3.1 Hz, 2H), 7.74 (dd, J = 5.5, 3.0 Hz, 2H), 5.03 (td, J = 8.0, 2.5 Hz, 1H), 2.36 (d, J = 2.5 Hz, 1H), 2.17 – 1.98 (m, 2H), 1.39 – 1.24 (m, 6H), 0.92 – 0.82 (m, 3H).

¹³C NMR (126 MHz, CDCl₃) δ 167.07, 134.12, 131.75, 123.45, 80.35, 71.78, 41.50, 33.31, 30.97, 25.91, 22.42, 13.95.

HRMS analysis (ESI): calculated for (M+H): C₁₆H₁₈NO₂ 256.1338; found: 256.1350

II-86 was synthesized from **II-85** (1.60 g, 4.83 mmol) through general procedure of cleavage of phthalimide and protection gave 55% yield in two steps as colorless oil.

R_f: 0.63 (30% EtOAc in Hexane, UV)

¹H NMR (500 MHz, CDCl₃) δ 7.81 – 7.70 (m, 2H), 7.41 (dt, J = 41.0, 7.4 Hz, 3H), 6.61 (d, J = 9.2 Hz, 1H), 4.92 (tdd, J = 8.3, 6.3, 2.4 Hz, 1H), 2.27 (d, J = 2.4 Hz, 1H), 1.83 – 1.61 (m, 2H), 1.45 (dp, J = 10.7, 3.5 Hz, 2H), 1.28 (dq, J = 7.1, 3.3 Hz, 4H), 0.90 – 0.78 (m, 3H).

¹³C NMR (126 MHz, CDCl₃) δ 166.50, 134.00, 131.64, 128.52, 127.10, 83.32, 71.27, 41.85, 35.72, 31.28, 25.32, 22.50, 14.00.

HRMS analysis (ESI): calculated for (M+H): C₁₅H₂₀NO 230.1545; found: 230.1559

II-87 was synthesized though general pathway C with cyclohexyl carboxaldehyde (6 mmol) in 71% yield.

yellow oil, R_f: 0.75 (30% EtOAc in Hexane, UV)

¹H NMR (500 MHz, CDCl₃) δ 7.42 (dq, J = 5.9, 2.1 Hz, 2H), 7.34 – 7.23 (m, 3H), 4.36 (td, J = 6.0, 2.1 Hz, 1H), 1.97 – 1.83 (m, 2H), 1.81 – 1.70 (m, 3H), 1.73 – 1.56 (m, 1H), 1.31 – 1.05 (m, 5H).

¹³C NMR (126 MHz, CDCl₃) δ 131.68, 128.32, 128.26, 122.72, 109.99, 89.18, 67.72, 44.32, 28.65, 28.20, 26.39, 25.92, 25.90.

II-88 was synthesized though general pathway **C** with benzaldehyde (5 mmol) in 99% yield.

yellow oil, R_f: 0.68 (30% EtOAc in Hexane, UV)

¹H NMR (500 MHz, CDCl₃) δ 7.64 (dd, J = 7.2, 1.8 Hz, 2H), 7.55 – 7.26 (m, 8H), 5.71 (d, J = 6.2 Hz, 1H), 2.37 – 2.26 (m, 1H).

¹³C NMR (126 MHz, CDCl₃) δ 140.61, 131.75, 128.69, 128.62, 128.47, 128.31, 126.74, 122.38, 88.65, 86.68, 65.14.

II-38 was synthesized through path **A**. **II-84** was subjected to the Sonagashira coupling condition with iodobenzene (2.1 mmol) to afford corresponding phthalimide in 100% yield. Then phthalimide was cleaved and protected with benzoyl group according general procedure, leading to 78% yield of **II-38** in two steps as white solids; M.P.: 115 °C -120 °C.

R_f: 0.78 (30% EtOAc in Hexane, UV)

¹H NMR (500 MHz, CDCl₃) δ 7.85 – 7.72 (m, 2H), 7.54 – 7.44 (m, 1H), 7.41 (ddd, J = 8.7, 5.1, 2.7 Hz, 4H), 7.34 – 7.24 (m, 3H), 6.53 (d, J = 8.1 Hz, 1H), 5.26 (dq, J = 8.0, 6.8 Hz, 1H), 1.58 (d, J = 6.8 Hz, 3H).

¹³C NMR (125 MHz, CDCl₃) δ 166.2, 134.1, 131.7, 131.6, 128.6, 128.4, 128.3, 127.0, 122.5, 89.3, 82.6, 38.2, 22.7

HRMS analysis (ESI): calculated for (M+H): $C_{17}H_{15}NO$ 250.1232; found: 250.1239 Resolution of enantiomers: Daicel Chiralpak AD-H, 15% IPA- Hex, 1.0 mL/min; 254 nm, RT1 = 5.2 min, RT2 = 6.1 min.

$$[\alpha]D^{20} = -42.4$$
 (C 1.0, CH₂Cl₂, $ee = 95\%$)

II-39 was synthesized with **II-86** (2 mmol) through path **B**, Sonagashira coupling gave 90% yield as white solids;

white solids; M.P.: 84 °C - 92 °C

R_f: 0.72 (30% EtOAc in Hexane, UV)

¹H NMR (500 MHz, CDCl₃) δ 7.80 (d, J = 7 Hz, 2H), 7.49 -7.38 (m, 5H), 7.28 - 7.26 (m, 3H), 6.57 (d, J = 7 Hz, 1H), 5.19 (dd, J = 7 Hz, 1H), 1.86 -1.80 (m, 2H), 1.55-1.52 (m, 2H), 1.34 -1.29 (m, 4H), 0.87 (t, J = 7 Hz, 3H)

13C NMR (125 MHz, CDCl₃) δ 166.4, 134.2, 131.8, 131.6, 128.5, 128.3, 127.1, 122.7, 88.6,
83.2, 45.2, 36.1, 31.4, 25.5, 22.6, 14.0

HRMS analysis (ESI): calculated for (M+H): $C_{21}H_{23}NO$ 306.1858; found: 306.1878 Resolution of enantiomers: Daicel Chiralpak AD-H, 15% IPA- Hex, 1.0 mL/min; 254 nm, RT1 = 5.5 min, RT2 = 5.9 min.

 $[\alpha]_D^{20} = -33.6 \text{ (C 1.0, CH}_2\text{Cl}_2, ee = 99\%)$

II-40 was synthesized with **II-86** (0.87 mmol) through path **B**, Sonagashira coupling gave 86% yield as white solids; M.P.: 83 °C - 87 °C

R_f: 0.73 (30% EtOAc in Hexane, UV)

¹H NMR (500 MHz, CDCl₃) δ 7.78 (d, J = 7 Hz, 2H), 7.51 -7.41 (m, 3H), 7.30 (d, J = 7 Hz, 2H), 7.09 (d, J = 7 Hz, 2H), 6.31 (d, J = 7 Hz, 1H), 5.17 (dd, J = 7 Hz, 1H), 2.32 (s, 3H), 1.82 (m, 2H), 1.56-1.54 (m, 2H), 1.35 -1.23 (m, 4H), 0.88 (t, J = 7 Hz, 3H)

13C NMR (125 MHz, CDCl₃) δ 166.2, 138.5, 134.2, 131.6, 129.0, 128.6, 127.0, 119.5, 87.8,
83.4, 42.6, 36.2, 31.4, 25.4, 22.5, 21.5, 14.0

HRMS analysis (ESI): calculated for (M+H): C₂₂H₂₅NO 320.2014; found: 320.2027

Resolution of enantiomers: Daicel Chiralpak IA, 10% IPA- Hex, 0.5 mL/min; 254 nm, RT1

= 14.3 min, RT2 = 15.6 min.

 $[\alpha]_D^{20} = -27.9 \text{ (C 1.0, CH}_2\text{Cl}_2, ee = 82\%)$

II-43 was synthesized with **II-86** (2.0 mmol) through path **B**, Sonagashira coupling gave 85% yield as white solids; M.P.: 68 °C - 71 °C

R_f: 0.69 (30% EtOAc in Hexane, UV)

¹H NMR (500 MHz, CDCl₃) δ 7.78 (d, J = 7 Hz, 2H), 7.52 -7.37 (m, 4H), 7.23 - 7.18 (m, 2H), 7.17 - 7.09 (m, 1H), 6.30 (d, J = 7 Hz, 1H), 5.21 (dd, J = 7 Hz, 1H), 2.41 (s, 3H), 1.89 -1.82 (m, 2H), 1.58-1.54 (m, 2H), 1.35 -1.32 (m, 4H), 0.88 (t, J = 7 Hz, 3H)

¹³C NMR (125 MHz, CDCl₃) δ 166.3, 140.2, 132.0, 131.6, 129.4, 128.6, 128.4, 127.0, 125.5, 122.4, 92.4, 82.2, 42.8, 36.2, 31.4, 25.5, 22.6, 20.8, 14.0

HRMS analysis (ESI): calculated for (M+H): C₂₂H₂₅NO 320.2014; found: 320.2036

Resolution of enantiomers: Daicel Chiralpak AD-H, 15% IPA- Hex, 1 mL/min; 254 nm, RT1 = 5.0 min, RT2 = 5.4 min.

 $[\alpha]_D^{20} = -25.7$ (C 1.0, CH₂Cl₂, *ee* = 83%)

II-41 was synthesized with **II-86** (0.74 mmol) through path **B**, Sonagashira coupling gave 95% yield as white solids; M.P.: 69 °C - 73 °C

R_f: 0.60 (30% EtOAc in Hexane, UV)

¹H NMR (500 MHz, CDCl₃) δ 7.78 (d, J = 7 Hz, 2H), 7.48 (t, J = 7 Hz, 1H), 7.42 (t, J = 7 Hz, 2H), 7.34 (d, J = 7 Hz, 2H), 6.81 (d, J = 7 Hz, 2H), 6.31 (d, J = 7 Hz, 1H), 5.15 (dd, J = 7 Hz, 1H), 3.79 (s, 3H), 1.84 -1.80 (m, 2H), 1.55-1.52(m, 2H), 1.35 -1.32 (m, 4H), 0.88 (t, J = 7 Hz, 3H)

¹³C NMR (125 MHz, CDCl₃) δ 166.2, 159.6, 134.2, 133.2, 131.6, 128.6, 127.0, 114.7, 113.9, 87.1, 83.2, 55.3, 42.6, 36.2, 31.4, 25.4, 22.5, 14.0

HRMS analysis (ESI): calculated for (M+H): C₂₂H₂₅NO₂ 336.1964; found: 336.1980

Resolution of enantiomers: Daicel Chiralpak IA, 5% IPA- Hex, 0.5 mL/min; 254 nm, RT1 = 33.5 min, RT2 = 37.2 min.

 $[\alpha]_D^{20} = -3.5^{\circ}$ (C 1.0, CH₂Cl₂, ee = 20%)

II-42 was synthesized with **II-86** (0.74 mmol) through path **B**, Sonagashira coupling gave 99% yield white solids; M.P.: 69 °C - 73 °C

R_f: 0.60 (30% EtOAc in Hexane, UV)

¹H NMR (500 MHz, CDCl₃) δ 7.79 (d, J = 7.5 Hz, 2H), 7.48 – 7.40 (m, 3H), 7.18 (t, J = 8 Hz, 1H), 7.00 (d, J = 8 Hz, 1H), 6.86 (s, 1H), 6.45 (d, J = 8 Hz, 1H), 5.17 (dd, J = 7 Hz, 8 Hz, 1H), 3.79 (s, 3H), 1.86 -1.80 (m, 2H), 1.55-1.52(m, 2H), 1.34 -1.30 (m, 4H), 0.88 (t, J = 7 Hz, 3H)

¹³C NMR (125 MHz, CDCl₃) δ 166.3, 159.3, 134.2, 131.6, 129.4, 128.6, 127.0, 124.3, 123.6, 116.6, 114.9, 88.4, 83.2, 55.3, 42.5, 36.2, 31.6, 31.3, 25.5, 22.5, 14.0 HRMS analysis (ESI): calculated for (M+H): $C_{17}H_{14}CINO$ 336.1964; found: 336.1975 Resolution of enantiomers: Daicel Chiralpak AD-H, 15% IPA- Hex, 1 mL/min; 280 nm, RT1 = 6.7 min, RT2 = 7.8 min.

 $[\alpha]_D^{20} = -30.4$ (C 1.0, CH₂Cl₂, ee = 99%)

II-53 was synthesized through path **C** with **II-87** (1.56 mmol) in 53% yield for 3 steps.

white solids; M.P.: 145 °C - 152 °C

Rf: 0.61 (30% EtOAc in Hexane, UV)

¹H NMR (500 MHz, CDCl₃) δ 7.79 (d, J = 9 Hz, 2H), 7.51 - 7.48 (m, 1H), 7.44 - 7.41 (m, 4H), 7.29 - 7.27 (m, 3H), 6.37 (d, J = 9 Hz, 1H), 5.09 (dd, J = 6 Hz, 2.5 Hz, 1H), 1.92 - 1.66 (m, 7H), 1.28 -1.21 (m, 4H),

13C NMR (125 MHz, CDCl₃) δ 166.4, 134.3, 131.8, 131.7, 128.6, 128.3, 127.0, 122.7, 87.4,
 84.1, 47.5, 42.8, 29.5, 28.5, 26.3, 26.0, 25.9

HRMS analysis (ESI): calculated for (M+H): C₂₂H₂₃NO 318.1858; found: 318.1876

Resolution of enantiomers: Daicel Chiralpak AD-H, 10% IPA- Hex, 1 mL/min; 228 nm, RT1 = 8.2 min, RT2 = 9.0 min.

 $[\alpha]_D^{20} = -19.4$ (C 1.0, CH₂Cl₂, ee = 67%)

II-45 was synthesized with **II-86** (1.3 mmol) through path **B**, Sonagashira coupling gave product as white solids in 66% yield.

white solids; M.P.: 120 °C - 125 °C

R_f: 0.60 (30% EtOAc in Hexane, UV)

¹H NMR (500 MHz, CDCl₃) δ 8.15 (d, J = 8.5 Hz, 2H), 7.79 - 7.77 (d, J = 9 Hz, 2H), 7.56 - 7.49 (m, 3H), 7.44 (t, J = 8 Hz, 2H), 6.27 (d, J = 8.5 Hz, 1H), 5.20 (dd, J = 7 Hz, 8.5 Hz, 1H), 1.88 -1.83 (m, 2H), 1.55 – 1.50 (m, 2H), 1.39 -1.33 (m, 4H), 0.88 (t, J = 7 Hz, 3H) ¹³C NMR (125 MHz, CDCl₃) δ 166.4, 147.1, 133.9, 132.5, 131.9, 129.6, 128.7, 128.5, 127.0, 123.5, 94.1, 81.4, 42.4, 35.8, 31.3, 25.5, 22.5, 14.0

HRMS analysis (ESI): calculated for (M+H): $C_{21}H_{22}N_2O_3$ 351.1709; found: 351.1720 Resolution of enantiomers: Daicel Chiralpak AD-H, 15% IPA- Hex, 1 mL/min; 254 nm, RT1 = 11.2 min, RT2 = 12.9 min.

 $[\alpha]_D^{20} = -3.0^{\circ}$ (C 1.0, CH₂Cl₂, *ee* = 11%)

II-44 was synthesized with **II-86** (0.74 mmol) through path **B**, Sonagashira coupling gave 99% yield product as white solids; M.P.: 80 °C - 86 °C.

R_f: 0.60 (30% EtOAc in Hexane, UV)

¹H NMR (500 MHz, CDCl₃) δ 7.78(d, J = 7 Hz, 2H), 7.44 - 7.37 (m, 4H), 6.98 (t, J = 7 Hz, 2H), 6.32 (d, J = 7 Hz, 1H), 5.15 (dd, J = 7 Hz, 1H), 1.84 - 1.81 (m, 2H), 1.55 - 1.51 (m, 2H), 1.35 -1.32 (m, 4H), 0.88 (t, J = 7 Hz, 3H)

¹³C NMR (125 MHz, CDCl₃) δ 166.3, 134.1, 133.6, 131.7, 128.6, 127.0, 118.7, 115.6, 115.5, 88.3, 82.2, 42.5, 36.1, 31.3, 25.5, 22.5, 14.0

HRMS analysis (ESI): calculated for (M+H): C₂₁H₂₂FNO 324.1764; found: 324.1787

Resolution of enantiomers: Daicel Chiralpak AD-H, 15% IPA- Hex, 1 mL/min; 254 nm, RT1 = 6.09 min, RT2 = 6.4 min.

 $[\alpha]_D^{20} = -30.4$ (C 1.0, CH₂Cl₂, ee = 97%)

II-52 was synthesized through path **A** with **II-84** (7.03 mmol), propargyl amine was protected with *p*-toluoylchloride according general procedure, leading to 75% yield of **II-52** as white solids; M.P.: 92 °C - 100 °C

R_f: 0.53 (30% EtOAc in Hexane, UV)

¹H NMR (500 MHz, CDCl₃) δ 7.71(d, J = 7.5 Hz, 2H), 7.44 - 7.43 (m, 2H), 7.32 -7.26 (m, 5H), 6.35 (d, J = 8 Hz, 1H), 5.27 (dd, J = 8 Hz, 6.5 Hz, 1H), 2.40 (s, 3H), 1.60 (d, J = 6.5 Hz, 3H)

¹³C NMR (125 MHz, CDCl₃) δ 166.2, 131.8, 131.2, 130.2, 129.2, 129.1, 128.4, 128.3, 127.0, 89.4, 82.5, 38.1, 22.8, 21.5

HRMS analysis (ESI): calculated for (M+H): C₁₈H₁₇NO 264.1388; found: 264.1404

Resolution of enantiomers: Daicel Chiralpak IA, 10% IPA- Hex, 0.5 mL/min; 254 nm, RT1

= 19.0 min, RT2 = 24.0 min.

 $[\alpha]_D^{20} = -24.9 \text{ (C 1.0, CH}_2\text{Cl}_2, ee = 99\%)$

II-47 was synthesized through path **C** with **II-88** (4.88 mmol). **II-88** was subjected to Mitsunobu reaction to afford phthalimide in 50% yield. Phthalimide was cleaved and protected with benzoyl group to get 44% yield of **II-47** in two steps.

white solids; M.P.: 164 °C - 171 °C

Rf: 0.64 (30% EtOAc in Hexane, UV)

¹H NMR (500 MHz, CDCl₃) δ 7.80(d, J = 7.5 Hz, 2H), 7.64 (d, J = 7Hz, 2H), 7.50 - 7.37 (m, 7H), 7.34 - 7.31 (m, 4H), 6.63 (d, J = 8.5 Hz, 1H), 6.47 (d, J = 8 Hz, 1H)

¹³C NMR (125 MHz, CDCl₃) δ 166.3, 139.0, 133.8, 131.9, 130.2, 128.8, 128.6, 128.5,
 128.4, 128.2, 127.2, 127.1, 122.4, 86.9, 85.1, 45.6

HRMS analysis (ESI): calculated for (M+H): C₂₂H₁₇NO 312.1388; found: 312.1408

Resolution of enantiomers: Daicel Chiralpak IA, 15% IPA- Hex, 1 mL/min; 254 nm, RT1

= 8.6 min, RT2 = 10.8 min.

 $[\alpha]_D^{20} = -2.9$ (C 1.0, CH₂Cl₂, ee = 82%)

II-50 was synthesized through path **A** with **II-84** (3.92 mmol), Sonagashira coupling with 1-iodonapthalene gave 70% yield of phthalimde, then pthalimide cleavage and protection gave 21% yield of **II-50** for two steps.

white solids; M.P.: 114 °C - 120 °C

R_f: 0.47 (30% EtOAc in Hexane, UV)

¹H NMR (500 MHz, CDCl₃) δ 8.27(d, J = 8.5 Hz, 1H), 7.83 - 7.80 (m, 4H), 7.65 (d, J = 6.5 Hz, 1H), 7.56 - 7.38 (m, 6H), 6.44 (d, J = 7 Hz, 1H), 5.41 (q, J = 7.5 Hz, 1H), 1.72 (d, J = 7 Hz, 3H)

¹³C NMR (125 MHz, CDCl₃) δ 166.3, 134.1, 133.3, 133.1, 131.7, 130.7, 128.9, 128.6, 128.3, 127.0, 126.9, 126.7, 126.4, 126.0, 125.2, 94.2, 80.7, 38.5, 22.9

HRMS analysis (ESI): calculated for (M+H): $C_{21}H_{17}NO$ 300.1388; found: 300.1397

Resolution of enantiomers: Daicel Chiralpak AD-H, 15% IPA- Hex, 1 mL/min; 254 nm, RT1 = 5.7 min, RT2 = 7.1··min.

 $[\alpha]_D^{20} = -30.1$ (C 1.0, CH₂Cl₂, ee = 95%)

II-49 was synthesized through path **A** with **II-84** (5.02 mmol), Sonagashira coupling with 1-iodo-4-(trifluoromethyl)benzene (5.02 mmol) gave 64% yield of phathalimde, then phthalimide cleavage and protection gave 45% yield of **II-49** for two steps.

white solids; M.P.: 141 °C - 150 °C

R_f: 0.58 (30% EtOAc in Hexane, UV)

¹H NMR (500 MHz, CDCl₃) δ 7.78(d, J = 8.5 Hz, 2H), 7.54 - 7.48 (m, 5H), 7.42 (t, J = 8 Hz, 2H), 6.41 (d, J = 8 Hz, 1H), 5.27 (q, J = 7.5 Hz, 1H), 1.58 (d, J = 7 Hz, 3H) ¹³C NMR (125 MHz, CDCl₃) δ 166.3, 133.9, 132.0, 131.8, 128.6, 127.0, 125.2, 91.9, 81.2, 38.0, 22.5 HRMS analysis (ESI): calculated for (M+H): $C_{18}H_{14}F_3NO$ 318.1106; found: 318.1113 Resolution of enantiomers: Daicel Chiralpak IA, 10% IPA- Hex, 0.5 mL/min; 254 nm, RT1 = 16.3 min, RT2 = 18.0 min.

 $[\alpha]_D^{20} = -13.3 \text{ (C } 1.0, \text{ CH}_2\text{Cl}_2, ee = 42\%)$

II-51 was synthesized through path **B** with **II-85** (1.5 mmol). Propargyl amine was protected with *p*-F-benzoylchloride in 81% yield. Then Sonagashira coupling of protected propargyl amine with iodobenzene gave **II-51** in 91% yield.

yellow solids; M.P.: 65 °C - 70 °C

Rf: 0.49 (30% EtOAc in Hexane, UV)

¹H NMR (500 MHz, CDCl₃) δ 7.80 (dt, J = 6 Hz, 2H), 7.40 (m, 2H), 7.30 - 7.27 (m, 3H), 7.08 (t, J = 9 Hz, 2H), 6.40 (d, J = 8.5 Hz, 1H), 5.15 (q, J = 7.5 Hz, 1H), 1.86 -1.78 (m, 2H), 1.56 -1.50 (m, 2H), 1.34 -1.30 (m, 4H), 0.88 (t, J = 7.5 Hz, 3H)

¹³C NMR (125 MHz, CDCl₃) δ 165.8, 165.3, 163.8, 131.8, 130.4, 129.4, 129.3, 128.3,
122.6, 115.7, 115.5, 88.4, 83.4, 42.7, 36.2, 31.3, 25.5, 22.5, 14.0

HRMS analysis (ESI): calculated for (M+H): C₂₁H₂₂FNO 324.1764; found: 324.1778

Resolution of enantiomers: Daicel Chiralpak AD-H, 15% IPA- Hex, 1 mL/min; 254 nm, RT1 = 5.1 min, RT2 = 5.8 min.

 $[\alpha]_D^{20} = -24.3$ (C 1.0, CH₂Cl₂, *ee* = 87%)

II-46 was synthesized starting with 1-heptyne (5.2 mmol). Procedure is same as path **C**. white solids; M.P.: 36 °C - 41 °C

Rf: 0.80 (30% EtOAc in Hexane, UV)

¹H NMR (500 MHz, CDCl₃) δ 7.81 – 7.68 (m, 2H), 7.56 – 7.35 (m, 3H), 6.17 (d, J = 8.8 Hz, 1H), 4.89 (dtd, J = 8.1, 5.8, 2.8 Hz, 1H), 2.16 (tdd, J = 7.1, 2.2, 1.0 Hz, 2H), 1.79 – 1.59 (m, 2H), 1.53 – 1.38 (m, 4H), 1.37 – 1.21 (m, 8H), 0.93 – 0.81 (m, 6H).

¹³C NMR (125 MHz, CDCl₃) δ 166.17, 134.37, 131.50, 128.54, 126.92, 83.89, 79.27, 42.35, 36.35, 31.36, 31.04, 28.37, 25.39, 22.55, 22.18, 18.62, 14.01, 13.99.

HRMS analysis (ESI): calculated for (M-H): C₂₀H₂₈NO 298.2171; found: 298.2173

II-89 was synthesized according to the reported literature. 18

II-54 was synthesized through procedure **C** with **II-89** (3.4 mmol), phthalimide was obtained in 56% yield for 2 steps; **II-54** was obtained in 60% yield for two steps.

vellow solids; M.P.: 45 °C - 52 °C

Rf: 0.70 (30% EtOAc in Hexane, UV)

¹H NMR (500 MHz, CDCl₃) δ 7.82 – 7.74 (m, 2H), 7.51 – 7.35 (m, 5H), 7.28 (dd, J = 5.3, 2.0 Hz, 3H), 6.66 (d, J = 8.3 Hz, 1H), 5.24 (dt, J = 8.2, 6.6 Hz, 1H), 3.78 – 3.56 (m, 2H), 2.03 – 1.62 (m, 4H), 0.88 (d, J = 8.7 Hz, 9H), 0.10 – -0.04 (m, 6H).

¹³C NMR (125 MHz, CDCl₃) δ 166.33, 134.21, 131.76, 131.66, 131.62, 128.57, 128.34, 128.26, 128.21, 127.04, 122.64, 88.33, 83.38, 62.70, 42.21, 32.75, 29.01, 25.98, 25.95, 25.92, 18.39, -5.20, -5.27.

HRMS analysis (ESI): calculated for (M-H): C₂₅H₃₂NO₂Si 406.2202; found: 406.2212

Resolution of enantiomers: Daicel Chiralpak AD-H, 5% IPA- Hex, 1 mL/min; 254 nm, RT1

= 6.2 min, RT2 = 6.8 min.

 $[\alpha]_D^{20} = -25.8$ (C 1.0, CH₂Cl₂, ee = 77%)

II-48 was synthesized through path **C** with pivaldehyde (6 mmol).

white solids; M.P.: 80 - 82 °C

Rf: 0.69 (30% EtOAc in Hexane)

¹H NMR (500 MHz, Chloroform-*d*) δ 7.85 – 7.72 (m, 2H), 7.53 – 7.38 (m, 5H), 7.28 (dd, J = 5.1, 1.9 Hz, 3H), 6.27 (d, J = 9.6 Hz, 1H), 5.07 (d, J = 9.6 Hz, 1H), 1.11 (s, 9H). ¹³C NMR (126 MHz, cdcl₃) δ 166.65, 134.43, 131.72, 131.67, 128.66, 128.29, 128.27, 127.00, 122.77, 87.48, 83.89, 51.31, 36.35, 26.14.

HRMS analysis (ESI): calculated for (M+H): C₂₀H₂₂NO 292.1701; found: 292.1707

Path D:

II-91 was synthesized according to our groups' previous work.¹⁹ **II-91**(1.2 g, 4.8 mmol) was dissolved in EtOAc (30 mL). To the solution was added Lindlar's catalyst (200 mg). The reaction mixture was degassed for 3 times under vacuum and then stirred under H₂ balloon for 12 h. After the reaction was complete, filter the catalyst thru celite and remove solvent to afford the crude. Purify the compound through flash column chromatography (silica gel, 15% EtOAc in Hexane) to get final product as white solid (90% yield).

R_f =0.55 (30% EtOAc in Hexane)

white solid; M.P. = 47 - 51°C

¹H NMR (500 MHz, CDCl₃) δ 8.23 (d, J = 8.8 Hz, 2H), 7.89 (d, J = 8.8 Hz, 2H), 6.23 (d, J = 7.5 Hz, 1H), 5.57 – 5.47 (m, 1H), 5.30 (tt, J = 10.5, 1.6 Hz, 1H), 4.97 (dddd, J = 8.8, 7.6, 6.6, 1.1 Hz, 1H), 2.16 (td, J = 7.5, 1.6 Hz, 2H), 1.30 (d, J = 6.7 Hz, 3H), 0.97 (t, J = 7.5 Hz, 3H).

¹³C NMR (126 MHz, cdcl₃) δ 164.41, 149.39, 140.41, 134.59, 129.69, 128.13, 123.68, 43.70, 21.76, 21.09, 14.18.

HRMS analysis (ESI): calculated for (M+H): $C_{13}H_{17}N_2O_3$ 249.1239; found: 249.1245 Resolution of enantiomers: Daicel Chiralpak OJ-H, 15% IPA- Hex, 0.5 mL/min; 254 nm, RT1 = 21.1 min, RT2 = 25.8 min.

2.7 ¹H NMR study

In order to elucidate the nature that catalyst can differentiate two enantiomers of substrate and therefore lead to different reaction rate, we did solvent-suppression ¹H NMR in trifluoroethanol which is the reaction solvent. Enantiopure (*R*)- and (*S*)- substrate **1a** were mixed with stoichiometric amount of (DHQD)₂PHAL in trifluoroethanol. The methyl proton shows slightly different chemical shift. This observation indicates that different binding affinity between enantiomers and catalyst lead to different reaction rate.

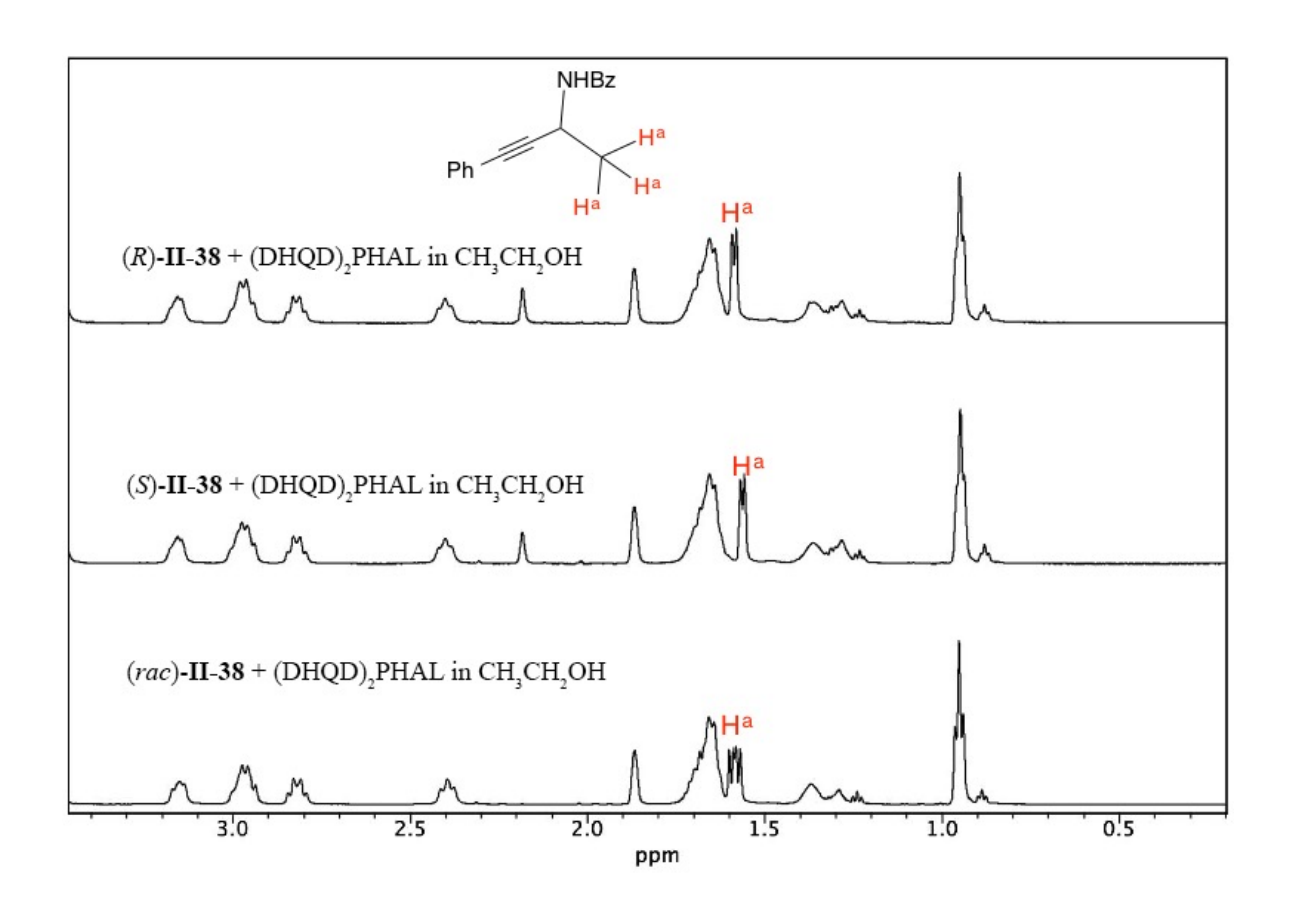
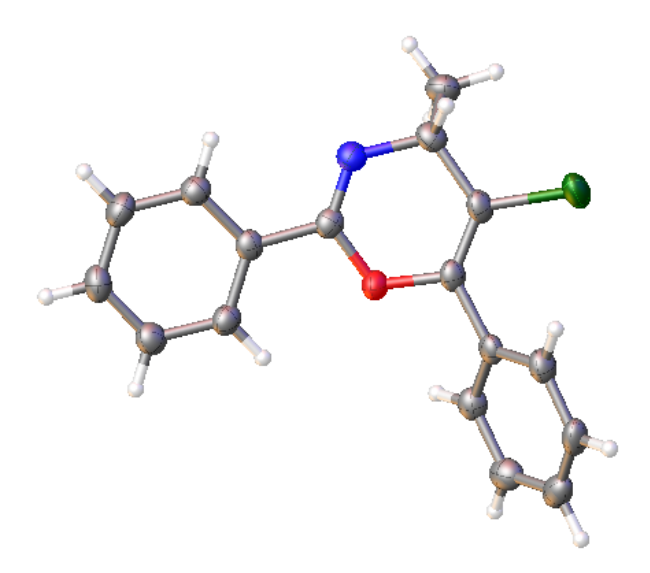


Figure 2.2 Stoichiometric NMR studies of substrate-catalyst mixtures in CF₃CH₂OH at ambient temperature and 0.02 M concentration of substrate and catalyst.

2.8 X-ray crystallography structure data

2.8.1 X-ray crystal structure data of II-55

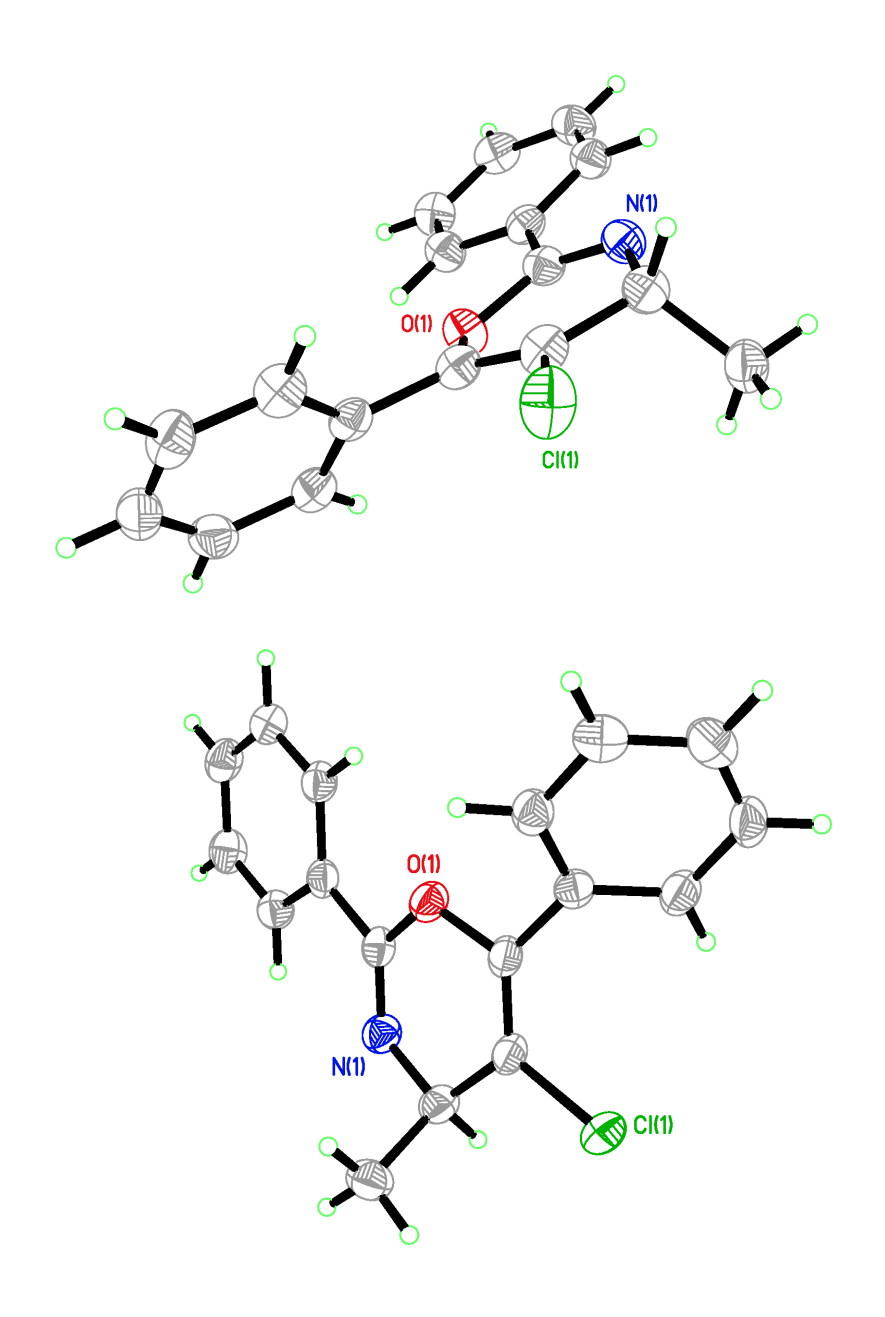


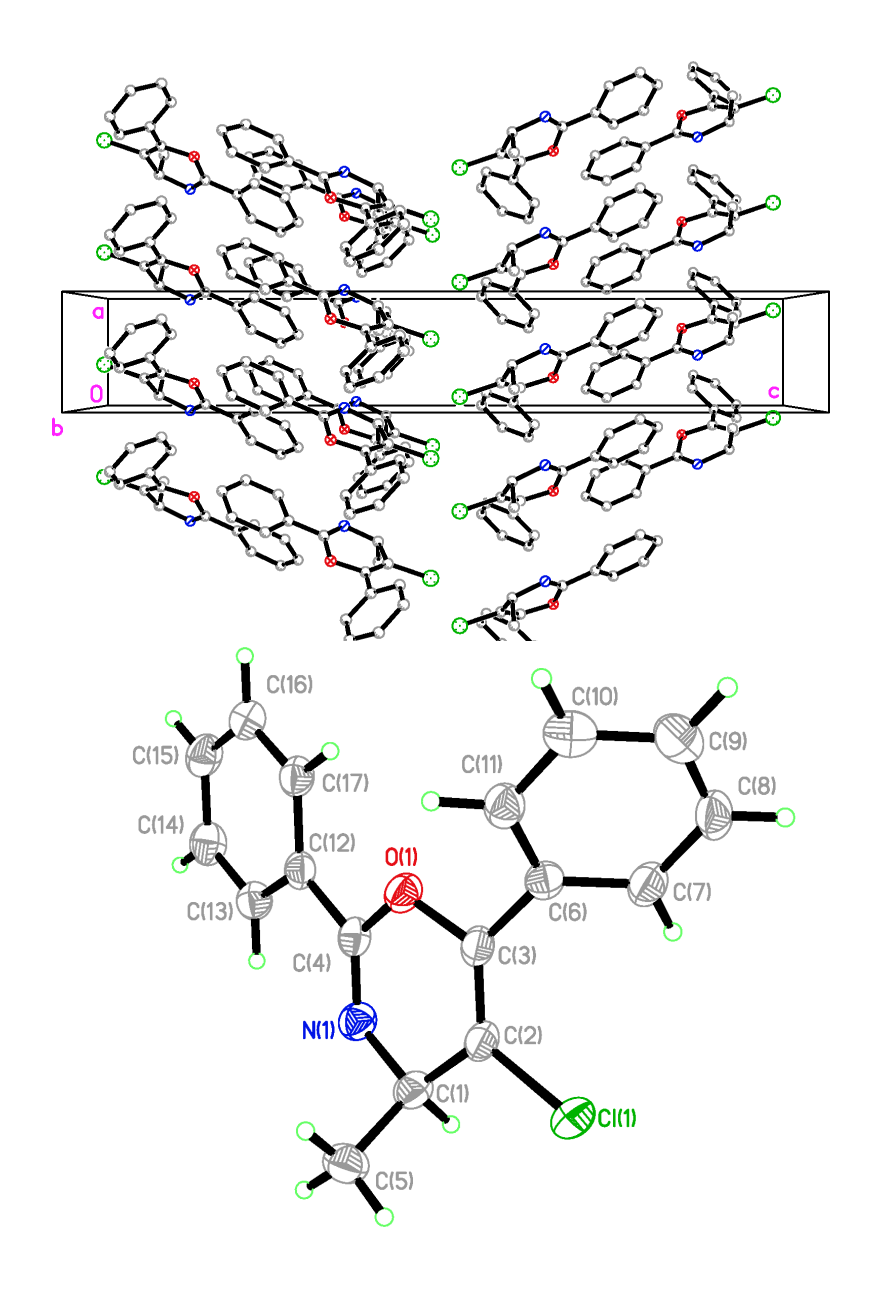
Experimental. Single colourless needle-shaped crystals of (**BB614a**) were used as supplied. A suitable crystal ($0.54 \times 0.08 \times 0.06 \text{ mm}^3$) was selected and mounted on a nylon loop with paratone oil on a Bruker APEX-II CCD diffractometer. The crystal was kept at T = 173(2) K during data collection. Using **Olex2** (Dolomanov et al., 2009), the structure was solved with the **SheIXS** (Sheldrick, 2008) structure solution program, using the Direct Methods solution method. The model was refined with version 2013-4 of **XL** (Sheldrick, 2008) using Least Squares minimisation.

Crystal Data. C₁₇H₁₄CINO, M_r = 283.74, orthorhombic, P2₁2₁2₁ (No. 19), a = 4.5922(3) Å, b = 10.4221(5) Å, c = 29.1253(13) Å, α = β = γ = 90 °, V = 1393.95(13) Å³, T = 173(2) K, Z = 4, Z' = 1.000, μ (CuK $_{\alpha}$) = 2.369, 13565 reflections measured, 2712 unique (R_{int} = 0.0823) which were used in all calculations. The final wR_2 was 0.0978 (all data) and R_1 was 0.0410 (I > 2(I)).

Crystal data and structure refinement

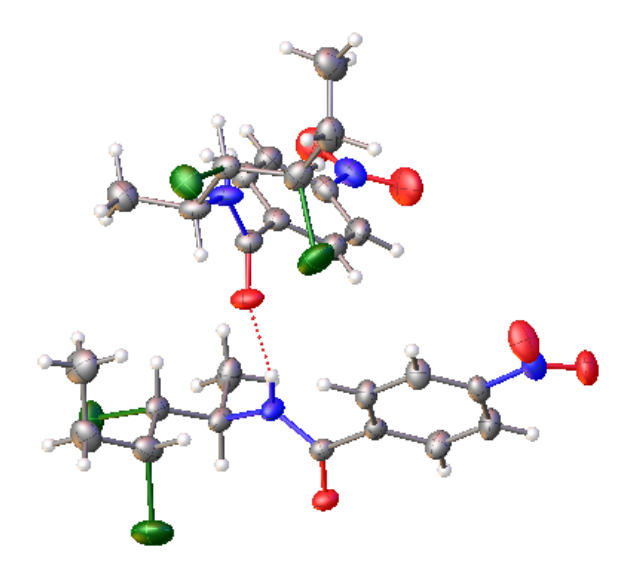
CCDC n/a Formula C ₁₇ H ₁₄ CINO D _{calc} / g cm ⁻³ 1.352 μ/mm ⁻¹ 2.369 Formula Weight 283.74 Colour colourless Shape needle Max Size/mm 0.08 Mid Size/mm 0.06 T/K 173(2) Crystal System orthorhombic Space Group P2₁2121 a/Å 4.5922(3) b/Å 10.4221(5) c/Å 29.1253(13) α/² 90 β/² 90 γ/² 1.000 Θ _{min} /² 3.034 Θ _{max} /² 72.147 Measured Refl. 13565 Independent Refl. 2712 Reflections Use	Compound	BB614a
Formula $C_{17}H_{14}CINO$ D_{calc}/g g cm-3 1.352 μ /mm-1 2.369 Formula Weight 283.74 Colour colourless Shape needle Max Size/mm 0.08 Min Size/mm 0.06 T/K 173(2) Crystal System orthorhombic Space Group P212121 $a/Å$ 4.5922(3) $b/Å$ 10.4221(5) $c/Å$ 29.1253(13) $\alpha/^\circ$ 90 $\beta/^\circ$ 90 $y/^\circ$ 90 $y/^$	•	
μ /mm ⁻¹ 2.369 Formula Weight 283.74 Colour colourless Shape needle Max Size/mm 0.54 Mid Size/mm 0.08 Min Size/mm 0.06 T/K 173(2) Crystal System orthorhombic Space Group P212121 $a/Å$ 4.5922(3) $b/Å$ 10.4221(5) $c/Å$ 29.1253(13) $\alpha/^\circ$ 90 $\beta/^\circ$ 90 $\gamma/^\circ$ 9		C ₁₇ H ₁₄ CINO
μ /mm ⁻¹ 2.369 Formula Weight 283.74 Colour colourless Shape needle Max Size/mm 0.54 Mid Size/mm 0.08 Min Size/mm 0.06 T/K 173(2) Crystal System orthorhombic Space Group P212121 $a/Å$ 4.5922(3) $b/Å$ 10.4221(5) $c/Å$ 29.1253(13) $\alpha/^\circ$ 90 $\beta/^\circ$ 90 $\gamma/^\circ$ 9	D _{calc} ./ g cm ⁻³	1.352
Formula Weight 283.74 Colour colourless Shape needle Max Size/mm 0.54 Mid Size/mm 0.08 Min Size/mm 0.06 T/K $173(2)$ Crystal System orthorhombic Space Group $P2:12:12:1$ $a/Å$ $4.5922(3)$ $b/Å$ $10.4221(5)$ $c/Å$ $29.1253(13)$ α/C 90 β/C 90 γ/C 90 β/C 90 β/C 90 β/C 90 β/C 90 β/C 90	_	2.369
Colour colourless Shape needle Max Size/mm 0.54 Mid Size/mm 0.08 Min Size/mm 0.06 T/K 173(2) Crystal System orthorhombic Space Group $P2_12_12_1$ $a/Å$ $4.5922(3)$ $b/Å$ $10.4221(5)$ $c/Å$ $29.1253(13)$ $\alpha/^\circ$ 90 $\beta/^\circ$ 90 $\gamma/^\circ$ 90	•	
Max Size/mm 0.54 Mid Size/mm 0.06 T/K 173(2) Crystal System orthorhombic Space Group $P2_12_12_1$ $a/Å$ $4.5922(3)$ $b/Å$ $10.4221(5)$ $c/Å$ $29.1253(13)$ $\alpha/^\circ$ 90 $\beta/^\circ$ 90 $\gamma/^\circ$ 1.000 <t< td=""><td>_</td><td>colourless</td></t<>	_	colourless
Max Size/mm 0.08 Min Size/mm 0.06 T/K 173(2) Crystal System orthorhombic Space Group $P2_12_12_1$ $a/Å$ $4.5922(3)$ $b/Å$ $10.4221(5)$ $c/Å$ $29.1253(13)$ $\alpha/^\circ$ 90 $\beta/^\circ$ 90 $\gamma/^\circ$ 90	Shape	needle
Min Size/mm 0.06 T/K 173(2) Crystal System orthorhombic Space Group $P2_12_12_1$ $a/Å$ $4.5922(3)$ $b/Å$ $10.4221(5)$ $c/Å$ $29.1253(13)$ $\alpha/^\circ$ 90 $\beta/^\circ$ 90 $\gamma/^\circ$	•	0.54
T/K 173(2) Crystal System orthorhombic Space Group $P2_12_12_1$ $a/Å$ $4.5922(3)$ $b/Å$ $10.4221(5)$ $c/Å$ $29.1253(13)$ $\alpha/°$ 90 $\beta/°$ 90 $\gamma/°$ 90 </td <td>Mid Size/mm</td> <td>0.08</td>	Mid Size/mm	0.08
Crystal System orthorhombic Space Group $P2_12_12_1$ $a/Å$ $4.5922(3)$ $b/Å$ $10.4221(5)$ $c/Å$ $29.1253(13)$ $\alpha/^\circ$ 90 $\beta/^\circ$ 90 $\gamma/^\circ$	Min Size/mm	0.06
Crystal System orthorhombic Space Group $P2_12_12_1$ $a/Å$ $4.5922(3)$ $b/Å$ $10.4221(5)$ $c/Å$ $29.1253(13)$ $\alpha/^\circ$ 90 $\beta/^\circ$ 90 $\gamma/^\circ$	T/K	173(2)
$a/Å$ $4.5922(3)$ $b/Å$ $10.4221(5)$ $c/Å$ $29.1253(13)$ $\alpha/^{\circ}$ 90 $\beta/^{\circ}$ 90 $\gamma/^{\circ}$ 90	Crystal System	orthorhombic
$b/Å$ $10.4221(5)$ $c/Å$ $29.1253(13)$ $\alpha/^{\circ}$ 90 $\beta/^{\circ}$ 90 $\gamma/^{\circ}$ 1000 0.000 900 $\gamma/^{\circ}$	Space Group	P2 ₁ 2 ₁ 2 ₁
$c/Å$ $29.1253(13)$ $\alpha/^{\circ}$ 90 $\beta/^{\circ}$ 90 $\gamma/^{\circ}$ 1000 90 90 $\gamma/^{\circ}$ 1000 90 90 $\gamma/^{\circ}$ 1000 90 90 90 90 90 90 90 90 90 90 90 90 90 90 90 9	a/Å	4.5922(3)
$\alpha/^{\circ}$ 90 $\beta/^{\circ}$ 90 $\gamma/^{\circ}$ 90 V/\mathring{A}^3 1393.95(13) Z 4 Z' 1.000 $\Theta_{min}/^{\circ}$ 3.034 $\Theta_{max}/^{\circ}$ 72.147 Measured Refl. 13565 Independent Refl. 2712 Reflections Used 2246 R_{int} 0.0823 Parameters 182 Restraints 0 Largest Peak 0.174 Deepest Hole -0.174 GooF 1.027 wR_2 (all data) 0.0978 WR_2 0.0915 R_1 (all data) 0.0553		10.4221(5)
β/l° 90 γ/l° 90 V/l^{3} 1393.95(13) Z 4 Z' 1.000 Θ_{min}/l° 3.034 Θ_{max}/l° 72.147 Measured Refl. 13565 Independent Refl. 2712 Reflections Used 2246 R_{int} 0.0823 Parameters 182 Restraints 0 Largest Peak 0.174 Deepest Hole -0.174 GooF 1.027 wR_2 (all data) 0.0978 wR_2 0.0915 R_1 (all data) 0.0553	<i>c</i> /Å	29.1253(13)
$\gamma/^{\circ}$ 90 V/ų 1393.95(13) Z 4 Z' 1.000 $\Theta_{min}/^{\circ}$ 3.034 $\Theta_{max}/^{\circ}$ 72.147 Measured Refl. 13565 Independent Refl. 2712 Reflections Used 2246 R_{int} 0.0823 Parameters 182 Restraints 0 Largest Peak 0.174 Deepest Hole -0.174 GooF 1.027 wR_2 (all data) 0.0978 wR_2 0.0915 R_1 (all data) 0.0553	$lpha/^{\circ}$	90
V/ų 1393.95(13) Z 4 Z' 1.000 $\Theta_{min}/^{\circ}$ 3.034 $\Theta_{max}/^{\circ}$ 72.147 Measured Refl. 13565 Independent Refl. 2712 Reflections Used 2246 R_{int} 0.0823 Parameters 182 Restraints 0 Largest Peak 0.174 Deepest Hole -0.174 GooF 1.027 wR_2 (all data) 0.0978 wR_2 0.0915 R_1 (all data) 0.0553	β/°	90
Z' 4 Z' 1.000 $\Theta_{min}/^{\circ}$ 3.034 $\Theta_{max}/^{\circ}$ 72.147 Measured Refl. 13565 Independent Refl. 2712 Reflections Used 2246 R_{int} 0.0823 Parameters 182 Restraints 0 Largest Peak 0.174 Deepest Hole -0.174 GooF 1.027 wR_2 (all data) 0.0978 wR_2 0.0915 R_1 (all data) 0.0553		90
Z' 1.000 $\Theta_{min}/^{\circ}$ 3.034 $\Theta_{max}/^{\circ}$ 72.147 Measured Refl. 13565 Independent Refl. 2712 Reflections Used 2246 R_{int} 0.0823 Parameters 182 Restraints 0 Largest Peak 0.174 Deepest Hole -0.174 GooF 1.027 wR_2 (all data) 0.0978 wR_2 0.0915 R_1 (all data) 0.0553	V/ų	1393.95(13)
$\Theta_{min}/^{\circ}$ 3.034 $\Theta_{max}/^{\circ}$ 72.147 Measured Refl. 13565 Independent Refl. 2712 Reflections Used 2246 R_{int} 0.0823 Parameters 182 Restraints 0 Largest Peak 0.174 Deepest Hole -0.174 GooF 1.027 wR_2 (all data) 0.0978 wR_2 0.0915 R_1 (all data) 0.0553	Z	4
$\Theta_{max}/^{\circ}$ 72.147 Measured Refl. 13565 Independent Refl. 2712 Reflections Used 2246 R_{int} 0.0823 Parameters 182 Restraints 0 Largest Peak 0.174 Deepest Hole -0.174 GooF 1.027 wR_2 (all data) 0.0978 wR_2 0.0915 R_1 (all data) 0.0553	<i>Z'</i>	1.000
Measured Refl. 13565 Independent Refl. 2712 Reflections Used 2246 Rint 0.0823 Parameters 182 Restraints 0 Largest Peak 0.174 Deepest Hole -0.174 GooF 1.027 wR2 (all data) 0.0978 wR2 0.0915 R1 (all data) 0.0553	$\Theta_{min}/\!\!\!/^\circ$	3.034
Independent Refl. 2712 Reflections Used 2246 Rint 0.0823 Parameters 182 Restraints 0 Largest Peak 0.174 Deepest Hole -0.174 GooF 1.027 wR2 (all data) 0.0978 wR2 0.0915 R1 (all data) 0.0553	$\Theta_{max}/\!\!\!/^\circ$	72.147
Reflections Used 2246 R _{int} 0.0823 Parameters 182 Restraints 0 Largest Peak 0.174 Deepest Hole -0.174 GooF 1.027 wR2 (all data) 0.0978 wR2 0.0915 R1 (all data) 0.0553	Measured Refl.	13565
Rint 0.0823 Parameters 182 Restraints 0 Largest Peak 0.174 Deepest Hole -0.174 GooF 1.027 wR2 (all data) 0.0978 wR2 0.0915 R1 (all data) 0.0553	Independent Refl.	2712
Parameters182Restraints0Largest Peak 0.174 Deepest Hole -0.174 GooF 1.027 wR_2 (all data) 0.0978 wR_2 0.0915 R_1 (all data) 0.0553	Reflections Used	2246
Restraints 0 Largest Peak 0.174 Deepest Hole -0.174 GooF 1.027 wR2 (all data) 0.0978 wR2 0.0915 R1 (all data) 0.0553	Rint	0.0823
Largest Peak 0.174 Deepest Hole -0.174 GooF 1.027 wR_2 (all data) 0.0978 wR_2 0.0915 R_1 (all data) 0.0553	Parameters	182
Deepest Hole -0.174 GooF 1.027 wR2 (all data) 0.0978 wR2 0.0915 R1 (all data) 0.0553		
GooF 1.027 wR_2 (all data) 0.0978 wR_2 0.0915 R_1 (all data) 0.0553	Largest Peak	0.174
wR_2 (all data) 0.0978 wR_2 0.0915 R_1 (all data) 0.0553	•	-0.174
wR_2 0.0915 R_1 (all data) 0.0553		
R₁ (all data) 0.0553		
·	=	
H_1 0.0410		
	R_1	0.0410





The Model has Chirality at C1 R

2.8.2 X-ray crystal structure data of II-79



Experimental. Single colourless needle-shaped crystals of (**bb1015b**) were used as received. A suitable crystal $(0.49\times0.09\times0.04)$ was selected and mounted on a nylon loop with paratone oil on a Bruker APEX-II CCD diffractometer. The crystal was kept at T = 173(2) K during data collection. Using **Olex2** (Dolomanov et al., 2009), the structure was solved with the **SheIXS** (Sheldrick, 2008) structure solution program, using the Direct Methods solution method. The model was refined with version 2014/6 of **XL** (Sheldrick, 2008) using Least Squares minimisation.

Crystal Data. C₂₆H₃₂Cl₄N₄O₆, M_r = 638.35, orthorhombic, P2₁2₁2₁ (No. 19), a = 12.9069(2) Å, b = 13.3255(2) Å, c = 18.0382(3) Å, $\alpha = \beta = \gamma = 90^{\circ}$, V = 3102.41(8) Å³, T = 173(2) K, Z = 4, Z' = 1, μ (CuK $_{\alpha}$) = 3.847, 22480 reflections measured, 5929 unique ($R_{int} = 0.0436$) which were used in all calculations. The final wR_2 was 0.0763 (all data) and R_1 was 0.0317 (I > 2(I)).

Crystal data and structure refinement

Compound bb1015b Formula C₂₆H₃₂CI₄N₄O₆ Dcalc./ g cm⁻³ 1.367 \square /mm⁻¹ 3.847 Formula Weight 638.35 Colour colourless Shape needle Max Size/mm 0.49 Mid Size/mm 0.09 Min Size/mm 0.04 T/K 173(2) Crystal System orthorhombic Flack Parameter 0.005(7)**Hooft Parameter** -0.001(8)P2₁2₁2₁ Space Group a/Å 12.9069(2) b/Å 13.3255(2) c/Å 18.0382(3) $\alpha/^{\circ}$ 90 $\beta / ^{\circ}$ 90 90 γſ° V/Å³ 3102.41(8) Ζ 4 Z'1 $\Theta_{min}/^{\circ}$ 4.125 $\Theta_{\text{max}}/^{\circ}$ 72.367 Measured Refl. 22480 Independent Refl. 5929 Reflections Used 5413 Rint 0.0436 **Parameters** 365 Restraints 0 Largest Peak 0.255 Deepest Hole -0.219GooF 1.028 wR_2 (all data) 0.0763 wR_2 0.0736 R₁ (all data) 0.0369 R_1 0.0317

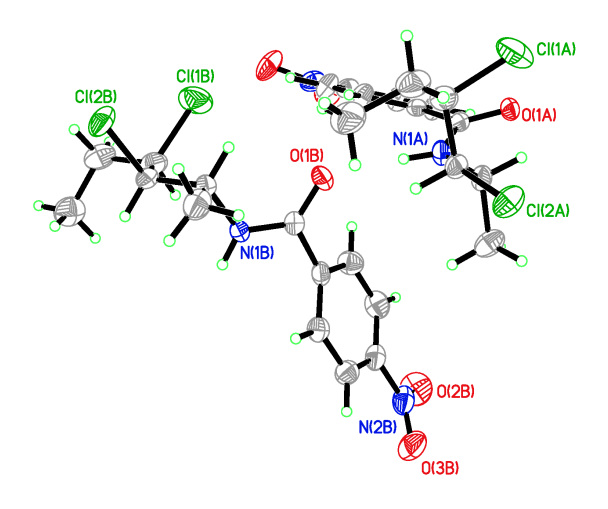


Figure 1:

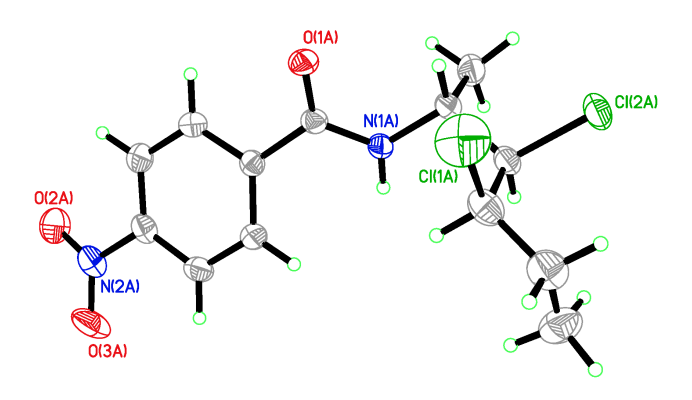


Figure 2:

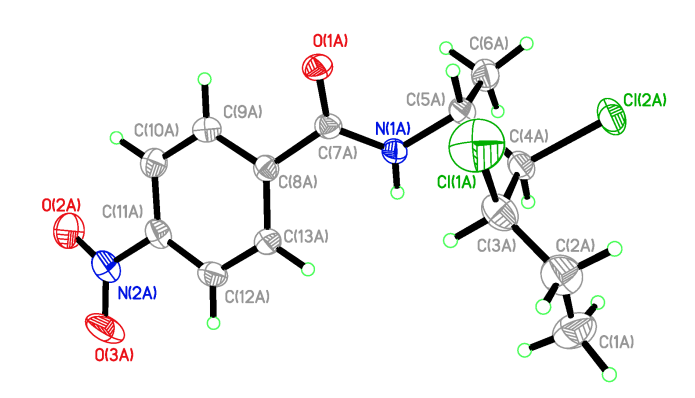


Figure 3: The Model has Chirality at C3A (Chiral SPGR) R Verify; The Model has Chirality at C4A (Chiral SPGR) R Verify; The Model has Chirality at C5A (Chiral SPGR) R Verify

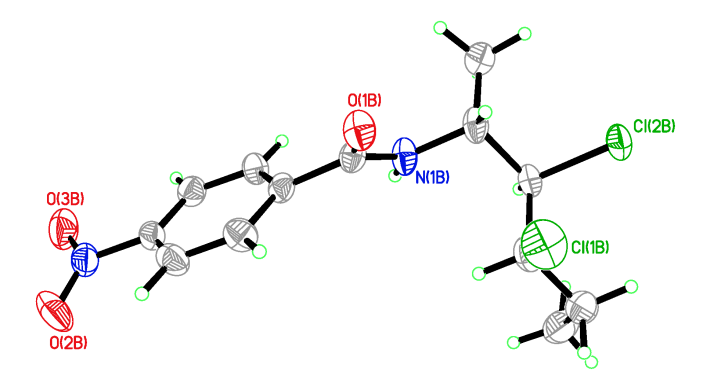


Figure 4:

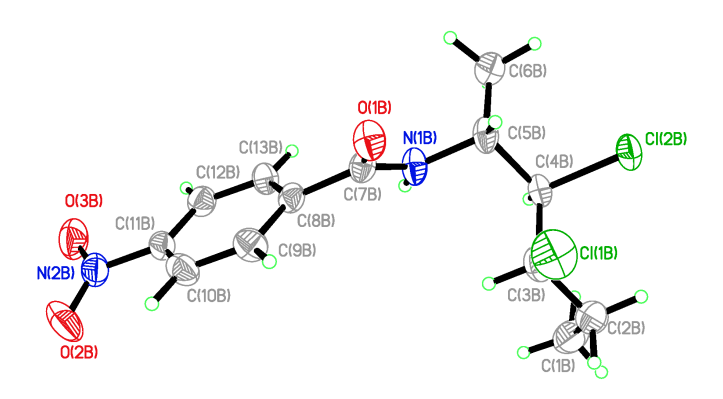


Figure 5: The Model has Chirality at C3B (Chiral SPGR) R Verify; The Model has Chirality at C4B (Chiral SPGR) R Verify; The Model has Chirality at C5B (Chiral SPGR) R Verify

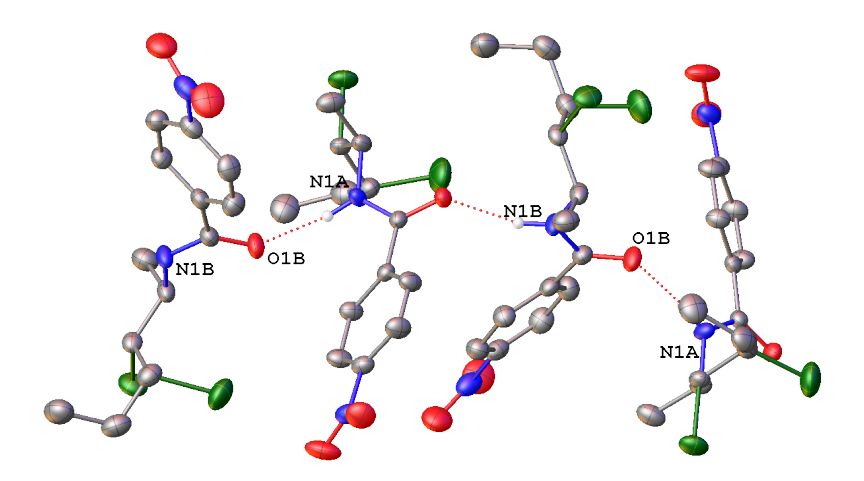


Figure 6: The following hydrogen bonding interactions with a maximum D-D distance of

2.9 Å and a minimum angle of 120 $^{\circ}$ are present in $BB1015b\colon$ N1B-O1A(1) =2.808 Å, N1A-O1B =2.857 Å.

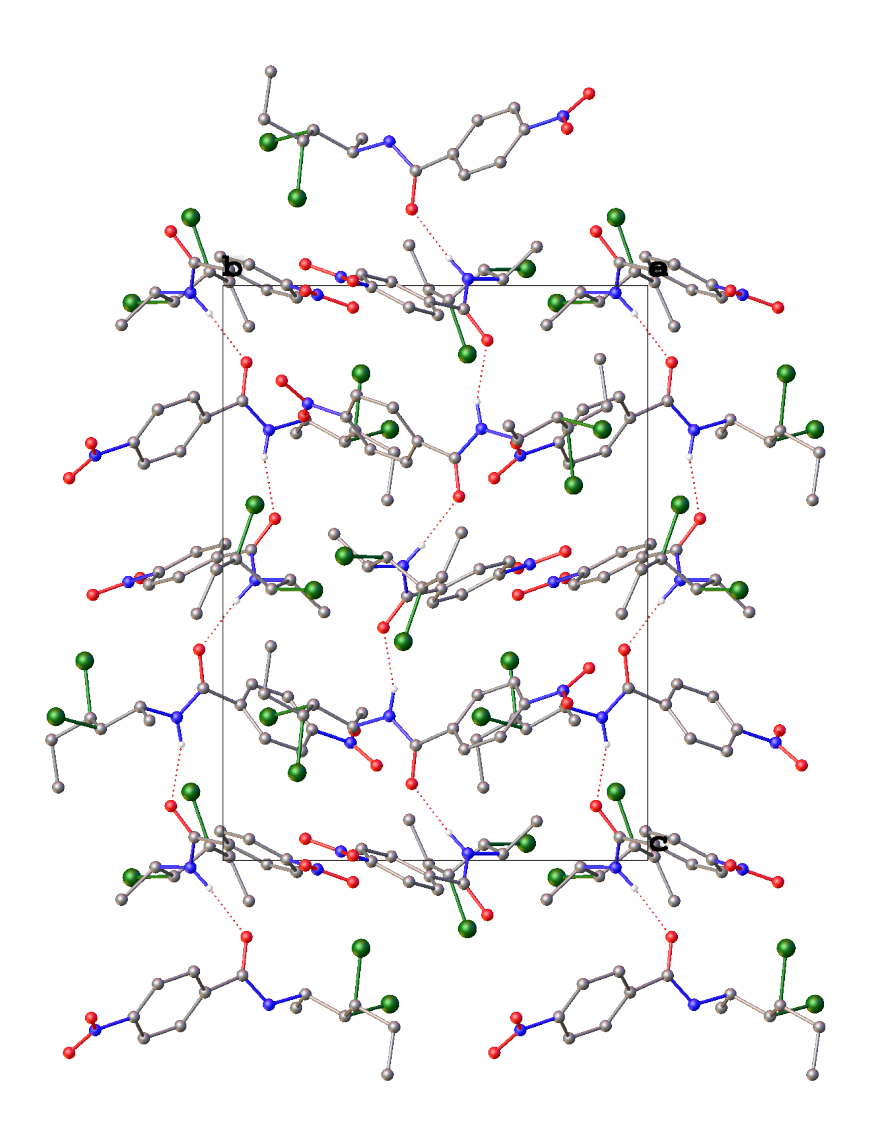


Figure 7: Packing diagram of BB1015b.

REFERENCES

REFERENCES

- 1. Keith, John M.; Larrow, Jay F.; Jacobsen, Eric N., Practical Considerations in Kinetic Resolution Reactions. *Advanced Synthesis & Catalysis* **2001**, *343* (1), 5-26.
- 2. Martin, V. S.; Woodard, S. S.; Katsuki, T.; Yamada, Y.; Ikeda, M.; Sharpless, K. B., Kinetic resolution of racemic allylic alcohols by enantioselective epoxidation. A route to substances of absolute enantiomeric purity? *Journal of the American Chemical Society* **1981**, *103* (20), 6237-6240.
- 3. Corey, E. J.; Noe, M. C.; Guzman-Perez, A., Kinetic Resolution by Enantioselective Dihydroxylation of Secondary Allylic 4-Methoxybenzoate Esters Using a Mechanistically Designed Cinchona Alkaloid Catalyst. *Journal of the American Chemical Society* **1995**, *117* (44), 10817-10824.
- 4. Hashiguchi, S.; Fujii, A.; Haack, K.-J.; Matsumura, K.; Ikariya, T.; Noyori, R., Kinetic Resolution of Racemic Secondary Alcohols by Rull-Catalyzed Hydrogen Transfer. *Angewandte Chemie International Edition in English* **1997**, *36* (3), 288-290.
- 5. Schaus, S. E.; Brandes, B. D.; Larrow, J. F.; Tokunaga, M.; Hansen, K. B.; Gould, A. E.; Furrow, M. E.; Jacobsen, E. N., Highly Selective Hydrolytic Kinetic Resolution of Terminal Epoxides Catalyzed by Chiral (salen)Colll Complexes. Practical Synthesis of Enantioenriched Terminal Epoxides and 1,2-Diols. *Journal of the American Chemical Society* **2002**, *124* (7), 1307-1315.
- 6. Hang, J.; Tian, S.-K.; Tang, L.; Deng, L., Asymmetric Synthesis of α-Amino Acids via Cinchona Alkaloid-Catalyzed Kinetic Resolution of Urethane-Protected α-Amino Acid N-Carboxyanhydrides. *Journal of the American Chemical Society* **2001**, *123* (50), 12696-12697.
- 7. Yu, C.; Huang, H.; Li, X.; Zhang, Y.; Wang, W., Dynamic Kinetic Resolution of Biaryl Lactones via a Chiral Bifunctional Amine Thiourea-Catalyzed Highly Atropoenantioselective Transesterification. *Journal of the American Chemical Society* **2016**, *138* (22), 6956-6959.
- 8. Sorrentino, E.; Connon, S. J., Enantioselective Alkylative Kinetic Resolution of 2-Oxindole-Derived Enolates Promoted by Bifunctional Phase Transfer Catalysts. *Organic Letters* **2016**, *18* (20), 5204-5207.
- 9. Kolleth, A.; Christoph, S.; Arseniyadis, S.; Cossy, J., Kinetic resolution of propargylamines via a highly enantioselective non-enzymatic N-acylation process. *Chemical Communications* **2012**, *48* (85), 10511-10513.

- 10. Tanaka, K.; Fu, G. C., Enantioselective Synthesis of Cyclopentenones via Rhodium-Catalyzed Kinetic Resolution and Desymmetrization of 4-Alkynals. *Journal of the American Chemical Society* **2002**, *124* (35), 10296-10297.
- 11. Tanaka, K.; Shoji, T., Cationic Rhodium(I)/BINAP Complex-Catalyzed Isomerization of Secondary Propargylic Alcohols to α,β -Enones. *Organic Letters* **2005**, *7* (16), 3561-3563.
- 12. Nakamura, S.; Ohara, M.; Nakamura, Y.; Shibata, N.; Toru, T., Copper-Catalyzed Enantioselective Three-Component Synthesis of Optically Active Propargylamines from Aldehydes, Amines, and Aliphatic Alkynes. *Chemistry A European Journal* **2010**, *16* (8), 2360-2362.
- 13. Wei, C.; Li, C.-J., A Highly Efficient Three-Component Coupling of Aldehyde, Alkyne, and Amines via C-H Activation Catalyzed by Gold in Water. *Journal of the American Chemical Society* **2003**, *125* (32), 9584-9585.
- 14. Gommermann, N.; Koradin, C.; Polborn, K.; Knochel, P., Eine enantioselektive, Kupfer(I)-katalysierte Drei-Komponenten-Reaktion zur Synthese von Propargylaminen. *Angewandte Chemie* **2003**, *115* (46), 5941-5944.
- 15. Jaganathan, A.; Staples, R. J.; Borhan, B., Kinetic Resolution of Unsaturated Amides in a Chlorocyclization Reaction: Concomitant Enantiomer Differentiation and Face Selective Alkene Chlorination by a Single Catalyst. *Journal of the American Chemical Society* **2013**, *135* (39), 14806-14813.
- 16. Klauber, E. G.; Mittal, N.; Shah, T. K.; Seidel, D., A Dual-Catalysis/Anion-Binding Approach to the Kinetic Resolution of Allylic Amines. *Organic Letters* **2011**, *13* (9), 2464-2467.
- 17. Soltanzadeh, B.; Jaganathan, A.; Yi, Y.; Yi, H.; Staples, R. J.; Borhan, B., Highly Regio- and Enantioselective Vicinal Dihalogenation of Allyl Amides. *Journal of the American Chemical Society* **2017**, *139* (6), 2132-2135.
- 18. Moragas, T.; Liffey, R. M.; Regentová, D.; Ward, J.-P. S.; Dutton, J.; Lewis, W.; Churcher, I.; Walton, L.; Souto, J. A.; Stockman, R. A., Sigmatropic Rearrangement of Vinyl Aziridines: Expedient Synthesis of Cyclic Sulfoximines from Chiral Sulfinimines. *Angewandte Chemie International Edition* **2016**, *55* (34), 10047-10051.
- 19. Jaganathan, A.; Garzan, A.; Whitehead, D. C.; Staples, R. J.; Borhan, B., A Catalytic Asymmetric Chlorocyclization of Unsaturated Amides. *Angewandte Chemie International Edition* **2011**, *50* (11), 2593-2596.

CHAPTER THREE Intramolecular *ipso*-Halocyclization to Construct a Chiral Spiro-Center

3.1 Introduction

Dearomative *ipso*-cyclization of arene compounds is an important transformation in organic synthesis and has been widely used in the total synthesis of natural products.¹ Intramolecular *ipso*-cyclization reactions enable the construction of a spiro-centre in a straightforward way, which can overall efficiently transform easily accessible molecules to more complicated structures.² However enantioselective processes are rare, especially catalytic ones. The two major challenges in developing enantioselective dearomative *ipso*-cyclization are: 1) the high energy barrier encountered in dearomatization processes; 2) the competitive *ortho*-cyclization process.

In 2008, the first enantioselective oxidative dearomatization of phenols **III-1** to synthesize a chiral spirolactone using chiral hypervalent iodine reagent **III-2** was reported by Kita's group (Scheme 3.1).³ Nucleophilic attack on an intermediate which was formed via ligand exchange afford quinone variants in up to 86% *ee*.

Scheme 3.1 C-O bond forming *ipso*-cyclization.

More recently transition-metal catalyzed dearomative *ipso*-cyclizations are emerging. In 2010, You's group reported a highly enantioselective synthesis of spiroindolenines via Ir-catalyzed asymmetric allylic alkylation reaction (Scheme 3.2).⁴ An electrophilic π-allyliridium intermediate was generated when the Iridium catalyst was subjected to allyl carbonate substrate **III-4** and indole functioned as a good carbon nucleophile. The BINOL derived phosphoramidite ligand **III-5** furnished excellent *ee* and *dr*. Similarly, they developed the first Ir-catalyzed intramolecular asymmetric allylic dearomatization of phenols **III-7**.⁵ Spirocyclohexenone derivatives **III-9** were obtained up to 97% *ee*.

Scheme 3.2 *ipso*-cyclization catalyzed by Iridium catalyst.

Hamada's group and Buchwald's group developed palladium catalyzed dearomatization of phenols (Scheme 3.3).⁶⁻⁷ Hamada dearomatized phenols **III-10** using Pd-catalyzed intramolecular *ipso*-Friedel-Crafts allylic alkylation. They demonstrated a single example of catalytic asymmetric synthesis of spiro[4,5]cyclohexadienones **III-12**

with 89% *ee*. Buchwald's group dearomatized phenol **III-13** using palladium catalyzed C-arylation. The reaction proceeds through reductive elimination of a palladacycle intermediate. Applying chiral phosphine ligands **III-14** enables a practical asymmetric catalytic process with up to 91% *ee*, albeit only 2 examples of asymmetric version.

Scheme 3.3 *ipso*-cyclization catalyzed by a Palladium catalyst.

Zhang reported a copper catalyzed oxidative *ipso*-cylization of an activated alkyne to synthesize azaspiro[4,5]trienones **III-17** with silanes through selective activation of Si-H and C-H bond (Scheme 3.4, a).⁸ They proposed that the reaction proceeds via a radical mechanism. Hence it would be difficult to develop an asymmetric version under this system. Very similarly Wang's group reported a metal-free synthesis of sulfonated azaspiro[4,5]trienones **III-19** through oxidative spirocyclization of arylpropioamides **III-18**

with sulfonylhydrazides (Scheme 3.4, b).⁹ The reaction proceeds through single electron oxidation of sulfonyl hydrazide mediated by I₂O₅.

a. Ph
$$+ \text{HSiPh}_3$$
 $\frac{5 \text{ mol}\% \text{ Cul}}{7 \text{ equiv TBHP}}$ $\frac{5 \text{ mol}\% \text{ Cul}}{7 \text{ equiv TBHP}}$ $\frac{5 \text{ mol}\% \text{ Cul}}{100 \text{ N}}$ $\frac{5 \text{ mol}\% \text{ Cul}}{100 \text{ N}}$ $\frac{100 \text{ N}}{100 \text{ N}}$

b.
$$\begin{array}{c} Ph \\ O \\ + Ph - \ddot{S} - NHNH_2 \end{array} \xrightarrow{\begin{array}{c} 1 \text{ equiv } I_2O_5 \\ \hline 3 \text{ equiv TBHP} \\ 1,4-\text{dioxane, } 80 \text{ °C} \end{array} \xrightarrow{\begin{array}{c} O \\ O \\ O \end{array}} SO_2Ph \\ \begin{array}{c} O \\ O \\ O \end{array} \xrightarrow{\begin{array}{c} O \\ O \\ O \end{array}} Ph - \ddot{S} - NHNH_2 \xrightarrow{\begin{array}{c} O \\ O \\ O \end{array}} Ph - \ddot{S} - NHNH_2 \xrightarrow{\begin{array}{c} O \\ O \\ O \end{array}} Ph - \ddot{S} - NHNH_2 \xrightarrow{\begin{array}{c} O \\ O \\ O \end{array}} Ph - \ddot{S} - NHNH_2 \xrightarrow{\begin{array}{c} O \\ O \\ O \end{array}} Ph - \ddot{S} - NHNH_2 \xrightarrow{\begin{array}{c} O \\ O \\ O \end{array}} Ph - \ddot{S} - NHNH_2 \xrightarrow{\begin{array}{c} O \\ O \\ O \end{array}} Ph - \ddot{S} - NHNH_2 \xrightarrow{\begin{array}{c} O \\ O \\ O \end{array}} Ph - \ddot{S} - NHNH_2 \xrightarrow{\begin{array}{c} O \\ O \\ O \end{array}} Ph - \ddot{S} - NHNH_2 \xrightarrow{\begin{array}{c} O \\ O \\ O \end{array}} Ph - \ddot{S} - NHNH_2 \xrightarrow{\begin{array}{c} O \\ O \\ O \end{array}} Ph - \ddot{S} - NHNH_2 \xrightarrow{\begin{array}{c} O \\ O \\ O \end{array}} Ph - \ddot{S} - NHNH_2 \xrightarrow{\begin{array}{c} O \\ O \\ O \end{array}} Ph - \ddot{S} - NHNH_2 \xrightarrow{\begin{array}{c} O \\ O \\ O \end{array}} Ph - \ddot{S} - NHNH_2 \xrightarrow{\begin{array}{c} O \\ O \\ O \end{array}} Ph - \ddot{S} - NHNH_2 \xrightarrow{\begin{array}{c} O \\ O \\ O \end{array}} Ph - \ddot{S} - NHNH_2 \xrightarrow{\begin{array}{c} O \\ O \\ O \end{array}} Ph - \ddot{S} - NHNH_2 \xrightarrow{\begin{array}{c} O \\ O \\ O \end{array}} Ph - \ddot{S} - NHNH_2 \xrightarrow{\begin{array}{c} O \\ O \\ O \end{array}} Ph - \ddot{S} - NHNH_2 \xrightarrow{\begin{array}{c} O \\ O \\ O \end{array}} Ph - \ddot{S} - NHNH_2 \xrightarrow{\begin{array}{c} O \\ O \\ O \end{array}} Ph - \ddot{S} - NHNH_2 \xrightarrow{\begin{array}{c} O \\ O \\ O \end{array}} Ph - \ddot{S} - NHNH_2 \xrightarrow{\begin{array}{c} O \\ O \\ O \end{array}} Ph - \ddot{S} - NHNH_2 \xrightarrow{\begin{array}{c} O \\ O \\ O \end{array}} Ph - \ddot{S} - NHNH_2 \xrightarrow{\begin{array}{c} O \\ O \\ O \end{array}} Ph - \ddot{S} - NHNH_2 \xrightarrow{\begin{array}{c} O \\ O \\ O \end{array}} Ph - \ddot{S} - NHNH_2 \xrightarrow{\begin{array}{c} O \\ O \\ O \end{array}} Ph - \ddot{S} - NHNH_2 \xrightarrow{\begin{array}{c} O \\ O \\ O \end{array}} Ph - \ddot{S} - NHNH_2 \xrightarrow{\begin{array}{c} O \\ O \end{array}} Ph - \ddot{S} - NHNH_2 \xrightarrow{\begin{array}{c} O \\ O \end{array}} Ph - \ddot{S} - NHNH_2 \xrightarrow{\begin{array}{c} O \\ O \end{array}} Ph - \ddot{S} - NHNH_2 \xrightarrow{\begin{array}{c} O \\ O \end{array}} Ph - \ddot{S} - NHNH_2 \xrightarrow{\begin{array}{c} O \\ O \end{array}} Ph - \ddot{S} - NHNH_2 \xrightarrow{\begin{array}{c} O \\ O \end{array}} Ph - \ddot{S} - NHNH_2 \xrightarrow{\begin{array}{c} O \\ O \end{array}} Ph - \ddot{S} - NHNH_2 \xrightarrow{\begin{array}{c} O \\ O \end{array}} Ph - \ddot{S} - NHNH_2 \xrightarrow{\begin{array}{c} O \\ O \end{array}} Ph - \ddot{S} - NHNH_2 \xrightarrow{\begin{array}{c} O \\ O \end{array}} Ph - \ddot{S} - \ddot{S$$

Scheme 3.4 ipso-cyclization of an activated alkyne by single electron oxidation path.

Unsworth's group reported a silver catalyzed dearomatization of indole to synthesize spirocyclic indolenines (Scheme 3.5). 10 Activation of the alkyne with π -acidic Ag(I) catalyst promotes spirocyclization via nucleophilic attack by the indole at the 3-position. They have not demonstrated an asymmetric version yet.

$$R^{4O}$$
 R^{1} R^{4O} R^{1} R^{4O} R^{1} R^{4O} R^{2} R^{2} R^{2} R^{2} R^{3} R^{2} R^{2} R^{3} R^{3} R^{2} R^{3} R^{3} R^{2} R^{3} R^{3} R^{3} R^{2} R^{3} R^{3}

Scheme 3.5 Silver catalyzed dearomatization of indole.

Another type of *ipso*-cyclization involves C-N bond formation instead of C-C bond formation: oxidation of arenes to a carbocation in advance of trapping by an NH-nucleophile. For example, an oxidative cyclization of phenolic alkylsulfonamides **III-22** mediated by hypervalent iodine reagent to form spiro-pyrrolidine **III-23** has been reported (Scheme 3.6, a).¹¹ Contrary to this method, phenol could behave like a nucleophile in a redox neutral environment. More recently a conceptually simple method of C-N bond forming dearomatization has been reported by Bower's group (Scheme 3.6, b).¹² The process involves a SEAr-like attack of the aromatic moiety onto the activated tosyloxyammonium intermediate which is in situ generated upon deprotection of Boc with TFA.

а

Scheme 3.6 C-N bond forming *ipso*-cyclization.

We have witnessed a large body of research focused on the catalytic asymmetric halofunctionalization of alkenes in the last few years, however catalytic asymmetric dearomatizations through halofunctionalization are still underdeveloped.¹³ There are generally two ways to realize dearomatization via halofunctionalization. In the first class, electrophilic halogenation occurs at a substituted aromatic ring, like phenol and indole, then a stabilized dearomatized product is generated directly (Scheme 3.7, a) or halonium intermediate is trapped by a tethered nucleophile (Scheme 3.7, b). In the second class, electrophilic halogenation occurs at an alkyne or alkene moiety to yield the halonium

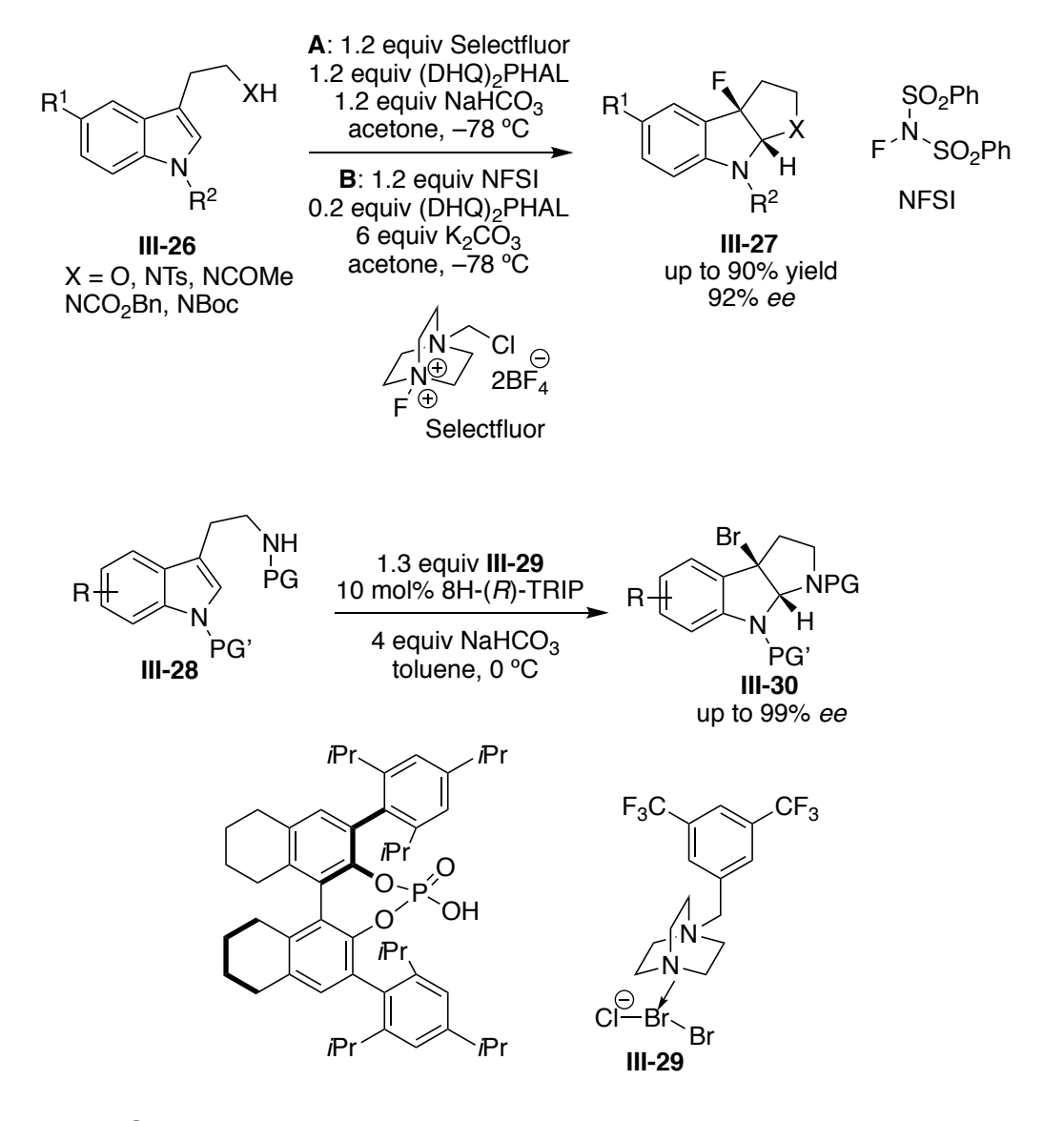
intermediate which is subsequently trapped intramolecularly by an aromatic ring at the *ipso* position (Scheme 3.7, c). So far, to the best of our knowledge, examples that fall into the second class are all racemic.

a.
$$OH$$
 R
 X^{+}
 NU
 X^{+}
 NU
 X^{+}
 NU
 X^{+}
 NU
 X^{+}
 NU
 X^{+}
 $X^$

Scheme 3.7 Types of dearomatization via halofunctionalization.

As opposed of the second type of reaction, many catalytic asymmetric dearomatization reactions initiated by electrophilic halogenation on arenes have been reported. In 2011, Gouverneur's group reported the first organocatalyzed asymmetric fluorocyclization through dearomatization of indoles III-26 (Scheme 3.8).¹⁴ Two sets of conditions with stoichiometric and catalytic amounts of (DHQ)₂PHAL, respectively, lead to fluorocyclization of tryptamine or tryptophol derivatives with moderate to high *ee*.

Electrophilic fluorine sources Selectfluor and NFSI were utilized. Like many other organocatalytic asymmetric halofunctionalization reactions, the major conceptual difficulty of this reaction is that the in situ generated transient chiral N-F cinchona species is similarly reactive or less reactive with respect to the achiral fluorinating reagent. Similarly an analogous bromine cyclization of tryptamine derivative III-28 was later reported by Xie (Scheme 3.8). 15 They used the DABCO derived bromine reagent III-29 as bromine source and chiral phosphoric acid as catalyst.



Scheme 3.8 Fluorocyclization of tryptamine and tryptophol.

You's group developed a highly enantioselective chlorocyclization of indole derived benzamides **III-31** and **III-33** using (DHQD)₂PHAL as catalyst (Scheme 3.9). ¹⁶⁻¹⁷ By using different substrates, both *spiro*-cyclization and fused ring products were obtained in high *ee*, respectively. They proposed a catalytic model in which the phthalazine nitrogen forms a hydrogen bond with benzamide NH to increase the nucleophilicity of the amide group and the quinuclidine nitrogen can activate the chlorenium to provide a chiral environment.

Scheme 3.9 Enantioselective *ipso*-chlorocyclization of indoles.

Unlike a lot of asymmetric examples of dearomatization that are initiated by halogenation of arenes, asymmetric version of the dearomatization by halogenation of tethered alkynes and alkenes remains underdeveloped (Scheme 3.7, c). So far most reported examples of this type of reaction are racemic. The earliest work of this area dates back to 2005, when Larock reported a straightforward route to spiro[4,5]trienones via intramolecular *ipso*-halocyclization of simple methoxy-substituted-4-aryl-1-alkynes (Scheme 3.10). ¹⁸ This reaction shows that the linkage of amine, ether and CH₂ were well tolerated. ICI or I₂ proved to be an efficient electrophile to give the iodonium intermediate,

which can undergo intramolecular *ipso*-attack by the electron-rich aromatic ring. The methyl group of methoxy can be removed through nucleophilic displacement by the base. This work represents a general model for future work on *ipso*-halocyclization initiated by halogenation of alkynes or alkenes.

$$\begin{array}{c} X \\ Y \\ \hline \\ NaHCO_3 \text{ or NaOMe} \\ CH_2Cl_2, -78 \text{ °C} \\ \hline \\ NaHCO_3 \text{ or NaOMe} \\ CH_2Cl_2, -78 \text{ °C} \\ \hline \\ NaHCO_3 \text{ or NaOMe} \\ \hline \\ NaHCO_3 \text{$$

Scheme 3.10 Larock's *ipso*-iodocyclization.

In 2008, Li reported electrophilic ipso-iodocyclization N-(4an of methylphenyl)propiolamides to access 4-methyleneazaspiro[4,5]trienes 3.11a).¹⁹ The major difference of this work in comparison to Larock's system is using para-methyl as the activating group instead of para-methoxy substituent. Similarly, the same group then reported the *ipso*-cyclization of N-(4-methoxylphenyl)propiolamide III-39 through an electrophile exchange process (Scheme 3.11b).20 Electrophilic fluoride reagent III-41 or Selectfluor can react with CuX (X= Br, I, SCN) to generate electrophilic cation X⁺, which reacts with an alkyne to initiate the *ipso*-cyclization. Besides the alkoxy or alkyl activating group at the para-position of phenyl group, non-activated substrates have also been studied by Li's group (Scheme 3.12).²¹ In the presence of a suitable nucleophile like AcOH or trifluroethanol, the cationic allyl intermediate can be captured by AcO⁻ or CF₃CH₂O⁻ anion, respectively. The yields ranged from moderate to good, however the *dr* were generally between 1:1 to 2:1.

Scheme 3.11 Electrophilic *ipso*-iodocyclization with *para*-activating group.

NIS

HOAc or
$$CF_3CH_2OH$$
 $Z = NMe, O$
 R'

NIS

HOAc or CF_3CH_2OH
 R'

Up to 98% yield up to 3:1 dr
 CF_3CH_2O/AcO
 R'
 R

Scheme 3.12 Electrophilic *ipso*-iodocyclization without *para*-activating group.

Majumdar and coworkers used the *ipso*-iodocyclization strategy to synthesize spiro-coumarin, quinolone and pyrimidine heterocyclic compounds (Scheme 3.13). They used l_2 as the electrophilic iodine source and NaHCO₃ as the base, which is similar to Larock's conditions.¹⁸

Scheme 3.13 *ipso*-iodocyclization to access *spiro*-pyrimidine/coumarin.

Although a lot of high yielding examples of dearomatization through halofunctionalization have been reported, the lack of catalytic enantioselective versions is still the downside of this area. Possible reasons why developing highly efficient asymmetric dearomatization via halofunctionalization is challenging are 1) the competitive background reactions or side reactions override the catalytic reactions due to the highly reactive electrophilic halogenating reagent; 2) the mechanism of catalytic asymmetric dearomatizations through halofunctionalization are not well understood, which prevents rational design of highly efficient catalytic systems.¹³ Inspired by recent success of asymmetric chlorofunctionalizations of olefins developed in the Borhan labs,

an effort was undertaken to develop catalytic asymmetric dearomatization via halofunctionalization.²²⁻²⁴ This chapter will depict the efforts towards the catalytic asymmetric *ipso*-halocyclization of 4-aryl-1-alkyne derivatives.

3.2 Results and discussion

3.2.1 Screen the halogen source with *N*-(4-methoxyphenyl)-4-methyl-*N*-(3-phenylprop-2-yn-1-yl)benzenesulfonamide

The initial evaluations of various halogenating reagents in racemic non-catalytic reactions employed Larock's substrate **III-48** (Table 3.1). Halogenated-succinimides, halogenated hydantoins and halogenated isocyanuric acids were screened. Reactions were run at room temperature. TCCA and *N*-halo succinimide species gave high conversion and yield after 3 h. Among the various electrophilic halogen reagents, NIS and TCCA gave ~90% yields within 3 h. However, DCDMH led to sluggish reaction and only gave 16% conversion after 3 h, although in a very clean reaction. Hence, DCDMH might be a good choice for catalytic reactions in terms of its slow background reaction.

Table 3.1 Halogen screening for substrate III-48

3.2.2 Asymmetric *ipso*-halocyclization of N-(4-methoxy-2-methylphenyl)-4-methyl-N-(3-phenylprop-2-yn-1-yl)benzenesulfonamide

The asymmetric reaction with *N*-tethered propargyl substrate **III-52** was evaluated. DCDMH and TCCA were used for screening cinchona alkaloid dimer catalysts (Table 3.2). TCCA was more reactive as compared to DCDMH, and reactions were done within half an hour in acetonitrile. However, complicated mixtures products were obtained and the yield was low. Reactions were not complete with DCDMH even after 27 h. (DHQD)₂PQN, (DHQD)₂Pyr and (DHQD)₂PHAL all gave racemic products.

^a reactions are quenched after 3 h; ^b conversions and yield were determined based on crude ¹H NMR using MTBE as internal standard

Table 3.2 Optimization of reaction conditions for substrate III-52

entry	catalyst	CI	time (h)	conversion (%) a	yield (%) b	ee (%) ^c
1	none	DCDMH	1	68	55	_
2	(DHQ) ₂ AQN	DCDMH	27	54	37	2
3	(DHQD) ₂ Pyr	DCDMH	27	69	22	2
4	(DHQD) ₂ PHAL	DCDMH	24	76	55	3
5	DABCO	TCCA	4	100	44	-
6	(DHQ) ₂ AQN	TCCA	0.5	100	44	8
7	(DHQD) ₂ Pyr	TCCA	0.5	100	37	2
8	(DHQD) ₂ Pyr	NCS	24	0	0	-

 $^{^{\}rm a}$ conversions were determined from crude $^{\rm 1}H$ NMR; $^{\rm b}~$ yields were determined from isolated products; $^{\rm c}$ ee were determined from chiral HPLC.

3.2.3 Asymmetric *ipso*-halocyclization with 2-bromo- 4-methoxy- 1-((3-phenylprop-2-yn-1-yl) oxy) benzene

Scheme 3.14 Ipso-chlorocylization of O-linker Substrate

In addition to the *N*-tethered propargyl substrates, the O-tethered substrate **III-54** has also been evaluated which contains an *ortho*-Br substituent on the benzene ring to install a prechiral center. Intramolecular chlorocyclization with TCCA as electrophilic chlorine source and DABCO as Lewis base catalyst leads to a major product **III-55** in 65% yield (Scheme 3.14). The product was characterized by X-ray crystallography. The proposed mechanism is that the benzene ring undergoes chlorine substitution at the *ortho*-position to the methoxy and chlorenium is formed on the propargyl group which lead to *ipso*-cyclization. The generated trienone **II** is converted to the chlorenium **III** which is trapped by the anion of isocyanuric acid. Different cinchona alkaloid derived catalysts were screened for the asymmetric reaction of **III-54** (Table 3.3). Both monomer and dimer hydroquinine or hydroquinidine derived catalysts induced no noticeable enantioselectivity,

also led to low yields. The best result was obtained from (DHQ)₂AQN as catalyst, which gave 75% yield and 7% *ee*. In consideration of the practicality and poor enantioselectivity of the product, O-tethered propargyl substrates were not further investigated.

Table 3.3 Catalyst screen for substrate III-54

ent	ry catalyst	yield % (III-55) ^a	<i>ee</i> % (III-55) ^b
1	III-95	25	3
2	III-96	34	3
3	III-97	25	5
4	III-98	38	< 2
5	III-99	44	< 2
6	(DHQD) ₂ PH	AL 44	3
7	(DHQ) ₂ AQI	N 75	7
8	hydroquinidi	ne 25	3

^a yield was determined by isolated product;

^b ee was determined by chiral HPLC.

3.2.4 Use of Brønsted acid (R)-VANOL hydrogenphosphate as catalyst

The discouraging results from using cinchona alkaloid based catalysts might indicate that a Lewis-base is not a suitable catalyst for this reaction. Instead, a Brønsted acid since there is precedence of tried Brønsted acid-catalyzed halofunctionalization in the literature. For example, Denmark's group reported the bromocycloetherification catalyzed by chiral Brønsted acid TRIP.25 Hennecke and coworkers also reported the haloetherification catalyzed by the sodium salt of VAPOL phosphoric acid and other BINOL derived phosphoric acids.²⁶ Thanks to the generosity of Prof. Wulff's lab, (R)-VANOL hydrogenphosphate III-58 was used as a Brønsted acid catalyst representative. The tosyl protected N-linked substrate III-52 was treated with Nbromosuccinimide and (R)-VANOL hydrogen phosphate (Table 3.4), however the enantioselectivity and yield were poor for the expected product III-56. The major product was indeed dibrominated methyl product III-57. Different solvents and catalyst loadings were screened. Dichloromethane and chloroform gave the best enantioselectivity, leading to only 15% ee, and the yields were generally poor. In addition, reactions were not complete when 1 equiv of NBS was used, which was ascribed to the formation of the dibrominated product III-57. When 3 equiv of NBS were applied, the reaction was finished within 3 h in DCM. In addition to the tosyl protected substrate, the benzoyl protected substrate III-59 was evaluated in the presence of DBDMH and (R)-VANOL hydrogenphosphate in MeCN (Scheme 3.15), however only racemic product III-60 was obtained.

Table 3.4 Evaluation of (R)-VANOL-hydrogen phosphate

entry	solvent	equiv of cat.	time (h)	conversion (%) ^a	yield (III-56)(%) ^a	ee (III-56)(%) ^b
1	MeCN	0.1	2	ND	49	3
2 ^c	MeCN	0.1	2	ND	29	3
3^{d}	toluene	0.3	18	100	17	3
4 ^d	CH ₂ Cl ₂	0.3	3	100	26	15
5	CH ₂ Cl ₂	0.1	48	75	11	3
6	CH ₂ Cl ₂	0.05	48	64	10	3
7	benzene	0.1	24	56	14	3
8	CHCl ₃	0.1	24	75	5	14

 $^{^{\}rm a}$ conversions and yield were determined from GC ; $^{\rm b}$ ee were determined from chiral HPLC; $^{\rm c}$ 2 equiv NaHCO_3 was added; $^{\rm d}$ 3 equiv NBS was used instead of 1 equiv.

III-58 (R)-VANOL hydrogen phosphate

100% conversion, 50% yield, 2% ee

Scheme 3.15 ipso-bromocyclization of benzoyl protected N-tethered substrate

3.2.5 Asymmetric *ipso*-halocyclization with *N*-(4-methoxy-2-methylphenyl)-3-phenyl-*N*-tosylpropiolamide

The failure of achieving any enantioselectivity by using Lewis base and Brønsted acids made us re-examine the interactions of the catalysts with the substrate. Based on previous studies in the Borhan's group on the enantioselective Lewis base catalyzed chlorocyclization and dichlorination reactions, all the successful examples are either amides, carboxylic acids or carbamates. In general, for Brønsted acid catalysis in the literature, these catalysts function through hydrogen binding with the substrates. So maybe the lack of hydrogen bond acceptor on the substrate III-52 prohibits the delivery of enantioselective delivery from the Brønsted acid catalyst. This would suggest the need for substrates to be modified if we want to continue to apply Lewis base or Brønsted acid catalysts. To this end, the methylene next to the triple bond was replaced with a carbonyl, depicted as III-61, which indeed has precedence in literature. 19-21 There are reported nonasymmetric electrophilic *ipso*-cyclization using similar substrates.²⁰ The screening commenced with different halogen sources using acetonitrile as solvent at room temperature (Table 3.5). The electrophilic iodine sources NIS and ICI furnished good yield when 2 equiv of NaHCO₃ were added. Chlorenium reagents like NCS, DCDMH and chloramine-T were less reactive leading to sluggish reactions. The bromine containing reagent NBS gave poor yield.

Table 3.5 Halogen screening for substrate III-61

X+	conversion (%) ^a	yield (%) ^a
NIS	100	44
NIS ^b	100	80°
ICIb	100	95 ^c
NCS	38	5
NBS	100	21 ^c
DCDMH	62	30
Chloramine-T	35	0

^a conversion and yield were decided by crude ¹H NMR using methyl-*t*-butyl ether as internal standard; ^b 2 equiv NaHCO₃ were added; ^c yields were determined by isolated product through column chromatography.

With optimal halogen reagents ICI and NIS in hand, our continued effort was focused on asymmetric catalysis (Table 3.6). In general, the presence of NaHCO₃ as a base can improve the yield (Table 3.6, entries 2, 4, 5 15, 16). When monomeric cinchona alkaloid catalysts quinine and quinidine were used, no enantioselectivity was induced at room temperature or even when the temperature was lowered to –30°C (Table 3.6, entries 2 to 6). Reactions were sluggish at –30 °C and could not be brought to completion even after an extended time frame. Cinchona alkaloid dimer catalysts (DHQD)₂PHAL and (DHQD)₂Pyr furnished racemic products as well (Table 3.6, entries 8, 9, 10, 12 and 13). The combination of (DHQD)₂PHAL and highly polar protic solvent TFE, which normally gave good *ee* for the lab's chlorofunctionalization chemistry led to racemic product (Table

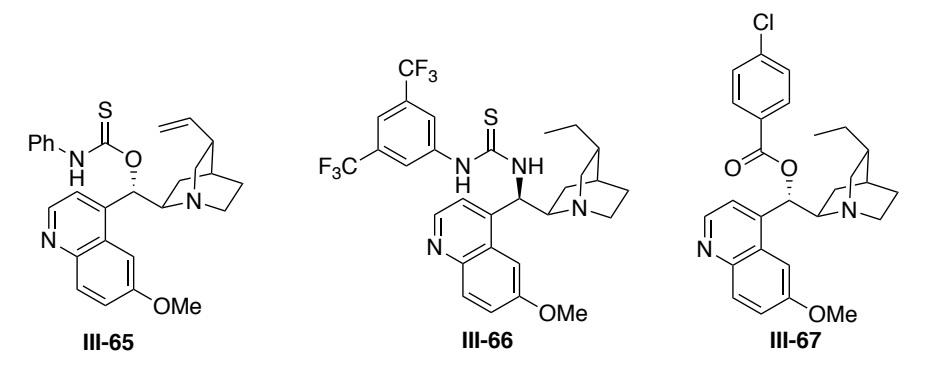
3.6, entry 9), albeit with good yield. Other quinine or quinidine derived monomeric catalysts, such as thiocarbamate III-65 and ester III-67 induced no enantioselectivity (Table 3.6, entries 7 and 16). Chiral Brønsted acid (*R*)-VANOL hydrogen phosphate and thiourea III-66 gave poor yield and no enantioselectivity was obtained (Table 3.6, entries 11, 14 and 15). Reaction with chlorenium reagent NCS catalyzed by (DHQD)₂PHAL in TFE led to good yield and improved *ee* (Table 3.6, entry 12). So far this substrate failed to give any practical enantioselectivity with the catalysts we have tested. NBS induced bromo-*ipso* cyclization, catalyzed by (DHQD)₂PHAL, and gave racemic product in moderate yield (Table 3.6, entry 17).

Table 3.6 Optimization of reaction conditions for substrate III-61

entry	, X	temp. (°C)	catalyst	conversion (%) a	yield (%) b	<i>ee</i> (%) ^c
1	ICI (1 equiv) 23	(DHQD) ₂ PHAL	80	73	2
2	NIS	-30	quinine	62	56	0
3	NISe	-30	quinine	60	40	0
4	NIS	23	quinine	100	75	0
5	NIS	-10	quinine	100	80	0
6	NIS ^e	-10	quinidine	100	41	0
7	NIS	-10	III-65	100	43	0
8	NISe	23	(DHQD) ₂ Pyr	100	74	0
9	NIS ^{d,e}	23	(DHQD) ₂ PHAL	100	80	2
10	NISe	23	(DHQD) ₂ PHAL	80	40	1
11	NCS ^{f,e}	23	(R)-VANOL PA	56	36	2
12	NCS ^{d,e}	23	((DHQD) ₂ PHAL	100	78	6
13	DCDMH	23	(DHQD) ₂ PHAL	100	48	0
14	NIS ^g	23	III-66	100	36	0
15	ICI	23	III-66	100	94	0
16	NIS	-30	III-67	100	94	1
17	NBS ^{d,e}	23	(DHQD) ₂ PHAL	100	68	0

 $^{^{\}rm a}$ conversions were decided by crude $^{\rm 1}H$ NMR using methyl- $\it t$ -butyl ether as internal standard; ; $^{\rm b}$ yields were determined by isolated product through column chromatography; $^{\rm c}$ ee were determined by chiral HPLC column

f DCM was used as solvent instead of MeCN.g CHCl3 was used as solvent



^d TFE was used as solvent instead of MeCN; ^e no NaHCO₃ was added;

3.2.6 Asymmetric *ipso*-halocyclization with *N*-(2-hydroxyphenyl)-*N*-methyl-3-phenylpropiolamide

After exhaustive search for the asymmetric *ipso*-halocyclization of *N*-tethered *para*-activating phenyl substrate **III-61**, we realized that this reaction might not be compatible with our group's catalytic system. I got some inspiration from recent work from Schneider's group (Scheme 3.16, a).²⁷ They reported an *ortho*-directing group assisted nucleophilic substitution of propargylic alcohols **III-68** catalyzed by chiral phosphoric acid **III-71**. Based on the mechanism, *o*-hydroxy group of **III-68** helps to form highly reactive *o*-quinone methides, which are readily attacked by enamides **III-69**. More importantly a chiral phosphoric acid helps bring quinone and enamides close together and subjects the cyclization step to a chiral environment by hydrogen binding. Inspired by this catalytic model, I designed a new *ortho*-activating substrate **III-72**, which could be interacting with Brønsted acid through hydrogen binding with carbonyl and hydroxyl groups (Scheme 3.16, b), which presumably direct *ipso*-cyclization in a chiral pocket.

Scheme 3.16 *ortho*-directing group assisted nucleophilic substitution of propargylic alcohols

The investigation began with the substrate **III-72** with halogen screening using (*S*)-VANOL phosphoric acid **III-75** (Table 3.7). Reactions were conducted under Schneider's condition, using dichloromethane as solvent at room temperature. Not surprisingly, electrophilic iodine sources, such as I₂, ICI and NIS were more reactive than bromine and chlorine reagents in terms of yield, although in poor *ee*. Chlorinated hydantoin species (DCDMH, DCDPH) and NCS resulted mostly in the recovery of starting materials recovery. No enantioselectivity was obtained under conditions with different halonium reagent.

Table 3.7 Screen of different electrophilic halogen reagent for III-72

III-75

Next, I screened other chiral phosphoric acids using NIS, which turned out to be the optimal halogen reagent in the study above (Table 3.8). (*R*)-BINOL phosphoric acid increased the *ee* to 6% as compared with (*S*)-VANOL phosphoric acid (2% *ee*). Lowering the temperature from rt to –20 °C further increased the *ee* to 12%. Switching solvent from DCM to toluene further increased *ee* to 16%. Adding Lewis acids such as Zn(OTf)₂ increased the yield but had minor effect on *ee*. More sterically hindered (*R*)-*t*-butyl VANOL phosphoric acid III-78 at –20 °C gave comparable *ee* as the (*R*)-BINOL phosphoric acid. BINOL derived thio-phosphoramide III-80 gave 3% *ee* at –30 °C in toluene. Last, but not least, 30% *ee* was obtained when (*R*)-TRIP III-79 was used as catalyst at –30 °C. The major side product observed in this reaction was the aromatic electrophilic iodination product III-76.

Table 3.8 Catalyst screening for III-72

condition		ee % ^b
(R)-BINOL phophoric acid III-77, DCM (0.1M), rt	68	6
(<i>R</i>)-BINOL phophoric acid III-77 , toluene (0.1M), -30 °C	_	16
(R)-BINOL phophoric acid III-77, DCM (0.1M), Zn(OTf)2, rt	86	4
(<i>R</i>)-BINOL phophoric acid III-77 , DCM (0.1M), $^-$ 20 $^{\circ}$ C	85	12
(R)-t-butyl VANOL phophoric acid III-78, DCM(0.1M), -20 °C	53	12
5 mol% (<i>R</i>)-TRIP III-79 , toluene (0.1M), -30 °C	49	30
5 mol% III-80 , toluene (0.1 M), -30 °C	42	3

a yields were determined from isolated product; b ee were determined from chiral HPLC

The strategy of using the combination of metal and chiral ligand was also examined. (Table 3.9). I assumed that chiral ligands like VANOL, VANOL phosphoric acid and tartaric acid along with Lewis acid can have some cooperative chiral control. However different Lewis acids such as Pd(OAc)₂, Ti(O*i*Pr)₄ and Yb(OTf)₃ combined with chiral ligands gave no enantioselectivity. Other halogen sources such as NBS were also evaluated using (*R*)-TRIP as catalyst. **III-73** was obtained in 40% yield and 8% ee (Scheme 3.17).

Table 3.9 Evaluation of chiral ligand with different Lewis acid

catalyst	yield %	ee %
Pd(OAc) ₂ , (S)-VANOL phosphoric acid	64	2
Pd(OAc) ₂ , (S)-t-butyl-VANOL	37	0
Ti(O <i>i</i> Pr) ₄ , (<i>R</i>)- <i>t</i> -butyl-VANOL	43	0
Yb(OTf) ₃ ·H ₂ O, (<i>D</i>)-tartaric acid	80	0
(DHQD) ₂ PHAL	0	_

Scheme 3.17 Evaluation of NBS with chiral dihydrogen phosphate

It is noteworthy to point out that if phenol was protected with methyl, no *ipso*-cyclized product was observed (Scheme 3.18). The major product was **III-81**, which might be due to the generated iodonium being trapped by H₂O when the reaction was worked up. Same product was observed when acetic acid and H₂O were used. However, when glacial acetic acid was used alone as solvent, *ipso*-cyclized product **III-82** was obtained in moderate yield. Another interesting observation was that when the N was not protected (**III-83**), no reaction occurs using chiral phosphoric acid as the catalyst.

Scheme 3.18 Reactions of other derivatives

3.3 Summary and future work

We attempted to achieve enantioselective *ipso*-cyclization mediated by electrophilic halogen sources. We have tested different catalytic systems including Lewis base and Brønsted acid catalysts, however none of them could deliver practical *ee*. We also tried to modify the skeleton of substrates to tune its hydrogen-bonding affinity with catalysts, for example substrate **III-72** which was supposed to have good hydrogen binding affinity with chiral hydrogen phosphate catalyst furnished 30% *ee*.

For the future work, to achieve good enantioselectivity we could try other organocatalysts or some organometal catalysts. For example, we could modify substrate to **III-84**, which contains a triple bond that can be activated by gold catalyst with a chiral ligand (Scheme

3.19). There are a large body of work with chiral gold catalysis. For instance, Toste reported gold-TRIP as a tight ion pair to catalyze the enantioselective construction of C-O/C-N bond.²⁸⁻²⁹ You's group recently reported a gold catalyzed dearomatization of naphthols to construct spirocarbocylces, however they have not demonstrated asymmetric version yet.²⁹

Scheme 3.19 Gold catalyzed *ipso*-cylclization

Another future endeavor could be using the double bond as a halenium acceptor instead of triple bond. Based on our group's previous study, most successful examples of Lewis base catalyzed enantioselctive halofunctionalization is with olefinic amides. Besides *N*-linked, *C* and *O*-linked substrates can also be candidates (Scheme 3.20). Indeed *N*-linker itself is also a chiral center which could have different conformation of states due to the restricted rotation of the C-N bond. I surmise the possibility that different conformation of the substrate could scramble the cyclization, which is the enantiodeterming step.

Scheme 3.20 Other substrates for *ipso*-halocyclization

3.4 Experimental section

3.4.1 General information

NBS was used after recrystallization from 90-95 °C water. NIS was recrystallized from dioxane/CCl₄. DCDMH was used after recrystallization from CHCl₃ and then sublimation. Other halogen reagents were purchased from commercial sources without purification. TLC analyses were performed on silica gel plates (pre-coated on glass; 0.20 mm thickness with fluorescent indicator UV254) and were visualized by UV or charred in KMnO₄ stains. ¹H and ¹³C NMR spectra were collected on 500 MHz NMR spectrometers (Agilent) using CDCl₃. Chemical shifts are reported in parts per million (ppm) and are referenced to residual solvent peaks. For HRMS (ESI) analysis, a Water 2795 (Alliance HT) instrument was used and referenced against Polyethylene Glycol (PEG-400-600). Flash silica gel (32-63 μm, Silicycle 60 Å) was used for column chromatography. All known compounds were characterized by ¹H and ¹³C NMR and are in complete agreement with samples reported elsewhere. All new compounds were characterized by ¹H and ¹³C NMR, HRMS, and melting point (where appropriate). Enantiomeric excesses were determined using chiral HPLC (instrument: HP series 1100, Agilent 1260 infinity).

3.4.2 Synthesis of substrate III-48, III-52

$$\begin{array}{c|c} NH_2 & HN^{-1S} \\ \hline CH_3 & 1 \text{ equiv TsCl, Et}_3N \\ \hline CH_2Cl_2, 0 \text{ °C to rt} \\ \hline OCH_3 & OCH_3 \\ \hline \end{array}$$

4-Methoxy-2-methylaniline (2.74 g, 20.0 mmol, 1.0 equiv) was added to an oven-dried round bottom flask charged with Ar. Freshly distilled CH₂Cl₂ 100 mL was added into flask.

The solution was stirred in an ice bath for 5 min followed by addition of distilled Et₃N (3.47 g, 34.3 mmol, 1.7 equiv). Tosylchloride (3.8 g, 20.0 mmol, 1.0 equiv) was added. The solution mixture was stirred for 2 h in an ice bath. The reaction was quenched with water. The organic layer was extracted with CH₂Cl₂ (3×30 mL). The organic layer was separated and dried over Na₂SO₄. The solvent was removed under reduced pressure to afford the crude product. Recrystalization of the crude product with EtOAc/hexane afforded III-91 as a white solid in 75% yield. Melting point: 69 °C-72 °C.

¹H NMR (500 MHz, CDCl₃), δ 7.79 (d, 2H, J = 5.0 Hz), δ 7.30 (d, 2H, J = 10.0 Hz), δ 6.79 (d, 1H, J = 10.0 Hz), δ 6.71 (d, 1H, J = 5.0 Hz), δ 6.64 (dd, 1H, J = 5.0 Hz, 10.0 Hz), δ 3.78 (s, 1H), δ2.44 (s, 3H), δ 1.88 (s, 3H).

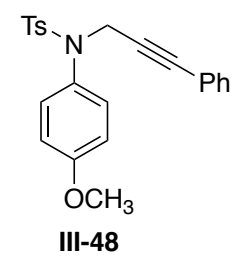
¹³C NMR (125 MHz, CDCl₃), δ 158.28, 143.57, 136.78, 135.41, 129.50, 128.03, 127.21, 126.89,116.00, 111.78.

3-Phenyl-2-propyn-1-ol (396 mg, 3.3 mmol, 1 equiv), triphenylphosphine (944 mg, 3.6 mmol, 1.1 equiv) and freshly distilled THF (16 mL) were added to a round bottom flask, followed by compound **III-91** (1.0 g, 3.6 mmol, 1.1 equiv) and the mixture was stirred at the 0 °C for 10 min. DIAD (728 mg, 3.6 mmol, 1.1 equiv) was added into the mixture. The reaction was stirred at 0 °C and gradually warmed to room temperature. After 2 h, the reaction was worked up with water (40 mL). The mixture was extracted with EtOAc and the organic layer was dried with anhydrous Na₂SO₄. The solids were filtered and the

solvent was removed under reduced pressure to afford a yellowish oil. The product was purified with column chromatography to yield **III-52** as a colorless oil 668 mg (50% yield). ¹H NMR (500 MHz, CDCl₃) δ 2.41 (s, 6H), δ 3.78 (s, 3H), δ 4.36 (d, 2H, J = 17.5 Hz), δ 4.78 (d, 2H, J = 17.5 Hz), δ 6.57 (dd, 1H, J = 3 Hz, 9 Hz), δ 6.81 (d, 1H, J = 3 Hz), δ 7.18 (dd, 2H, J = 1.5 Hz, 8 Hz), δ 7.24-7.29 (m, 5H), δ 7.69 (d, 2H, J = 7.5 Hz).

¹³C NMR (125 MHz, CDCl₃), δ 18.55, 21.43, 42.17, 55.21, 83.48, 85.15, 111.45, 116.11, 122.38, 128.09, 128.13, 128.31, 129.27, 129.72, 130.63, 131.35, 136.64, 141.21, 143.40, 159.36.

HRMS (ESI) (m/z): $[M+H]^+$ calculated for $[C_{24}H_{24}NO_3S]^+$: 406.1477, found: 406.1478.



71% yield of **III-48** was obtained using procedure above, colorless oil, $R_{\rm f}$ = 0.62 (30% EtOAc in Hexane, UV)

¹H NMR (500MHz, CDCl₃) δ 7.59 (d, 2H, *J* = 8 Hz), δ 7.24-7.27(m, 3H), δ 7.15-7.20 (m, 6H), δ 6.80 (d, 2H, *J* = 9 Hz), δ 4.61 (s, 2H), δ 3.78 (s, 3H), δ 2.36 (s, 3H).

¹³C NMR (125 MHz, CDCl₃), δ 21.49, 42.31, 55.39, 83.78, 85.47, 114.16, 122.41, 128.13, 128.16, 128.39, 129.21, 130.11, 131.46, 132.24, 136.09, 143.38, 159.31.

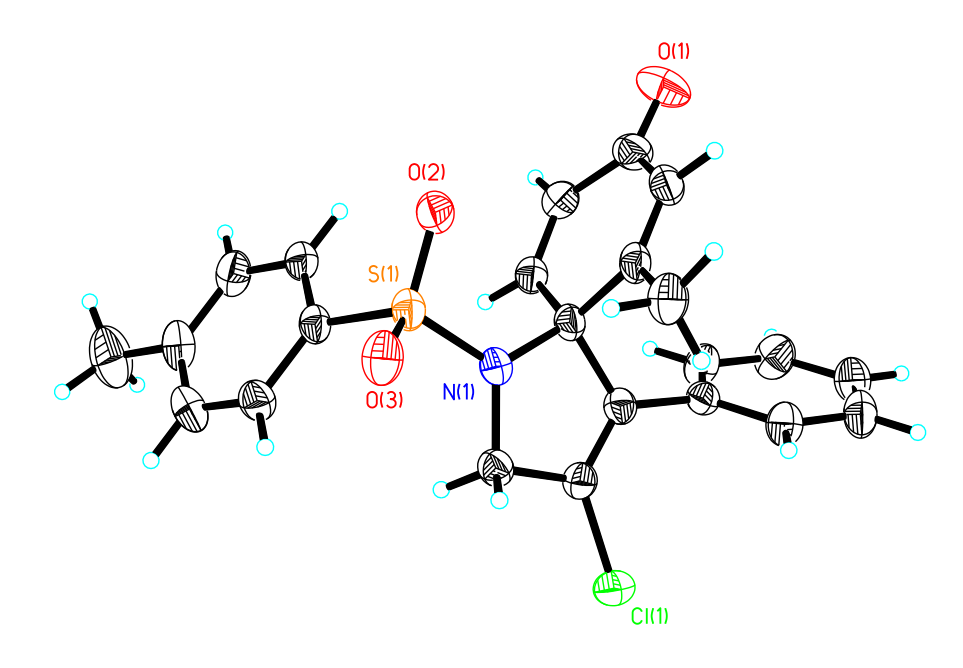
HRMS (ESI) (m/z): $[M+H]^+$ calculated for $[C_{23}H_{22}NO_3S]^+$: 392.1320, found: 393.1322.

3.4.3 General procedure of screening and optimization of *i*pso-halocyclization of substrate III-48 and III-52

Substrate III-52 (30 mg, 0.074 mmol, 1 equiv) was dissolved in dry solvent (1 mL). The appropriate catalyst (0.0074 mmol, 0.1 equiv) and the halogen source (0.074 mmol, 1 equiv) were added. The reaction was stirred at the room temperature for the stated time, and worked up with saturated Na₂S₂O₃. The organic layer was extracted with EtOAc and dried over anhydrous Na₂SO₄. The solvent was removed under the reduced pressure to yield a wax like solid.

X = CI (III-53): ¹H NMR (500 MHz, CDCl₃), δ 2.01 (s, 3H), δ 2.44 (s, 3H), δ 4.46 (d, 1H, J = 15 Hz), δ 4.58 (d, 1H, J = 15 Hz), δ 6.05 (s, 1H), δ 6.14 (dd, 1H, J = 10 Hz, 5 Hz), δ 6.50 (d, 1H, J = 10 Hz), δ 7.00 (d, 2H, J = 5 Hz), δ 7.22-7.33 (m, 5H), δ 7.72 (d, 2H, J = 5 Hz); ¹³C NMR (125 MHz, CDCl₃), δ 19.11, 21.58, 57.01, 75.05, 127.03, 127.67, 128.38, 128.51, 129.04, 129.26, 129.32, 129.77, 129.89, 135.16, 136.24, 144.35, 145.77, 156.75, 184.78.

HRMS (ESI) (m/z): [M+H]⁺ calculated for [C₂₃H₂₁NO₃SCI]⁺: 426.0931, found: 426.0927. The structure was further verified by X-ray crystallography:



Resolution of enantiomers: Daicel Chiralpak OD-H, 20% IPA/Hex, 1 mL/min; 254 nm, RT1= 10.6 min, RT2 = 15.2 min.

X = Br (III-56): White solids, melting point: 170-172 °C.

¹H NMR (500 MHz, CDCl₃) δ 2.01 (s, 3H), δ 2.44 (s, 3H), δ 4.49 (d, 1H, J = 14 Hz), δ 4.62 (d, 1H, J = 14 Hz), δ 6.03 (s, 1H), δ 6.13 (dd, 1H, J = 9.5 Hz, 2 Hz), δ 6.49 (d, 1H, J = 10 Hz), δ 6.83 (d, 2H, J = 8 Hz) δ 7.22-7.33 (m, 5H), δ 7.72 (d, 2H, J = 8 Hz); ¹³C NMR (125 MHz, CDCl₃) δ 19.14, 21.60, 59.09, 75.51, 116.49, 127.68, 128.35, 128.54, 129.23, 129.34, 129.79, 129.87, 130.04, 136.30, 138.50, 144.34, 145.56, 156.63, 184.77. HRMS (ESI) (m/z): [M+H]+ calculated for [$C_{23}H_{21}NO_{3}SBr$]+: 470.0426, found: 470.0397. Resolution of enantiomers: Daicel Chiralpak OD-H, 20% IPA/Hex, 1 mL/min; 254 nm, RT1= 10.3 min, RT2 = 14.8 min.

X = I (III-92): White solids, melting point:190-192 °C.

¹H NMR (500 MHz, CDCl₃) δ 2.01 (s, 3H), δ 3.44 (s, 3H), δ 4.46 (d, 1H, J = 13 Hz), δ 4.61 (d, 1H, J = 13 Hz), δ 6.01 (s, 1H), δ 6.11 (dd, 1H, J =10 Hz, 2 Hz), δ 6.46 (d, 1H, J = 10 Hz), δ 6.90 (d, 1H, J =8 Hz), δ 7.25-7.33 (m, 5H), δ 7.72 (d, 2H, J = 8 Hz). ¹³C NMR (125 MHz, CDCl₃) δ 19.19, 21.60, 63.11, 75.54, 90.79, 127.66, 128.33, 128.60, 129.11, 129.33, 129.73, 129.79, 131.97, 136.38, 144.30, 144.75, 145.53, 156.68, 184.78. HRMS (ESI) (m/z): [M+H]+ calculated for [$C_{23}H_{21}NO_3SI$]+: 518.0287, found: 518.0284. Resolution of enantiomers: Daicel Chiralpak OD-H, 15% IPA/Hex, 1 mL/min; 254 nm, RT1=22 min, RT2 = 36 min.

X = CI (III-49): ¹H NMR (500 MHz, CDCl₃) δ 7.75 (d, *J* = 8.3 Hz, 2H), 7.38 – 7.21 (m, 5H), 6.72 (d, *J* = 10.0 Hz, 2H), 6.15 (d, *J* = 10.0 Hz, 2H), 4.52 (s, 2H), 2.47 (s, 3H).

¹³C NMR (125 MHz, CDCl₃) δ 184.34, 146.71, 144.49, 142.61, 135.81, 134.90, 129.83, 129.25, 129.11, 128.31, 127.91, 127.28, 72.28, 56.48, 21.64.

HRMS (ESI) (m/z): [M+H]⁺ calculated for [C₂₂H₁₉NO₃SCI]⁺: 412.0774, found: 412.0764. **X = Br (III-50)**: ¹H NMR (500 MHz, CDCl₃) δ 7.75 (d, J = 8.3 Hz, 2H), 7.41 – 7.21 (m, 5H), 7.05 – 6.93 (m, 2H), 6.71 (d, J = 10.0 Hz, 2H), 6.14 (d, J = 10.1 Hz, 2H), 4.57 (s, 2H), 2.47 (s, 3H).

¹³C NMR (125 MHz, CDCl₃) δ 184.28, 146.50, 144.47, 138.19, 135.85, 130.12, 129.83, 129.80, 129.23, 129.12, 128.26, 127.90, 116.63, 72.70, 58.51, 21.64.

HRMS (ESI) (m/z): $[M+H]^+$ calculated for $[C_{22}H_{19}NO_3SBr]^+$: 456.0269, found: 456.0266.

X = I (III-51): ¹H NMR (500 MHz, CDCl₃) δ 7.75 (d, J = 8.3 Hz, 2H), 7.43 – 7.21 (m, 5H), 7.00 – 6.89 (m, 2H), 6.69 (d, J = 10.0 Hz, 2H), 6.12 (d, J = 10.0 Hz, 2H), 4.56 (s, 2H), 2.47 (s, 3H).

¹³C NMR (125 MHz, CDCl₃) δ 184.32, 146.50, 144.42, 144.33, 135.89, 132.07, 129.81, 129.65, 129.20, 129.19, 128.24, 127.90, 91.09, 72.68, 62.46, 21.64.

HRMS (ESI) (m/z): $[M+H]^+$ calculated for $[C_{22}H_{19}NO_3SI]^+$: 504.0130, found: 504.0090.

3.4.4 Procedure of synthesis and ipso-halocyclization of substrate III-54

2-Bromo-4-methoxyphenol (950 mg, 4.7 mmol, 1 equiv) and K₂CO₃ (0.68 g, 4.9 mmol, 1 equiv) was dissolved in distilled DMF (25 mL), followed by adding phenyl propargyl bromide (1000 mg, 5.13 mmol, 1.1 equiv). The reaction mixture was refluxed at 120 °C for 1.5 h. The reaction was quenched with H₂O, and the mixture was extracted with ethyl acetate. The organic layer was dried with anhydrous Na₂SO₄. The solvent was removed under the reduced pressure to afford crude residue, which was then purified in column chromatography to yield III-54 as yellow oil in 81% yield. (This compound is stable on bench for more than 5 years!)

Rf = 0.76 (30% EtOAc in Hex, UV)

¹H NMR (500 MHz, CDCl₃) δ 7.40 (dd, J = 7.6, 1.9 Hz, 2H), 7.34 – 7.25 (m, 3H), 7.16 – 7.05 (m, 2H), 6.81 (dd, J = 9.0, 3.0 Hz, 1H), 4.91 (s, 2H), 3.75 (s, 3H).

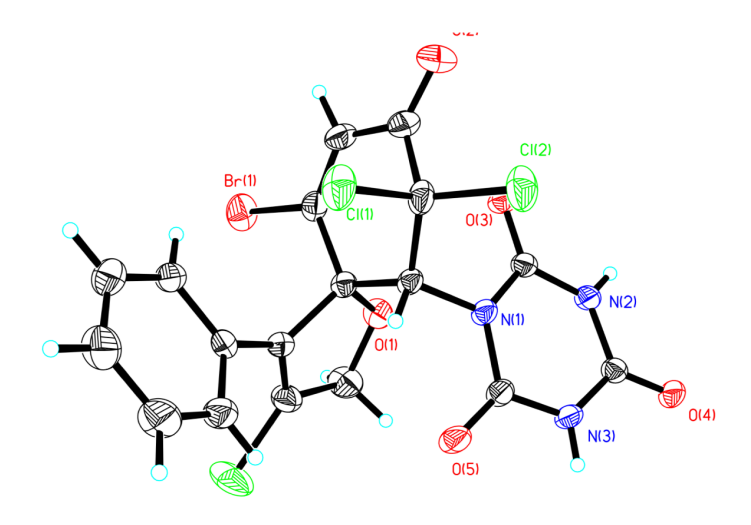
¹³C NMR (125 MHz, CDCl₃) δ 154.93, 148.54, 131.77, 128.69, 128.29, 122.23, 118.77, 116.70, 113.71, 113.47, 87.58, 83.76, 58.91, 55.87.

Compound III-54 (100.0 mg, 0.3 mmol, 1 equiv) was dissolved in acetonitrile (1 mL). NaHCO₃ (50.4 mg, 0.6 mmol, 2 equiv) was added into the solution, followed by DABCO (33.7 mg, 0.03 mmol, 0.1 equiv), and TCCA (139.4 mg, 0.6 mmol, 2 equiv). The reaction was stirred at room temperature for the statetd time, the reaction was worked up with saturated Na₂S₂O₃. The mixture was extracted with EtOAc and dried over the anhydrous Na₂SO₄, and the solvent was removed under reduced pressure to get a viscous yellow oil 105 mg (66% yield).

¹H NMR (500 MHz, CDCl₃), δ 4.60 (d, 1H, J = 12.5 Hz), δ 4.84 (d, 1H, J = 12.5 Hz), δ 6.02 (s, 1H), δ 6.87 (s, 1H), δ 7.40-7.41 (m, 5H).

¹³C NMR (125 MHz, CDCl₃), δ 65.37, 77.63, 82.99, 90.86, 128.86, 128.93, 129.82, 129.92, 130.26, 130.85, 135.30, 145.58, 147.09, 148.45, 148.87, 176.82.

The structure was verified by X-ray crystallography.



Resolution of enantiomers: Daicel Chiralpak AD-H, 20% IPA/Hex, 1 mL/min; 250 nm, RT1= 9.9 min, RT2 = 10.2 min.

3.4.5 Synthesis and ipso-cyclization of substrate III-61

III-61 was synthesized with III-91 (1000 mg, 3.43 mmol) according to the reported procedure.³⁰ 1.15g III-61 was obtained as yellow glue (81% yield).

 $R_f = 0.37 \text{ (UV, } 30\% \text{ EtOAc / Hex)}$

¹H NMR (500 MHz, Chloroform-*d*) δ 8.08 – 7.95 (m, 2H), 7.40 – 7.30 (m, 3H), 7.29 – 7.19 (m, 2H), 7.11 – 7.02 (m, 3H), 6.95 – 6.86 (m, 1H), 6.82 (dd, J = 8.7, 2.9 Hz, 1H), 3.87 (d, J = 0.9 Hz, 3H), 2.48 (s, 3H), 2.40 (s, 3H).

¹³C NMR (126 MHz, cdcl₃) δ 160.66, 152.88, 145.31, 140.92, 135.69, 132.98, 131.31, 130.81, 129.46, 129.41, 128.45, 127.21, 119.25, 116.18, 112.20, 93.15, 81.64, 55.54, 21.75, 18.75.

HRMS (ESI) (m/z): [M+H]+ calculated for [C₂₄H₂₂NO₄S]+: 420.1270, found: 420.1273.

X = CI (III-62):

¹H NMR (500 MHz, CDCl₃) δ 8.06 – 7.97 (m, 2H), 7.47 – 7.30 (m, 5H), 7.24 – 7.15 (m, 2H), 6.50 (d, *J* = 0.9 Hz, 2H), 6.35 – 6.25 (m, 1H), 2.46 (s, 3H), 1.96 (d, *J* = 1.4 Hz, 3H). ¹³C NMR (126 MHz, CDCl₃) δ 184.26, 162.83, 152.26, 151.47, 146.27, 142.07, 135.03, 132.77, 131.36, 130.93, 129.84, 128.86, 128.79, 127.72, 127.67, 127.38, 71.29, 21.79, 18.21.

HRMS (ESI) (m/z): [M+H]+ calculated for [$C_{23}H_{19}NO_4SCI$]+: 440.0723, found: 440.0717. Resolution of enantiomers: Daicel Chiralpak AD-H, 20% IPA/Hex, 1 mL/min; 250 nm, RT1= 13.7min, RT2 = 15.2 min.

X = Br (III-63):

¹H NMR (500 MHz, Chloroform-*d*) δ 8.10 – 7.96 (m, 2H), 7.50 – 7.29 (m, 5H), 7.21 – 7.10 (m, 2H), 6.50 (s, 2H), 6.30 (d, J = 1.7 Hz, 1H), 2.48 (s, 3H), 2.00 (d, J = 1.4 Hz, 3H). ¹³C NMR (126 MHz, cdcl₃) δ 184.22, 163.37, 156.05, 151.32, 146.23, 141.81, 135.05, 132.71, 131.25, 130.83, 129.84, 128.85, 128.80, 128.73, 127.55, 118.41, 72.96, 21.81, 18.26.

HRMS (ESI) (m/z): [M+H]⁺ calculated for [C₂₃H₁₉NO₄SBr]⁺: 484.0218, found: 484.0237. Resolution of enantiomers: Daicel Chiralpak IA, 20% IPA/Hex, 1 mL/min; 254 nm, RT1= 13.9 min, RT2 = 16.4 min.

X = I (III-64):

¹H NMR (500 MHz, CDCl₃) δ 8.03 (d, J = 8.4 Hz, 2H), 7.46 – 7.29 (m, 5H), 7.13 – 6.94 (m, 2H), 6.56 – 6.40 (m, 2H), 6.26 (t, J = 1.5 Hz, 1H), 2.47 (s, 3H), 2.00 (d, J = 1.4 Hz, 3H).

¹³C NMR (126 MHz, CDCl₃) δ 184.26, 164.92, 162.40, 151.41, 146.16, 141.81, 135.06, 132.49, 130.99, 130.67, 130.59, 129.83, 128.88, 128.75, 127.41, 96.22, 74.96, 21.81, 18.31.

HRMS (ESI) (m/z): $[M+H]^+$ calculated for $[C_{23}H_{19}NO_4SI]^+$: 532.0079, found: 532.0091. Resolution of enantiomers: Daicel Chiralpak IA, 20% IPA/Hex, 1 mL/min; 250 nm, RT1= 17.3 min, RT2 = 20.7 min.

3.4.6 Synthesis and ipso-cyclization of substrate III-72

III-93 was synthesizd according to reported procedure³¹: Na (2.3 g, 100 mmol) was slowly added to MeOH (40 mL). Once the evolution of H₂ gas had ceased, anisidine (2.46 g, 20 mmol) was added and the resulting hot solution was poured into a suspension of paraformaldehyde (840 mg, 28 mmol) in MeOH. The mixture was stirred at rt for 5 h and NaBH₄ (700 mg, 20 mmol) was added. The solution was heated under reflux and hydrolyzed with 1 M KOH solution (20 mL). Most of the MeOH was removed under reduced pressure and DCM was added to the residue. The organic layer was separated and the solvent was removed under reduced pressure to afford the crude. The crude was purified by column chromatography in silica gel with 15% EtOAc in Hexane as eluent. 820 mg of III-93 as white solid was obtained (30% yield).

¹H NMR (500 MHz, CDCl₃) δ 6.92 (td, J = 7.6, 1.4 Hz, 1H), 6.79 (dd, J = 8.0, 1.3 Hz, 1H), 6.69 (td, J = 7.7, 1.5 Hz, 1H), 6.62 (dd, J = 7.8, 1.5 Hz, 1H), 4.25 (s, 1H), 3.86 (s, 3H), 2.88 (s, 3H).

¹³C NMR (126 MHz, CDCl₃) δ 146.88, 139.38, 121.34, 116.28, 109.31, 109.21, 55.39, 30.39.

III-94 was synthesized with **III-93** (1.1 g, 8.02 mmol) followed the same procedure as **III-61** described above. Ginger color solid was obtained in 83% yield.

¹H NMR (500 MHz, Chloroform-*d*) δ 7.39 (ddt, J = 9.2, 8.0, 1.4 Hz, 1H), 7.31 (ddt, J = 8.1, 6.1, 1.6 Hz, 2H), 7.26 – 7.16 (m, 2H), 7.10 (dt, J = 8.4, 1.6 Hz, 2H), 7.05 – 6.98 (m, 2H), 3.94 – 3.76 (m, 3H), 3.30 (d, J = 1.6 Hz, 3H).

¹³C NMR (126 MHz, cdcl₃) δ 155.82, 155.12, 132.43, 132.42, 131.75, 129.76, 128.54, 128.27, 120.57, 120.56, 111.86, 89.28, 82.64, 55.68, 35.22.

HRMS (ESI) (m/z): [M+H]+ calculated for [C₁₇H₁₆NO₂]+: 266.1181, found: 266.1194.

$$\begin{array}{c} O \\ N \end{array} \begin{array}{c} O \\ \longrightarrow Ph \end{array}$$

$$\begin{array}{c} O \\ \longrightarrow Ph \end{array}$$

To a solution of **III-94** (770 mg, 2.9 mmol) in distilled dichloremethane (10 mL) was added a solution of BBr₃ (11.6 mmol, 1 M in DCM) at room temperature. The mixture was protected with Ar balloon. After completion, the reaction was quenched the reaction with H₂O to hydrolize excess BBr₃ and boron complexes. The organic layer was extracted with dichloromethane. The solvent was removed under reduced pressure to give crude residue. The crude was purified with column chromatography (silica gel, 15% to 25%

EtOAc /hexane) to give colorless crystals **III-72** in 59% yield. M.P. = 108-113 $^{\circ}$ C. R_f = 0.24 (UV, 30% EtOAc in Hexane)

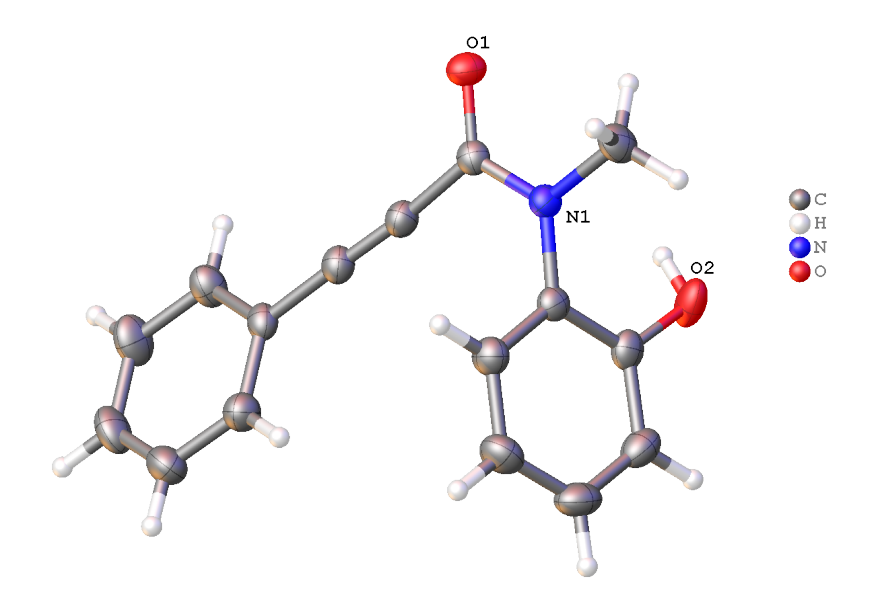
amide *cis/trans* isomer mixture:

¹H NMR (500 MHz, CDCl₃) δ 7.65 – 7.60 (m, 1H), 7.51 – 7.39 (m, 1H), 7.36 – 7.29 (m, 1H), 7.29 – 7.13 (m, 5H), 7.13 – 6.93 (m, 6H), 6.83 (d, *J* = 12.8 Hz, 1H), 3.76 (s, 2H), 3.36 (s, 3H).

¹³C NMR (126 MHz, CDCl₃) δ 156.09, 155.39, 153.44, 151.31, 132.63, 132.62, 130.60, 130.13, 129.94, 129.68, 129.26, 129.09, 128.62, 128.16, 125.51, 121.21, 120.08, 120.07, 119.85, 117.72, 93.48, 91.72, 82.07, 81.51, 40.26, 35.64.

HRMS (ESI) (m/z): [M+H]+ calculated for [C₁₆H₁₄NO₂]+: 252.1025, found: 252.1028.

The structure has been confirmed by X-ray crystallography:



brownish oil, $R_f = 0.12$ (UV, 30% EtOAc in Hexane)

¹H NMR (500 MHz, CDCl₃) δ 7.44 – 7.30 (m, 3H), 7.23 – 7.13 (m, 2H), 6.93 (ddd, J = 9.9, 6.0, 1.7 Hz, 1H), 6.51 (dd, J = 9.4, 5.9 Hz, 1H), 6.19 – 6.07 (m, 2H), 2.84 (s, 3H).

¹³C NMR (126 MHz, CDCl₃) δ 194.36, 168.80, 157.28, 141.98, 136.94, 131.97, 129.78, 128.42, 127.65, 127.55, 127.10, 97.85, 77.90, 27.54.

HRMS (ESI) (m/z): [M+H]+ calculated for [$C_{16}H_{13}NO_2I$]+: 377.9991, found: 378.0006. Resolution of enantiomers: Daicel Chiralpak AD-H, 10% IPA/Hex, 1 mL/min; 250 nm, RT1= 18.4 min, RT2 = 22.2 min.

¹H NMR (500 MHz, Chloroform-*a*) δ 7.43 – 7.28 (m, 5H), 7.02 (ddd, J = 9.9, 6.0, 1.7 Hz, 1H), 6.56 (ddd, J = 9.4, 6.0, 0.8 Hz, 1H), 6.21 (dt, J = 9.9, 0.9 Hz, 1H), 6.14 (ddd, J = 9.4, 1.7, 0.9 Hz, 1H), 2.83 (s, 3H).

¹³C NMR (126 MHz, cdcl₃) δ 194.35, 167.20, 150.88, 141.94, 137.20, 130.26, 129.94, 128.51, 127.68, 127.54, 127.21, 119.58, 75.23, 29.61.

HRMS (ESI) (m/z): [M+H]⁺ calculated for [$C_{16}H_{12}NO_2Br$]⁺: 330.0130, found: 330.0135. Resolution of enantiomers: Daicel Chiralpak AD-H, 10% IPA/Hex, 1 mL/min; 250 nm, RT1= 16.2 min, RT2 = 19.1 min.

diastereomers mixtures:

¹H NMR (500 MHz, Chloroform-*d*) δ 7.77 – 7.67 (m, 2H), 7.58 – 7.40 (m, 4H), 7.41 – 7.25 (m, 6H), 7.17 (ddd, J = 8.3, 7.5, 1.7 Hz, 1H), 7.05 (td, J = 7.6, 1.3 Hz, 1H), 6.92 (ddd, J = 7.4, 5.7, 1.5 Hz, 2H), 6.81 (dd, J = 8.3, 1.3 Hz, 1H), 6.67 (td, J = 7.6, 1.2 Hz, 1H), 5.95 (s, 1H), 5.85 (s, 1H), 3.90 (s, 3H), 3.58 (s, 3H), 3.25 (d, J = 5.2 Hz, 6H).

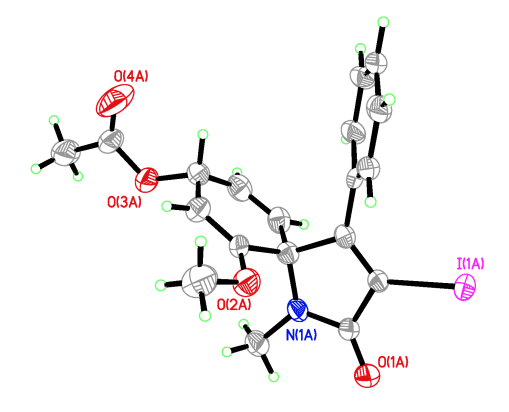
¹³C NMR (126 MHz, cdcl₃) δ 190.96, 188.72, 166.06, 164.71, 154.86, 154.63, 133.44, 133.37, 133.29, 130.91, 130.90, 130.39, 130.30, 130.03, 129.08, 128.78, 128.75, 128.50, 128.42, 128.37, 121.33, 112.13, 112.04, 55.82, 55.20, 37.84, 37.52, 28.60, 26.72.

The structure was confirmed by X-ray crystallography:

diastereomers mixtures (ratio= 5:4)

¹H NMR (500 MHz, CDCl₃) δ 7.46 – 7.28 (m, 7H), 7.26 – 7.12 (m, 2H), 6.15 (ddd, J = 9.8, 3.9, 1.4 Hz, 1H), 6.09 (ddd, J = 9.8, 3.4, 1.5 Hz, 1H), 5.81 (td, J = 4.0, 1.1 Hz, 1H), 5.57 (td, J = 3.7, 1.4 Hz, 1H), 5.48 (ddd, J = 18.1, 9.8, 1.2 Hz, 2H), 5.18 (dd, J = 4.2, 1.4 Hz, 1H), 5.12 (dd, J = 4.0, 1.5 Hz, 1H), 3.54 (d, J = 4.7 Hz, 5H), 2.86 (s, 3H), 2.78 (s, 3H), 2.07 (s, 3H), 1.93 (s, 2H).

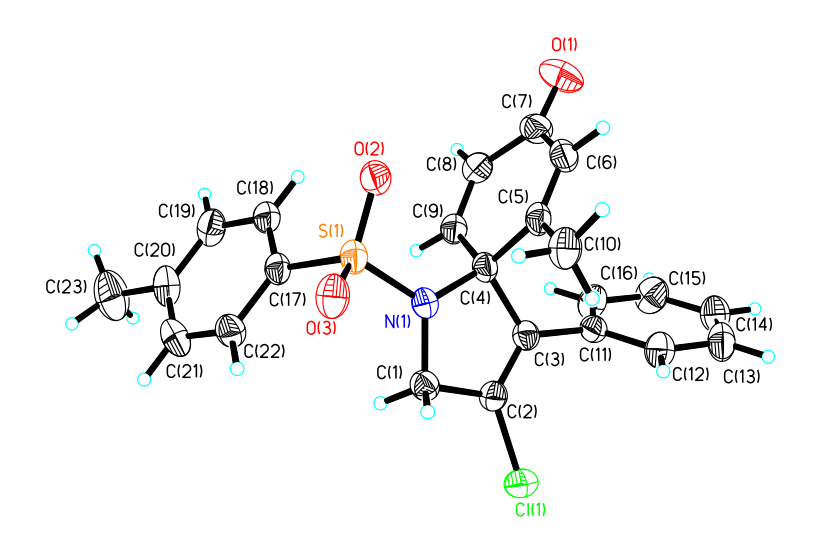
X-ray crystallography:



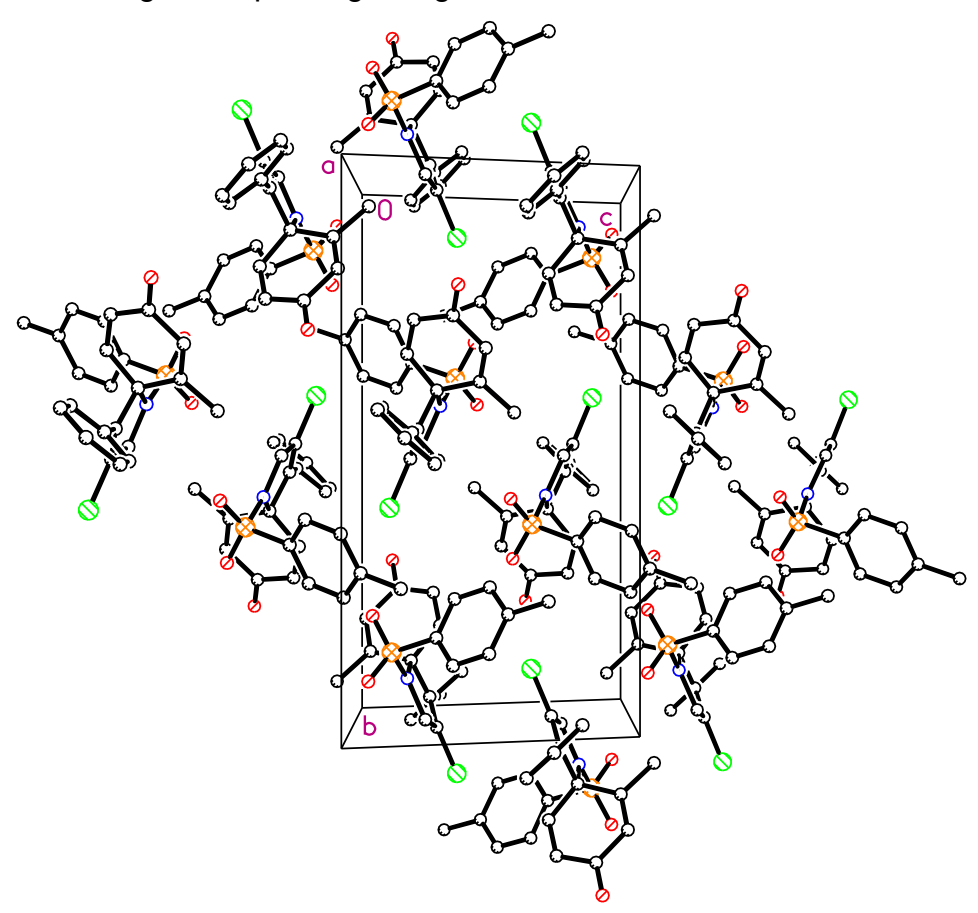
3.5 X-ray crystallography data

3.5.1 X-ray crystallography data of III-53

The following are 50% thermal ellipsoidal drawings of the molecule in the asymmetric cell with various amount of labeling:



This is a drawing of the packing along the a-axis:



Crystal data and structure refinement for bb104

Identification code	bb104		
Empirical formula	C23 H20 CI N O3 S		
Formula weight	425.91		
Temperature	173(2) K		
Wavelength	1.54178 Å		
Crystal system	Monoclinic		
Space group	P 21/c		
Unit cell dimensions	a = 13.1210(2) Å	α = 90°.	
	b = 17.7164(3) Å	$\beta = 110.5720(10)^{\circ}$	
	c = 9.7092(2) Å	$\gamma = 90^{\circ}$	
Volume	2113.05(6) Å ³		
Z	4		
Density (calculated)	1.339 Mg/m ³		
Absorption coefficient	2.721 mm ⁻¹		

F(000) 888

Crystal size 0.12 x 0.12 x 0.09 mm³

Theta range for data collection 4.38 to 67.71°.

Index ranges -15<=h<=15, -21<=k<=20, -10<=l<=11

Reflections collected 12122

Independent reflections 3666 [R(int) = 0.0309]

Completeness to theta = 67.71° 95.7%

Absorption correction Semi-empirical from equivalents

Max. and min. transmission 0.7840 and 0.7325

Refinement method Full-matrix least-squares on F²

Data / restraints / parameters 3666 / 0 / 264

Goodness-of-fit on F² 1.135

Final R indices [l>2sigma(l)] R1 = 0.0479, wR2 = 0.1389 R indices (all data) R1 = 0.0569, wR2 = 0.1448

Largest diff. peak and hole 1.014 and -0.367 e.Å-3

Experimental Section:

A colorless needle crystal with dimensions 0.12 x 0.12 x 0.09 mm was mounted on a Nylon loop using very small amount of paratone oil.

Data were collected using a Bruker CCD (charge coupled device) based diffractometer equipped with an Oxford Cryostream low-temperature apparatus operating at 173 K. Data were measured using omega and phi scans of 0.5° per frame for 30 s. The total number of images was based on results from the program COSMO¹ where redundancy was expected to be 4.0 and completeness to 0.83 Å to 100%. Cell parameters were retrieved using APEX II software² and refined using SAINT on all observed reflections. Data reduction was performed using the SAINT software³ which corrects for Lp. Scaling and absorption corrections were applied using SADABS⁴ multiscan technique, supplied by George Sheldrick. The structures are solved by the direct method using the SHELXS-97 and refined by least squares method on F², SHELXL- 97,

which are incorporated in SHELXTL-PC V 6.10.5

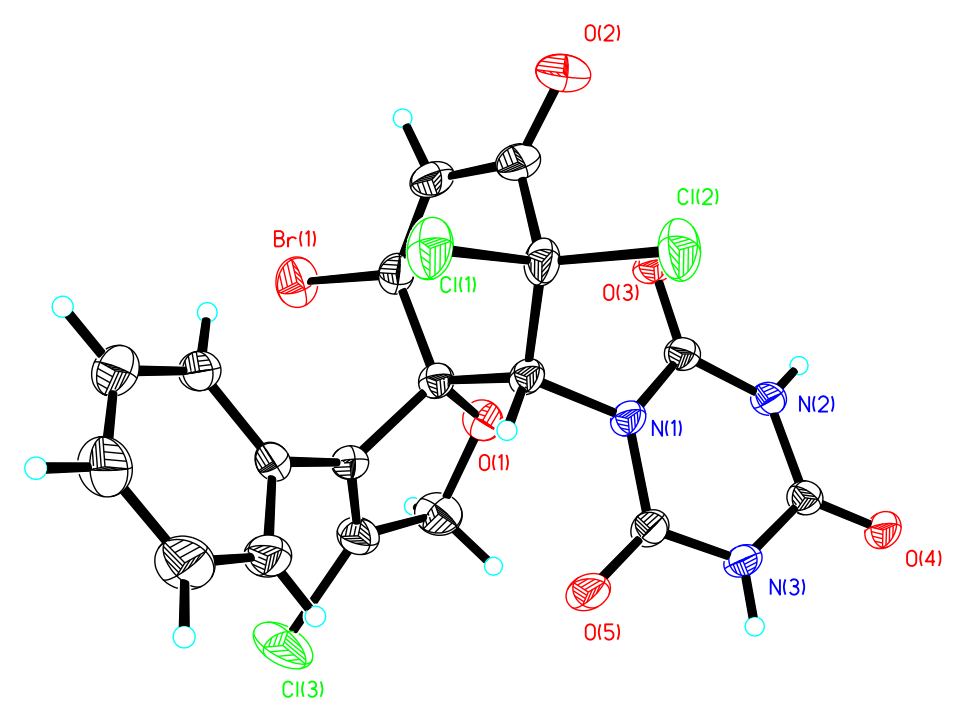
The structure was solved in the space group P2₁/c (# 14). All non-hydrogen atoms are refined anisotropically. Hydrogens were calculated by geometrical methods and refined as a riding model. The crystal used for the diffraction study showed no decomposition during data collection. All drawings are done at 50% ellipsoids.

Citations:

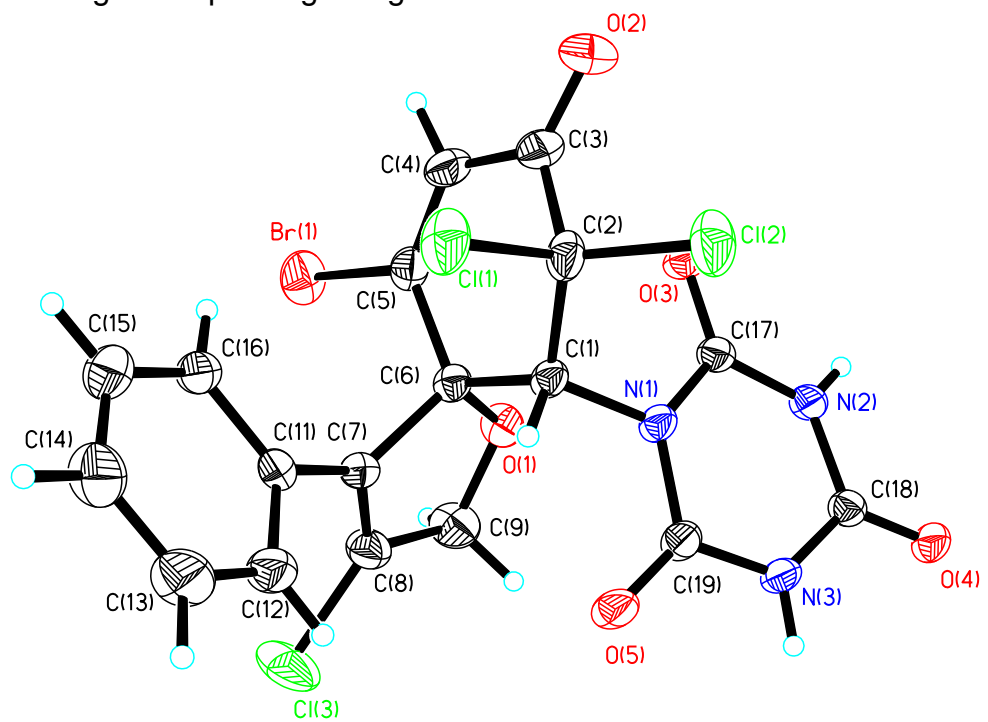
- 1. COSMO V1.61, Software for the CCD Detector Systems for Determining Data Collection Parameters. Bruker Analytical X-ray Systems, Madison, WI (2009).
- 2. APEX2 V2010.11-3. Software for the CCD Detector System; Bruker Analytical X-ray Systems, Madison, WI (2010).
- SAINT V 7.68A Software for the Integration of CCD Detector System Bruker
 Analytical X-ray Systems, Madison, WI (2010).
- 4. SADABS V2008/2 Program for absorption corrections using Bruker-AXS CCD based on the method of Robert Blessing; Blessing, R.H. Acta Cryst. A51, 1995, 33-38.
- 5. Sheldrick, G.M. "A short history of SHELX". Acta Cryst. A64, 2008, 112-122.

3.5.2 X-ray crystallography data of III-55

The following are 50% thermal ellipsoidal drawings of the molecule in the asymmetric cell with various amount of labeling:



This is a drawing of the packing along the a-axis:



Crystal data and structure refinement

Identification code bb105_0m

Empirical formula C19 H12 Br Cl6 N3 O5

Formula weight 654.93
Temperature 173(2) K
Wavelength 1.54178 Å
Crystal system Monoclinic
Space group P 21/c

Unit cell dimensions $a = 15.67910(10) \text{ Å} \qquad \alpha = 90^{\circ}.$

b = 10.46970(10) Å β = 116.7272(1)°.

 $c = 16.93680(10) \text{ Å} \qquad \gamma = 90^{\circ}.$

Volume 2483.22(3) Å³

Z 4

Density (calculated) 1.752 Mg/m³
Absorption coefficient 8.536 mm⁻¹

F(000) 1296

Crystal size 0.19 x 0.11 x 0.09 mm³

Theta range for data collection 5.14 to 67.94°.

Index ranges -18<=h<=17, -12<=k<=11, -20<=l<=20

Reflections collected 18304

Independent reflections 4480 [R(int) = 0.0264]

Completeness to theta = 67.94° 99.0%

Absorption correction Semi-empirical from equivalents

Max. and min. transmission 0.5272 and 0.2982

Refinement method Full-matrix least-squares on F²

Data / restraints / parameters 4480 / 17 / 377

Goodness-of-fit on F² 0.986

Final R indices [I>2sigma(I)] R1 = 0.0355, wR2 = 0.0938 R indices (all data) R1 = 0.0389, wR2 = 0.0968

Largest diff. peak and hole 0.899 and -1.018 e.Å-3

Experimental:

A colorless block crystal with dimensions 0.19 x 0.11 x 0.09 mm was mounted on a

Nylon loop using very small amount of paratone oil.

Data were collected using a Bruker CCD (charge coupled device) based diffractometer equipped with an Oxford Cryostream low-temperature apparatus operating at 173 K. Data were measured using omega and phi scans of 0.5° per frame for 30 s. The total number of images was based on results from the program COSMO¹ where redundancy was expected to be 4.0 and completeness of 100% out to 0.83 Å. Cell parameters were retrieved using APEX II software² and refined using SAINT on all observed reflections. Data reduction was performed using the SAINT software³ which corrects for Lp. Scaling and absorption corrections were applied using SADABS⁴ multiscan technique, supplied by George Sheldrick. The structures are solved by the direct method using the SHELXS-97 program and refined by least squares method on F², SHELXL-97, which are incorporated in SHELXTL-PC V 6.10.5

The structure was solved in the space group P2₁/c (# 14). All non-hydrogen atoms are refined anisotropically. Hydrogen atoms were found by difference Fourier methods and refined isotropically. The crystal used for the diffraction study showed no decomposition during data collection. All drawings are done at 50% ellipsoids.

Citations:

- COSMO V1.61, Software for the CCD Detector Systems for Determining Data Collection Parameters. Bruker Analytical X-ray Systems, Madison, WI (2009).
- APEX2 V2010.11-3. Software for the CCD Detector System; Bruker Analytical Xray Systems, Madison, WI (2010).
- SAINT V 7.68A Software for the Integration of CCD Detector System Bruker
 Analytical X-ray Systems, Madison, WI (2010).

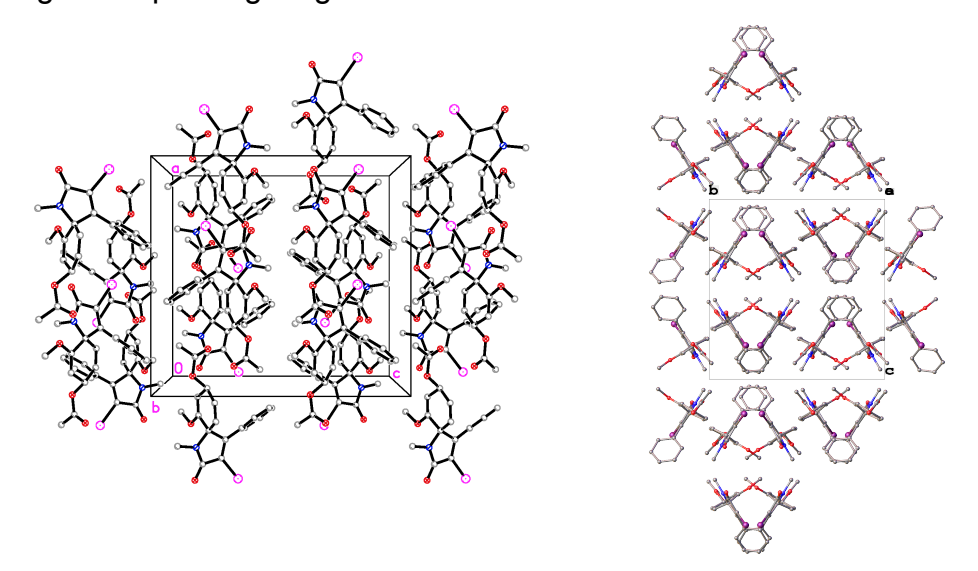
- SADABS V2.008/2 Program for absorption corrections using Bruker-AXS CCD based on the method of Robert Blessing; Blessing, R.H. Acta Cryst. A51, 1995, 33-38.
- 5. Sheldrick, G.M. "A short history of SHELX". Acta Cryst. A64, 2008, 112-122.

3.5.3 X-ray crystallography data of III-82

The Model has Chirality at C1A (Polar SPGR) R Verify: The Model has Chirality at C7A (Polar SPGR) R Verify:

The Model has Chirality at C1B (Polar SPGR) S Verify; The Model has Chirality at C7B (Polar SPGR) S Verify:

This is a drawing of the packing diagram:



Crystal data and structure refinement

Compound BB315b Formula C₁₉H₁₈INO₄ Dcalc./ g cm⁻³ 1.634 μ /mm⁻¹ 1.768 Formula Weight 451.24 Colour colourless Shape chunk Max Size/mm 0.30 Mid Size/mm 0.20 Min Size/mm 0.18 T/K 173(2) Crystal System orthorhombic Flack Parameter -0.036(12) **Hooft Parameter** -0.027(12)Space Group Pna2₁ a/Å 14.7594(7) b/Å 15.5768(8) c/Å 15.9589(8) $\alpha/^{\circ}$ 90 $\beta / ^{\circ}$ 90 90 γſ° V/Å³ 3669.0(3) Ζ 8 Z'2 $\Theta_{min}/^{\circ}$ 1.827 $\Theta_{\text{max}}/^{\circ}$ 25.379 Measured Refl. 29546 Independent Refl. 6736 Reflections Used 5996 Rint 0.0423 **Parameters** 457 Restraints 1 Largest Peak 1.199 Deepest Hole -0.395GooF 1.057 wR_2 (all data) 0.0841 wR_2 0.0801 R_1 (all data) 0.0396

0.0342

 R_1

Experimental

Single crystals of C₂₃H₁₇NO₂Br₂ were crystallized from [Chloroform]. A suitable crystal was selected and mounted on a nylon loop using Paratone Oil. The crystal was kept at 173.15 K during data collection. Data were collected using a Bruker APEX-II CCD (charge coupled device) based diffractometer equipped with an Oxford Cryostream low-temperature apparatus operating at 173 K. Data were measured using omega and phi scans of 0.5°per frame for 30 s. The total number of images was based on results from the program COSMO,¹ where redundancy was expected to be 4.0 and completeness to 0.83 Å to 100%. Cell parameters were retrieved using APEX II software<sup2 and refined using SAINT on all observed reflections. Data reduction was performed using the SAINT software³ which corrects for Lp. Scaling and absorption corrections were applied using SADABS⁴ multi-scan technique, supplied by George Sheldrick. Using Olex2 ⁴, the structure was solved with the XS ⁵ structure solution program using Direct Methods and refined with the XL ⁶ refinement package using Least Squares minimisation.

The structure was solved in the space group P2₁/c (no. 14). All non-hydrogen atoms are refined anisotropically. Hydrogens were calculated by geometrical methods and refined as a riding model. The Flack⁷ parameter is used to determine chirality of the crystal studied, the value should be near zero, a value of one is the other enantiomer and a value of 0.5 is racemic. The Flack parameter was refined to -0.001(19), confirming the absolute stereochemistry. Determination of absolute structure using Bayesian statistics on Bijvoet differences using the program within Platon⁸ also report that we have the correct enantiomer based on this comparison.⁹ All drawings are done at 50% ellipsoids.

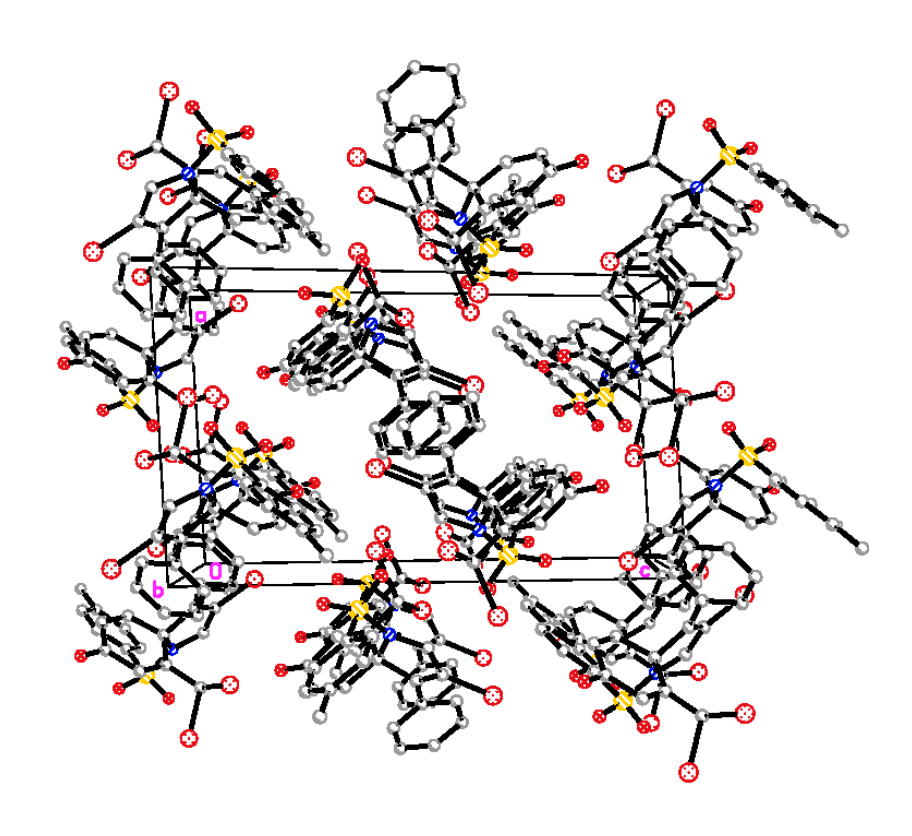
Citations:

- COSMO V1.61, Software for the CCD Detector Systems for Determining Data Collection Parameters. Bruker Analytical X-ray Systems, Madison, WI (2009).
- APEX2 V2010.11-3. Software for the CCD Detector System; Bruker Analytical Xray Systems, Madison, WI (2010).
- SAINT V 7.68A Software for the Integration of CCD Detector System Bruker Analytical X-ray Systems, Madison, WI (2010).
- SADABS V2008/2 Program for absorption corrections using Bruker-AXS CCD based on the method of Robert Blessing; Blessing, R.H. Acta Cryst. A51, 1995, 33-38.
- O. V. Dolomanov, L. J. Bourhis, R. J. Gildea, J. A. K. Howard and H. Puschmann,
 OLEX2: a complete structure solution, refinement and analysis program. J. Appl.
 Cryst. (2009). 42, 339-341.
- 6. XS, G.M. Sheldrick, Acta Cryst. (2008). A64, 112-122
- 7. XL, G.M. Sheldrick, Acta Cryst. (2008). A64, 112-122
- 8. Flack, H. D. Acta Cryst. A39, 1983, 876-881.
- 9. Spek, A.L. (2003), J.Appl.Cryst. 36, 7-13.
- 10. Hooft, R.W.W.; Straver, L.H. & A. L. Spek, A.L.. J. Appl. Cryst. 41, 2008, 96-103

3.5.4 X-ray crystallography data of III-57

The following are 50% thermal ellipsoidal drawings of the molecule in the asymmetric cell with various amount of labeling:

This is a drawing of the packing along the b-axis:



Crystal data and structure refinement

Identification code YY-02-82 Side spot Empirical formula C₄₆H₃₄Br₆N₂O₆S

Formula weight 1254.33
Temperature/K 173.15
Crystal system triclinic
Space group P-1

a/Å 10.4886(6)b/Å 12.5265(7)c/Å 17.9881(10) $\alpha/^{\circ}$ 103.9000(10) $\beta/^{\circ}$ 93.0900(10) $\gamma/^{\circ}$ 91.0890(10)

Volume/Å³ 2289.6(2)

 $\begin{array}{cccc} Z & & 2 & & \\ \rho_{calc}mg/mm^3 & & 1.819 & \\ m/mm^{-1} & & 5.403 & \\ F(000) & & 1228.0 & \\ \end{array}$

Crystal size/mm³ $0.351 \times 0.283 \times 0.064$

20 range for data collection 3.36 to 50.72°

Index ranges $-12 \le h \le 12, -15 \le k \le 15, -21 \le l \le 21$

Reflections collected 38138

exptl absorpt T max, min 0.7452, 0.5676

Independent reflections 8404[R(int) = 0.0388]

Data/restraints/parameters 8404/0/561

2O 25.36 fraction collected 0.999 Goodness-of-fit on F² 1.023

Final R indexes [I>= 2σ (I)] R₁ = 0.0340, wR₂ = 0.0825 Final R indexes [all data] R₁ = 0.0464, wR₂ = 0.0882

Largest diff. peak/hole / e Å-3 1.53/-0.73

Experimental

Single crystals of C₄₆H₃₄Br₆N₂O₆S₂ (III-57) were crystallized from DCM. A suitable crystal was selected and mounted on a nylon loop using Paratone Oil. The crystal was kept at 173.15 K during data collection. Data were collected using a Bruker APEX-II CCD (charge coupled device) based diffractometer equipped with an Oxford Cryostream low-temperature apparatus operating at 173 K. Data were measured using omega and phi scans of 0.5°per frame for 30 s. The total number of images was based on results from the program COSMO,¹ where redundancy was expected to be 4.0 and completeness to 0.83 Å to 100%. Cell parameters were retrieved using APEX II software<sup2 and refined using SAINT on all observed reflections. Data reduction was performed using the SAINT software³ which corrects for Lp. Scaling and absorption corrections were applied using SADABS⁴ multi-scan technique, supplied by George Sheldrick. Using Olex2 ⁴, the structure was solved with the XS ⁵ structure solution program using Direct Methods and refined with the XL ⁶ refinement package using Least Squares minimisation.

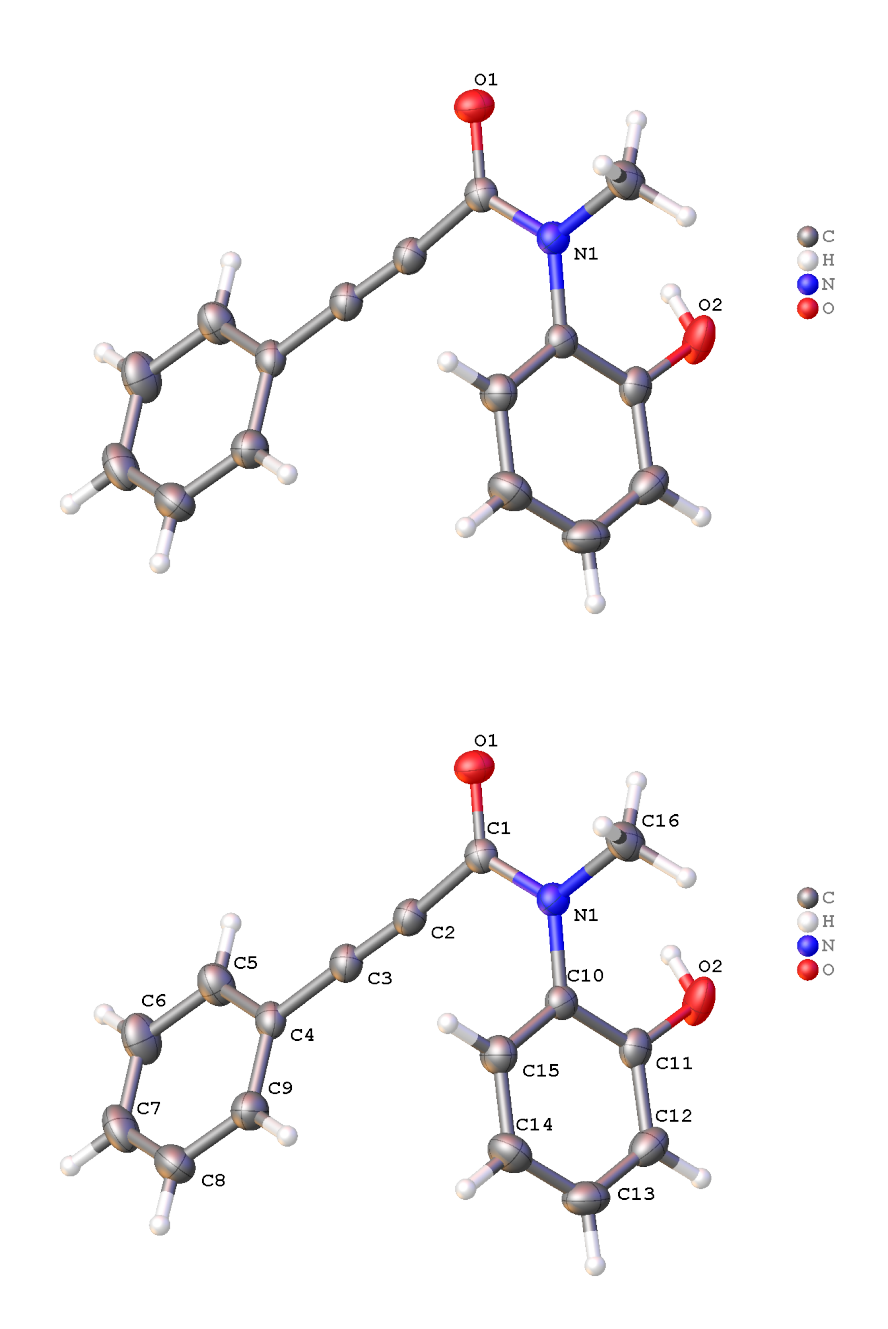
The structure was solved in the space group P-1 (no. 2). All non-hydrogen atoms are refined anisotropically. Hydrogens were calculated by geometrical methods and refined as a riding model. All drawings are done at 50% ellipsoids.

Citations:

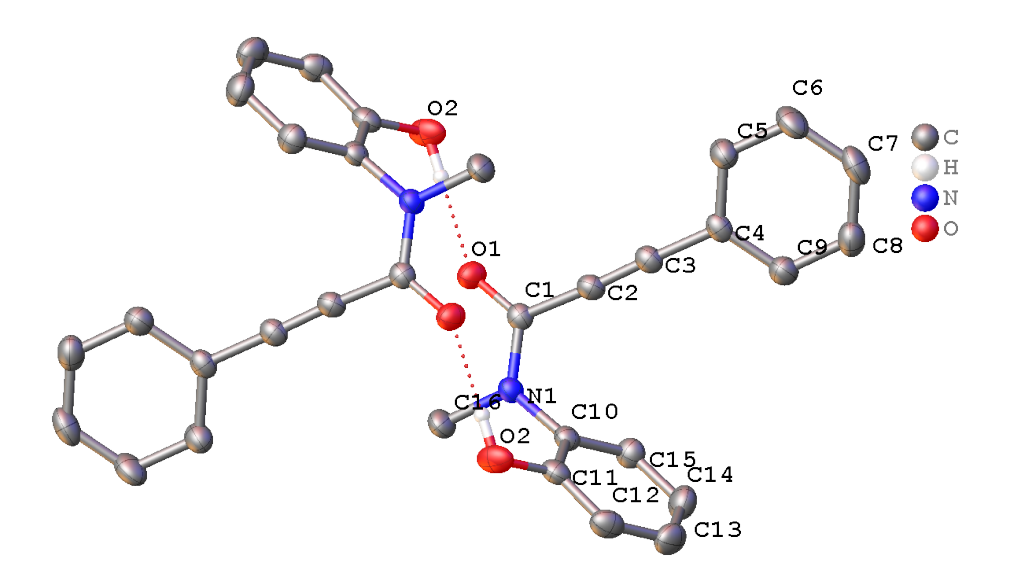
- COSMO V1.61, Software for the CCD Detector Systems for Determining Data Collection Parameters. Bruker Analytical X-ray Systems, Madison, WI (2009).
- APEX2 V2010.11-3. Software for the CCD Detector System; Bruker Analytical Xray Systems, Madison, WI (2010).
- SAINT V 7.68A Software for the Integration of CCD Detector System Bruker Analytical X-ray Systems, Madison, WI (2010).
- SADABS V2008/2 Program for absorption corrections using Bruker-AXS CCD based on the method of Robert Blessing; Blessing, R.H. Acta Cryst. A51, 1995, 33-38.
- O. V. Dolomanov, L. J. Bourhis, R. J. Gildea, J. A. K. Howard and H. Puschmann,
 OLEX2: a complete structure solution, refinement and analysis program. J. Appl.
 Cryst. (2009). 42, 339-341.
- 6. XS, G.M. Sheldrick, Acta Cryst. (2008). A64, 112-122
- 7. XL, G.M. Sheldrick, Acta Cryst. (2008). A64, 112-122

3.5.5 X-ray crystallography data of III-72

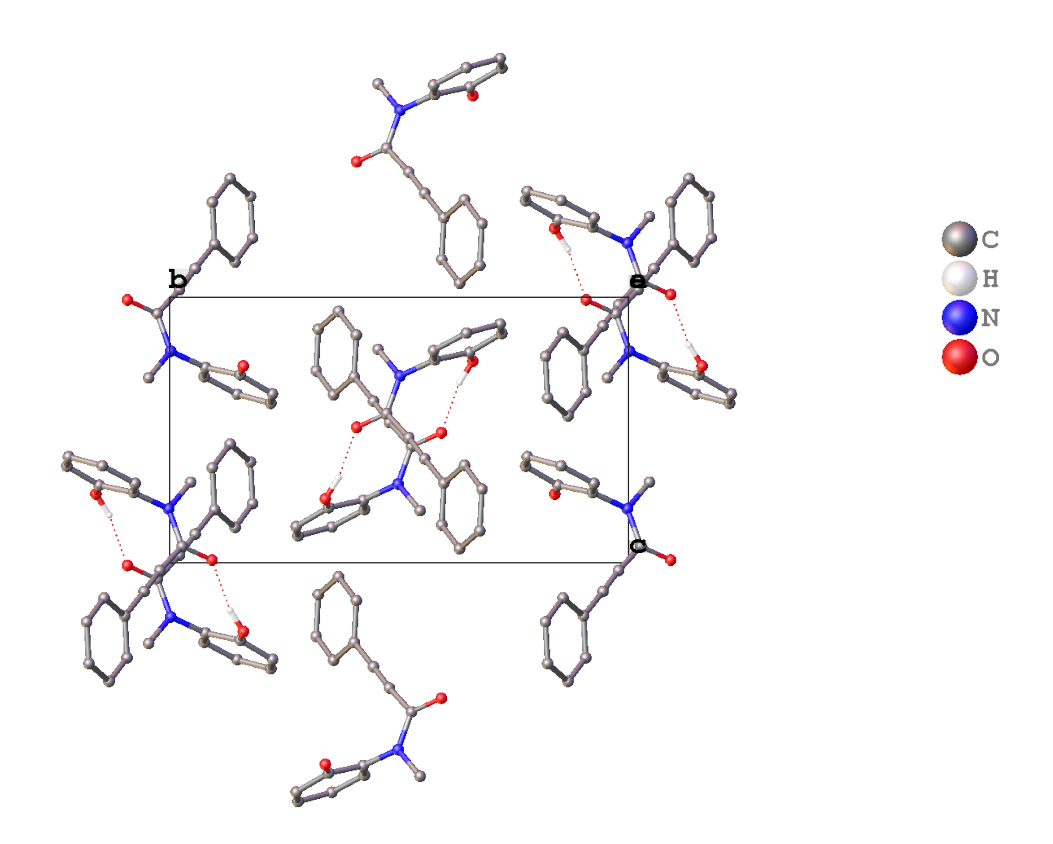
The following are 50% thermal ellipsoidal drawings of the molecule in the asymmetric cell with various amount of labeling:



The following hydrogen bonding interactions with a maximum D-D distance of 2.9 Å and a minimum angle of 120 $^{\circ}$ are present in **BB1017A**: O2–O1_1: 2.705 Å:



Packing diagram of BB1017A:



Crystal data and structure refinement

Compound BB1017A Formula C₁₆H₁₃NO₂ Dcalc./ g cm⁻³ 1.236 μ /mm⁻¹ 0.660 Formula Weight 251.27 Colour colourless Shape needle

Size/mm³ 0.46×0.17×0.15

T/K 173(2) Crystal System monoclinic Space Group $P2_1/c$ a/Å 10.0246(5) b/Å 15.2711(8) c/Å 9.1744(5) $\alpha/^{\circ}$ 90

 $\beta / \hat{}$ 105.936(3)

90

γſ°

V/Å³ 1350.50(12)

Z 4 Z'

Wavelength/Å 1.541838 Radiation type CuK_{α} 4.587 $\Theta_{min}/^{\circ}$ 70.158 $\Theta_{\text{max}}/^{\circ}$ Measured Refl. 2345 Independent Refl. 2345 Reflections Used 2117

Rint 175 **Parameters**

Restraints 0 Largest Peak 0.398 Deepest Hole -0.203 GooF 1.082 wR_2 (all data) 0.1171 wR_2 0.1126 R_1 (all data) 0.0437 R_1 0.0391

Experimental:

Single colourless needle-shaped crystals of (**BB1017A**) were used as received. A suitable crystal ($0.46\times0.17\times0.15$) mm³ was selected and mounted on a nylon loop with paratone oil on a Bruker APEX-II CCD diffractometer. The crystal was kept at T = 173(2) K during data collection. Using **Olex2** (Dolomanov et al., 2009), the structure was solved with the **SheIXT** (Sheldrick, 2015) structure solution program, using the Intrinsic Phasing solution method. The model was refined with version of **XL** (Sheldrick, 2008) using Least Squares minimisation.

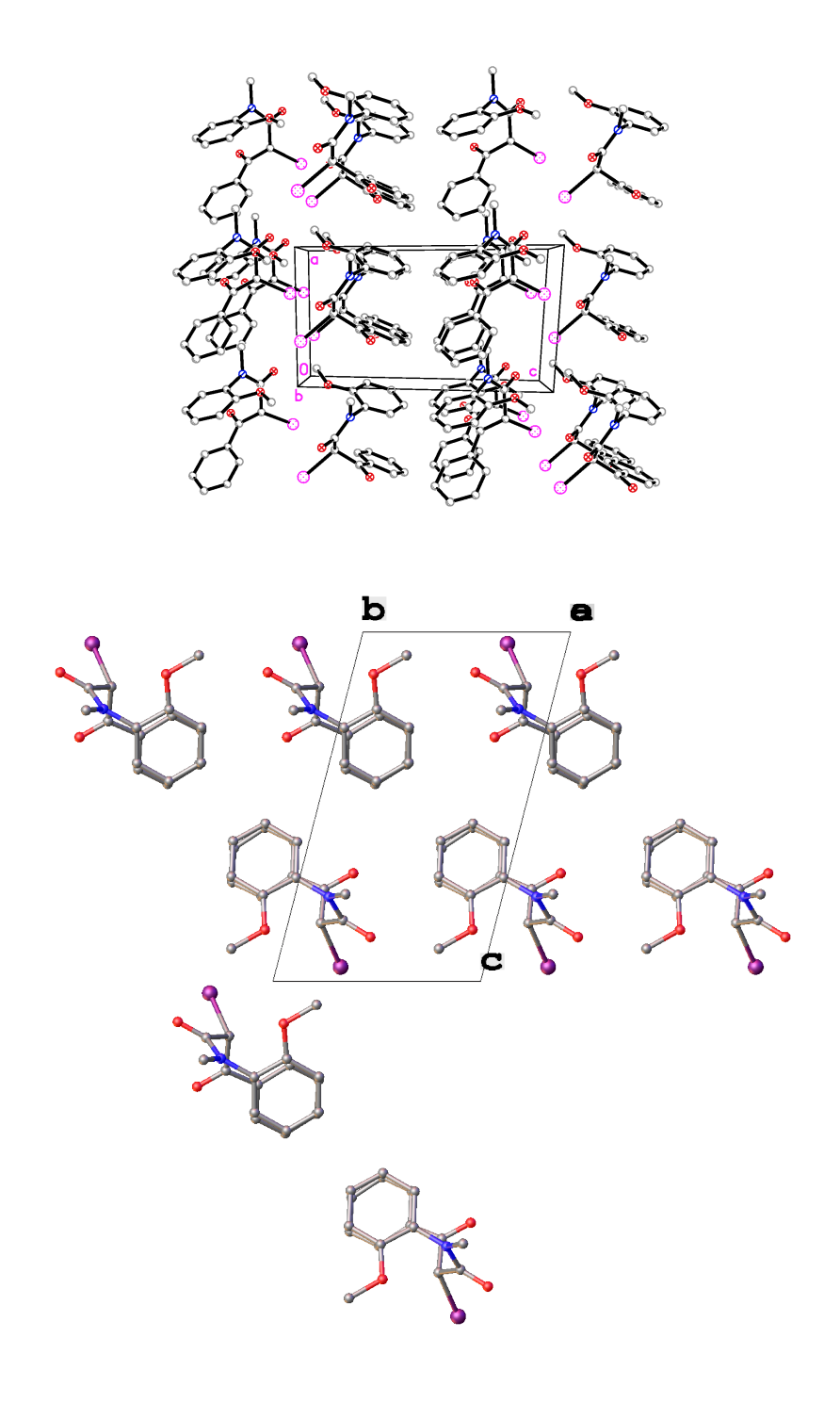
Citations:

- COSMO-V1.61 Software for the CCD Detector Systems for Determining Data
 Collection Parameters, Bruker axs, Madison, WI (2000).
- 2. O.V. Dolomanov and L.J. Bourhis and R.J. Gildea and J.A.K. Howard and H. Puschmann, Olex2: A complete structure solution, refinement and analysis program, *J. Appl. Cryst.*, (2009), **42**, 339-341.
- 3. Sheldrick, G.M., A short history of ShelX, Acta Cryst., (2008), A64, 339-341.
- 4. Sheldrick, G.M., ShelXT-Integrated space-group and crystal-structure determination, *Acta Cryst.*, (2015), **A71**, 3-8.
- 5. Software for the Integration of CCD Detector System Bruker Analytical X-ray Systems, Bruker axs, Madison, WI (after 2013).

3.5.6 X-ray crystallography data of III-81

The following are 50% thermal ellipsoidal drawings of the molecule in the asymmetric cell with various amount of labeling:

Packing diagram of bb315d:



Crystal data and structure refinement

Compound	bb315d
Formula	C34H32I2N2O6
D _{calc.} / g cm ⁻³	1.667
μ/mm^{-1}	1.976
Formula Weight	818.41
Colour	colourless
Shape	chunk
Max Size/mm	0.53
Mid Size/mm	0.32
Min Size/mm	0.20
T/K	173(2)
Crystal System	triclinic
Flack Parameter	0.464(15)
Hooft Parameter	0.464(6)
	0.404(0) P1
Space Group <i>al</i> Å	
a/A b/Å	8.1207(6) 8.6889(6)
c/Å	` '
$\alpha \beta^{\circ}$	13.5841(10)
	73.1960(10)
βf°	81.1990(10)
η [°]	62.6900(10)
V/Å ³	815.06(10)
Z	1
Z'	1
Θ_{min} / $^{\circ}$	2.724
$\Theta_{max} \int_{0}^{\infty} dt$	25.349
Measured Refl.	13687
Independent Refl.	5970
Reflections Used	5878
Rint	0.0171
Parameters	402
Restraints	3
Largest Peak	0.343
Deepest Hole	-0.258
GooF	1.062
wR₂ (all data)	0.0430
wR ₂	0.0426
R_1 (all data)	0.0173
R_1	0.0169

Experimental:

Single colourless chunk-shaped crystals of (**BB315b**) were used as received. A suitable crystal ($0.30\times0.20\times0.18$) was selected and mounted on a nylon loop with paratone oil on a Bruker APEX-II CCD diffractometer. The crystal was kept at T = 173(2) K during data collection. Using **Olex2** (Dolomanov et al., 2009), the structure was solved with the **SheIXS** (Sheldrick, 2008) structure solution program, using the Direct Methods solution method. The model was refined with version 2014/6 of **XL** (Sheldrick, 2008) using Least Squares minimisation.

Citations:

- 1.COSMO-V1.61 •Software for the CCD Detector Systems for Determining Data Collection Parameters, Bruker axs, Madison, WI (2000).
- 2. O.V. Dolomanov and L.J. Bourhis and R.J. Gildea and J.A.K. Howard and H. Puschmann, Olex2: A complete structure solution, refinement and analysis program, *J. Appl. Cryst.*, (2009), **42**, 339-341.
- 3. SAINT-8.34A-2013 Software for the Integration of CCD Detector System Bruker Analytical X-ray Systems, Bruker axs, Madison, WI (2013).
- 4. Sheldrick, G.M., A short history of ShelX, Acta Cryst., (2008), A64, 339-341.

REFERENCES

REFERENCES

- 1. Roche, S. P.; Porco, J. A., Dearomatization Strategies in the Synthesis of Complex Natural Products. *Angewandte Chemie International Edition* **2011**, *50* (18), 4068-4093.
- 2. Zhuo, C.-X.; Zhang, W.; You, S.-L., Catalytic Asymmetric Dearomatization Reactions. *Angewandte Chemie International Edition* **2012**, *51* (51), 12662-12686.
- 3. Dohi, T.; Maruyama, A.; Takenaga, N.; Senami, K.; Minamitsuji, Y.; Fujioka, H.; Caemmerer, S. B.; Kita, Y., A Chiral Hypervalent Iodine(III) Reagent for Enantioselective Dearomatization of Phenols. *Angewandte Chemie* **2008**, *120* (20), 3847-3850.
- 4. Wu, Q.-F.; He, H.; Liu, W.-B.; You, S.-L., Enantioselective Construction of Spiroindolenines by Ir-Catalyzed Allylic Alkylation Reactions. *Journal of the American Chemical Society* **2010**, *132* (33), 11418-11419.
- 5. Wu, Q.-F.; Liu, W.-B.; Zhuo, C.-X.; Rong, Z.-Q.; Ye, K.-Y.; You, S.-L., Iridium-Catalyzed Intramolecular Asymmetric Allylic Dearomatization of Phenols. *Angewandte Chemie International Edition* **2011**, *50* (19), 4455-4458.
- 6. Nemoto, T.; Ishige, Y.; Yoshida, M.; Kohno, Y.; Kanematsu, M.; Hamada, Y., Novel Method for Synthesizing Spiro[4.5]cyclohexadienones through a Pd-Catalyzed Intramolecular ipso-Friedel–Crafts Allylic Alkylation of Phenols. *Organic Letters* **2010**, *12* (21), 5020-5023.
- 7. Rousseaux, S.; García-Fortanet, J.; Del Aguila Sanchez, M. A.; Buchwald, S. L., Palladium(0)-Catalyzed Arylative Dearomatization of Phenols. *Journal of the American Chemical Society* **2011,** *133* (24), 9282-9285.
- 8. Gao, P.; Zhang, W.; Zhang, Z., Copper-Catalyzed Oxidative ipso-Annulation of Activated Alkynes with Silanes: An Approach to 3-Silyl Azaspiro[4,5]trienones. *Organic Letters* **2016**, *18* (22), 5820-5823.
- 9. Wen, J.; Wei, W.; Xue, S.; Yang, D.; Lou, Y.; Gao, C.; Wang, H., Metal-Free Oxidative Spirocyclization of Alkynes with Sulfonylhydrazides Leading to 3-Sulfonated Azaspiro[4,5]trienones. *The Journal of Organic Chemistry* **2015**, *80* (10), 4966-4972.
- 10. James, M. J.; Clubley, R. E.; Palate, K. Y.; Procter, T. J.; Wyton, A. C.; O'Brien, P.; Taylor, R. J. K.; Unsworth, W. P., Silver(I)-Catalyzed Dearomatization of Alkyne-Tethered Indoles: Divergent Synthesis of Spirocyclic Indolenines and Carbazoles. *Organic Letters* **2015**, *17* (17), 4372-4375.

- 11. Liang, H.; Ciufolini, M. A., Oxidative Spirocyclization of Phenolic Sulfonamides: Scope and Applications. *Chemistry A European Journal* **2010**, *16* (44), 13262-13270.
- 12. Farndon, J. J.; Ma, X.; Bower, J. F., Transition Metal Free C–N Bond Forming Dearomatizations and Aryl C–H Aminations by in Situ Release of a Hydroxylamine-Based Aminating Agent. *Journal of the American Chemical Society* **2017**, *139* (40), 14005-14008.
- 13. Liang, X.-W.; Zheng, C.; You, S.-L., Dearomatization through Halofunctionalization Reactions. *Chemistry A European Journal* **2016**, *22* (34), 11918-11933.
- 14. Lozano, O.; Blessley, G.; Martinez del Campo, T.; Thompson, A. L.; Giuffredi, G. T.; Bettati, M.; Walker, M.; Borman, R.; Gouverneur, V., Organocatalyzed Enantioselective Fluorocyclizations. *Angewandte Chemie International Edition* **2011**, *50* (35), 8105-8109.
- 15. Xie, W.; Jiang, G.; Liu, H.; Hu, J.; Pan, X.; Zhang, H.; Wan, X.; Lai, Y.; Ma, D., Highly Enantioselective Bromocyclization of Tryptamines and Its Application in the Synthesis of (–)-Chimonanthine. *Angewandte Chemie International Edition* **2013**, *52* (49), 12924-12927.
- 16. Yin, Q.; You, S.-L., Enantioselective Chlorocyclization of Indole Derived Benzamides for the Synthesis of Spiro-indolines. *Organic Letters* **2013**, *15* (16), 4266-4269.
- 17. Yin, Q.; You, S.-L., Asymmetric Chlorocyclization of Indole-3-yl-benzamides for the Construction of Fused Indolines. *Organic Letters* **2014**, *16* (9), 2426-2429.
- 18. Zhang, X.; Larock, R. C., Synthesis of Spiro[4.5]trienones by Intramolecular ipso-Halocyclization of 4-(p-Methoxyaryl)-1-alkynes. *Journal of the American Chemical Society* **2005**, *127* (35), 12230-12231.
- 19. Yu, Q.-F.; Zhang, Y.-H.; Yin, Q.; Tang, B.-X.; Tang, R.-Y.; Zhong, P.; Li, J.-H., Electrophilic ipso-lodocyclization of N-(4-Methylphenyl)propiolamides: Selective Synthesis of 8-Methyleneazaspiro[4,5]trienes. *The Journal of Organic Chemistry* **2008**, 73 (9), 3658-3661.
- 20. Tang, B.-X.; Yin, Q.; Tang, R.-Y.; Li, J.-H., Electrophilic ipso-Cyclization of N-(p-Methoxyaryl)propiolamides Involving an Electrophile-Exchange Process. *The Journal of Organic Chemistry* **2008**, *73* (22), 9008-9011.
- 21. Tang, B.-X.; Tang, D.-J.; Tang, S.; Yu, Q.-F.; Zhang, Y.-H.; Liang, Y.; Zhong, P.; Li, J.-H., Selective Synthesis of Spiro[4,5]trienyl Acetates via an Intramolecular Electrophilic ipso-lodocyclization Process. *Organic Letters* **2008**, *10* (6), 1063-1066.

- 22. Jaganathan, A.; Garzan, A.; Whitehead, D. C.; Staples, R. J.; Borhan, B., A Catalytic Asymmetric Chlorocyclization of Unsaturated Amides. *Angewandte Chemie International Edition* **2011**, *50* (11), 2593-2596.
- 23. Garzan, A.; Jaganathan, A.; Salehi Marzijarani, N.; Yousefi, R.; Whitehead, D. C.; Jackson, J. E.; Borhan, B., Solvent-Dependent Enantiodivergence in the Chlorocyclization of Unsaturated Carbamates. *Chemistry A European Journal* **2013**, *19* (27), 9015-9021.
- 24. Whitehead, D. C.; Yousefi, R.; Jaganathan, A.; Borhan, B., An Organocatalytic Asymmetric Chlorolactonization. *Journal of the American Chemical Society* **2010**, *132* (10), 3298-3300.
- 25. Denmark, S. E.; Burk, M. T., Enantioselective Bromocycloetherification by Lewis Base/Chiral Brønsted Acid Cooperative Catalysis. *Organic Letters* **2012**, *14* (1), 256-259.
- 26. Hennecke, U.; Müller, C. H.; Fröhlich, R., Enantioselective Haloetherification by Asymmetric Opening of meso-Halonium Ions. *Organic Letters* **2011**, *13* (5), 860-863.
- 27. Saha, S.; Schneider, C., Directing Group Assisted Nucleophilic Substitution of Propargylic Alcohols via o-Quinone Methide Intermediates: Brønsted Acid Catalyzed, Highly Enantio- and Diastereoselective Synthesis of 7-Alkynyl-12a-acetamido-Substituted Benzoxanthenes. *Organic Letters* **2015**, *17* (3), 648-651.
- 28. LaLonde, R. L.; Wang, Z. J.; Mba, M.; Lackner, A. D.; Toste, F. D., Gold(I)-Catalyzed Enantioselective Synthesis of Pyrazolidines, Isoxazolidines, and Tetrahydrooxazines. *Angewandte Chemie International Edition* **2010**, *49* (3), 598-601.
- 29. Wu, W.-T.; Xu, R.-Q.; Zhang, L.; You, S.-L., Construction of spirocarbocycles via gold-catalyzed intramolecular dearomatization of naphthols. *Chemical Science* **2016**, *7* (5), 3427-3431.
- 30. Qian, D.; Zhang, J., Catalytic oxidation/C-H functionalization of N-arylpropiolamides by means of gold carbenoids: concise route to 3-acyloxindoles. *Chemical Communications* **2012**, *48* (56), 7082-7084.
- 31. Barluenga, J.; Bayon, A. M.; Asensio, G., A new and specific method for the monomethylation of primary amines. *Journal of the Chemical Society, Chemical Communications* **1984**, (20), 1334-1335.

CHAPTER FOUR

XtalFluor-E[®] Mediated Proto-functionalization of N-vinyl Amides: Access to *N*-acetyl *N,O*-acetals

4.1 Introduction

Within the family of organic reactions, functionalization of olefins is one of the most well studied and important transformations. Some of the milestone reactions in this realm are epoxidation,¹ dihydroxylation,² hydroamination,³ dihalogenation,⁴ halofuntionalization⁵ to name a few. Proto-functionalization of olefins i.e., activation of a double bond with a proton and interception of the resulting carbocation with a nucleophile, is a highly prevalent method. This generally requires the application of strong acids and relatively harsh reaction conditions,⁶ not compatible with molecules bearing sensitive functionalities. In this vein, introduction of approaches that catalyze the reaction by *in situ* generation of proton under mild conditions is of interest. Here we report such a system and utilize this mild condition towards hydroalkoxylation of enamides to access *N,O*-acetals.

Hydroalkoxylation of olefin is a straightforward and commonly used strategy to construct C-O bonds. Acid catalyzed additions of alcohols to alkenes are classic reactions in organic chemistry. Recently, a number of different catalytic processes for the intramolecular hydroalkoxylation of olefin to construct cyclic ether has been reported. In 2004, Widenhoefer and coworkers developed the first catalytic intramolecular hydroalkoxylation of γ-hydroxy alkenes **IV-1** using platinum (II) complex (Scheme 4.1).⁷⁻⁸ He's group used silver triflate to catalyze intramolecular addition of a hydroxyl group to unactivated olefins **IV-3** (Scheme 4.1).⁸ In this method Ag(I) activates the double bond to form a π-complex. Similarly Duñach achieved the same transformation in the presence of catalytic amount of TfOH (Scheme 4.1).⁶ Interestingly other organic or inorganic acids such as H₂SO₄, *p*-toluenesulfonic acid and TFA afforded no reaction. Hartwig's group also found that

catalytic amount of TfOH can promote the intermolecular alcohol addition to norbornene, styrene and cyclohexne (Scheme 4.2). However, products undergo decomposition when a large loading of acid is used.

Widenhoefer's work:

Scheme 4.1 Catalytic intramolecular hydroalkoxylation.

Scheme 4.2 TfOH catalyzed intermolecular hydroalkoxylation.

More recently Yamamoto's group developed a novel catalytic system using I_2 and PhSiH $_3$ for the intramolecular hydroalkoxylation of unactivated olefins **IV-3** (Scheme 4.3). 10 In situ generated PhSiH $_2$ I can react with hydroxyl groups to generate HI and γ -silyloxy alkene. The electrophilic activation of the double bond by HI led to the following intramolecular alkoxylation to form cyclic ether. The yield was comparable with He's method using AgOTf as catalyst metioned above. 8

$$\begin{array}{c} \text{OH} \\ \text{Ph} \\ \text{IV-3} \end{array} \begin{array}{c} \text{10 mol\% l}_2 \\ \text{10 mol\% PhSiH}_3 \end{array} \begin{array}{c} \text{Ph} \\ \text{Ph} \\ \text{IV-4} \\ \text{95\%} \end{array}$$

$$\begin{array}{c} \text{Mechanism:} \\ \text{OH} \\ \text{R} \end{array} \begin{array}{c} \text{PhSiH}_2 \\ \text{OH} \\ \text{H} \end{array} \begin{array}{c} \text{Ph-SiH}_2 \\ \text{OH} \\ \text{OH} \end{array} \begin{array}{c} \text{Ph-SiH}_2 \\ \text{OH} \\ \text{OH} \end{array} \begin{array}{c} \text{Ph-SiH}_2 \\ \text{OH} \\ \text{OH} \end{array} \begin{array}{c} \text{Ph-SiH}_2 \\ \text{OH} \end{array} \begin{array}{c} \text{Ph-SiH}_2 \\ \text{OH} \\ \text{OH} \end{array} \begin{array}{c} \text{Ph-SiH}_2 \\ \text{Ph-SiH}_2 \\ \text{OH} \end{array} \begin{array}{c} \text{Ph-SiH}_2 \\ \text{P$$

Scheme 4.3 Intramolecular alkoxylation catalyzed by I₂ and PhSiH₃.

To date, several strategies have been devised that give rise to *N*,*O*-acetals, but surprisingly the more straightforward strategy of hydroalkoxylation of enamides has not been reported yet. Katrizsky's protocol employed benzotriazole as a good leaving group in the first step for the condensation of an amide and an aldehyde to yield adduct **IV-12**, followed by installation of the alkoxy group by sodium alkoxide (Scheme 4.4).¹¹⁻¹² Wen and co-workers developed the method of condensation of amides and aldehydes in the presense of Ti(OEt)₄ to construct *N*-benzoyl-*O*-ethyl-*N*,*O*-acetals (Scheme 4.4).¹³ They can easily obtain *N*-benzoyl-*O*-isopropyl-*N*,*O*-acetals by using Ti(O*i*Pr)₄ instead. This is a mild and efficient way to access *N*,*O*-acetals for both aliphatic and aromatic aldehydes with moderate to high yield. Zhu reported a multicomponent one-pot synthesis of α-amidosulfides (Scheme 4.4). Aldehyde, primary carbamates or amides, and phenylsulfinic acid can lead to a

highly reactive α -amidosulfones **IV-15**, which then react with sodium thiolate or sodium methoxide via S_N1or S_N2 pathways to form *N,S*-acetals or *N,O*-acetals. ¹⁴⁻¹⁵

All methods described above involved the condensation of aldehydes and amides. Floreancig's group reported an alternative one-pot synthesis which consists of hydrozirconation of nitriles, followed by acylation and nucleophilic addition (Scheme 4.5). The reaction proceeds via an acylimine intermediate **IV-20**, which then undergoes nucleophilic addition of different alcohols, including methanol, *t*-BuOH, phenol and thiophenol. Considering the numerous methods that are available for nitrile preparation and the capacity for variation of nucleophiles, this method can lead to a large number of "oxidized" amides.

Scheme 4.4 Access to N-acetyl-N,O-acetals via condensation of amides with aldehydes

R
N
$$\frac{Cp_2Zr(H)Cl, CH_2Cl_2}{\text{then } iPrCOCl}}{\text{then MeOH}}$$

$$|V-17|$$

$$|V-19|$$

$$|V-20|$$

$$|V-20|$$

Scheme 4.5 Access to *N*-acetyl-*N*,*O*-acetals via activation of nitriles.

Antilla and coworkers developed the enantioselective addition of alcohols to *N*-acyl imines **IV-21** to form chiral *N*,*O*-aminals catalyzed by BINOL-derived phosphoric acid **IV-22** (Scheme 4.6).¹⁷ A variety of *N*,*O*-aminals can be obtained in high yield and *ee*. However, this method requires freshly prepared unstable *N*-benzoylimines, which might limit its practicality.

Scheme 4.6 Chiral phosphoric acid catalyzed addition of alcohols to imines.

It is noteworthy to point out that Toste and coworkers developed an enantioselective oxyfluorination of enamides **IV-24** using chiral phosphoric acid and Selectfluor to access the α-fluoro-*N*,*O*-aminal **IV-25** (Scheme 4.7).¹⁸ This method is based on phase-transfer catalysis using chiral anionic phosphate which reacts with Selectfluor to generate a chiral

electrophilic fluorinating reagent. Upon enamide fluorination, the generated protonated *N*-acyliminium ion can be trapped by an oxygen nucleophile.

Ph N
$$\oplus$$
 2BF₄ \oplus 5 mol% (R , R)-PhDAP \oplus Na₂CO₃ \oplus toluene, rt \oplus IV-25 \oplus Selectfluor \oplus Selectfluor \oplus No \oplus

Scheme 4.7 Chiral phosphoric acid catalyzed oxyfluorination

Our approach takes advantage of the fact that the interaction of XtalFluor-E® with alcohols leads to a mild method for generation of protons that promote the hydroalkoxylation of enamides. Similar to many other sulfur-based fluorination or fluoroalkylation reagents (Scheme 4.8), XtalFluor-E® is best known as a reagent for deoxyfluorination of carbonyl compounds and alcohols. 19-20 The combination of "soft" sulfur and "hard" fluorine along with the rich chemistry of sulfur-containing species make them ideal for transferring fluorine atoms. The strong affinity of the sulfur atom towards oxygen (S-O bond 124 Kcal/mol vs S-F bond 82 Kcal/mol) makes DAST the most commonly used deoxyfluorination reagent since it was first introduced in the 1970s. However, its propensity of violent decomposition renders it unsuitable for some reactions. Aminodifluorosulfinium tetrafluoroborates: XtalFluor-E® and XtalFluor-M® are easy-handled crystalline salts, having emerged as good substitutes for DAST due to their high thermal stability and strong fluorinating ability. 21

Scheme 4.8 Sulfur-based fluorinating reagents.

XtalFluor-E® consists of a sulfur nitrogen double bond with a highly electron deficient sulfur atom, bearing two electronegative fluorine atoms. Indeed, this polarized bond is the key feature for its reactivity of activating oxygenated organic compounds towards substitution reactions. In 2009 L'Heureux and coworkers found that XtalFluor-E[®] is capable of performing deoxofluorinations of hydroxyls and carbonyls when promoted by an exogenous fluoride source (Scheme 4.9).21 It is noteworthy that XtalFluor-E® alone cannot perform deoxofluorination of carbonyls, whereas alcohols can be transformed to alkyl fluorides, albeit sluggishly. Mechanistically, XtalFluor-E® is an electrophile that leads to a reactive dialkylaminodifluorosulfane intermediate.²² Since the reaction mixture is absent of fluoride, exogenous fluoride is required. In this context, XtalFluor-E® combined with other nucleophilic halogen sources have also been used for halogenation of primary alcohols (Scheme 4.9).²³ More recently Paquin and coworkers reported the eliminative deoxofluorination of cyclohexanone derivatives IV-26 using XtalFluor-E® (Scheme 4.9).24 In this context, the ketone would get converted to fluoroalkoxy-N,N-diethylaminodifluorosulfane IV-27, which then undergo E2 triggered by Et₃N.

deoxofluorination: R OH
$$\frac{1.5 \text{ equiv XtalFluor-E}^{\oplus}}{1.5 \text{ equiv XtalFluor-E}^{\oplus}}$$
 $\frac{1.5 \text{ equiv XtalFluor-E}^{\oplus}}{1.5 \text{ equiv XtalFluor-E}^{\oplus}}$ $\frac{1.5 \text{ equiv XtalFluor-E}^{\oplus}}{1.5 \text{$

Scheme 4.9 XtalFluor-E[®] as deoxofluorinating reagent.

XtalFluor-E® has also been used for activation of hydroxyl, carboxylic acid²⁵ or carbonyl for further transformations. The commonality of these transformations is the activation of the oxygen with XtalFluor-E® into a good leaving group for the subsequent displacement reaction. Paquin's group reported a transition metal and Lewis acid-free Friedel-Crafts benzylation of arenes activated by XtalFluor-E® (Scheme 4.10).²⁶ Benzylic alcohol **IV-29** reacts with XtalFluor-E® to generate an alkoxy-*N*,*N*-diethylaminodifluorosulfane, and ionization provides a stabilized

carbocation which is ready for electrophilic substitution. Similarly, they reported XtalFluor-E® promoted allylation of benzyl alcohol afterwards.²⁷

Ar OH
$$\xrightarrow{\text{IV-29}}$$
 $1.1 \text{ equiv XtalFluor-E} \atop \text{5 equiv } p\text{-xylene} \atop \text{CH}_2\text{Cl}_2\text{-HFIP (9:1)} \atop \text{rt, 4h}$
 $1.1 \text{ equiv XtalFluor-E} \atop \text{5 equiv } p\text{-xylene} \atop \text{CH}_2\text{Cl}_2\text{-HFIP (9:1)} \atop \text{rt, 4h}$
 $1.1 \text{ equiv XtalFluor-E} \atop \text{5 equiv } p\text{-xylene} \atop \text{CH}_2\text{Cl}_2\text{-HFIP (9:1)} \atop \text{rt, 4h}$
 $1.1 \text{ equiv XtalFluor-E} \atop \text{5 equiv } p\text{-xylene} \atop \text{CH}_2\text{Cl}_2\text{-HFIP (9:1)} \atop \text{rt, 4h}$
 $1.1 \text{ equiv XtalFluor-E} \atop \text{5 equiv } p\text{-xylene} \atop \text{R} \xrightarrow{\text{IV-30}}$
 $1.1 \text{ equiv XtalFluor-E} \atop \text{5 equiv } p\text{-xylene} \atop \text{R} \xrightarrow{\text{IV-30}}$
 $1.1 \text{ equiv XtalFluor-E} \atop \text{5 equiv } p\text{-xylene} \atop \text{CH}_2\text{Cl}_2\text{-HFIP (9:1)} \atop \text{rt, 4h}$
 $1.1 \text{ equiv XtalFluor-E} \atop \text{5 equiv } p\text{-xylene} \atop \text{CH}_2\text{Cl}_2\text{-HFIP (9:1)} \atop \text{R} \xrightarrow{\text{IV-30}}$
 $1.1 \text{ equiv XtalFluor-E} \atop \text{5 equiv } p\text{-xylene} \atop \text{R} \xrightarrow{\text{IV-30}}$
 $1.1 \text{ equiv XtalFluor-E} \atop \text{5 equiv } p\text{-xylene} \atop \text{R} \xrightarrow{\text{IV-30}}$
 $1.1 \text{ equiv XtalFluor-E} \atop \text{5 equiv } p\text{-xylene} \atop \text{IV-30}}$
 $1.1 \text{ equiv XtalFluor-E} \atop \text{5 equiv } p\text{-xylene} \atop \text{IV-30}}$
 $1.1 \text{ equiv XtalFluor-E} \atop \text{5 equiv } p\text{-xylene} \atop \text{IV-30}}$
 $1.1 \text{ equiv XtalFluor-E} \atop \text{5 equiv } p\text{-xylene} \atop \text{IV-30}}$
 $1.1 \text{ equiv XtalFluor-E} \atop \text{5 equiv } p\text{-xylene} \atop \text{IV-30}}$
 $1.1 \text{ equiv XtalFluor-E} \atop \text{5 equiv } p\text{-xylene} \atop \text{IV-30}}$
 $1.1 \text{ equiv XtalFluor-E} \atop \text{1.1 equiv } p\text{-xylene} \atop \text{$

Scheme 4.10 XtalFluor-E® mediated benzylation.

Moreover, XtalFuor-E® has been extensively used to activate aziridines for fluoride opening of the ring (Scheme 4.11).²⁸ Bicyclic compound **IV-31** was treated with XtalFuor-E® to afford fluorinated ester containing an imidazolidinone ring system. They believed that the sulfonamide group activates the aziridine through neighboring group participation. Partially negatively polarized O of the sulfonamide attacks the S of XtalFuor-E® to form adduct **IV-32** with the concomitant generation of a fluoride anion. Fluoride leads to nucleophilic aziridine ring opening intermediate **IV-33**, which then undergoes intramolecular acylation of N giving rise to bicyclic imidazolidinone product **IV-35**.

Scheme 4.11 XtalFluor-E® mediated aziridine opening.

Looking deeply into the literature about XtalFluor-E® activation, in most cases, it has been used as reagent, however XtalFluor-E® as catalyst has rarely been reported. Here we developed a practical, straightforward synthesis of *N*-acetyl-*N*,*O*-acetals catalyzed by XtalFluor-E® (Scheme 4.12). We surmised addition of alcohol to XtalFluor-E® generates protons that can initiate the protonation of enamides. The protonated enamide can be intercepted by the excess nucleophile to yield *N*,*O*-acetal products.

Scheme 4.12 XtalFluor-E[®] catalyzed hydroalkoxylation of enamides.

4.2 Results and discussion

4.2.1 Optimization for intermolecular hydroalkoxylation of enamide

We commenced our study with phenyl substituted enamide **IV-36**. Our initial attempt of using stoichiometric amount of XtalFluor-E® with excess MeOH (10 equiv) renders quantatitive yield of hydromethoxylation product (Table 4.1, entry 1). However, the reaction became slower when only 10% XtalFluor-E® was applied, and led to lower yield (Table 4.1, entry 2). This might be due to the attenuated activity of the *in situ* generated proton in methanol, thus we resorted to aprotic solvents. A variety of aprotic solvents have been screened. Reaction is sluggish in toluene, and much faster in dichloromethane, chloroform, dichloroethane and nitromethane, albeit with 5% substrates remaining after extended time. Ultimately it was found that DCM-MeOH (1:1, v:v) co-solvent system furnished 98% yield in 8 h. Another aminodifluorosulfinium tetrafluoroborates salt XtalFluor-M® also gave 86% yield, albeit with lower reaction rate. In case of alcohols with low molecular weight, the excess amount is not an issue since the remaining alcohol can be evaporated. It is noteworthy that reaction was sluggish when acids such as TFA were used as the catalyst instead of XtalFluor-E®.

Table 4.1 Reaction condition optimization

entry	solvent	time (h)	conversion (yield) ^a	
1 ^b	MeOH	36	99% (>98%)	
2	MeOH	48	88% (57%)	
3	Toluene	22	74% (66%)	
4	CH ₂ Cl ₂	10	95% (89%)	
5	CHCl ₃	10	93% (83%)	
6	Nitromethane	10	95% (85%)	
7	CICH ₂ CH ₂ CI	10	95% (85%)	
8	Acetonitrile	22	85% (68%)	
9 ^c	CH ₂ Cl ₂	36	97% (86%)	
10 ^d	CH ₂ Cl ₂	8	100% (>98%)	
11 ^{d,e}	CH ₂ Cl ₂	38	50%	

^aYields were estimated by ¹H NMR analysis of the crude reaction mixture. ^bOne equivalent of XtalFluor-E[®] was used ^cXtalFluor-M[®] (10 mol%) was used instead of XtalFluor-E[®]. ^dMeOH:DCM (1:1 v:v, 0.1 M) was used. ^e 20% mol TFA was used instead of XtalFluor-E[®].

4.2.2 The scope for intermolecular hydroalkoxylation of enamides

To demonstrate the generality of the reaction, a handful of enamide substrates were synthesized and subjected to the reaction condition (Table 4.2). Gratifyingly, the reaction resulted in the corresponding *N,O* or *N,S*-acetals with nearly quantitative yield for most of the substrates. The electronic and steric influence of the aryl group on the reactivity of the enamide was screened, with minimal effect on the yield and efficiency of the reaction. Nevertheless, the *p*-methoxy benzoyl group generally gave better results. The transformation was equally effective with aliphatic enamides, delivering high yield of the *N,O*-acetal products. The reaction is not limited to secondary enamides, as cyclic-tertiary enamides resulted in products with excellent yield. Furthermore, the cyclic nature of the enamide did not diminish the reaction outcome. With regard to the nature of the protic nucleophile,

light alcohols can be used to successfully give the corresponding *N,O*-acetal products. Thiols also yield *N,S*-acetals with excellent yields (IV-59, IV-60). The thiol mediated reactions typically proceed faster as compared to alcohols as nucleophiles. The reaction can also be performed on a large scale without deterioration in efficiency (IV-55, *trans*). The stereoisomerism of the starting enamide (*cis* or *trans*) had minimal effect on the reaction. Of note is the incompatibility of the methodology with bulky nucleophiles. As illustrated in Table 2, hydroalkoxylation of enamide with *n*-propyl alcohol results in high yield of IV-57, however the reaction is less efficient with *iso*-propyl alcohol (IV-58). The reaction of enamide with *tert*-butyl alcohol failed to give any product. Substrate IV-51 is unreactive under this condition, which might be due to the steric hindrance of two methyl groups on enamide. When the enamide is substituted by phenyl group, no reaction occurred as well (IV-52 and IV-53).

Table 4.2 Substrates scope.

$^{\rm c}$ reaction was performed at 1.0 mmol scale.

4.2.3 Mechanistic studies

To propose a reasonable mechanism, we conducted a few control experiments. As reported by Paquin and coworkers, alcohols can react with XtalFluor-E[®] to give a non-reversible adduct.^{22, 27} In our optimized reaction condition, catalytic XtalFluor-E[®] is exposed to protic nucleophiles in large excess. As a result, the

^a yield was determined by ¹H NMR using methyl-*tert*-butyl ether as internal standard; the rest of the reported yields were based on isolated products. ^b HFIP/MeOH(v/v, 9:1) was used as solvent.

formation of the putative adduct and its implication on the reaction progress is obscured by the presence of excess nucleophile. To circumvent this issue, the reaction of IV-46 was conducted in the presence of only one equivalent of methanol and the loading of XtalFluor-E® was varied. As illustrated in Table 4.3 the yield of N,O-acetal product IV-66 decreases as XtalFluor-E® loading increases. At a 1:1 ratio of methanol:XtalFluor-E®, no desired product was detected based on ¹H NMR analysis albeit with all substrate consumed. The complete disappearance of the enamide IV-46 in the reaction with methanol and XtalFluor-E® (1 equiv each) is illustrative of the fact that the protonation of the enamaide most likely is taking place under this condition, however in the absence of free methanol the protonated enamide undergoes deleterious side reactions. This set of experiments does suggest the formation of an adduct such as I, depicted in Scheme 4.13 (dashed box).

Table 4.3 Control experiments with increasing loadings of XtalFluor-E[®].

entry	XtalFluor-E (equiv)	yield ^a
1	0.1	90%
2	0.2	69%
3	0.5	40%
4	1.0	0%
5 ^b	1.0	0%

^a Yield was estimated by ¹HNMR analysis of the crude reaction mixture.

^b After 2 hours another 5 equivalents of methanol was added.

Table 4.4 Control experiments of nucleophiles with different nucleophilicity and acidity.

Since the nucleophile acts as the proton source in this reaction, we designed experiments to investigate the contribution of nucleophilicity as well as the acidity of the protic nucleophiles on the course of the reaction. As illustrated in Table 4.4, comparing reactions of the enamide IV-37 revealed that the reaction with sulfur-based nucleophiles is faster than oxygen-based nucleophiles (compare entries 1 and 2, Table 4.4). On the other hand, the acidity of the protic nucleophile proved to have minimal effect on the reaction progress i.e., benzoic acid, despite its higher acidity, was an incompetent reagent. This can be interpreted by the weaker nucleophilicity of benzoic acid that prevents adduct formation with XtalFluor-E®. This hypothesis is in accordance with the reported data that adduct formation of carboxylic acids with XtalFluor-E® requires the presence of a base. The increased nucleophilicity of thiobenzoic acid in comparison resulted in the fast consumption of substrate and formation of the corresponding product was observed.

^a Yield was estimated by ¹H NMR analysis of the crude reaction mixture.

^b ~ 65% starting material was recovered.

We also conducted NMR study to further understand the mechanism. Upon addition of methanol to a solution of XtalFluor-E® in d_3 -acetonitrile, substantial changes in the ¹⁹F NMR of the mixture were observed. XtalFluor-E® has two peaks in the ¹⁹F NMR that correspond to the fluorine atoms on the sulfur (12.9 ppm) and the tetrafluoroborate anion (–151.6 ppm). Addition of one equivalent of methanol resulted in the disappearance of the peak at 12 ppm concomitant with the appearance of multiple peaks in the 50–60 ppm range. Addition of two equivalents of methanol simplified the spectrum into a single peak at 54 ppm (see Figure 4.1 for NMR traces). This newly emerged peak did not undergo any further changes upon increasing the equivalents of methanol (up to 10 equivalents). These results further suggest the formation of the putative adduct I.

Our experimental and NMR data, along with observations and mechanistic suggestions that have appeared in the literature, lead us to the mechanistic proposal depicted in Scheme 4.13. We surmised that addition of an alcohol to XtalFluor-E® provides a *catalytic* proton source as the initial step of the reaction. The protonated enamide can be intercepted by the excess nucleophile to yield the protonated *N,O*-acetal product. This protonated *N,O*-acetal product can act as proton source to activate another enamide. Putative complexes (shown in the dashed box, Scheme 4.13) can potentially collapse to generate tetrafluoroboric acid (HBF₄) and subsequently this acid can protonate the enamide. This suggest that HBF₄ itself should be able to catalyze this reaction. Indeed, we find the latter statement is true (Table 4.5).

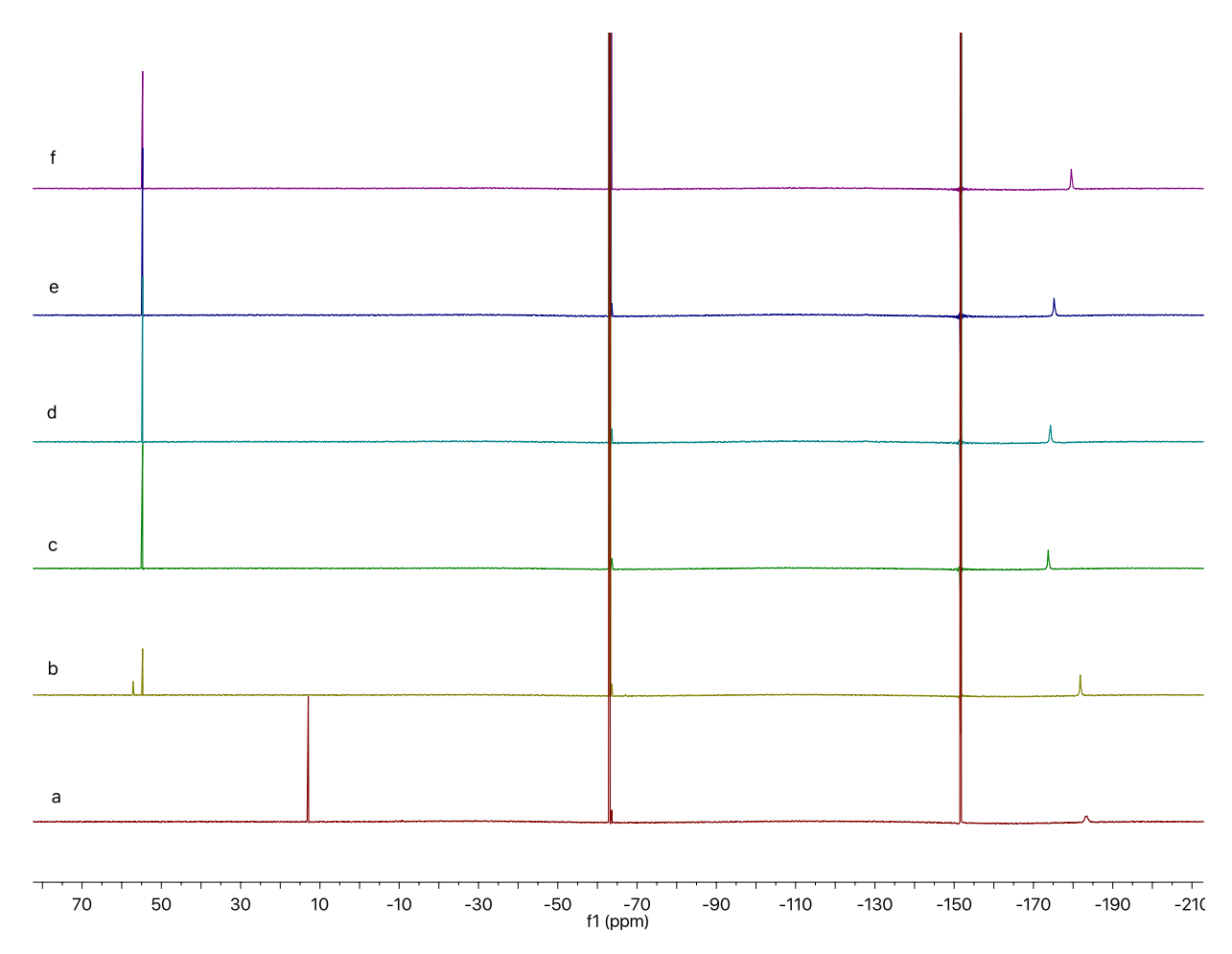


Figure 4.1. ¹⁹F NMR spectrum of a) XtalFluor-E[®]; b) XtalFluor-E[®] + 1 equiv MeOH; c) XtalFluor-E[®] + 2 equiv MeOH; d) XtalFluor-E[®] + 4 equiv MeOH; e) XtalFluor-E[®] + 5 equiv MeOH; f) XtalFluor-E[®] + 10 equiv MeOH (δ 63.21 was from standard compound benzotrifluoride 1 equiv.).

RXH
$$X = 0$$
 or S
 $R = 0$ o

Scheme 4.13 Proposed mechanism

4.2.4 HBF₄ catalyzed hydroalkoxylation

Based on our proposed mechanism, we believe that HBF₄, putatively generated from XtalFluor-E[®] and alcohol, is the species that catalyzes the reaction. To verify this, HBF₄•OEt₂ (20 mol%) was used as the catalyst instead of XtalFluor-E[®] with different substrates. We observed comparable results to those obtained with XtalFluor-E[®]. Most reactions with HBF₄OEt₂ proceeded faster than XtalFluor-E[®] catalyzed reactions. However, for some substrates yields are a bit lower than with XtalFluor-E[®] as catalysts since products are prone to decomposition under strong acidic conditions.

Table 4.5 Comparison of yields between XtalFluor-E® and HBF₄•OEt₂ as catalyst.

entry	substrate	XtalFluor-E ^{® a}	HBF ₄ •OEt ₂ ^a
1	O OMe N H	98	98
2	O OMe N H	91	98
3	O OMe N H	98	70
4	O OMe N H	95	98
5	F O OMe N H	60	99
6	HN O OMe	86	75
7	O OMe	94	98
8	O OMe	98	83
9	trans H N O OMe	83	83
10	MeO Cis	98	64

^a isolated yield of *N,O*-acetal products

4.2.5 Study of intramolecular hydroalkoxylation

In addition to the intermolecular hydroalkoxylation, intramolecular hydroalkoxylation has also been evaluated (**Table 4.6**). Unsaturated amide **IV-72** was subjected to catalytic amount of XtalFluor-E® in DCM at ambient temperature, after 20 h only 4% conversion was observed. However, when stoichiometric amount of XtalFluor-E® was used, 80% yield of lactam product was obtained after 24 h. For primary alcohol substrate **IV-74**, cyclized product bearing a tetrahydrofuran ring was obtained in 94% yield when 10 mol% XtalFluor-E® was used. The external alcohol reagent MeOH seems not to affect the reaction outcome. Other unsaturated amide **IV-76** and allyl amine **IV-77** did not give desired cyclized products even in the presence of stoichiometric amount of XtalFluor-E®.

Table 4.6 Intramolecular cyclization mediated by XtalFluor-E[®]

entry	MeOH (equiv)	time (hours)	conversion ^a (yield) ^b
1	10	18	100% (93%)
2	0	6	100% (94%)

^a yield was estimated by ¹H NMR analysis of the crude reaction mixture.

b isolated yield.

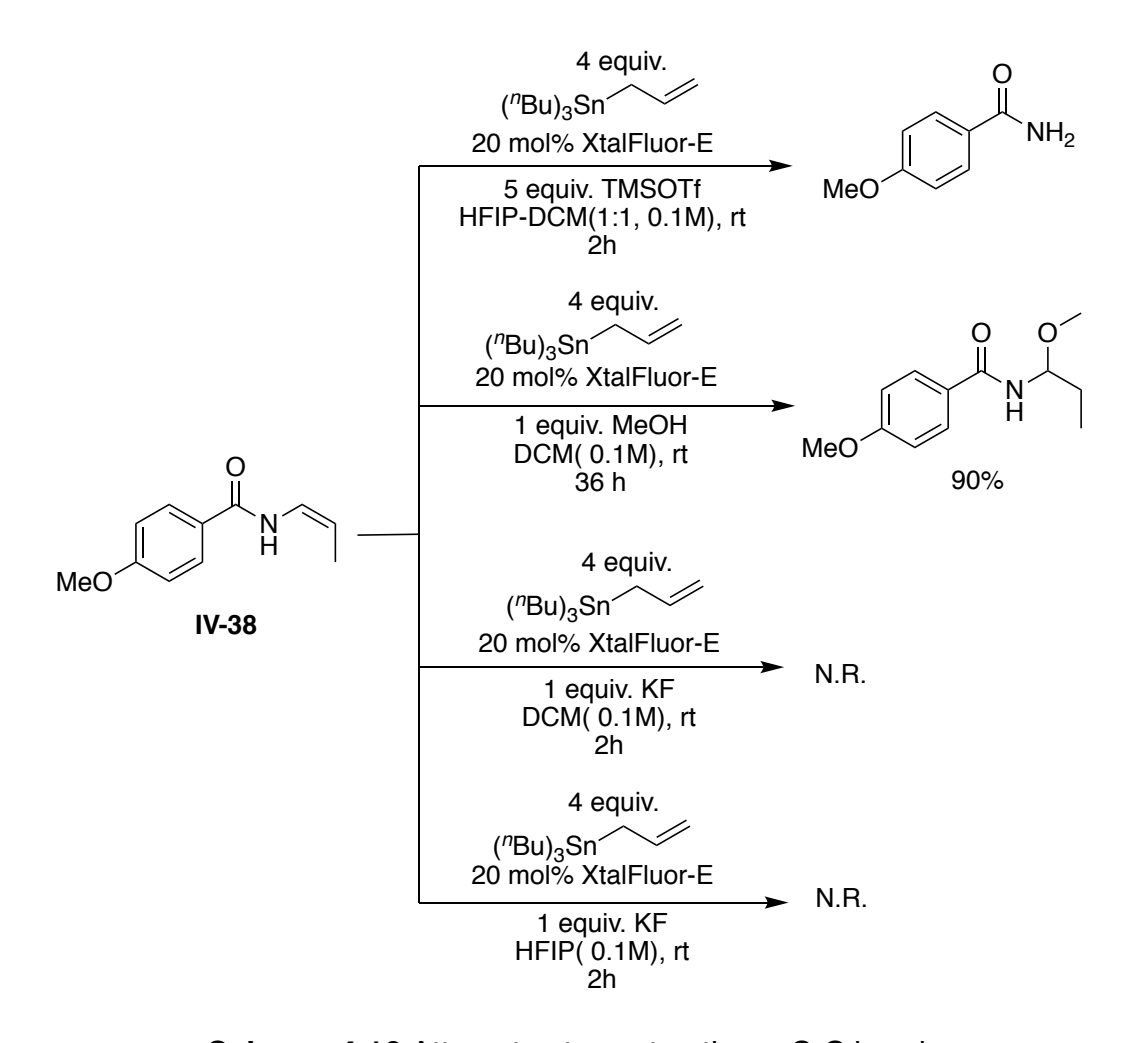
Scheme 4.14 Other attempts for intramolecular cyclization.

4.2.6 Attempts of constructing C-N/C-C bond mediated by XtalFluor-E®

As an extension of the C-O/S bond formation, we next endeavored to build C-N bonds with chemistry mediated by XtalFluor-E[®]. Substrate **IV-38** was treated with excess *n*-butylamine in DCM with 20 mol% XtalFluor-E[®], however no reaction occurred. We ascribed this to the fact that the generated acid would protonate the amine first, and thus there is no more acid to activate the enamide for further reaction.

Scheme 4.15 Attempts at constructing a C-N bond.

Besides constructing a C-heteroatom bond, we also attempted to construct more challenging C-C bond using XtalFluor-E® as catalyst. We chose a strong nucleophile, allyltributylsilane, which usually reacts with a variety of cationic carbon electrophiles and is used with Lewis acids. Different Lewis acids and solvent combinations have been tested, however, either benzamide formed as a result of substrate decomposition or no reaction occurred.



Scheme 4.16 Attempts at constructing a C-C bond.

4.2.7 Summary

We developed a mild and simple method for the generation of protons from the reaction of XtalFluor-E® with a protic solvent. Reaction of enamides under the prescribed conditions lead to the protofunctionalization of olefins, yielding *N,O*-acetals or *N,S*-acetals. The *N,O/N,S*-acetal products can be accessed in nearly quantatitive yield in most cases, often without need for further purification. XtalFluor-E® is commercially available and the water-soluble side product can be removed easily. Constructing C-N or C-C bonds using XtalFluor-E® could be our future endeavors. Also, combining XtalFluor-E® with other chiral catalysts to construct C-O bond enantioselectively is also our interest.

4.3 Experimental section

4.3.1 General information

All reagents were purchased from commercial sources and were used without purification. XtalFluor-E® and *N*-vinylcaprolactam were purchased from Aldrich. *N*-vinyl-2-pyrrolidone was purchased from Combi-Blocks. TLC analyses were performed on silica gel plates (pre-coated on glass; 0.20 mm thickness with fluorescent indicator UV254) and were visualized by UV or charred in PMA stains. ¹H and ¹³C NMR spectra were collected on 500 MHz NMR spectrometers (Agilent) using CDCl₃. Chemical shifts are reported in parts per million (ppm) and are referenced to residual solvent peaks. Flash silica gel (32-63 μm, Silicycle 60 Å) was used for column chromatography. All known compounds were characterized by ¹H and ¹³C NMR and are in complete agreement with samples reported elsewhere. All new compounds were characterized by ¹H and ¹³C NMR, HRMS, and melting point (where appropriate).

4.3.2 General procedure A for screening and optimization

A 5 mL vial equipped with a magnetic stir bar was charged with the substrate (0.1 mmol, 1 equiv.) and XtalFluor-E® (20 mol%). The mixture was dissolved with freshly distilled dichloromethane (0.5 mL) and alcohol (0.5 mL). The vial was flushed with argon and sealed. The reaction was stirred at ambient temperature for 1-24 h. The reaction was then quenched with saturated Na₂SO₃ and extracted with dichloromethane. The combined organics were dried over anhydrous Na₂SO₄ and filtered. Conversions were calculated by 1H NMR. Pure product was isolated by column chromatography on silica gel

or aluminum oxide (activated, neutral) as stationary phase (EtOAc in Hexanes as gradient).

4.3.3 Analytical data for products

General procedure **A** was used with 19.1 mg (0.1 mmol) of **IV-38** yielding 21.8 mg (98%) of **IV-55**; 19.1 mg (0.1 mmol) of **IV-39** yielding 19 mg (85%) of **IV-55**.

white solids; M.P.: 66 - 70 °C; Rf: 0.23 (30% EtOAc in Hexane, UV).

¹H NMR (500 MHz, CDCl₃) δ 7.74 (d, J = 8.5 Hz, 2H), 6.91 (d, J = 9 Hz, 2H), 6.17 (d, J = 9.5 Hz, 1H), 5.24 (tt, J = 5 Hz, 13 Hz, 1H), 3.83 (s, 3H), 3.37 (s, 3H), 1.76 (m, 1H), 1.63 (m, 1H), 0.96 (t, J = 7.5 Hz, 3H).

¹³C NMR (125 MHz, CDCl₃) δ 167.2, 162.5, 128.8, 126.2, 113.8, 82.7, 56.0, 55.4, 28.8, 9.2.

HRMS analysis (ESI): calculated for (M+Na): C₁₂H₁₇NO₃Na 246.1106; found: 246.1113

General procedure **A** was used with 19.1 mg (0.1 mmol) of **IV-38** yielding 22.5 mg (95%) of **IV-56** as a clear oil.

R_f: 0.33 (30% EtOAc in Hexane, UV)

¹H NMR (500 MHz, CDCl₃) δ 7.76 (d, J = 8.5 Hz, 2H), 6.94 (d, J = 9 Hz, 2H), 6.2 (d, J = 9 Hz, 1H), 5.36 (m, 1H), 3.86 (s, 3H), 3.70 (m, 1H), 3.57 (m, 1H), 1.78 (m, 1H), 1.66 (m, 1H), 1.20 (t, J = 7 Hz, 3H), 0.99 (t, J = 7.5 Hz, 3H).

¹³C NMR (125 MHz, CDCl₃) δ 166.8, 162.4, 128.8, 126.2, 113.8, 81.2, 63.8, 55.4, 29.1, 15.2, 9.3.

HRMS analysis (ESI): calculated for (M+Na): C₁₃H₁₉NO₃Na 260.1263; found: 260.1270

General procedure **A** was used with 19.1 mg (0.1 mmol) of **IV-38** yielding 20 mg (80%) of **IV-57** as a clear oil.

Rf: 0.29 (30% EtOAc in Hexane, UV)

¹H NMR (500 MHz, CDCl₃) δ 7.74 (d, J = 9 Hz, 2H), 6.92 (d, J = 9 Hz, 2H), 6.17 (d, J = 9 Hz, 1H), 5.34 (m, 1H), 3.85 (s, 3H), 3.59 (m, 1H), 3.47 (m, 1H), 1.79 (m, 1H), 1.71-1.56 (m, 3H), 0.99 (t, J = 7.5 Hz, 3H), 0.91 (t, J = 7.5 Hz, 3H).

¹³C NMR (125 MHz, CDCl₃) δ 166.7, 162.4, 128.8, 126.3, 113.8, 81.4, 70.2, 55.4, 29.1, 22.9, 10.6, 9.4

HRMS analysis (ESI): calculated for (M+Na): C₁₄H₂₁NO₃Na 274.1419; found: 274.1425

General procedure **A** was used with 19.1 mg (0.1 mmol) of **IV-38** yielding 20 mg (40%) of **IV-58** as a clear oil.

R_f: 0.41 (30% EtOAc in Hexane, UV)

¹H NMR (500 MHz, CDCl₃) δ 7.73 (d, J = 8.8 Hz, 2H), 6.92 (d, J = 8.8 Hz, 2H), 6.19 (d, J = 9.4 Hz, 1H), 5.43 – 5.35 (m, 1H), 3.87 (dt, J = 12.3, 6.1 Hz, 1H), 3.83 (s, 3H), 1.75 – 1.66 (m, 1H), 1.67 – 1.58 (m, 1H), 1.19 (d, J = 6.0 Hz, 3H), 1.13 (d, J = 6.2 Hz, 3H), 0.96 (t, J = 7.4 Hz, 3H).

¹³C NMR (125 MHz, CDCl₃) δ 166.57, 162.38, 128.77, 126.36, 113.82, 79.32, 69.22, 55.45, 29.48, 23.52, 21.70, 9.45.

HRMS analysis (ESI): calculated for (M+Na): C₁₄H₂₁NO₃Na 274.1419; found: 274.1420

General procedure **A** was used with 19.1 mg (0.1 mmol) of **IV-39** yielding 29 mg (98%) of **IV-59** as a wax.

R_f: 0.43 (30% EtOAc in Hexane, UV)

¹H NMR (500 MHz, CDCl₃) δ 7.73 (d, J = 8.8 Hz, 2H), 6.91 (d, J = 8.8 Hz, 2H), 6.12 (d, J = 9.8 Hz, 1H), 5.30 (ddd, J = 9.8, 7.3, 6.3 Hz, 1H), 3.83 (s, 3H), 2.64 (ddd, J = 12.7, 8.0,

6.0 Hz, 1H), 2.46 (ddd, J = 12.8, 8.2, 6.9 Hz, 1H), 1.86 – 1.69 (m, 2H), 1.69 – 1.52 (m, 2H), 1.02 (t, J = 7.4 Hz, 3H), 0.93 (t, J = 7.3 Hz, 3H).

¹³C NMR (125 MHz, CDCl₃) δ 166.20, 162.35, 128.71, 126.19, 113.82, 56.00, 55.44, 32.80, 29.59, 23.11, 13.53, 10.86.

HRMS analysis (ESI): calculated for (M+Na): C₁₄H₂₁NO₂SNa 290.1191; found: 290.1197

General procedure **A** was used with 19.1 mg (0.1 mmol) of **IV-39** yielding 20 mg (85%) of **IV-60** as a white solid.

white solids; M.P.: 75 - 80 °C

Rf: 0.52 (30% EtOAc in Hexane, UV)

¹H NMR (500 MHz, CDCl₃) δ 7.73 (d, J = 8.8 Hz, 2H), 6.91 (d, J = 8.8 Hz, 2H), 6.09 (d, J = 9.8 Hz, 1H), 5.31 (ddd, J = 9.8, 7.3, 6.3 Hz, 1H), 3.83 (s, 3H), 2.65 (ddd, J = 12.7, 8.3, 6.0 Hz, 1H), 2.49 (ddd, J = 12.7, 8.4, 6.7 Hz, 1H), 1.87 – 1.69 (m, 2H), 1.64 – 1.48 (m, 2H), 1.34 (ddq, J = 13.9, 8.8, 7.2 Hz, 2H), 1.02 (t, J = 7.4 Hz, 3H), 0.85 (t, J = 7.3 Hz, 3H). ¹³C NMR (125 MHz, CDCl₃) δ 166.19, 162.35, 128.69, 128.69, 126.22, 113.82, 56.04, 55.44, 31.83, 30.49, 29.59, 21.99, 13.63, 10.86.

HRMS analysis (ESI): calculated for (M+Na): C₁₅H₂₃NO₂SNa 304.1347; found: 304.1362

General procedure **A** was used with 18 mg (0.102 mmol) of **IV-41** yielding 21 mg (98%) of **IV-62** as a clear oil.

Rf: 0.13 (30% EtOAc in Hexane, UV)

¹H NMR (500 MHz, CDCl₃) δ 7.76 (d, J = 8.8 Hz, 1H), 6.93 (d, J = 8.8 Hz, 2H), 6.25 (d, J = 9.5 Hz, 1H), 5.49 (dd, J = 9.5, 5.8 Hz, 1H), 3.85 (s, 4H), 3.39 (s, 3H), 1.43 (d, J = 5.9 Hz, 4H).

¹³C NMR (125 MHz, CDCl₃) δ 166.67, 162.45, 128.83, 126.09, 113.81, 78.17, 55.78, 55.43, 21.82.

HRMS analysis (ESI): calculated for (M+Na): C₁₁H₁₅NO₃Na 232.0950; found: 232.0954

General procedure **A** was used with 17.5 mg (0.1 mmol) of **IV-42** yielding 18.9 mg (9%) of **IV-63**; 17.5 mg (0.1 mmol) of **IV-43** yielding 14.9 mg (72%) of **IV-63**.

Yellowish solid, M.P.: 56 - 63 °C

Rf: 0.35 (30% EtOAc in Hexane, UV)

¹H NMR (500 MHz, CDCl₃) δ 7.71 – 7.67 (m, 2H), 7.28 – 7.18 (m, 2H), 6.22 (d, J = 9.7 Hz, 1H), 5.26 (dtd, J = 9.8, 6.1, 1.8 Hz, 1H), 3.38 (d, J = 1.4 Hz, 3H), 2.38 (s, 2H), 1.77 (dddd, J = 13.7, 7.6, 6.1, 1.5 Hz, 1H), 1.67 – 1.57 (m, 1H), 0.97 (td, J = 7.5, 1.4 Hz, 3H). ¹³C NMR (125 MHz, CDCl₃) δ 167.44, 142.35, 131.10, 129.30, 126.96, 82.73, 56.01, 28.83, 21.47, 9.22.

HRMS analysis (ESI): calculated for (M+Na): C₁₂H₁₇NO₂Na 230.1157; found: 230.1154

General procedure **A** was used with 16.1 mg (0.1 mmol) of **IV-36** yielding 18.4 mg (95%) of **IV-54**; 16.1 mg (0.1 mmol) of **IV-37** yielding 18.9 mg (98%) of **IV-54**;

Rf: 0.71 (30% EtOAc in Hexane, UV)

¹H NMR (500 MHz, CDCl₃) δ 7.81 – 7.71 (m, 2H), 7.55 – 7.47 (m, 1H), 7.43 (dd, J = 8.2, 6.9 Hz, 2H), 6.26 (d, J = 9.6 Hz, 1H), 5.26 (dt, J = 9.6, 6.2 Hz, 1H), 3.39 (s, 3H), 1.78 (ddd, J = 14.0, 7.7, 6.5 Hz, 1H), 1.65 (ddd, J = 14.0, 7.7, 6.5 Hz, 1H), 0.98 (t, J = 7.5 Hz, 3H). ¹³C NMR (125 MHz, CDCl₃) δ 167.56, 134.01, 131.85, 128.67, 126.97, 82.83, 56.06, 28.82, 9.21.

HRMS analysis (ESI): calculated for (M+Na): C₁₁H₁₅NO₂Na 216.1000; found: 216.1004

General procedure **A** was used with 17.9 mg (0.1 mmol) of **IV-44** yielding 14.2 mg (67%) of **IV-64** as a clear oil.

Rf: 0.53 (30% EtOAc in Hexane, UV)

¹H NMR (500 MHz, CDCl₃) δ 8.06 (td, J = 7.9, 1.9 Hz, 1H), 7.47 (dddd, J = 8.3, 7.2, 5.2, 1.9 Hz, 1H), 7.27 – 7.21 (m, 1H), 7.11 (ddd, J = 12.1, 8.2, 1.1 Hz, 1H), 6.77 (d, J = 12.4 Hz, 1H), 5.29 (dddd, J = 9.0, 6.1, 6.1, 2.7 Hz, 1H), 3.39 (s, 3H), 1.76 (dddd, J = 14.9, 13.5, 7.5, 7.5, 6.0 Hz, 1H), 1.73 – 1.62 (m, 1H), 0.97 (t, J = 7.5 Hz, 3H).

¹³C NMR (125 MHz, CDCl₃) δ 163.56 (d, J = 2.9 Hz), 161.59, 159.62, 133.60 (d, J = 9.3 Hz), 132.17 (d, J = 2.2 Hz), 124.88 (d, J = 3.2 Hz), 116.11 (d, J = 24.8 Hz), 82.77, 56.05, 28.68, 9.01.

HRMS analysis (ESI): calculated for (M+Na): C₁₁H₁₄NO₂FNa 234.0906; found: 234.0904

General procedure **A** was used with 20 mg (0.202 mmol) of **IV-48** yielding 18.8mg (71%) of **IV-68** as a clear oil.

R_f: 0.08 (30% EtOAc in Hexane, dye with PMA)

¹H NMR (500 MHz, CDCl₃) δ 5.70 (s, 1H), 5.32 – 5.12 (m, 1H), 3.29 (d, J = 1.3 Hz, 2H), 2.21 (q, J = 7.6, 2H), 1.29 (dd, J = 5.9, 1.3 Hz, 3H), 1.14 (td, J = 7.6, 1.2 Hz, 3H). ¹³C NMR (125 MHz, CDCl₃) δ 173.79, 77.47, 55.60, 29.77, 21.57, 9.68.

HRMS analysis (ESI): calculated for (M+Na): C₆H₁₃NO₂Na 154.0844; found: 154.0843

General procedure **A** was used with 25 mg (0.2 mmol) of **IV-49** yielding 31 mg (98%) of **IV-69** as a clear oil.

R_f: 0.09 (30% EtOAc in Hexane, dye with PMA)

¹H NMR (500 MHz, CDCl₃) δ 5.05 (t, J = 6.9 Hz, 1H), 3.34 (dt, J = 9.9, 6.9 Hz, 1H), 3.27 (dt, J = 9.9, 7.2 Hz, 1H), 3.24 (s, 3H), 2.51 – 2.37 (m, 2H), 2.09 – 1.94 (m, 2H), 1.82 – 1.65 (m, 2H), 1.60 – 1.42 (m, 2H), 0.88 (t, J = 7.5, 3H).

¹³C NMR (125 MHz, CDCl₃) δ 176.27, 83.80, 55.62, 40.83, 31.68, 25.55, 18.26, 9.25.

HRMS analysis (ESI): calculated for (M+Na): C₈H₁₅NO₂Na 180.1000; found: 180.1000

General procedure **A** was used with 22.2 mg (0.2 mmol) of **IV-50** yielding 26.8 mg (100%) of **IV-70** as a clear oil.

Rf: 0.14 (30% EtOAc in Hexane, dye with PMA)

¹H NMR (500 MHz, CDCl₃) δ 5.28 (q, J = 6.1 Hz, 1H), 3.37 – 3.24 (m, 2H), 3.18 (d, J = 1.1 Hz, 3H), 2.47 – 2.34 (m, 2H), 2.08 – 1.89 (m, 2H), 1.27 (dd, J = 6.1, 1.1 Hz, 3H). ¹³C NMR (125 MHz, CDCl₃) δ 175.74, 78.77, 55.41, 40.73, 31.68, 18.67, 18.09.

HRMS analysis (ESI): calculated for (M+Na): C₇H₁₃NO₂Na 166.0844; found: 166.0844

General procedure **A** was used with 22.2 mg (0.2 mmol) of **IV-50** yielding 31 mg (100%) of **IV-71**as a clear oil.

Rf: 0.14 (30% EtOAc in Hexane, dye with PMA)

¹H NMR (500 MHz, CDCl₃) δ 5.40 (q, J = 6.1 Hz, 1H), 3.42 – 3.27 (m, 4H), 2.41 (td, J = 8.2, 1.7 Hz, 2H), 2.00 (p, J = 7.7 Hz, 2H), 1.27 (s, 2H), 1.15 (t, J = 7.1 Hz, 3H).

 ^{13}C NMR (125 MHz, CDCl₃) δ 175.55, 77.18, 63.14, 40.83, 31.71, 18.88, 18.07, 14.98.

HRMS analysis (ESI): calculated for (M+Na): C₈H₁₅NO₂Na 180.1000; found: 180.0996

General procedure **A** was used with 31 mg (0.22 mmol) of **IV-46** yielding 37 mg (98%) of **IV-66** as a clear oil.

R_f: 0.15 (30% EtOAc in Hexane, dye with PMA)

¹H NMR (500 MHz, CDCl₃) δ 5.71 (q, J = 6.1 Hz, 1H), 3.30 (ddd, J = 15.4, 7.7, 1.7 Hz, 1H), 3.23 – 3.07 (m, 4H), 2.56 (ddd, J = 13.8, 10.3, 1.8 Hz, 1H), 2.47 (ddd, J = 13.8, 9.3, 1.6 Hz, 1H), 1.78 – 1.43 (m, 6H), 1.20 (d, J = 6.1 Hz, 3H).

¹³C NMR (125 MHz, CDCl₃) δ 176.66, 80.78, 55.47, 40.83, 37.73, 30.09, 29.32, 23.59, 19.13.

HRMS analysis (ESI): calculated for (M+Na): C₉H₁₇NO₂Na 194.1157; found: 194.1160

General procedure A was used with 22.6 mg (0.2 mmol) of **IV-47** yielding 24 mg (83%) of **IV-67** as a colorless oil.

Rf: 0.30 (30% EtOAc in Hexane, dye with PMA)

¹H NMR (500 MHz, CDCl₃) δ 5.86 – 5.68 (m, 1H), 5.26 (dq, J = 9.6, 5.4 Hz, 1H), 3.29 (d, J = 1.1 Hz, 3H), 2.43 – 2.24 (m, 1H), 1.30 (dd, J = 5.9, 1.0 Hz, 3H), 1.15 (ddd, J = 12.8, 7.0, 1.0 Hz, 6H).

 ^{13}C NMR (125 MHz, CDCl₃) δ 177.12, 77.40, 55.49, 35.78, 21.55, 19.73, 19.35.

HRMS analysis (ESI): calculated for (M+Na): C₇H₁₅NO₂Na 168.1000 found: 168.1002

General procedure A was used with 25.4 mg (0.2 mmol) of **IV-45** yielding 27.4 mg (86%) of **IV-65** as a clear oil.

R_f: 0.26 (30% EtOAc in Hexane, dye with PMA)

¹H NMR (500 MHz, CDCl₃) δ 5.76 (d, J = 9.6 Hz, 1H), 5.27 (dq, J = 9.5, 5.9 Hz, 1H), 3.30 (d, J = 0.9 Hz, 3H), 2.19 (t, J = 7.6 Hz, 2H), 1.67 – 1.46 (m, 2H), 1.32 (dd, J = 19.5, 6.7 Hz, 5H), 0.90 (t, J = 7.3 Hz, 3H).

¹³C NMR (125 MHz, CDCl₃) δ 173.18, 77.44, 55.59, 36.59, 27.64, 22.37, 21.60, 13.77. HRMS analysis (ESI): calculated for (M+Na): C₈H₁₇NO₂Na 182.1157; found: 182.1156

General procedure **A** was used with 23.3 mg (0.1 mmol) of **IV-40** yielding 26.5 mg (100%) of **IV-61** as a clear oil.

Rf: 0.39 (30% EtOAc in Hexane, UV)

¹H NMR (500 MHz, CDCl₃) δ 7.80 – 7.70 (m, 2H), 6.96 – 6.84 (m, 2H), 6.17 (d, J = 9.7 Hz, 1H), 5.31 (dt, J = 9.7, 6.2 Hz, 1H), 3.83 (s, 4H), 3.37 (s, 3H), 1.82 – 1.64 (m, 1H), 1.50 – 1.31 (m, 1H), 1.32 – 1.23 (m, 6H), 0.86 (q, J = 6.9, 5.5 Hz, 3H).

¹³C NMR (125 MHz, CDCl₃) δ 166.90, 162.45, 128.82, 126.18, 113.83, 81.61, 55.96, 55.45, 35.81, 31.53, 24.60, 22.54, 14.00.

HRMS analysis (ESI): calculated for (M+Na): C₁₅H₂₃NO₃Na 288.1576; found: 288.1574

Rf: 0.86 (30% EtOAc in Hexane, dye with PMA)

¹H NMR (500 MHz, CDCl₃) δ 7.32 – 7.28 (m, 2H), 6.86 – 6.82 (m, 2H), 4.00 – 3.94 (m, 1H), 3.91 – 3.84 (m, 1H), 3.78 (d, J = 0.7 Hz, 3H), 2.19 – 2.11 (m, 1H), 2.02 – 1.90 (m, 2H), 1.79 (dt, J = 7.2, 0.8 Hz, 1H), 1.49 (d, J = 0.7 Hz, 3H).

¹³C NMR (125 MHz, CDCl₃) δ 158.05, 140.24, 125.81, 113.38, 83.98, 67.44, 55.23, 39.43, 29.76, 25.76.

HRMS analysis (ESI): calculated for (M+H): C₁₂H₁₇O₂ 193.1229; found: 193.1227

R_f: 0.26 (30% EtOAc in Hexane, UV)

¹H NMR (500 MHz, CDCl₃) δ 7.33 – 7.19 (m, 4H), 7.16 (t, J = 7.4 Hz, 1H), 7.04 (dd, J = 7.4, 1.6 Hz, 2H), 6.95 – 6.87 (m, 2H), 3.82 (s, 3H), 2.76 – 2.63 (m, 1H), 2.63 – 2.53 (m, 1H), 2.26 (dd, J = 9.5, 6.3 Hz, 2H), 1.68 (s, 3H).

¹³C NMR (125 MHz, CDCl₃) δ 175.06, 158.75, 136.94, 136.85, 128.61, 126.76, 126.36, 126.33, 113.94, 67.20, 55.29, 38.19, 30.27, 26.11.

HRMS analysis (ESI): calculated for (M+Na): C₁₈H₁₉NO₂Na 304.1313; found: 304.1315

4.3.4 General procedure for synthesis of unsaturated amides and analytical data

$$R + CI \xrightarrow{3 \text{ equiv allylamine}} R + CI \xrightarrow{1 \text{ equiv. } K_2CO_3 \\ DCM, \text{ rt, 2 h}} R + CI \xrightarrow{2.2 \text{ equiv } LDA} CI \xrightarrow{1 \text{ equiv. } K_2CO_3 \\ DCM, \text{ rt, 2 h}} R + CI \xrightarrow{1 \text{ equiv. } K_2CO_3 \\ DCM, \text{ rt, 2 h}} R + CI \xrightarrow{1 \text{ equiv. } K_2CO_3 \\ DCM, \text{ rt, 2 h}} R + CI \xrightarrow{1 \text{ equiv. } K_2CO_3 \\ DCM, \text{ rt, 2 h}} R + CI \xrightarrow{1 \text{ equiv. } K_2CO_3 \\ DCM, \text{ rt, 2 h}} R + CI \xrightarrow{1 \text{ equiv. } K_2CO_3 \\ DCM, \text{ rt, 2 h}} R + CI \xrightarrow{1 \text{ equiv. } K_2CO_3 \\ DCM, \text{ rt, 2 h}} R + CI \xrightarrow{1 \text{ equiv. } K_2CO_3 \\ DCM, \text{ rt, 2 h}} R + CI \xrightarrow{1 \text{ equiv. } K_2CO_3 \\ DCM, \text{ rt, 2 h}} R + CI \xrightarrow{1 \text{ equiv. } K_2CO_3 \\ DCM, \text{ rt, 2 h}} R + CI \xrightarrow{1 \text{ equiv. } K_2CO_3 \\ DCM, \text{ rt, 2 h}} R + CI \xrightarrow{1 \text{ equiv. } K_2CO_3 \\ DCM, \text{ rt, 2 h}} R + CI \xrightarrow{1 \text{ equiv. } K_2CO_3 \\ DCM, \text{ rt, 2 h}} R + CI \xrightarrow{1 \text{ equiv. } K_2CO_3 \\ DCM, \text{ rt, 2 h}} R + CI \xrightarrow{1 \text{ equiv. } K_2CO_3 \\ DCM, \text{ rt, 2 h}} R + CI \xrightarrow{1 \text{ equiv. } K_2CO_3 \\ DCM, \text{ rt, 2 h}} R + CI \xrightarrow{1 \text{ equiv. } K_2CO_3 \\ DCM, \text{ rt, 2 h}} R + CI \xrightarrow{1 \text{ equiv. } K_2CO_3 \\ DCM, \text{ rt, 2 h}} R + CI \xrightarrow{1 \text{ equiv. } K_2CO_3 \\ DCM, \text{ rt, 2 h}} R + CI \xrightarrow{1 \text{ equiv. } K_2CO_3 \\ DCM, \text{ rt, 2 h}} R + CI \xrightarrow{1 \text{ equiv. } K_2CO_3 \\ DCM, \text{ rt, 2 h}} R + CI \xrightarrow{1 \text{ equiv. } K_2CO_3 \\ DCM, \text{ rt, 2 h}} R + CI \xrightarrow{1 \text{ equiv. } K_2CO_3 \\ DCM, \text{ rt, 2 h}} R + CI \xrightarrow{1 \text{ equiv. } K_2CO_3 \\ DCM, \text{ rt, 2 h}} R + CI \xrightarrow{1 \text{ equiv. } K_2CO_3 \\ DCM, \text{ rt, 2 h}} R + CI \xrightarrow{1 \text{ equiv. } K_2CO_3 \\ DCM, \text{ rt, 2 h}} R + CI \xrightarrow{1 \text{ equiv. } K_2CO_3 \\ DCM, \text{ rt, 2 h}} R + CI \xrightarrow{1 \text{ equiv. } K_2CO_3 \\ DCM, \text{ rt, 2 h}} R + CI \xrightarrow{1 \text{ equiv. } K_2CO_3 \\ DCM, \text{ rt, 2 h}} R + CI \xrightarrow{1 \text{ equiv. } K_2CO_3 \\ DCM, \text{ rt, 2 h}} R + CI \xrightarrow{1 \text{ equiv. } K_2CO_3 \\ DCM, \text{ rt, 2 h}} R + CI \xrightarrow{1 \text{ equiv. } K_2CO_3 \\ DCM, \text{ rt, 2 h}} R + CI \xrightarrow{1 \text{ equiv. } K_2CO_3 \\ DCM, \text{ rt, 2 h}} R + CI \xrightarrow{1 \text{ equiv. } K_2CO_3 \\ DCM, \text{ rt, 2 h}} R + CI \xrightarrow{1 \text{ equiv. } K_2CO_3 \\ DCM, \text{ rt, 2 h}} R + CI \xrightarrow{1 \text{ equiv. } K_2CO_3 \\ DCM, \text{ rt, 2 h}} R + CI \xrightarrow{1 \text{ equiv. } K_2CO_3 \\ DCM, \text{ rt, 2 h}} R + CI \xrightarrow{1 \text{ equiv. } K_2CO_3 \\ DCM, \text{ rt, 2 h$$

IV-36-IV-39, IV-42-IV-44

General procedure **B**: The appropriate aryl chloride (1 equiv) was dissolved in freshly distilled dichloromethane (15 mL) at room temperature. K₂CO₃ (1 equiv) was added in one portion to the solution at 0 °C. After stirring for 5 min, allylamine (3 equiv) was added in one portion. The reaction mixture was stirred for 2 h and gradually warmed to room temperature. The reaction was quenched with addition of H₂O, the organic layer was separated and washed with dichloromethane. The combined organic fraction was dried over Na₂SO₄, and concentrated in vacuo. The residue was purified by silica gel chromatography (25% EtOAc in Hexane). The purified allyl amide product was used in the next step. Freshly distilled i-Pr₂NH (2.2 equiv) was dissolved in anhydrous THF (0.3 M) and the solution was cooled down to -78 °C. n-BuLi (2.5 M in hexane, 2.2 equiv) was added dropwise to the solution. After stirring for 15 min, allyl amide (1 equiv) in anhydrous THF was added dropwise to the LDA solution at -78 °C. The reaction mixture was warmed to room temperature gradually. After 1 h, saturated NH₄Cl solution was added to work up the reaction. The organics were separated and dried over Na₂SO₄. The organic fraction was concentrated under vacuo and the residue was purified by silica gel column chromatography (15% EtOAc in Hex).

General procedure **B** was used with 2.0 g (12.5 mmol) of benzoyl chloride yielding 1.1 g (55%) of **IV-36** and 600 mg (30%) of **IV-37** as a white solid.

For **IV-36**:

White solid, M.P.: 68 - 73 °C

Rf: 0.72 (30% EtOAc in Hexane, UV)

¹H NMR (500 MHz, CDCl₃) δ 7.81 – 7.74 (m, 2H), 7.59 (d, J = 9.6 Hz, 1H), 7.55 – 7.48 (m, 1H), 7.47 – 7.39 (m, 2H), 6.92 (ddq, J = 10.8, 8.9, 1.8 Hz, 1H), 4.97 – 4.87 (m, 1H), 1.69 (dd, J = 7.1, 1.8 Hz, 3H).

¹³C NMR (126 MHz, CDCl₃) δ 164.30, 133.98, 131.92, 128.75, 126.99, 122.24, 106.08, 10.99.

HRMS analysis (ESI): calculated for (M+H): C₁₀H₁₂NO 162.0919; found: 162.0920

For **IV-37**:

White solid, M.P.: 92 - 97 °C

Rf: 0.51 (30% EtOAc in Hexane, UV)

¹H NMR (500 MHz, CDCl₃) δ 7.86 – 7.72 (m, 2H), 7.63 (s, 1H), 7.54 – 7.39 (m, 3H), 6.94 (ddq, J = 14.0, 10.4, 1.7 Hz, 1H), 5.29 (dq, J = 13.6, 6.7 Hz, 1H), 1.72 (dd, J = 6.7, 1.7 Hz, 3H).

¹³C NMR (126 MHz, CDCl₃) δ 164.16, 133.84, 131.78, 128.67, 126.95, 123.55, 108.79, 14.97.

HRMS analysis (ESI): calculated for (M+H): C₁₀H₁₂NO 162.0919; found: 162.0920

General procedure $\bf B$ was used with 2.0 g (11.72 mmol) of $\it p$ -MeObenzoyl chloride yielding 560 mg (26%) of $\bf IV$ -38 and 630 mg (28%) of $\bf IV$ -39 after 2 steps as a white solid.

For **IV-38**:

white solids; M.P.: 70 - 75 °C

R_f: 0.38 (30% EtOAc in Hexane, UV)

¹H NMR (500 MHz, CDCl₃) δ 7.78 – 7.72 (m, 2H), 7.54 (d, J = 10.4 Hz, 1H), 6.96 – 6.88 (m, 3H), 4.94 – 4.80 (m, 1H), 3.83 (s, 3H), 1.68 (dd, J = 7.1, 1.7 Hz, 3H).

¹³C NMR (126 MHz, CDCl₃) δ 163.79, 162.49, 128.88, 126.13, 122.38, 113.91, 105.46, 55.44, 10.97.

HRMS analysis (ESI): calculated for (M+H): C₁₁H₁₄NO₂ 192.1025; found: 192.1025

For **IV-39**:

white solids; M.P.: 122 -125 °C

Rf: 0.33 (30% EtOAc in Hexane, UV)

¹H NMR (500 MHz, CDCl₃) δ 7.76 – 7.70 (m, 2H), 7.66 (d, J = 10.4 Hz, 1H), 6.94 (dq, J = 12.5, 1.7 Hz, 1H), 6.91 – 6.86 (m, 2H), 5.26 (dq, J = 13.6, 6.7 Hz, 1H), 3.82 (s, 3H), 1.70 (dd, J = 6.7, 1.7 Hz, 3H).

¹³C NMR (126 MHz, CDCl₃) δ 163.71, 162.37, 128.85, 126.02, 123.73, 113.82, 108.17, 55.42, 14.98.

HRMS analysis (ESI): calculated for (M+H): C₁₁H₁₄NO₂ 192.1025; found: 192.1028

General procedure **B** was used with 1.5 g (11.72 mmol) of *p*-Mebenzoyl chloride yielding 937 mg (56%) of **IV-42** and 468 mg (28%) of **IV-43** after 2 steps as a white solid.

For **IV-42**:

white solid, M.P.: 54 -58 °C

Rf: 0.58 (30% EtOAc in Hexane, UV)

¹H NMR (500 MHz, CDCl₃) δ 7.67 (d, J = 7.9 Hz, 3H), 7.20 (d, J = 7.8 Hz, 2H), 6.88 (ddd, J = 11.0, 8.9, 2.1 Hz, 1H), 4.92 – 4.83 (m, 1H), 2.36 (s, 3H), 1.67 (dd, J = 7.0, 1.9 Hz, 3H). ¹³C NMR (126 MHz, CDCl₃) δ 164.33, 142.40, 131.06, 129.33, 127.04, 122.31, 105.89, 21.47, 10.99.

HRMS analysis (ESI): calculated for (M+H): C₁₁H₁₄NO 176.1075; found: 176.1073

For **IV-43**:

white solid, M.P.: 117 - 122 °C

Rf: 0.47 (30% EtOAc in Hexane, UV)

¹H NMR (500 MHz, CDCl₃) δ 7.98 (d, J = 10.3 Hz, 1H), 7.67 (d, J = 7.8 Hz, 2H), 7.17 (d, J = 7.8 Hz, 2H), 6.91 (t, J = 12.2 Hz, 1H), 5.29 (dq, J = 13.6, 6.7 Hz, 1H), 2.35 (s, 3H), 1.68 (d, J = 6.7 Hz, 3H).

¹³C NMR (126 MHz, CDCl₃) δ 164.31, 142.18, 130.94, 129.23, 127.08, 123.71, 108.62, 21.46, 14.99.

HRMS analysis (ESI): calculated for (M+H): C₁₁H₁₄NO 176.1075; found: 176.1073

General procedure B was used with 1.0 g (6.3 mmol) of *o*-fluorobenzoyl chloride yielding 332 mg (29%) of **IV-44** after 2 steps as a colorless crystal.

colorless crystal, M.P.: 30 - 35 °C

Rf: 0.77 (30% EtOAc in Hexane, UV)

¹H NMR (500 MHz, CDCl₃) δ 8.32 (s, 1H), 8.15 (tt, J = 8.0, 1.4 Hz, 1H), 7.53 – 7.45 (m, 1H), 7.28 (td, J = 7.6, 1.1 Hz, 1H), 7.14 (ddd, J = 12.6, 8.3, 1.2 Hz, 1H), 6.97 (m, 1H), 5.00 – 4.87 (m, 1H), 1.69 (dd, J = 7.1, 1.8 Hz, 3H).

¹³C NMR (126 MHz, CDCl₃) δ 161.72, 160.09 (d, J = 3.7 Hz), 159.76, 133.77 (d, J = 9.7 Hz), 132.39 (d, J = 1.9 Hz), 125.06 (d, J = 3.2 Hz), 122.01, 116.06 (d, J = 25 Hz), 106.82, 11.01.

HRMS analysis (ESI): calculated for (M+H): C₁₀H₁₁NOF 180.0825; found: 180.0826

General procedure C: Freshly distilled *N*-vinyl formamide (1 equiv), Et₃N (1.2 equiv), DMAP (5 mol%) and anhydrous THF (1M) were added to a round bottom flask. The resulting mixture was cooled to 0 °C. Acyl chloride (1.2 equiv) was then slowly added and the mixture was stirred at 0-5 °C for 2 h, 5N NaOH solution was added at 0 °C and the solution was stirred for another 2 h. Organic layers were separated and dried over Na₂SO₄ and concentrated under vacuo. The residue was isolated by silica gel column chromatography.

General procedure **C** was used with 543 mg (7.64 mmol) of *N*-vinylformamide yielding 788 mg (58%) of **IV-41** as a white solid.

White solid, M.P.: 76 - 83 °C

Rf: 0.32 (30% EtOAc in Hexane, UV)

¹H NMR (500 MHz, CDCl₃) δ 8.42 (d, J = 10.5 Hz, 1H), 7.83 – 7.70 (m, 2H), 7.21 – 7.06 (m, 1H), 6.88 – 6.78 (m, 2H), 4.76 (d, J = 15.8 Hz, 1H), 4.43 (d, J = 8.7 Hz, 1H), 3.78 (s, 3H).

¹³C NMR (126 MHz, CDCl₃) δ 164.47, 162.54, 129.29, 129.19, 125.62, 113.80, 95.88, 55.40.

HRMS analysis (ESI): calculated for (M+Na): C₁₀H₁₁NO₂Na 200.0687; found: 200.0679

General procedure **C** was used with 668 mg (9.40 mmol) of *N*-vinylformamide and propanoyl chloride 1 g (10.80 mmol) yielding 120 mg (29%) of **IV-48** as a purplish liquid. R_f: 0.30 (30% EtOAc in Hexane, UV)

¹H NMR (500 MHz, CDCl₃) δ 9.23 (s, 1H), 6.50 (ddd, J = 15.9, 8.8, 0.6 Hz, 1H), 5.42 (dd, J = 15.9, 0.7 Hz, 1H), 5.35 – 5.24 (m, 1H), 2.66 (q, J = 7.2 Hz, 2H), 1.18 (t, J = 7.2 Hz, 3H).

¹³C NMR (126 MHz, CDCl₃) δ 171.90, 128.72, 95.17, 29.42, 9.50.

HRMS analysis (ESI): calculated for (M+H): C₅H₁₀NO 100.0762; found: 100.0754

General procedure **C** was used with 600 mg (8.44 mmol) of *N*-vinylformamide and *iso*-butyryl chloride 1.03 g (9.70 mmol) yielding 563 mg (59%) of **IV-47** as a white solid.

White solid, M.P.: 40 - 45 °C

Rf: 0.47 (30% EtOAc in Hexane, UV)

¹H NMR (500 MHz, CDCl₃) δ 7.19 (d, J = 47.1 Hz, 1H), 6.97 (ddd, J = 15.8, 10.8, 8.7 Hz, 1H), 4.58 (d, J = 15.8 Hz, 1H), 4.37 (d, J = 8.7 Hz, 1H), 2.37 (p, J = 6.9 Hz, 1H), 1.16 (d, J = 7.0 Hz, 6H).

¹³C NMR (126 MHz, CDCl₃) δ 174.39, 128.78, 94.90, 35.56, 19.35.

HRMS analysis (ESI): calculated for (M+H): C₆H₁₂NO 114.0919; found: 114.0918

General procedure C was used with 1.0 g (14.10 mmol) of *N*-vinylformamide and valeroyl chloride 1.95 g (16.20 mmol) yielding 310 mg (17%) of **IV-45** as a white solid.

White solid, M.P.: 41 − 45 °C

R_f: 0.44 (30% EtOAc in Hexane, UV)

¹H NMR (500 MHz, CDCl₃) δ 7.07 – 6.89 (m, 3H), 4.56 (dd, J = 15.8, 0.8 Hz, 1H), 4.36 (dd, J = 8.2, 0.8 Hz, 1H), 2.25 – 2.14 (m, 2H), 1.68 – 1.55 (m, 2H), 1.34 (h, J = 7.4 Hz, 2H), 0.90 (t, J = 7.4 Hz, 3H).

¹³C NMR (126 MHz, CDCl₃) δ 170.98, 128.64, 94.66, 36.38, 27.42, 22.36, 13.77. HRMS analysis (ESI): calculated for (M+H): C₇H₁₄NO 128.1075; found: 128.1063

(E)-1-(prop-1-en-1-yl)pyrrolidin-2-one **IV-49** was synthesized according to the reported literature.²⁹

Rf: 0.20 (30% EtOAc in Hexane, UV)

¹H NMR (500 MHz, CDCl₃) δ 6.85 (dq, J = 14.3, 1.9 Hz, 1H), 4.97 – 4.84 (m, 1H), 3.45 (dd, J = 8.6, 5.9 Hz, 2H), 2.44 (td, J = 8.1, 3.3 Hz, 2H), 2.11 – 1.98 (m, 2H), 1.69 (dt, J = 6.5, 1.6 Hz, 3H).

¹³C NMR (126 MHz, CDCl₃) δ 172.61, 124.31, 106.83, 45.22, 31.23, 17.40, 15.19. HRMS analysis (ESI): calculated for (M+H): C₇H₁₂NO 126.0919; found: 126.0921

$$\frac{2.5 \text{ equiv KCO}_2\text{N} = \text{NCO}_2\text{K}}{5 \text{ equiv AcOH}} \\ \frac{5 \text{ equiv AcOH}}{7.5 \text{ equiv pyridine}} \\ \text{MeOH, rt} \\ (Z)\text{-1-iodohex-1-ene} \\ \frac{20 \text{ mol}\% \text{ Cul}}{2 \text{ equiv CsCO}_3} \\ \frac{40 \text{ mol}\% \text{ DMEDA}}{\text{THF, 70 °C, 12 h}} \\ \text{IV-40}$$

1-iodohexyne was synthesized accord to reported literature procedure in quantitative yield.³⁰ 1-iodohexyne (1.15 g, 5.53 mmol) was dissolved in methanol (10 mL) and pyridine (1.65 mL), followed by adding potassium diazodiimide (2.7 g, 13.8 mmol) with vigorous stiring. Acetic acid (1.66 g) was added via syringe to the reaction mixture dropwise at room temperature. The reaction was followed by GC. After 8 h 15% of the hexyne was observed via GC. To the reaction 0.5 equiv of potassium diazodiimide and 1 equiv of

AcOH were added. Aq. HCI (5%, 20 mL) was added and the mixture was extracted with Et₂O. The organics were washed with brine, dried over Na₂SO₄ and the solvents were removed in vacuo. The residue was purified through a flash column of SiO₂ (100% hexane). A pale yellow liquid 604 mg was isolated as (Z)-1-iodohex-1-ene (52% yield).

The enamide substrate **IV-40** was synthesized accord to reported literature.³¹ An oven-dried 25 mL screw-cap seal tube equipped with a Teflon-coated magnetic stir bar was charged with (*Z*)-1-iodohex-1-ene (540 mg, 2.57 mmol, 1 equiv), *p*-methoxybenzamide (466 mg, 3.08 mmol, 1.2 equiv), CuI (98 mg, 0.514 mmol, 20 mol%), and Cs₂CO₃ (1.67 g, 5.14 mmol, 2 equiv). The tube was then evacuated and backfilled with argon. DMEDA (91 mg, 1.03 mmol, 40 mol%) was added into the tube followed by anhydrous THF (10 mL) via a syringe. The sealed tube was placed in a preheated oil bath (70 °C). After stirring at the same temperature for 12 h, the reaction mixture was allowed to cool to room temperature. The reaction mixture was filtered through a thin layer of celite and washed by EtOAc. The filtrate was concentrated in vacuo. The crude residue was purified by flash chromatography, 402 mg **IV-40** was given as oil in 67% yield.

Rf: 0.46 (30% EtOAc in Hexane, UV)

¹H NMR (500 MHz, CDCl₃) δ 7.80 – 7.71 (m, 2H), 7.71 – 7.17 (m, 1H), 7.01 – 6.81 (m, 3H), 4.89 – 4.73 (m, 1H), 3.83 (s, 3H), 2.08 (qd, J = 7.2, 1.7 Hz, 2H), 1.53 – 1.28 (m, 4H), 0.91 (t, J = 7.1 Hz, 3H).

¹³C NMR (126 MHz, CDCl₃) δ 163.80, 162.46, 128.87, 126.14, 121.27, 113.89, 111.74, 55.42, 31.49, 25.55, 22.33, 13.94.

HRMS analysis (ESI): calculated for (M+H): C₁₄H₂₀NO₂ 234.1494; found: 234.1497

4-(4-methoxyphenyl)pent-4-enoic acid was synthesized via Wittig reaction according to reported procedure.³² To 4-(4-methoxyphenyl)pent-4-enoic acid (1 mmol, 206 mg) in freshly distilled dichloromethane (5 mL) was added DMAP (1.4 mmol, 171 mg) and *N,N'*-dicyclohexylcarbodiimide (1.3 mmol, 268 mg) sequentially at 0 °C. After stirring for 5 min at 0 °C, aniline (1.2 mmol, 1.1 mL) was added in one portion. After 8 h, reaction was quenched with 1N HCl solution (2 mL) and H₂O (5 mL). The reaction was extracted with DCM three times and the organic portion was dried with Na₂SO₄. The organic portion was concentrated under reduced pressure to afford crude residue. The product was purified via flash column (silica gel, 15% EtOAc in Hexane) to afford **IV-72**.

Rf: 0.41 (30% EtOAc in Hexane, UV)

¹H NMR (500 MHz, CDCl₃) δ 7.47 – 7.42 (m, 2H), 7.37 – 7.32 (m, 2H), 7.31 – 7.25 (m, 2H), 7.19 (s, 1H), 7.07 (tt, J = 7.3, 1.1 Hz, 1H), 6.89 – 6.83 (m, 2H), 5.24 (s, 1H), 5.02 (s, 1H), 3.79 (s, 3H), 2.94 – 2.87 (m, 2H), 2.47 (dd, J = 8.4, 6.8 Hz, 2H).

¹³C NMR (126 MHz, CDCl₃) δ 170.62, 159.27, 146.13, 137.83, 132.57, 128.96, 127.27, 124.21, 119.76, 113.85, 112.03, 55.31, 36.49, 31.14.

HRMS analysis (ESI): calculated for (M+H): C₁₈H₂₀NO₂ 282.1494; found: 282.1506

¹H NMR (500 MHz, CDCl₃) δ 7.37 (d, J = 8.8 Hz, 2H), 6.87 (d, J = 8.8 Hz, 2H), 5.24 (d, J = 1.5 Hz, 1H), 5.02 (d, J = 1.4 Hz, 1H), 3.82 (s, 3H), 3.66 (t, J = 6.4 Hz, 2H), 2.64 – 2.52 (m, 2H), 1.80 – 1.67 (m, 2H), 1.61 (s, 1H).

¹³C NMR (126 MHz, CDCl₃) δ 159.04, 147.19, 133.33, 127.17, 113.66, 111.02, 62.42, 55.27, 31.58, 31.18.

4.4 Acknowledgement

Thanks are due to Dr Gholami who worked as a wonderful originator and collaborator in this project. I had a lot of helpful discussions with him. He also did a lot of work for preparing the paper for publication. Cheers Man!

REFERENCES

REFERENCES

- 1. Grigoropoulou, G.; Clark, J. H.; Elings, J. A., Recent developments on the epoxidation of alkenes using hydrogen peroxide as an oxidant. *Green Chemistry* **2003**, *5* (1), 1-7.
- 2. Kolb, H. C.; VanNieuwenhze, M. S.; Sharpless, K. B., Catalytic Asymmetric Dihydroxylation. *Chemical Reviews* **1994**, *94* (8), 2483-2547.
- 3. Müller, T. E.; Hultzsch, K. C.; Yus, M.; Foubelo, F.; Tada, M., Hydroamination: Direct Addition of Amines to Alkenes and Alkynes. *Chemical Reviews* **2008**, *108* (9), 3795-3892.
- 4. Cresswell, A. J.; Eey, S. T. C.; Denmark, S. E., Catalytic, Stereoselective Dihalogenation of Alkenes: Challenges and Opportunities. *Angewandte Chemie International Edition* **2015**, *54* (52), 15642-15682.
- 5. Denmark, S. E.; Kuester, W. E.; Burk, M. T., Catalytic, Asymmetric Halofunctionalization of Alkenes—A Critical Perspective. *Angewandte Chemie International Edition* **2012**, *51* (44), 10938-10953.
- 6. Coulombel, L.; Dunach, E., Triflic acid-catalysed cyclisation of unsaturated alcohols. *Green Chemistry* **2004**, *6* (10), 499-501.
- 7. Qian, H.; Han, X.; Widenhoefer, R. A., Platinum-Catalyzed Intramolecular Hydroalkoxylation of γ and δ -Hydroxy Olefins to Form Cyclic Ethers. *Journal of the American Chemical Society* **2004**, *126* (31), 9536-9537.
- 8. Liu, C.; Bender, C. F.; Han, X.; Widenhoefer, R. A., Platinum-catalyzed hydrofunctionalization of unactivated alkenes with carbon, nitrogen and oxygen nucleophiles. *Chemical Communications* **2007**, (35), 3607-3618.
- 9. Rosenfeld, D. C.; Shekhar, S.; Takemiya, A.; Utsunomiya, M.; Hartwig, J. F., Hydroamination and Hydroalkoxylation Catalyzed by Triflic Acid. Parallels to Reactions Initiated with Metal Triflates. *Organic Letters* **2006**, *8* (19), 4179-4182.
- 10. Fujita, S.; Abe, M.; Shibuya, M.; Yamamoto, Y., Intramolecular Hydroalkoxylation of Unactivated Alkenes Using Silane–Iodine Catalytic System. *Organic Letters* **2015**, *17* (15), 3822-3825.
- 11. Katritzky, A. R.; Pernak, J.; Fan, W. Q.; Saczewski, F., N-(1-benzotriazol-1-ylalkyl)amides, versatile .alpha.-amidoalkylation reagents. 1. .alpha.-Amidoalkylation of CH acids. *The Journal of Organic Chemistry* **1991**, *56* (14), 4439-4443.

- 12. Katritzky, A. R.; Fan, W. Q.; Black, M.; Pernak, J., N-[1-(Benzotriazol-1-yl)alkyl]amides, versatile amidoalkylation reagents. 5. A general and convenient route to N-(.alpha.-alkoxyalkyl)amides. *The Journal of Organic Chemistry* **1992**, *57* (2), 547-549.
- 13. Li, M.; Luo, B.; Liu, Q.; Hu, Y.; Ganesan, A.; Huang, P.; Wen, S., Synthesis of N-Acyl-N,O-acetals Mediated by Titanium Ethoxide. *Organic Letters* **2014**, *16* (1), 10-13.
- 14. George, N.; Bekkaye, M.; Masson, G.; Zhu, J., A Practical, One-Pot Multicomponent Synthesis of α-Amidosulfides and Their Application as Latent N-Acylimines in the Friedel–Crafts Reaction. *European Journal of Organic Chemistry* **2011**, *2011* (20-21), 3695-3699.
- 15. Gizecki, P.; Ait Youcef, R.; Poulard, C.; Dhal, R.; Dujardin, G., Diastereoselective preparation of novel tetrahydrooxazinones via heterocycloaddition of N-Boc, O-Meacetals. *Tetrahedron Letters* **2004**, *45* (52), 9589-9592.
- 16. Wan, S.; Green, M. E.; Park, J.-H.; Floreancig, P. E., Multicomponent Approach to the Synthesis of Oxidized Amides through Nitrile Hydrozirconation. *Organic Letters* **2007**, *9* (26), 5385-5388.
- 17. Li, G.; Fronczek, F. R.; Antilla, J. C., Catalytic Asymmetric Addition of Alcohols to Imines: Enantioselective Preparation of Chiral N,O-Aminals. *Journal of the American Chemical Society* **2008**, *130* (37), 12216-12217.
- 18. Honjo, T.; Phipps, R. J.; Rauniyar, V.; Toste, F. D., A Doubly Axially Chiral Phosphoric Acid Catalyst for the Asymmetric Tandem Oxyfluorination of Enamides. *Angewandte Chemie International Edition* **2012**, *51* (38), 9684-9688.
- 19. Ni, C.; Hu, M.; Hu, J., *Chemical Reviews* **2015**, *115*, 765-825.
- 20. Nielsen, M. K.; Ugaz, C. R.; Li, W.; Doyle, A. G., PyFluor: A Low-Cost, Stable, and Selective Deoxyfluorination Reagent. *J. Am. Chem. Soc.* **2015**, *137* (30), 9571-9574.
- 21. Beaulieu, F.; Beauregard, L.-P.; Courchesne, G.; Couturier, M.; LaFlamme, F.; L'Heureux, A., Aminodifluorosulfinium Tetrafluoroborate Salts as Stable and Crystalline Deoxofluorinating Reagents. *Organic Letters* **2009**, *11* (21), 5050-5053.
- 22. L'Heureux, A.; Beaulieu, F.; Bennett, C.; Bill, D. R.; Clayton, S.; LaFlamme, F.; Mirmehrabi, M.; Tadayon, S.; Tovell, D.; Couturier, M., Aminodifluorosulfinium Salts: Selective Fluorination Reagents with Enhanced Thermal Stability and Ease of Handling. *The Journal of Organic Chemistry* **2010**, *75* (10), 3401-3411.
- 23. Pouliot, M.-F.; Mahé, O.; Hamel, J.-D.; Desroches, J.; Paquin, J.-F., Halogenation of Primary Alcohols Using a Tetraethylammonium Halide/[Et2NSF2]BF4 Combination. *Organic Letters* **2012**, *14* (21), 5428-5431.

- 24. Vandamme, M.; Paquin, J.-F., Eliminative Deoxofluorination Using XtalFluor-E: A One-Step Synthesis of Monofluoroalkenes from Cyclohexanone Derivatives. *Organic Letters* **2017**, *19* (13), 3604-3607.
- 25. Vandamme, M.; Bouchard, L.; Gilbert, A.; Keita, M.; Paquin, J.-F., Direct Esterification of Carboxylic Acids with Perfluorinated Alcohols Mediated by XtalFluor-E. *Organic Letters* **2016**, *18* (24), 6468-6471.
- 26. Desroches, J.; Champagne, P. A.; Benhassine, Y.; Paquin, J.-F., In situ activation of benzyl alcohols with XtalFluor-E: formation of 1,1-diarylmethanes and 1,1,1-triarylmethanes through Friedel-Crafts benzylation. *Organic & Biomolecular Chemistry* **2015**, *13* (8), 2243-2246.
- 27. Lebleu, T.; Paquin, J.-F., Direct allylation of benzyl alcohols, diarylmethanols, and triarylmethanols mediated by XtalFluor-E. *Tetrahedron Letters* **2017**, *58* (5), 442-444.
- 28. Nonn, M.; Kiss, L.; Haukka, M.; Fustero, S.; Fülöp, F., A Novel and Selective Fluoride Opening of Aziridines by XtalFluor-E. Synthesis of Fluorinated Diamino Acid Derivatives. *Organic Letters* **2015**, *17* (5), 1074-1077.
- 29. Tamai, T.; Yoshikawa, M.; Higashimae, S.; Nomoto, A.; Ogawa, A., Palladium-Catalyzed Markovnikov-Selective Hydroselenation of N-Vinyl Lactams with Selenols Affording N,Se-Acetals. *The Journal of Organic Chemistry* **2016**, *81* (1), 324-329.
- 30. Hoye, R. C.; Anderson, G. L.; Brown, S. G.; Schultz, E. E., Total Synthesis of Clathculins A and B. *The Journal of Organic Chemistry* **2010**, *75* (21), 7400-7403.
- 31. Cheung, C. W.; Buchwald, S. L., Room Temperature Copper(II)-Catalyzed Oxidative Cyclization of Enamides to 2,5-Disubstituted Oxazoles via Vinylic C–H Functionalization. *The Journal of Organic Chemistry* **2012**, *77* (17), 7526-7537.
- 32. Sha, W.; Zhang, W.; Ni, S.; Mei, H.; Han, J.; Pan, Y., Photoredox-Catalyzed Cascade Difluoroalkylation and Intramolecular Cyclization for Construction of Fluorinated γ-Butyrolactones. *The Journal of Organic Chemistry* **2017**, *82* (18), 9824-9831.